

Targeting the tumour microenvironment with endosialin-directed CAR T-cells

Sarah L. Ash

A thesis submitted for the degree of Doctor of Philosophy

Breast Cancer Now Research Centre

The Institute of Cancer Research

237 Fulham Road

London

This thesis was completed under the supervision of Professor Clare M. Isacke and Dr France Turrell.

The work described here was carried out in the Breast Cancer Now Research Centre, The Institute of Cancer Research, 237 Fulham Road, London, SW3 6JB.

I, Sarah L. Ash, confirm that the work presented in this thesis is my own. Where information has been derived from other sources, I confirm that this has been indicated in the thesis.

Date: 31st March, 2022.



.....

Abstract

Advances in T-cell engineering have facilitated the generation of CAR T-cells that successfully deplete malignant cells of haematological cancers. However, attempts to target solid tumours with CAR T-cells have been hindered by the unfavourable environments surrounding the malignant cells in this setting. An alternative approach that circumvents the arduous journey to reach tumour cells is to target cells of the tumour microenvironment, especially those proximal to the vasculature. Endosialin is a transmembrane glycoprotein upregulated on tumour-associated pericytes and fibroblasts which has previously been shown by our laboratory to have a role in promoting tumour cell intravasation and metastatic dissemination.

The aim of this PhD was to evaluate endosialin-targeting CAR T-cells, known as Endo3 CAR T-cells, in the context of solid tumours. *In vitro* characterisation of Endo3 CAR T-cells demonstrated endosialin-specific activation and cytotoxicity against both mouse and human cells. Endo3 CAR T-cells were evaluated *in vivo* in the context of three syngeneic models of cancer: 4T1, AT-3 and LLC. Modest effects on primary tumour growth were observed in 4T1 and LLC tumour-bearing mice, however a significant reduction in spontaneous lung metastasis was observed in these models. Conversely, in AT-3 tumour-bearing mice, Endo3 CAR T-cell therapy resulted in a significant reduction of primary tumour growth but did not limit metastatic lung disease. Endo3 CAR T-cell therapy was associated with toxicity in BALB/c 4T1 tumour-bearing mice that was not alleviated by anti-IL-6R treatment or delivering multiple low T-cell doses. Interrogation of the strain-specific Endo3 CAR T-cell products revealed differences in the CD4⁺:CD8⁺ T-cell ratio and distinct efficacies in an immunodeficient setting.

This thesis proposes that Endo3 CAR T-cell therapy is a potential candidate for targeted therapy of solid tumours. Further studies are required to gain better

Abstract

understanding of Endo3 CAR T-cell dosing and tolerability in the context of different endogenous immune systems.

Statement regarding impact of COVID-19 on PhD studies

On 24th March 2020, the ICR went into lockdown due to the COVID-19 pandemic and I was unable to attend the laboratory to conduct experiments for approximately 3 months.

Upon returning to the lab on June 8th, 2020, the environment was different with additional challenges including:

- Strict restrictions on the number of people allowed in the building at any given time. This meant reduced hours in the laboratory compared to pre-COVID. Even stricter restrictions were in place in the animal house resulting an additional delay in restarting *in vivo* work
- Due to COVID/Brexit there have been multiple supply chain issues resulting in delays to experiments whilst waiting for reagents and equipment to arrive.
- We experienced a much slower turnaround of samples submitted to core facilities due to staff shielding and isolation.

Closure of our collaborator's laboratory in Birmingham during the first COVID-19 lockdown delayed the progression of my project further. The Birmingham laboratory reopened much later than ours and I did not receive another batch of CAR T-cells until 1st December 2020 and I was unable to start a new experiment until January 2021, giving a one year gap when I was unable to perform a CAR T-cell *in vivo* study (Jan 2020 to Jan 2021).

Date: 30th March, 2022.



Sarah Ash

.....



Professor Clare M. Isacke

.....

Acknowledgments

First and foremost, I would like to thank my supervisors Professor Clare Isacke and Dr Frances Turrell for giving me their support, guidance and wisdom throughout this project and the writing of this thesis.

Secondly, I would like to thank all members of the Isacke lab, past and present, who have helped support both myself and this project and become dear friends in doing so. I give special thanks to David Vicente and Rebecca Orha for their invaluable assistance with *in vivo* experiments. I also give thanks to my collaborator Dr Steven Lee and his colleagues for designing and generating mock transduced and CAR T-cells for this project.

I am extremely grateful to CRUK, Breast Cancer Now and the Institute of Cancer Research for funding this project and the facilities required to complete this research. Additionally, I thank the ICR BSU staff for their assistance with *in vivo* studies and the Breast Cancer Now histopathology facility for their continuous efforts to supply me with high quality sections and IHC stains for this project.

Je veux aussi remercier mon copain Arnaud pour son soutien sans limite et pour m'avoir donné de meilleurs repas que de la soupe en boite. Je ne sais pas ce que j'aurais pu faire sans toi. Merci beaucoup.

I give a special thanks to my parents, David & Mandy, without whom I would not be the person I am today. Your love and support have helped me not only through this PhD, but through every challenge I have faced in life so far.

Finally, I dedicate this thesis to the memory of my Grandad Keith Ash, who sadly lost his battle with lung cancer at the young age of 54 and to my Nan Margaret Rowbotham, who has been bravely surviving with breast cancer for the past 5 years.

Table of Contents

ABSTRACT	3
STATEMENT REGARDING IMPACT OF COVID-19 ON PHD STUDIES.....	5
ACKNOWLEDGMENTS	6
TABLE OF CONTENTS	7
LIST OF FIGURES	12
LIST OF TABLES.....	15
LIST OF ABBREVIATIONS.....	16
CHAPTER 1 INTRODUCTION	23
1.1 Breast Cancer	23
1.1.1 Breast cancer incidence	23
1.1.2 Risk factors associated with breast cancer	24
1.1.3 Breast cancer diagnosis, staging and subtypes.....	25
1.1.4 Breast cancer metastasis.....	27
1.1.5 Breast cancer treatment.....	30
1.2 The Tumour Microenvironment	32
1.2.1 Introduction.....	32
1.2.2 Tumour vasculature	33
1.2.3 Pericytes.....	38
1.2.3.1 Pericyte classification	38
1.2.3.2 Pericyte function.....	39
1.2.3.3 Pericytes & cancer	40
1.2.4 Cancer-associated fibroblasts.....	43
1.2.4.1 Normal fibroblasts	43
1.2.4.2 Function of cancer-associated fibroblasts (CAFs)	44
1.2.4.3 Cancer-associated fibroblast subtypes	45
1.2.4.4 The role of cancer-associated fibroblasts in tumour progression	47
1.3 Endosialin	48
1.3.1 Endosialin structure and family members	48
1.3.2 Endosialin expression	50
1.3.2.1 Endosialin-expressing cell types	50
1.3.2.2 Endosialin expression in embryonic and adult tissues.....	51
1.3.2.3 Endosialin expression in tumour tissue and other disease pathologies	53
1.3.2.4 Regulators of endosialin expression	54
1.3.3 Endosialin Function	54
1.3.3.1 Endosialin in development and cellular signalling.....	54

Table of Contents

1.3.3.2	Endosialin in angiogenesis.....	57
1.3.3.3	Endosialin in tumour angiogenesis and growth	60
1.3.3.4	Endosialin in metastasis.....	61
1.3.3.5	Soluble endosialin	62
1.3.4	Targeting Endosialin	63
1.3.4.1	Endosialin targeting with MORAb-004 (Ontuxizumab)	63
1.3.4.2	Endosialin targeting with antibody-drug conjugates.....	65
1.3.4.3	Alternative clinical uses for endosialin targeting	66
1.4	CAR T-cell therapy	67
1.4.1	Cancer Immunotherapy.....	67
1.4.2	CAR T-cell design, development & production	68
1.4.2.1	CAR T-cell generations	68
1.4.2.2	CAR T-cell production	71
1.4.3	FDA approved CAR T-cell therapies.....	72
1.4.3.1	Kymriah (tisagenlecleucel).....	73
1.4.3.2	Yescarta (axicabtagene ciloleucel)	77
1.4.3.3	Abecma (idecabtagene vicleucel)	81
1.4.3.4	Tecartus (brexucabtagene autoleucel)	83
1.4.3.5	Breyanzi (lisocabtagene maraleucel).....	84
1.4.4	Managing CAR T-cell associated toxicity.....	85
1.4.4.1	Managing Cytokine Release Syndrome (CRS).....	86
1.4.4.2	Managing Immune Effector Cell-Associated Neurotoxicity Syndrome (ICANS) ..	87
1.4.4.3	Managing Tumour Lysis Syndrome	89
1.4.5	Limitations of CAR T-cell therapy in solid tumours	89
1.4.6	CAR T-cells targeting the tumour stroma.....	93
1.4.6.1	Targeting cancer associated fibroblasts	93
1.4.6.2	Targeting the tumour vasculature	95
1.4.7	Next Generation CAR T-cells.....	97
1.4.7.1	Enhancing CAR T-cell migration and tumour infiltration	98
1.4.7.2	Enhancing CAR T-cell activation, proliferation and survival	99
1.4.7.3	Limiting CAR T-cell associated toxicity and overcoming therapeutic resistance	101
1.4.7.3.1	Bi-specific CAR T-cells.....	101
1.4.7.3.2	Low affinity CAR T-cells	105
1.4.7.3.3	Inducible CAR T-cell control.....	106
1.4.7.3.4	CAR T-cell exosomes.....	107
1.4.7.4	Universal CAR T-cells	108
1.4.8	CAR T-cells currently in clinical trials	112
1.5	Project rationale and aims	113
CHAPTER 2	MATERIALS AND METHODS	115
2.1	Materials.....	115
2.1.1	General reagents	115
2.1.2	Cell culture	115
2.1.3	Flow cytometry	116
2.1.4	Immunostaining.....	117
2.1.5	Western blotting	117
2.1.6	RNA isolation and RTqPCR	118
2.1.7	ELISA	119

Table of Contents

2.1.8	Cytotoxicity assays.....	119
2.1.9	Generation of Endo3 CAR and Mock T-cells	119
2.1.10	In vivo studies.....	120
2.2	Methods.....	121
2.2.1	Cell culture	121
2.2.2	Western blotting	121
2.2.3	In vivo studies.....	122
2.2.4	Histology.....	125
2.2.5	Immunostaining.....	125
2.2.6	Generation of Endo3 CAR and Mock T-cells	126
2.2.7	Flow cytometry	127
2.2.8	RNA extraction and RTqPCR analysis	128
2.2.9	Cell viability assays	129
2.2.10	Enzyme-linked immunosorbent assay (ELISA).....	129
2.2.11	Cytotoxicity assays.....	129
2.2.12	Statistical analysis.....	130
 CHAPTER 3 GENERATION OF ENDO3 CAR T-CELLS AND VALIDATION OF ENDOSIALIN AS A CAR T-CELL TARGET		131
3.1	Introduction	131
3.2	Results	132
3.2.1	mAb 3K2L recognises mouse and human endosialin.....	132
3.2.2	Endo3 CAR is transduced with high efficiency into mouse T-cells.....	134
3.2.3	Endosialin is upregulated in tumour tissue compared to normal tissues	135
3.2.4	Endosialin expression in human breast cancer	142
3.3	Discussion	145
3.3.1	Endo3 CAR is transduced with high efficiency into mouse T-cells.....	145
3.3.2	Syngeneic models of breast cancer for Endo3 CAR T-cell evaluation	145
3.3.3	Endosialin expression in human breast cancer	147
 CHAPTER 4 IN VITRO AND IN VIVO CHARACTERISATION OF ENDO3 CAR T-CELLS.....		149
4.1	Introduction	149
4.2	Results	150
4.2.1	Endo3 CAR T-cells exhibit target-specific activity in vitro.....	150
4.2.2	Optimisation of Endo3 CAR T-cell in vivo therapeutic strategy	154
4.2.3	Endo3 CAR T-cells expand in the circulation of BALB/c mice and deplete endosialin-positive cells in the 4T1 tumour stroma	157
4.2.4	Endo3 CAR T-cell therapy is associated with toxicity in BALB/c mice but limits metastatic spread of 4T1 tumours	162
4.2.5	Endo3 CAR T-cells do not cause toxicity in mice with healing wounds.....	163
4.3	Discussion	168
 CHAPTER 5 ENDO3 CAR T-CELL ACTIVITY IN BALB/C MICE.....		177

5.1	Introduction	177
5.2	Results	178
5.2.1	Endo3 CAR T-cell targeting is specific to tumour tissue in Cd248 ^{WT} mice	178
5.2.2	Endo3 CAR T-cell-associated toxicity is target and tumour specific.....	185
5.2.3	Anti-IL-6R treatment does not alleviate Endo3 CAR T-cell-associated toxicity	186
5.2.4	Multiple low doses of Endo3 CAR T-cells reduce the incidence of, but do not fully alleviate, Endo3 CAR T-cell-associated toxicity.....	192
5.3	Discussion	196
5.3.1	Endo3 CAR T-cells increase 4T1 tumour necrosis and limit spontaneous metastasis to the lungs in Cd248 ^{WT} mice.....	196
5.3.2	Endo CAR T-cells demonstrate no activity or toxicity in Cd248 ^{KO} mice.....	196
5.3.3	Endo3 CAR T-cells demonstrate tumour-specific toxicity and do not attack normal tissues	197
5.3.4	Endo3 CAR T-cell associated toxicity is not alleviated by anti-IL-6R co-treatment ..	199
5.3.5	Multiple low doses of Endo3 CAR T-cells reduces the incidence but does not alleviate Endo3 CAR T-cell-associated toxicity.....	201
 CHAPTER 6 ENDO3 CAR T-CELL ACTIVITY IN C57BL/6 MICE.....		203
6.1	Introduction	203
6.2	Results	204
6.2.1	Characterisation of Endo3 CAR T-cell therapy in AT-3 tumour-bearing C57BL/6 mice	204
6.2.2	Endo3 CAR T-cells do not expand in Cd248 ^{WT} or Cd248 ^{KO} AT-3 tumour bearing C57BL/6 mice.....	209
6.2.3	Endo3 CAR T-cells partially deplete endosialin-expressing cells in AT-3 tumours but not in the normal tissue	211
6.2.4	Endo3 CAR T-cells limit AT-3 tumour growth in Cd248 ^{WT} but not Cd248 ^{KO} mice	213
6.2.5	Endo3 CAR T-cells do not limit AT-3 spontaneous metastasis to the lungs	216
6.2.6	Endo3 CAR T-cells significantly limit spontaneous metastasis of LLC tumours to the lungs	218
6.3	Discussion	222
6.3.1	Endo3 CAR T-cells are not toxic in C57BL/6 mice at doses of up to 7.5 x 10 ⁶ CAR T-cells	222
6.3.2	Endo3 CAR T-cells limit AT-3 primary tumour growth but not metastasis to the lung	224
6.3.3	Endo3 CAR T-cells do not limit LLC primary tumour growth but suppress metastasis to the lung.....	226
 CHAPTER 7 COMPARING BALB/C AND C57BL/6 DERIVED ENDO3 CAR T-CELLS.....		228
7.1	Introduction	228
7.2	Results	229
7.2.1	CD4 ⁺ :CD8 ⁺ T-cell ratio in BALB/c and C57BL/6 derived Endo3 CAR T-cells.....	229
7.2.2	BALB/c derived Endo3 CAR T-cells show delayed killing in vitro.....	229

Table of Contents

7.2.3	C57BL/6 Endo3 CAR T-cells limit 4T1 metastasis, whereas BALB/c Endo3 CAR T-cells are non-toxic but display no efficacy in NSG mice	231
7.3	Discussion	238
7.3.1	BALB/c and C57BL/6 Endo3 CAR T-cells behave differently in vitro	238
7.3.2	BALB/c Endo3 CAR T-cells are non-toxic but display no efficacy in NSG mice, whereas C57BL/6 Endo3 CAR T-cells limit 4T1 metastasis.....	239
CHAPTER 8 FINAL DISCUSSION AND FUTURE DIRECTIONS.....		243
8.1	Targeting endosialin as a novel CAR T-cell approach.....	244
8.2	Endosialin blockade vs pericyte ablation.....	248
8.3	Is Endo3 CAR T-cell associated toxicity relevant to humans?	250
8.4	Next steps for Endo3 CAR T-cell therapy.....	253
8.5	Concluding remarks	255
REFERENCES		256

List of Figures

FIGURE 1. 1 THE MOLECULAR SUBTYPES OF BREAST CANCER.....	27
FIGURE 1. 2 THE METASTATIC CASCADE	28
FIGURE 1. 3 THE TUMOUR MICROENVIRONMENT.....	33
FIGURE 1. 4 MECHANISMS OF TUMOUR VASCULARISATION	37
FIGURE 1. 5 PERICYTES AND THE VASCULATURE	38
FIGURE 1. 6 PERICYTE ROLES IN CANCER PROGRESSION	41
FIGURE 1. 7 THE ENDOSIALIN FAMILY MEMBERS	49
FIGURE 1. 8 MULTIMERIN 2 (MMRN2) STRUCTURE AND PROPOSED FUNCTION	59
FIGURE 1. 9 CLASSIC T-CELL AND CAR T-CELL KILLING	70
FIGURE 1. 10 EARLY CAR GENERATIONS.....	72
FIGURE 1. 11 THE CAR T-CELL PRODUCTION PROCESS	73
FIGURE 1. 12 BISPECIFIC CAR T-CELLS.....	103
FIGURE 1. 13 THE UNICAR SYSTEM.....	111
FIGURE 3. 1 MAB 3K2L RECOGNISES MOUSE AND HUMAN ENDOSIALIN	133
FIGURE 3. 2 ENDO3 CAR CONSTRUCT.....	135
FIGURE 3. 3 TRANSDUCTION OF ENDO3 CAR CONSTRUCT INTO BALB/C AND C57BL/6 T-CELLS.....	136
FIGURE 3. 4 TRANSDUCTION EFFICIENCY OF ENDO3 CAR CONSTRUCT INTO BALB/C AND C57BL/6 DERIVED T-CELLS.....	137
FIGURE 3. 5 ENDOSIALIN EXPRESSION IN THE HEALTHY, ADULT BALB/C MOUSE	139
FIGURE 3. 6 ENDOSIALIN EXPRESSION IN THE HEALTHY, ADULT C57BL/6 MOUSE	140
FIGURE 3. 7 ENDOSIALIN EXPRESSION IN SYNGENEIC MOUSE MODELS OF BREAST CANCER	141
FIGURE 3. 8 DIRECT COMPARISON OF ENDOSIALIN EXPRESSION IN NORMAL SKIN AND 4T1 TUMOUR TISSUE	141
FIGURE 3. 9 ENDOSIALIN EXPRESSION IN HUMAN BREAST CANCER	143
FIGURE 3. 10 ENDOSIALIN EXPRESSION IN NORMAL HUMAN TISSUES	144
FIGURE 4. 1 IFN- γ RELEASE BY MOCK TRANSDUCED AND ENDO3 CAR T-CELLS CO- CULTURED WITH TARGET CELL LINES	152
FIGURE 4. 2 VIABILITY OF TARGET CELL LINES CO-CULTURED WITH MOCK TRANSDUCED OR ENDO3 CAR T-CELLS.....	153
FIGURE 4. 3 <i>IN VITRO</i> VALIDATION OF C57BL/6 DERIVED ENDO3 CAR T-CELLS GENERATED BY DR STEVEN LEE'S LABORATORY	154
FIGURE 4. 4 NON-LETHAL WHOLE BODY IRRADIATION SAFELY DEPLETES LYMPHOCYTES	156
FIGURE 4. 5 4T1 TUMOURS ARE VASCULARISED, ENDOSIALIN-POSITIVE AND HAVE NOT METASTASISED TO THE LUNGS AT 2-3 WEEKS POST-IMPLANTATION.	158
FIGURE 4. 6 ENDO3 CAR T-CELL <i>IN VIVO</i> THERAPEUTIC STRATEGY FOR BALB/C MICE BEARING 4T1 TUMOURS.....	159
FIGURE 4. 7 ENDO3 CAR T-CELLS EXPAND IN BALB/C MICE	160
FIGURE 4. 8 ENDO3 CAR T-CELLS DEplete ENDOSIALIN-POSITIVE CELLS IN 4T1 TUMOURS (1).....	161
FIGURE 4. 9 ENDO3 CAR T-CELL THERAPY LIMITS LUNG METASTASIS BUT IS ASSOCIATED WITH TOXICITY	164
FIGURE 4. 10 ENDO3 CAR T-CELL <i>IN VIVO</i> STRATEGY FOR BALB/C WOUNDED MICE	165
FIGURE 4. 11 ENDO3 CAR T-CELLS DO NOT AFFECT WOUND HEALING OR CAUSE TOXICITY IN WOUNDED MICE	166
FIGURE 4. 12 ENDO3 CAR T-CELLS DO NOT DEplete ENDOSIALIN-POSITIVE CELL IN THE HEALING WOUND	167

FIGURE 5. 1 THERAPEUTIC STRATEGY FOR TREATING CD248 ^{WT} AND CD248 ^{KO} MICE WITH ENDO3 CAR T-CELL THERAPY	178
FIGURE 5. 2 ENDO3 CAR T-CELL EXPANSION AND ACTIVITY IN CD248 ^{WT} AND CD248 ^{KO} MICE	180
FIGURE 5. 3 ENDO3 CAR T-CELLS DEplete ENDOSIALIN-POSITIVE CELLS IN 4T1 TUMOURS (2).....	181
FIGURE 5. 4 ENDO3 CAR T-CELLS DO NOT DEplete ENDOSIALIN-POSITIVE CELLS IN NORMAL TISSUE	182
FIGURE 5. 5 EFFICACY OF ENDO3 CAR T-CELL THERAPY AGAINST 4T1 TUMOURS IN CD248 ^{WT} AND CD248 ^{KO} MICE	184
FIGURE 5. 6 ENDO3 CAR T-CELLS LIMIT 4T1 LUNG METASTASIS IN CD248 ^{WT} BUT NOT CD248 ^{KO} MICE	185
FIGURE 5. 7 ENDO3 CAR T-CELL ASSOCIATED TOXICITY IS LIMITED TO CD248 ^{WT} , TUMOUR-BEARING MICE	187
FIGURE 5. 8 VALIDATION OF ANTI-IL-6R MAB 15A7 AND ISOTYPE CONTROL MAB LTF2	189
FIGURE 5. 9 EXPERIMENTAL STRATEGY FOR INVESTIGATING ENDO3 CAR T-CELL AND ANTI-IL-6R CO-THERAPY IN BALB/C MICE	190
FIGURE 5. 10 ANTI-IL-6R CO-THERAPY DOES NOT AFFECT ENDO3 CAR T-CELL PERSISTENCE	191
FIGURE 5. 11 ANTI-IL-6R CO-THERAPY DOES NOT ALLEVIATE ENDO3 CAR T-CELL ASSOCIATED TOXICITY IN BALB/C MICE	193
FIGURE 5. 12 EXPERIMENTAL STRATEGY FOR INVESTIGATING MULTIPLE LOW DOSES OF ENDO3 CAR T-CELL THERAPY IN BALB/C MICE	194
FIGURE 5. 13 DELIVERING MULTIPLE LOW DOSES OF ENDO3 CAR T-CELL THERAPY ALLEVIATES CAR T-CELL-MEDIATED TOXICITY IN A SUBSET OF BALB/C MICE ...	195
FIGURE 6. 1 AT-3 TUMOURS ARE VASCULARISED, ENDOSIALIN-POSITIVE AND HAVE NOT METASTASISED TO THE LUNGS AT 2-3 WEEKS POST-IMPLANTATION.	205
FIGURE 6. 2 ENDO3 CAR T-CELL <i>IN VIVO</i> THERAPEUTIC STRATEGY FOR C57BL/6 MICE BEARING AT-3 TUMOURS	206
FIGURE 6. 3 ENDO3 CAR T-CELLS DO NOT EXPAND IN C57BL/6 MICE	207
FIGURE 6. 4 ENDO3 CAR T-CELLS DEplete ENDOSIALIN-POSITIVE CELLS IN AT-3 TUMOURS	208
FIGURE 6. 5 ENDO3 CAR T-CELL THERAPY MAY LIMIT TUMOUR GROWTH IN AT-3 TUMOUR-BEARING MICE WITHOUT ASSOCIATED TOXICITY	210
FIGURE 6. 6 THERAPEUTIC STRATEGY FOR TREATING CD248 ^{WT} AND CD248 ^{KO} AT-3 TUMOUR-BEARING MICE WITH ENDO3 CAR T-CELL THERAPY	211
FIGURE 6. 7 ENDO3 CAR T-CELL NUMBERS AND ACTIVITY IN CD248 ^{WT} AND CD248 ^{KO} AT-3 TUMOUR-BEARING MICE	212
FIGURE 6. 8 ENDO3 CAR T-CELLS DEplete ENDOSIALIN-POSITIVE CELLS IN AT-3 TUMOURS	214
FIGURE 6. 9 ENDO3 CAR T-CELLS DO NOT DEplete ENDOSIALIN-POSITIVE CELLS IN NORMAL TISSUE IN AT-3 TUMOUR-BEARING MICE	215
FIGURE 6. 10 EFFICACY OF ENDO3 CAR T-CELL THERAPY AGAINST AT-3 TUMOURS IN CD248 ^{WT} AND CD248 ^{KO} MICE	217
FIGURE 6. 11 ENDO3 CAR T-CELLS DO NOT LIMIT AT-3 LUNG METASTASIS	218
FIGURE 6. 12 THERAPEUTIC STRATEGY FOR TREATING LLC TUMOUR-BEARING MICE WITH ENDO3 CAR T-CELL THERAPY	219
FIGURE 6. 13 LLC TUMOURS ARE VASCULARISED, ENDOSIALIN-POSITIVE AND HAVE NOT METASTASISED TO THE LUNGS AT 2 WEEKS POST-IMPLANTATION.	220

FIGURE 6. 14 ENDO3 CAR T-CELL NUMBERS AND ACTIVITY IN LLC TUMOUR-BEARING MICE	221
FIGURE 6. 15 ENDO3 CAR T-CELLS LIMIT METASTASIS OF LLC TUMOUR CELLS TO THE LUNGS.....	222
FIGURE 7. 1 BALB/C AND C57BL/6 DERIVED ENDO3 CAR T-CELLS HAVE DIFFERENT CD4 ⁺ :CD8 ⁺ RATIOS.....	230
FIGURE 7. 2 BALB/C AND C57BL/6 DERIVED ENDO3 CAR T-CELL CYTOTOXICITY	231
FIGURE 7. 3 4T1 TUMOURS GROW AND METASTASISE MORE RAPIDLY IN NSG MICE	232
FIGURE 7. 4 <i>IN VIVO</i> THERAPEUTIC STRATEGY FOR COMPARING BALB/C AND C57BL/6 DERIVED ENDO3 CAR T-CELLS SIMULTANEOUSLY	233
FIGURE 7. 5 NO TOXICITY OR EFFICACY AGAINST 4T1 TUMOURS IS OBSERVED IN NSG MICE TREATED WITH BALB/C OR C57BL/6 DERIVED ENDO3 CAR T-CELLS.....	235
FIGURE 7. 6 C57BL/6 DERIVED ENDO3 CAR T-CELLS MAY DEplete ENDOSIALIN-POSITIVE CELLS MORE EFFECTIVELY THAN BALB/C DERIVED ENDO3 CAR T-CELLS IN NSG MICE	236
FIGURE 7. 7 C57BL/6 DERIVED ENDO3 CAR T-CELLS LIMIT 4T1 LUNG METASTASIS BUT BALB/C DERIVED ENDO3 CAR T-CELLS HAVE NO EFFECT IN NSG MICE	237

List of Tables

TABLE 1.1 CLASSIFICATION OF BREAST CANCER.....	25
TABLE 1.2 THE RECEPTOR-BASED SUBTYPES OF BREAST CANCER.....	26
TABLE 1.3 ACTIVE CAR T-CELL CLINICAL TRIALS.....	112
TABLE 2.1 ANTIBODIES USED FOR FLOW CYTOMETRY.....	116
TABLE 2.2 ANTIBODIES USED FOR IMMUNOFLUORESCENT STAINING.....	117
TABLE 2.3 ANTIBODIES USED FOR WESTERN BLOTTING.....	118
TABLE 2.4 TAQMAN PROBES FOR RTQPCR.....	119
TABLE 2.5 MOUSE HEALTH SCORING CRITERIA.....	125

List of Abbreviations

Abbreviations

α -SMA – alpha-smooth muscle actin

ADC – antibody-drug conjugate

AIs – aromatase inhibitors

ALL - acute lymphoblastic leukaemia

alloHSCT - allogeneic haematopoietic stem cell transplant

AWERB – animal welfare ethical review body

BCMA – b-cell maturation antigen

BCN – Breast Cancer Now

BMSCs - bone marrow-derived stem cells

BSA – bovine serum albumin

CAFs – cancer-associated fibroblasts

CAIX – carboxy-anhydrase-IX

CAR - chimeric antigen receptor

Cd248^{KO} – endosialin knock-out

Cd248^{WT} – endosialin wild-type

CEA - carcinoembryonic antigen

CLEC14A – C-type lectin domain containing 14A

List of Abbreviations

CLL - chronic lymphocytic leukaemia

CNS - central nervous system

CRS - cytokine release syndrome

CRUK – Cancer Research UK

CSM – co-stimulatory molecule

CSSD – central sterile stores department

CTLA-4 - cytotoxic T-lymphocyte-associated protein 4

CTLD – C-type lectin-like domain

DCIS – ductal carcinoma in situ

DLBCL - diffuse large B-cell lymphoma

DMEM – Dulbecco's modified eagle medium

DMSO – dimethyl sulfoxide

ECL – enhanced chemiluminescence

ECM – extracellular matrix

EGF – epidermal growth factor

EGFR - epidermal growth factor receptor

ELISA – enzyme-linked immunosorbent assay

EMILIN – elastic microfibril interfacier

EMT – epithelial-to-mesenchymal transition

List of Abbreviations

ER – oestrogen reception

ERK – extracellular signal-regulated protein kinase

ET_BR - endothelin B receptor

FAP – fibroblast activation protein

FBS – fetal bovine serum

FFPE – formalin-fixed, paraffin-embedded

FGF – fibroblast growth factor

FITC – fluorescein isothiocyanate

FKBP2 - FK506-binding protein

FMO – fluorescence minus one

FR α - folate receptor α

GVHD - graft-versus-host disease

hCD34 – human CD34

HER2 – human epidermal growth factor receptor 2

HGF – hepatocyte growth factor

HIF1 α – hypoxia-inducible factor 1 α

HIF2 α – hypoxia inducible factor 2 α

HIV - human immunodeficiency virus

HLA - human leukocyte antigen

List of Abbreviations

HR – hormone receptor

HSV-TK - herpes simplex virus - thymidine kinase

HUVECs – human umbilical vein endothelial cells

ICAM-1 - intracellular adhesion molecule 1

ICANS - immune effector cell-associated neurotoxicity syndrome

ICOS - inducible T-cell costimulatory

IFF – immunofluorescence buffer

IFN- γ - interferon- γ

IHC – immunohistochemistry

IL- interleukin

IL-6R – IL-6 receptor

IP – intraperitoneal

ITAMs - immunoreceptor tyrosine-based activation motifs

IV - intravenous

KD – knock-down

KO – knock-out

LDH – lactate dehydrogenase

LLC – Lewis lung carcinoma

mAb – monoclonal antibody

List of Abbreviations

MHC - major histocompatibility complex

MM - multiple myeloma

MMPs – matrix metalloproteinases

MMRN2 – multimerin 2

MUC – mucin

NCI – National Cancer Institute

NG2 – chondroitin sulfate proteoglycan4/neural glial antigen 2

NHL - non-Hodgkin's lymphoma

NOX4 – NADPH oxidase 4

NSG - NOD-scid-gamma

PARP – poly (ADP-ribose) polymerase

PBMCs – peripheral blood mononuclear cells

PD-1 - programmed death protein 1

PDAC – pancreatic ductal adenocarcinoma

PDGF – platelet-derived growth factor

PDGFR – platelet-derived growth factor receptor

PD-L1 - programmed death-ligand 1

PDX - patient derived xenograft

PLGA – poly (lactic-co-glycolic acid)

List of Abbreviations

PNE - peptide neoepitope

PR – progesterone receptor

PSCA - prostate stem cell antigen

PSMA - prostate-specific membrane antigen

pSTAT3 – phosphorylated STAT3

PVDF – polyvinylidene difluoride

qPCR – quantitative polymerase chain reaction

RIPA – radioimmunoprecipitation assay

RPMI – Roswell park memorial institute

RTqPCR – real time qPCR

SAGE – serial analysis of gene expression

scFv – single chain variable fragment

SERDs – selective ER downregulators

SERMs – selective ERM modulators

SP1 – specificity protein 1

TALENs - transcription activator-like effector nucleases

TBS – tris-buffered saline

TCR - T-cell receptor

TEM1 – tumour endothelial cell marker 1

List of Abbreviations

TEM8 - tumour endothelial marker 8

TGF- β – transforming growth factor β

TLS - tumour lysis syndrome

TM - targeting molecule

TME – tumour microenvironment

TNBC - triple negative breast cancer

TNF - tumour necrosis factor

TRUCK - T-cells redirected for universal cytokine mediated killing

UniCAR - universal CAR T-cell

VEGF – vascular endothelial growth factor

VEGFR – vascular endothelial growth factor receptor

VHH - variable heavy chain

VSMCs – vascular smooth muscle cells

WHO – World Health Organisation

WT – wild-type

Chapter 1 Introduction

1.1 Breast Cancer

The definition of cancer is the uncontrolled division of abnormal cells in a given part of the body, triggered by genetic and epigenetic changes. However, the term cancer acts as an umbrella term for a wide range of diseases with different tissues of origin, treatment options and prognosis. In a seminal paper published in 2000, Hanahan and Weinberg defined the 6 common hallmarks of cancer: sustaining proliferative signalling, evading growth suppressors, activating invasion and metastasis, enabling replicative immortality, inducing angiogenesis and resisting cell death (Hanahan and Weinberg 2000). In 2011, the authors updated these hallmarks to include: avoiding immune destruction, tumour-promoting inflammation, genome instability and mutation and deregulating cellular energetics (Hanahan and Weinberg 2011) and in 2022 a further 4 hallmarks were added: unlocking phenotypic plasticity, nonmutational epigenetic reprogramming, polymorphic microbiomes and senescent cells (Hanahan 2022). Breast cancer occurs when breast tissue acquires some or all of the 10 defined hallmarks of cancer.

1.1.1 Breast cancer incidence

In the UK, breast cancer has the highest incidence of all cancers (excluding non-melanoma skin cancer) and accounts for 15% of all new cases, with 1 in 7 women and 1 in 870 men being diagnosed in their lifetime (CRUK 2022). Globally, over 2 million women were newly diagnosed with breast cancer in the year 2020 and in the same year there were over 7.8 million women surviving with breast cancer, making it the world's most prevalent cancer (WHO 2022). Although the incidence of breast cancer continues to increase in the UK and globally, survival rates are improving. The mortality rate of females with breast cancer has fallen by 21% over the last decade in the UK, with over

75% of women with breast cancer surviving their disease for 10 years or more (CRUK 2022). Despite the encouraging trend in survival rates, breast cancer still accounts for 15.5% of cancer related deaths in women worldwide (Sung *et al.* 2021).

1.1.2 Risk factors associated with breast cancer

Multiple factors that affect one's risk of developing breast cancer have been identified. Reproductive factors such as early menarche, late menopause, late pregnancy and low parity increase breast cancer risk. For each year that the menopause is delayed, the risk of developing breast cancer increases by 3% and for each year that menarche or pregnancy is delayed, the risk of developing breast cancer decreases by 5% and 10%, respectively (Sun *et al.* 2017). Several environmental factors are also associated with increased breast cancer risk including obesity, alcohol consumption and taking sources of exogenous oestrogen (such as the contraceptive pill and hormone replacement therapy).

Heritable factors that increase the risk of developing breast cancer include ethnicity and genetics. It has been reported that women of black and Asian decent have a slightly decreased risk of developing breast cancer when compared to women of white decent, however this is likely due to differences in other risk factors, for example non-white women were found to be less likely to drink alcohol, less likely to have been on hormone therapy and more likely to have given birth at a younger age (Chlebowski *et al.* 2005). Germline mutations in certain genes also increase the risk of developing breast cancer. For example, women with a *BRCA1* or *BRCA2* mutation have a cumulative breast cancer risk to age 80 of 72% and 69%, respectively (Kuchenbaecker *et al.* 2017). Similarly, moderately penetrant inherited mutations in *PALB2* and *FGFR2* are also associated with increased breast cancer incidence (Easton *et al.* 2007; Antoniou *et al.* 2014).

1.1.3 Breast cancer diagnosis, staging and subtypes

New cases of breast cancer are diagnosed either during routine screens or following symptomatic presentation by patients. Upon diagnosis, the breast cancer is defined as Stage 0-4 based on characteristics described in Table 1.1. Patients diagnosed with stage 0, 1 or 2 breast cancer generally have a good prognosis, however patients diagnosed with stage 3 or 4 breast cancer have a significantly poorer prognosis.

Table 1.1 Classification of breast cancer	
Stage	Classification (CRUK 2022)
Stage 0	Pre-invasive breast cancer/ ductal carcinoma in situ (DCIS)
Stage 1	A – Tumour \leq 2 cm with no extramammary spread B – Micrometastases in axillary lymph nodes and tumour \leq 2 cm.
Stage 2	A – Tumour \leq 2 cm with metastases in 1-3 axillary or internal mammary lymph nodes OR tumour size 2-5 cm, with no metastases to lymph nodes. B – Tumour size 2-5 cm with metastases in 1-3 axillary or internal mammary lymph nodes OR tumour size $>$ 5 cm with no metastases to lymph nodes.
Stage 3	A – No tumour in breast but metastases found in 4-9 axillary or internal mammary lymph nodes OR tumour $>$ 5 cm with metastases in 1-3 axillary or internal mammary lymph nodes. B – Tumour of any size involving skin or chest wall. Metastases in up to 9 axillary or internal mammary lymph nodes. C – Tumour of any size involving skin or chest wall with metastases in 10 or more axillary, internal mammary or supraclavicular lymph nodes.
Stage 4	Tumour of any size with or without lymph node involvement that has metastasised to distant sites (e.g., liver, lung, brain, bone).

Breast cancer can be divided into subtypes based on expression of certain receptors and gene expression profile. The receptors involved in breast cancer subtyping are the oestrogen receptor (ER), the progesterone receptor (PR) (together referred to as hormone receptors (HR)) and the signalling receptor ErbB2 (HER2). The receptor-based subtypes of breast cancer are summarised in Table 1.2. Classification based on gene expression profiling is referred to as the molecular or intrinsic subtype. Global gene expression profiling by Perou and colleagues divided breast tumours into five subtypes: luminal A, luminal B, basal-like, HER2-enriched and normal breast-like (Perou *et al.* 2000). Luminal A tumours are predominantly ER-positive and tend to be of low grade and proliferation rate. Luminal B tumours are also generally ER-positive, but may express lower levels of hormone receptors, be more proliferative, have a worse prognosis and be of a higher grade than luminal A tumours. The HER2-enriched subtype usually reflects amplification of the *ERBB2* gene in tumours that can be HR-negative or HR-positive. The basal subtype mostly overlaps with triple negative HR-negative, HER2-negative breast cancers (Figure 1.1).

Table 1.2 The receptor-based subtypes of breast cancer		
Receptor Status	Incidence*	5-year relative survival*
HR ⁺ HER2 ⁻	68%	94.3%
HR ⁺ HER2 ⁺	10%	90.5%
HR ⁻ HER2 ⁻	10%	76.9%
HR ⁻ HER2 ⁺	4%	84%
-	7%	76.1%
*statistics from (NCI 2022)		

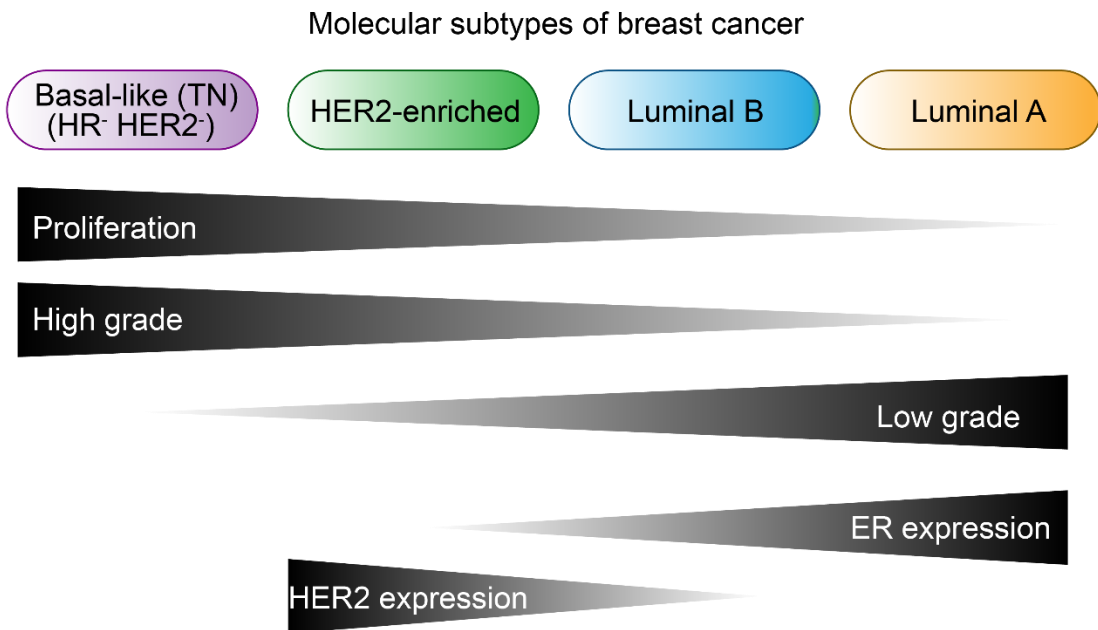


Figure 1. 1 The molecular subtypes of breast cancer

Breast cancers can be divided into subtypes based on their gene expression profiles, described as molecular or intrinsic subtypes. Basal-like (triple negative) breast cancers are negative for oestrogen and progesterone hormone receptors (HR⁻) and the HER2 receptor and are the most proliferative and of the highest grade. HER2-enriched tumours have increased HER2 expression and a high proliferation rate. Luminal A and B breast cancers are both generally oestrogen receptor (ER)-positive, however luminal B tumours may express lower levels of hormone receptors and tend to be more proliferative and of a higher grade than luminal A tumours. Adapted from (Harbeck *et al.* 2019).

1.1.4 Breast cancer metastasis

The metastatic progression of a tumour can be broken down into 5 key steps: (1) local invasion into the breast stroma, (2) intravasation into the vasculature, (3) survival in the circulation, (4) extravasation from the vasculature at the distal tissue, and (5) colonisation and proliferation to form a tumour at the secondary site. Collectively these steps are often referred to as the metastatic cascade (Figure 1.2).

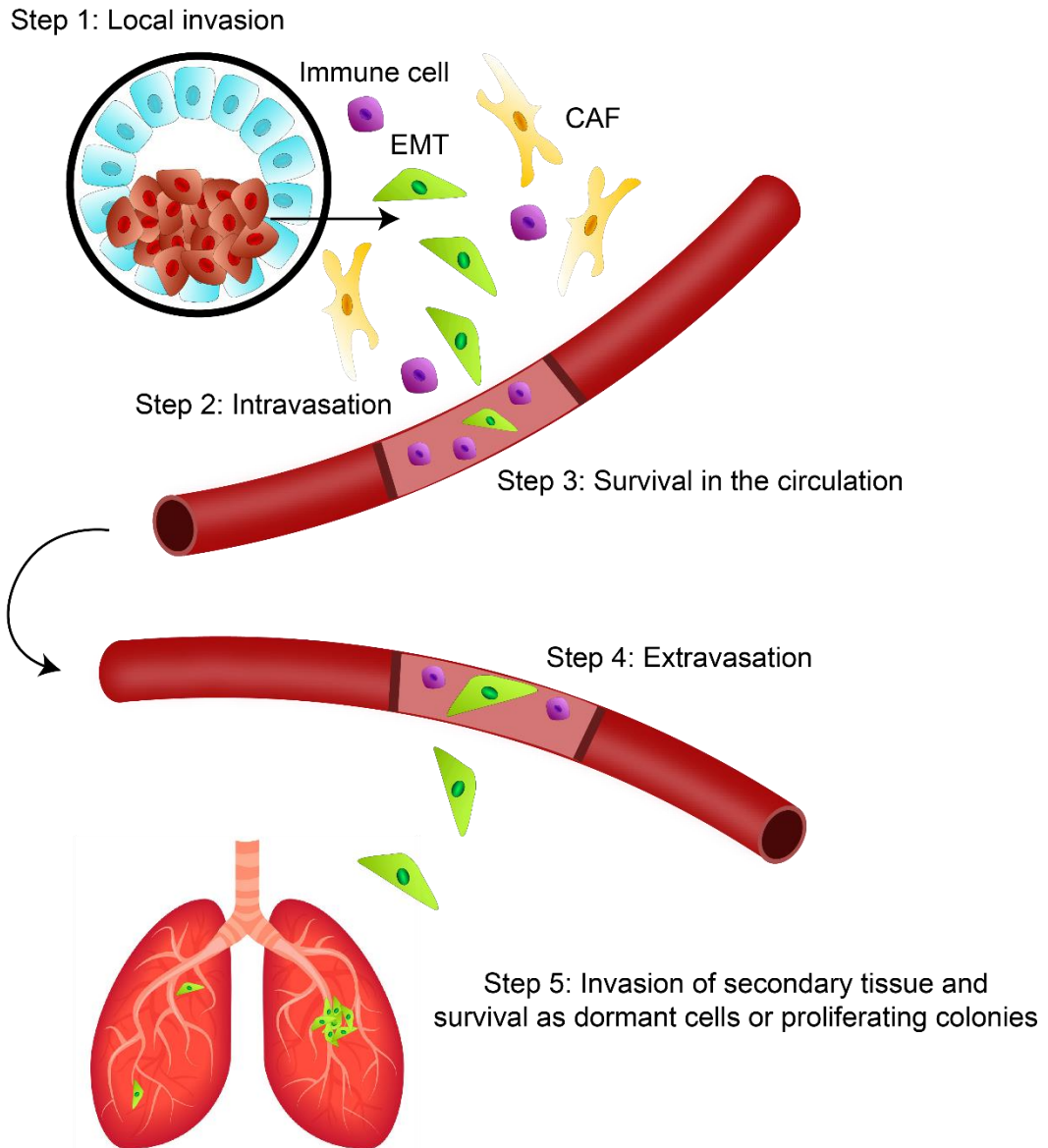


Figure 1. 2 The metastatic cascade

Diagram showing the 5 main steps of the metastatic cascade. **(1)** a single or cluster of tumour cells acquire epithelial-to-mesenchymal transition (EMT) features resulting in a more migratory and invasive phenotype. Tumour cells have to degrade and remodel the basement membrane and extracellular matrix allowing invasion into the local stromal tissue. **(2)** Tumour cells degrade the vascular basement membrane and disrupt tight endothelial cell-cell junctions to intravasate into the vasculature. **(3)** Once in the circulation, tumour cells must survive against extreme shearing forces and increased immune surveillance. Only small numbers of intravasated tumour cells will survive in the circulation. **(4)** At the secondary site, tumour cells adhere to the vascular wall and extravasate out of the blood vessels into the tissue parenchyma. **(5)** In the new microenvironmental niche, tumour cells can either die, become dormant or begin proliferating. Proliferating colonies result in micrometastases which will grow into clinically detectable macrometastases.

To invade through local tissue, tumour cells must secrete enzymes capable of degrading and remodelling the extracellular matrix (ECM), lose their anchorage dependence and increase their motility. The process during which tumour cells acquire these characteristics is commonly referred to as the epithelial-to-mesenchymal transition (EMT) (Thiery *et al.* 2009). Tumour cells may invade through local tissue alone or in clusters, in the latter case only the cells at the invading front undergo EMT and the following cells retain an epithelial state (Cheung *et al.* 2013). Disseminated tumour cells must then break down the basement membrane surrounding blood vessels and pass through the endothelial cell layer. In tumours, the vasculature is often poorly formed with loose endothelial cell junctions, which makes the passage of tumour cells into the circulation less challenging. Once inside the circulation, tumour cells face the challenge of surviving: they are exposed to the hydrodynamic shearing forces of the blood flow that can damage the tumour cell membrane; they are unanchored which can initiate anoikis, a type of programmed cell death triggered when anchorage-dependent cells are detached from the ECM; and they are in close proximity to circulating immune cells.

Upon arriving in the vasculature of the secondary tissue, tumour cells must exit the circulation by extravasation which presents the challenges of becoming static and breaking down the endothelial cell junctions and basement membrane at the secondary site. Finally, tumour cells must adapt to survive and proliferate in an unfamiliar microenvironmental niche. If tumour cells succeed in surviving at the secondary site, they will either continue to proliferate and form clinically detectable metastatic lesion or survive in a dormant state where they do not proliferate but remain viable. These dormant cells may become 'awakened', sometimes after long periods of time, resulting in relapse of the cancer, often many years after initial diagnosis (Dittmer 2017). The tumour microenvironment (TME) plays a significant role in multiple stages of the metastatic cascade and this will be further discussed in Section 1.3.

In 1889, Stephen Paget hypothesised that different types of cancer have preferences for different secondary sites and environments within the body, referred to as the “seed and soil hypothesis”. The most common sites of breast cancer metastasis are the bones, lungs, brain and liver (Minn *et al.* 2005). The bones are the most frequent site of metastasis in ER⁺ breast cancers, whereas for triple negative breast cancers metastasis to the lung is most common (Kennecke *et al.* 2010). Unfortunately, the prognosis for women with metastatic breast cancer is poor, with only 25% of patients surviving for 5 years or more after they are diagnosed (CRUK 2022). To date, metastatic breast cancer is not curable therefore treatments targeting or preventing breast cancer metastasis are a current clinical need.

1.1.5 Breast cancer treatment

The treatment a patient receives for their breast cancer depends on the stage with which they are diagnosed. Stage 0 breast cancer (DCIS) is primarily treated with lumpectomy plus radiation therapy or mastectomy. Early invasive (Stage 1a,b and 2a,b) and locally advanced (Stage 3a,b,c) breast cancers are non-metastatic and treatment for these breast cancers can be divided into three phases: pre-operative, surgical and post-operative. When the breast cancer is receptor-positive (ER, PR or HER2), pre-operative (neoadjuvant) endocrine therapy or anti-HER2 targeting therapy can be given. In the case of triple negative breast cancer neoadjuvant chemotherapy can be given. In the surgical phase, patients are either subjected to lumpectomy or mastectomy. Following surgery patients may be treated with radiotherapy followed by post-operative (adjuvant) chemotherapy, targeted therapy, endocrine therapy, immunotherapy, or a combination of these approaches. Stage 4 metastatic breast cancer is not usually surgically resected, as this does not increase the probability of survival in these patients. Instead, the aim in treating stage 4 patients is to control the tumour growth for as long

as possible and to treat the symptoms of the disease. This can include a combination of therapies listed above for earlier stage breast cancers (Trayes and Cokenakes 2021).

The aim of breast cancer surgery is to excise the tumour tissue along with a defined margin of normal breast tissue, whether this be a wide local excision, known as “lumpectomy” or by performing a mastectomy and removing the whole breast. Pre-operative neoadjuvant therapy may be given to the patient with the aim of reducing the size of the tumour prior to surgery to allow breast-conserving surgery rather than a more radical procedure. Neoadjuvant therapy can also allow for an early assessment of how well a patient's tumour responds to a given therapy which can guide future treatment decisions (Selli and Sims 2019).

Following surgery, patients with early invasive or locally advanced breast cancer are given post-operative (adjuvant) therapy to decrease the risk of recurrence. These therapies are given as a first line treatment to patients with advanced metastatic breast cancer.

Radiotherapy and chemotherapy both take advantage of the fact that tumour cells are more vulnerable to DNA damage and cell cycle interruption than non-malignant cells. Radiotherapy utilises the ionising waves of x-ray radiation to cause DNA breaks within cells in a given area of tissue and chemotherapy describes the systemic delivery of agents that target tumour cells such as anthracyclines that cause double stranded DNA breaks or taxanes that disrupt microtubule formation.

Targeted therapies exploit cellular targets which are upregulated by cancer cells and which the malignant cells depend on for survival. Examples include trastuzumab (Herceptin) which targets HER2 and prevents downstream signalling that promotes cell proliferation, palbociclib inhibits CDK4/6 causing cell cycle arrest and olaparib which inhibits poly(ADP-ribose) polymerase (PARP) and causes synthetic lethality in cells with *BRCA1* and *BRCA2* mutations.

Endocrine therapy focuses on perturbing oestrogen signalling which in turn prevents the proliferation of ER-positive tumour cells dependent on these pathways for survival. There are 3 categories of endocrine therapy: selective ER modulators (SERMs), such as tamoxifen, which bind to ER and competitively inhibit oestrogen binding, selective ER downregulators (SERDs), such as fulvestrant, which promote degradation of ER and aromatase inhibitors (AIs), such as letrozole, which prevent oestrogen production.

Immunotherapy is an emerging branch of cancer therapy and is not currently widely licenced for the treatment of breast cancer. However, patients with high-risk early stage or advanced triple negative breast cancer (TNBC) may be offered the immunotherapy agent pembrolizumab, a PD-1 inhibitor, in combination with chemotherapy if their cancer is PD-1-positive (Cortes *et al.* 2020; Schmid *et al.* 2022).

1.2 The Tumour Microenvironment

1.2.1 Introduction

The TME describes the environment associated with tumour cells which contains a variety of different cell types. These include fibroblasts, pericytes, vascular and lymphatic endothelial cells and immune cells (Figure 1.3). Cross-talk occurs between stromal cell types, as well as between stromal and tumour cells to promote tumour progression (Balkwill *et al.* 2012). In addition to the cellular compartments, the TME also consists of an aberrant ECM, which contributes to the tumour structure and stiffness.

The TME facilitates the growth and survival of malignant cells by creating an immunosuppressive niche, the production of growth factors, supporting angiogenesis and facilitating dissemination. The mechanisms by which the TME supports cancer progression and dissemination are numerous. This thesis will focus on the contribution

of tumour-associated pericytes and cancer-associated fibroblasts (CAFs), with a particular focus on their role in metastatic progression.

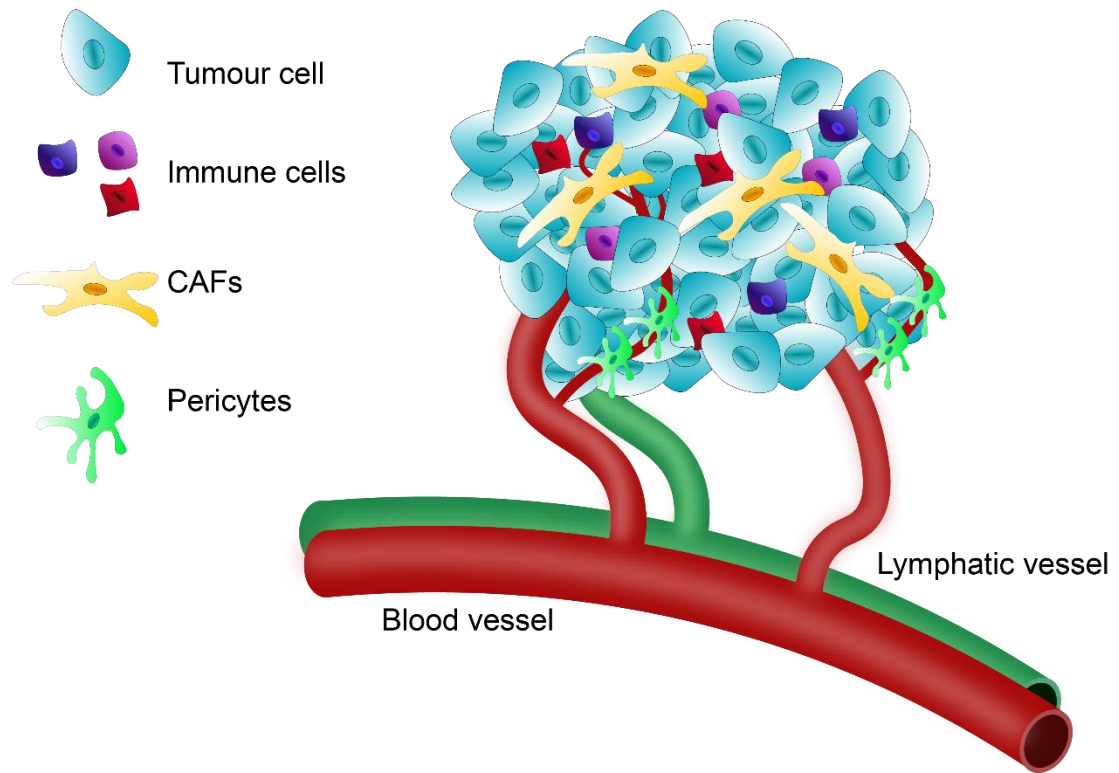


Figure 1. 3 The tumour microenvironment

Solid tumours consist of a mass of tumour cells together with extracellular matrix, vascular and lymphatic endothelial cells, mesenchymal cells (CAFs and pericytes) and immune cells. Cross-talk between tumour cells and cells of the tumour microenvironment can be both of a pro-and anti-tumour nature, as can interactions between different cell types within the microenvironment. Adapted from (Junttila and de Sauvage 2013).

1.2.2 Tumour vasculature

The vascular system is a critical network which permits the passage of oxygen, nutrients and immune cells between tissues. Normal vascular structures consist of a lumen formed by tightly joined endothelial cells and mural cells that support the vascular structure. Endothelial and mural cells are surrounded by a vascular basement

membrane, to which both cell types contribute. Under normal physiological conditions, the vascular network is hierarchically organised and remodelled in a controlled manner to allow adequate perfusion of oxygen and other nutrients to all cells.

Angiogenesis describes the process of new vessel formation from pre-existing vascular structures. In the human adult, angiogenesis only occurs under certain conditions of tissue remodelling, such as wound healing or pregnancy. Hypoxia within tissues is a key driver of angiogenesis, which results in the activation of pro-angiogenic pathways, such as the vascular endothelial growth factor (VEGF)-A pathway. Interaction of VEGF-A with vascular endothelial growth factor receptor (VEGFR)-2 on the endothelial cell surface results in an activated form of the endothelial cell, known as a tip cell, which is motile, invasive and protrudes filopodia. Tip cells produce factors to breakdown the basement membrane and spearhead new vascular sprouts towards the source of VEGF-A secretion. Following tip cells, stalk endothelial cells establish a lumen and proliferate to support sprout elongation. A basement membrane is then established and mural cells, such as pericytes, are recruited to stabilise the new vascular structure (Potente *et al.* 2011).

The angiogenic process is tightly regulated by a balance of pro-and anti-angiogenic factors in non-tumour tissues, however in tumour tissue this becomes dysregulated. A developing tumour can only grow to ~2 mm in size without vascular support, thus rapid establishment of a vascular network is essential for tumour survival and progression (Hanahan and Folkman 1996). One of the well-established hallmarks of cancer is the 'angiogenic switch', a process which occurs early in tumour development. The angiogenic switch describes an event in which the balance between pro-and anti-angiogenic factors shifts towards a pro-angiogenic outcome, resulting in rapid vascularisation of the tumour tissue (Hanahan and Folkman 1996) (Figure 1.4A). The angiogenic switch may be triggered by a number of factors, including local hypoxia, expression of pro-angiogenic factors and tumour-associated inflammation (Lugano *et al.*

2020). Excessive and sustained pro-angiogenic signalling results in inefficient tumour vascularisation, with a poorly structured and disorganised vascular network.

Unlike non-malignant cells, VEGF-A secretion by tumour cells is not only driven by ischaemia, but also by oncogenes and the loss of tumour suppressor genes, among other factors. Tumour cells therefore secrete a higher concentration of VEGF-A when compared to non-malignant cells. Intramuscular injection of high and low VEGF-A secreting myoblasts demonstrated that a higher local VEGF-A concentration is more likely to induce abnormal vascular structures (Ozawa *et al.* 2004). Therefore, the high concentration of VEGF-A secreted by tumour cells likely plays a key role in the development of abnormal tumour vessels.

Blood vessels within the tumour tissue are immature, tortuous and hyperpermeable, with different subtypes of microvessels being indistinguishable. Vessels are inconsistent in diameter and shape and are not optimally structured, with endothelial cell junctions being poorly formed (Hashizume *et al.* 2000). When compared to normal blood vessels, tumour-associated vessels have reduced pericyte coverage and the pericytes are associated with endothelial cells less efficiently (Morikawa *et al.* 2002). These properties render tumour-associated blood vessels leaky and poorly perfused, which results in excessive plasma leakage. The increased interstitial fluid pressure created by vessel hyperpermeability results in an accumulation of waste products in the tumour tissue, increased acidity and regions of hypoxia (Vaupel *et al.* 1987). This in turn further promotes tumour angiogenesis resulting in an entirely dysregulated process. Further, poor pericyte coverage and loose endothelial junctions gives rise to vessels that are more easily infiltrated by tumour cells, thus facilitating metastatic intravasation.

The dependency of tumours on the angiogenic process for survival led to the development of multiple anti-angiogenic agents for clinical use, such as the anti-VEGFA

and anti-VEGFR-2 monoclonal antibodies bevacizumab and ramucirumab, respectively. Although significant improvements in overall survival rates have been observed when such agents are combined with classical chemotherapy in cancers such as colorectal carcinoma (Hurwitz *et al.* 2004; Tabernero *et al.* 2015), in breast cancer limited success has been observed thus far (Brufsky *et al.* 2011; Gianni *et al.* 2013; Vrdoljak *et al.* 2016).

Resistance to anti-angiogenic therapy is frequently observed and is one of the main reasons for its limited success. By inhibiting angiogenesis, regions of hypoxia form within the tumour, which in turn results in the upregulation of hypoxia-inducible factor 1 α (HIF1 α) in tumour cells. An increase in HIF1 α expression leads to more pro-angiogenic factors being secreted by the tumour cells, which in turn promote angiogenesis and resistance to the anti-angiogenic therapy (Alessi *et al.* 2009; Hartwich *et al.* 2013). Further, hypoxia in the tumour and increased HIF1 α expression in the tumour cells can promote metastatic spread (Jing *et al.* 2012; Ebright *et al.* 2020). In human breast cancer, a high level of HIF1 α at diagnosis can predict early relapse and metastasis and correlated with poor clinical outcomes (Bos *et al.* 2003; Gruber *et al.* 2004; Generali *et al.* 2006).

As well as via angiogenesis, tumours can hijack blood vessels in the surrounding normal tissue for vascular support, a process known as vessel co-option (Kuczynski *et al.* 2019) (Figure 1.4B). An example of vessel co-option in lung cancer was described by Pezzella and colleagues in which tumour cells invaded the alveolar spaces in a distinct pattern and co-opted the alveolar capillaries (Pezzella *et al.* 1997). Further examples of vessel co-option can also be observed in primary liver, brain and skin cancers (Nakashima *et al.* 1995; Döme *et al.* 2002; Bernsen *et al.* 2005) as well as in various metastases (Colpaert *et al.* 2003; Stessels *et al.* 2004; Bentolila *et al.* 2016).

In some instances, tumours may also develop vascular structures from malignant cells in a process known as vascular mimicry (Figure 1.4C). Blood vessels created by vascular

mimicry lack endothelial cells and are instead lined with tumour cells with cancer stem cell features driving an epithelial-to-endothelial transition (Andonegui-Elguera *et al.* 2020). This phenomena was first described in melanoma (Maniotis *et al.* 1999) and has since been identified in many other tumour types, including breast cancer where it has been associated with a more aggressive phenotype (Shirakawa *et al.* 2001).

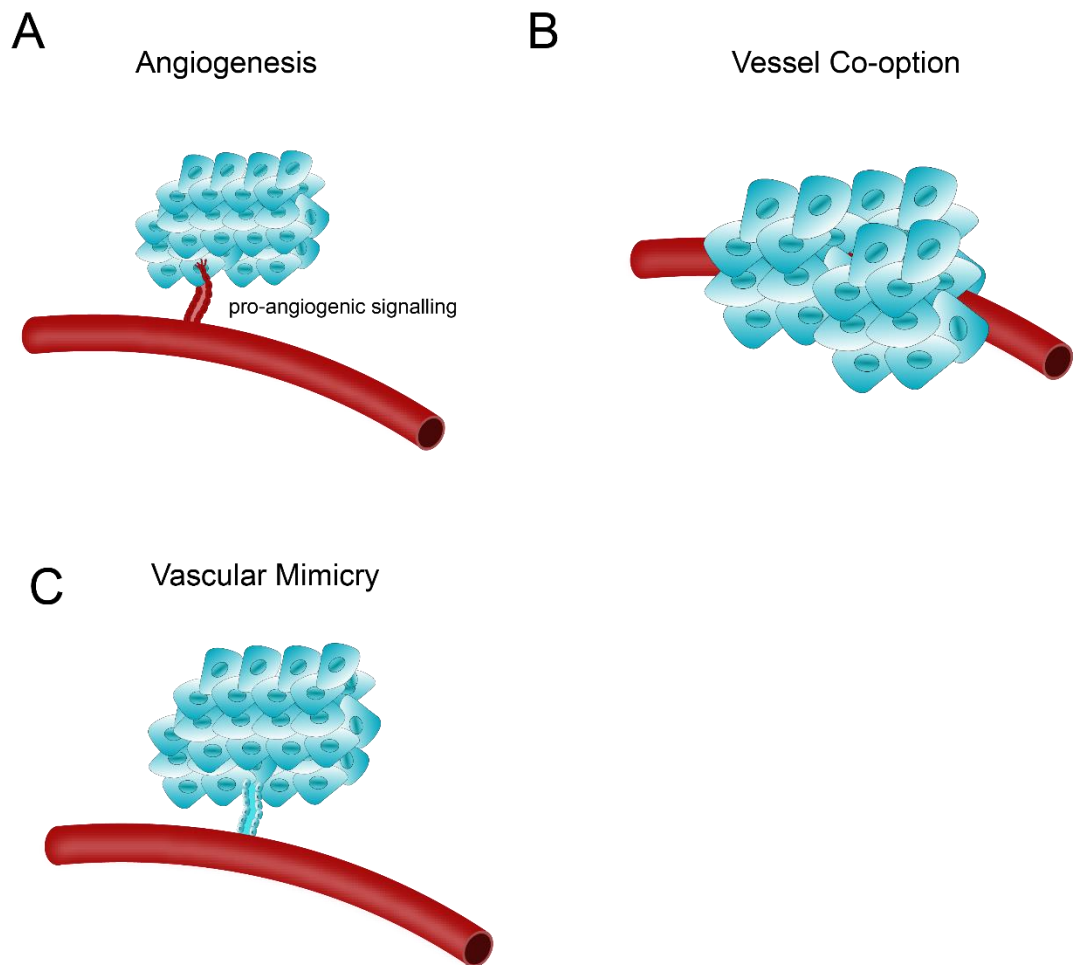


Figure 1. 4 Mechanisms of tumour vascularisation

Tumours require a vascular network to survive and can develop this by **(A)** stimulating the generation of new vessels via angiogenesis **(B)** co-option of blood vessels from the normal surrounding tissue and **(C)** vascular mimicry in which tumour cells undergo an epithelial-to-endothelial transition and vessels lined with transformed tumour cells are created.

1.2.3 Pericytes

1.2.3.1 Pericyte classification

Pericytes were first identified in 1879 by Rouget as contractile cells surrounding small blood vessels and thus were first named ‘Rouget cells’ until Zimmermann renamed them pericytes in 1923, with “peri” and “cyte” meaning around and cell, respectively (Zimmermann 1923). Pericytes are now accepted to be a mural cell subclass that surround microvessels and are embedded within the vascular basement membrane, providing structural support to these vessels (Sims 1986) (Figure 1.5). Large-diameter blood vessels, such as arteries and veins, are covered by vascular smooth muscle cells (VSMCs), the other subclass of mural cells. Although it is believed that VSMCs and pericytes belong to the same lineage, they can be distinguished by their location, morphology and marker expression. However, this distinction is not absolute and a range of phenotypes exist from the classical VSMC to a typical pericyte (Armulik *et al.* 2005).

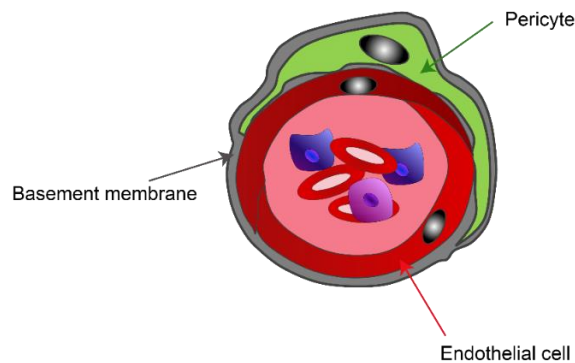


Figure 1. 5 Pericytes and the vasculature

Pericytes are a subclass of mural cell that embed within the vascular basement membrane and surround the endothelial cell structure, providing structural support to the vasculature.

Electron microscopy studies have morphologically defined pericytes as cells with prominent nuclei and several long processes that extend along the endothelial wall (Sims 1986). However, despite the extensive study of pericyte characteristics, pericytes

still remain a poorly defined cell type. To date, no marker with absolute pericyte specificity has been identified. Several markers have been used to identify pericytes such as α -smooth muscle actin (α -SMA), chondroitin sulfate proteoglycan4/neural glial antigen 2 (NG2), platelet-derived growth factor receptor (PDGFR)- β , desmin and vimentin, however none of these markers represent a pericyte-specific marker as they are also expressed by VSMCs and perivascular fibroblasts (Yamazaki and Mukoyama 2018). Therefore, identification of pericytes to date relies on a combination of one or more of these surface markers with morphological characteristics and spatial location.

1.2.3.2 Pericyte function

The functional roles of pericytes under normal physiological conditions have been studied extensively and several important functions have been identified. First, pericytes play an important role in the regulation of angiogenesis and vessel maturation. As pericytes can be found in close proximity to vascular endothelial cells, the two cell types are able to interact via a range of signalling axes. For example, sprouting endothelial cells secrete platelet derived growth factor (PDGF)-B, the ligand for PDGFR- β expressed by pericytes. The binding of PDGF-B to PDGFR- β results in the recruitment and adhesion of pericytes to the developing endothelial cell layer, which in turn promotes vascular stabilisation (Betsholtz 2004). When this pathway is defective, decreased pericyte coverage can be observed alongside aberrant vasculature and microaneurysms (Lindahl *et al.* 1997). Moreover, genetic deletion of *Pdgfb* or *Pdgfrb* in mice results in perinatal death which can be attributed to vascular dysfunction (Levéen *et al.* 1994; Soriano 1994). As well as the PDGF-B/PDGFR- β axis, pericyte-endothelial cell interactions via the angiopoietin2/Tie2, transforming growth factor beta (TGF- β) and VEGF signalling axes are also important for angiogenic homeostasis and correct vessel maturation (Gaengel *et al.* 2009). Together, these observations suggest a crucial role for pericytes in regulating the angiogenic process and maintaining a stable vasculature.

The contractile nature of pericytes gives them a role in regulating the blood flow through microvessels (Caporarello *et al.* 2019). Pericytes express both cholinergic (α -2) and adrenergic (β -2) receptors, the stimulation of which lead to pericyte contraction and relaxation, respectively (Rucker *et al.* 2000). Owing to this, capillary pericytes mediate blood flow in response to local metabolic needs, for example it has been reported that pericyte relaxation occurs in response to a local increase in carbon dioxide concentration (Matsugi *et al.* 1997). Moreover, in the brain, the dilation of capillaries by pericyte relaxation occurs faster than that of arteriole dilation (Mapelli *et al.* 2017) suggesting that pericyte relaxation is important in the immediate response to local hypoxia.

In addition to their physical properties, pericytes have been identified as a population of mesenchymal stem cells that are able to differentiate into other cell types, giving them roles that extend beyond vascular maintenance. For example, in the presence of chondrogenic or adipogenic medium, pericytes can differentiate into chondrocytes and adipocytes, which have the potential to form mineralised cartilage and adipocytic regions *in vivo* (Farrington-Rock *et al.* 2004). This suggests pericytes may also contribute to processes such as wound healing, growth and repair.

1.2.3.3 Pericytes & cancer

In pathological conditions such as cancer, pericytes have several roles in promoting disease progression (Figure 1.6). As outlined in Section 1.3.1, pericytes represent one of the many cell types found within the TME where they contribute towards tumour vascularisation, immunomodulation and metastasis (Ribeiro and Okamoto 2015). In tumours, pericytes support angiogenesis by interacting with endothelial cells to create stable vascular structures which support tumour growth. It has been shown that blockage

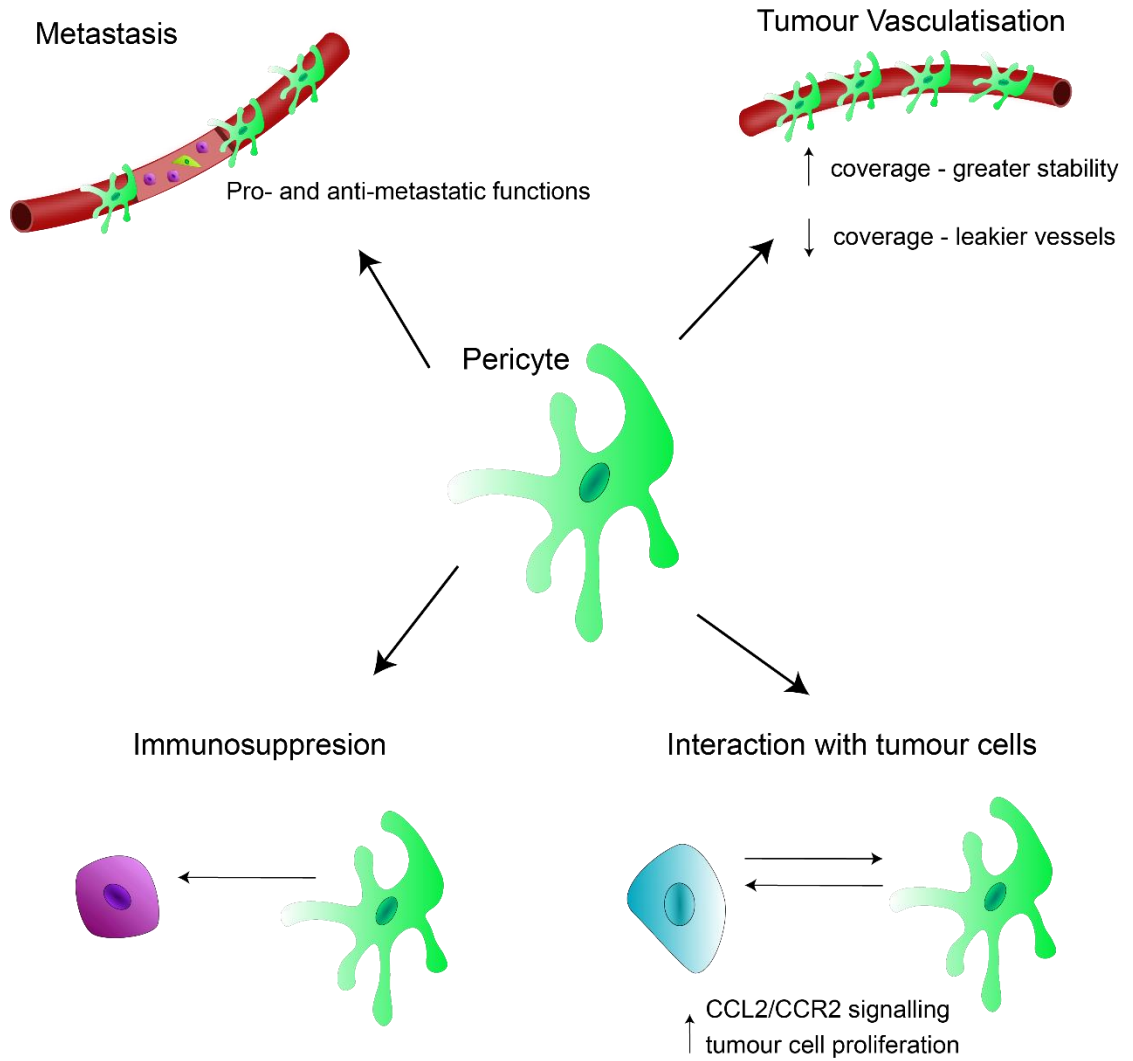


Figure 1. 6 Pericyte roles in cancer progression

Tumour-associated pericytes have multiple roles in cancer progression. Coverage and support of the tumour vasculature results in a more stable tumour vasculature, whereas decreased pericyte coverage gives rise to leakier vessel that facilitate easier intravasation of metastatic tumour cells. Pericytes can interact with tumour cells via the CCL2/CCR2 signalling axis to promote tumour cell proliferation and can interact with immune cells to promote an immunosuppressive phenotype, though the mechanisms behind the latter interaction are currently not well understood.

of pericyte recruitment by inhibiting the PDGF- β pathway leads to endothelial cell loss and regression of tumour vessels (Lindahl *et al.* 1997), whereas overexpression of PDGF- β results in increased pericyte coverage and supports tumour growth (Guo *et al.* 2003; Furuhashi *et al.* 2004). Owing to this, increased pericyte coverage correlates with poorer disease prognosis in renal carcinoma and bladder cancer (Yonenaga *et al.* 2005; O'Keeffe *et al.* 2008; Cao *et al.* 2013). However, conversely, it has been reported that decreased pericyte coverage in colorectal cancer results in increased metastasis and worse overall survival (Yonenaga *et al.* 2005). This may be due to increased leakiness of tumour vasculature, which in turn allows for increased tumour cell intravasation and metastasis. Therefore, it is likely that cancer subtypes are affected in different ways by the number of pericytes associated with their vasculature. This should be considered when targeting pericytes therapeutically in patients.

Alongside communicating with endothelial cells to facilitate tumour angiogenesis or vessel co-option, pericytes can also interact with other cell types within the tumour. It has been demonstrated that loss of β 3-integrin expression on tumour-associated pericytes promotes pericyte-tumour cell crosstalk via the CCL2/CCR2 axis, which results in enhanced tumour cell proliferation and tumour growth (Wong *et al.* 2020). Further, Ochs and colleagues have demonstrated that pericytes derived from gliomas have immunosuppressive properties when co-cultured with peripheral blood mononuclear cells (PBMCs) and that pericyte abundance in malignant glioma negatively correlates with the abundance of perivascular cytotoxic T-cells, suggesting an interaction between pericyte and immune populations in the TME (Ochs *et al.* 2013).

In addition to supporting primary tumour growth, pericytes may play an important role in the metastatic cascade. However, it remains unclear whether pericytes promote or suppress metastasis. Our laboratory has previously demonstrated that the expression of endosialin by tumour-associated pericytes facilitates tumour cell intravasation and promotes metastatic spread in breast cancer (Viski *et al.* 2016). Similarly, Sinha and

colleagues have demonstrated that co-injection of ovarian cancer cells with pericytes in a xenograft model results in accelerated tumour growth and aggressive metastases (Sinha *et al.* 2016). In contrast, Xian and colleagues have shown that defective pericyte-endothelial cell interactions lead to an enhanced metastatic potential in fibrosarcoma (Xian *et al.* 2006). It has also been demonstrated that pericyte ablation in tumours results in unstable and leaky tumour vasculature which in turn favour metastasis (Cooke *et al.* 2012). It is well known that microvessels without sufficient pericyte coverage are leakier, therefore it makes sense that poor pericyte coverage within a tumour would give rise to greater opportunity for tumour cell intravasation. However, on the other hand, microvessels with reduced pericyte coverage may be less functional and more collapsed than well covered vessels, which in turn may impede tumour cell dissemination. The mechanisms by which adhered tumour-associated pericytes facilitate tumour progression are less clear. Recent studies have made progress on understanding this by examining pericyte interactions with tumour-associated macrophages via the interleukin (IL)-33-ST2 pathway, as well as the differentiation of pericytes into stromal fibroblasts, both of which were found to aid tumour progression (Hosaka *et al.* 2016; Yang *et al.* 2016).

Taken together, these reported findings suggest that the presence of pericytes and their coverage of microvessels varies between different tumour types. It is therefore important to better understand the role of pericytes in the context of different cancer and translate this knowledge into pericyte-targeting therapies.

1.2.4 Cancer-associated fibroblasts

1.2.4.1 Normal fibroblasts

Fibroblasts are mesenchymal cells that comprise the main cell type of connective tissue and can be characterised by their spindle-like morphology, alongside an absence of epithelial, vascular or leukocyte markers. In normal tissue, fibroblasts are usually

found within the interstitial space where they exist in a quiescent state. The primary function of tissue resident fibroblasts is the deposition of ECM components. The ECM generates the biochemical and mechanical properties of each organ, including the tensile strength and elasticity of the tissue. Further, the ECM is able to alter the behaviour of cells that interact with it via numerous signalling axes (Frantz *et al.* 2010).

Under conditions of tissue remodelling, which includes remodelling of the ECM, fibroblasts become activated by mechanical stress and inflammatory mediators resulting in them differentiating to a myofibroblast phenotype. Myofibroblasts were first observed in the setting of wound healing (Gabbiani *et al.* 1971) and have been described as fibroblasts with smooth muscle cell-like features (Powell *et al.* 1999). At the electron microscope level, myofibroblasts are distinguishable from normal fibroblasts by their high levels of exocytotic vesicles and their stress fibres. In keeping with these morphological features, myofibroblasts secrete an array of growth factors and cytokines and can be distinguished from normal fibroblasts by their upregulation of the α -SMA protein (Baum and Duffy 2011). The principal role of myofibroblasts in wound healing is contraction of the wound, which they are able to do due to the presence of α -SMA fibres. Myofibroblasts also secrete an array of growth factors and cytokines which maintain the inflammatory response. Once the wound healing process is complete, myofibroblasts become apoptotic and disappear (Chitturi *et al.* 2015)

1.2.4.2 *Function of cancer-associated fibroblasts (CAFs)*

Much like in the aforementioned conditions of tissue remodelling, CAFs exhibit a myofibroblast-like phenotype. The key difference with CAFs however is that, unlike myofibroblasts involved in wound healing, they do not die by apoptosis but remain chronically active and proliferative. CAFs are the most effective cells within the tumour stroma at depositing and remodelling the tumour ECM, which is dysregulated and disorganised compared to normal tissues. The increased activity of matrix

metalloproteinases (MMPs) results in enhanced ECM degradation, which facilitates the migration of vessels into the tumour, as well as assisting with tumour cell dissemination. CAFs also produce matrix cross-linking enzymes, for example collagen cross-linking lysyl oxidases, which contribute to the increased stiffness of the tumour tissue. An increase in collagen deposition in the tumour TME facilitates the growth and survival of malignant cells by increasing the rigidity of the TME, as well as enhancing growth factor sequestration (Sahai *et al.* 2020).

CAFs are able to crosstalk with tumour cells via the secretion of growth factors and cytokines, for example TGF- β secretion by CAFs promotes a pro-migratory phenotype in the tumour cells (Shimao *et al.* 1999; Fuyuhiko *et al.* 2012). Alongside TGF- β , CAFs secrete a plethora of other factors that are known to affect tumour cell migration and invasion, including hepatocyte growth factor (HGF), fibroblast growth factor (FGF) and IL-6 (Erdogan and Webb 2017).

As well as crosstalk with tumour cells to promote cancer progression, CAFs can communicate with immune cells within the tumour stroma. It has been shown that CAFs act in an immunosuppressive manner to both induce differentiation of naïve T-cells to T regulatory cells (Kinoshita *et al.* 2013) and kill cytotoxic CD8⁺ T-cells via PD-L2 and Fas ligand engagement (Lakins *et al.* 2018). Further, normalisation of CAFs via NADPH oxidase 4 (NOX4) inhibition promotes the infiltration of CD8⁺ T-cells into the tumour, suggesting a role for CAFs in the exclusion of cytotoxic CD8⁺ lymphocytes from the tumour environment (Ford *et al.* 2020).

1.2.4.3 *Cancer-associated fibroblast subtypes*

Within solid tumours, CAFs are an abundant and heterogeneous populations. Single-cell RNA sequencing of mouse mammary carcinoma CAFs has revealed three distinct subpopulations of CAFs in breast cancer: vascular CAFs, matrix CAFs and developmental CAFs plus a group of actively proliferating vascular CAFs termed cycling

CAFs (Bartoschek *et al.* 2018). Vascular CAFs were found to significantly differentially express genes associated with angiogenesis and vascular regulation, whereas for matrix CAFs and developmental CAFs ECM-related genes and stem cell markers were found to be significantly differentially expressed, respectively. Further, based on their expression profiles, it was proposed that these distinct CAF subpopulations were derived from different sources including perivascular cells, tissue resident fibroblasts and malignant cells for the vascular, matrix and development CAFs, respectively (Bartoschek *et al.* 2018).

Similar single cell sequencing approaches have been performed on human breast cancers, where distinct subpopulations of CAFs were also identified. In the human setting, the subgroups identified were myofibroblastic CAFs, inflammatory CAFs and antigen-presenting CAFs. Myofibroblastic CAFs are characterised by activated fibroblast markers such as α -SMA, fibroblast activation protein (FAP) and podoplanin, inflammatory CAFs are characterised by the enrichment of CXCL12 chemokine expression and antigen-presenting CAFs are characterised by the specific expression of CD74 (Kieffer *et al.* 2020; Wu *et al.* 2021). In these studies, vascular CAFs were not identified and perivascular cells were considered an unrelated cell population.

In Section 1.3.4.2, a number of CAF functions were discussed. The identification of multiple CAF subtypes suggests that these different functions may be undertaken by distinct CAF subpopulations. For example, it is likely that inflammatory CAFs are responsible for the immunomodulatory effects of CAFs and matrix CAFs may be predominantly responsible for the CAF-mediated remodelling of the ECM in tumours. Further work is required to extend our understanding of CAF subpopulations, however these recent discoveries may allow for more specialised targeting of CAFs in the tumour stroma.

1.2.4.4 *The role of cancer-associated fibroblasts in tumour progression*

Although CAFs are generally considered to be a tumour-promoting cell type, in some cases CAFs have been found to play a role in tumour suppression. For example, in pancreatic ductal adenocarcinoma (PDAC) models, depletion of CAFs resulted in disease progression due to a decline in immune surveillance and increased infiltration of T regulatory cells (Özdemir *et al.* 2014; Rhim *et al.* 2014). Similarly, in a 3D co-culture of lung squamous carcinoma epithelial cells with CAFs, it was demonstrated that CAFs were able to reverse oncogenic changes within the epithelial cells, returning them from a state of dysplasia to a state of hyperplasia (Chen *et al.* 2018). In breast cancer, several studies have demonstrated that patients with stroma rich tumours have a poorer prognosis than those with less abundant stroma (de Kruijf *et al.* 2011; Moorman *et al.* 2012; Dekker *et al.* 2013). However, the impact of CAFs on long-term survival in breast cancer is less clear. Whilst studies utilising either α -SMA or PDGFR- β as markers of CAFs generally demonstrate a negative correlation between these markers and patient survival (Surowiak *et al.* 2007; Paulsson *et al.* 2009; Parikh *et al.* 2014; Sinn *et al.* 2014; Nordby *et al.* 2017; Yixuan *et al.* 2018), studies utilising FAP as a CAF marker have shown both positive and negative correlations with overall survival (Ariga *et al.* 2001; Li *et al.* 2020). These conflicting results are likely due to the heterogeneity within the CAF population, with different subpopulations of CAF expressing different combinations of the classical CAF markers and being present in differing quantities across solid tumour types. As previously mentioned, both tumour-promoting and tumour-suppressing functions of CAFs have been identified. It remains to be determined whether different subpopulations of CAF can be categorised more distinctly as either pro-or anti-tumour CAFs.

As well as affecting tumour progression, there is increasing evidence that CAFs can aid in mediating resistance to cancer chemotherapy. Straussman and colleagues conducted an extensive study in which 23 stromal cell lines were co-cultured with 45

tumour cell lines and co-cultures were challenged with 35 targeted and cytotoxic anti-cancer therapies (Straussman *et al.* 2012). This study demonstrated that CAFs were capable of directly mediating tumour cell resistance to an array of anti-cancer therapies. These findings have since been corroborated *in vivo* by studies demonstrating CAF-mediated resistance to cisplatin, BRAF inhibitors and epirubicin, among others (Hirata *et al.* 2015; Long *et al.* 2019; Broad *et al.* 2021).

Despite the tumour-promoting roles of CAFs and their contributions towards chemoresistance, both of which make CAFs good candidates for targeted therapy, the heterogeneity of the CAF population in solid tumours make this approach more challenging. As previously mentioned, total depletion of CAFs may result in undesirable disease progression (Özdemir *et al.* 2014; Rhim *et al.* 2014) and thus a more conservative approach may be required, such as targeting specific subpopulations or aiming to revert CAFs back to a more normal fibroblast phenotype. The latter approach has already seen some success in pancreatic cancer using a vitamin D receptor ligand to revert activated stellate cells back to a more quiescent state (Sherman *et al.* 2014).

1.3 Endosialin

1.3.1 Endosialin structure and family members

Endosialin was first identified in 1992 by Rettig and colleagues during a search for tumour-associated vascular proteins suitable for immunological targeting. Subsequently, the authors described endosialin as a highly sialylated cell surface glycoprotein. Human endosialin is encoded by an intronless gene, *CD248*, located on chromosome 11q.13, resulting in a protein with no alternative splice variants (Rettig *et al.* 1992; S. Christian *et al.* 2001). Similarly, murine *Cd248* is intronless and is located on chromosome 19, in a region that displays homology to the human chromosome region 11q (Opavsky *et al.* 2001). Coding of these genes results in an ~80 kDa protein core consisting of a large extracellular domain, a transmembrane domain and a short proline-

rich cytoplasmic tail. The extracellular domain contains an N-terminal C-type lectin-like domain (CTLN), a sushi domain, three epidermal growth factor (EGF) repeats and a membrane proximal mucin domain (Figure 1.7). The mucin domain is heavily modified by sialylated O-linked glycosylation, giving rise to a ~175 kDa mature glycoprotein (Christian *et al.* 2001). Consistently, a small portion of endosialin protein is found in the Golgi apparatus, the site of addition and modification of O-linked sugars (MacFadyen *et al.* 2005). Mammalian proteins containing a CTLN are classified into 17 groups, with endosialin belonging to C-type lectin family XIV (Zelensky and Gready 2005). Thrombomodulin, CD93 and C-type lectin domain containing 14A (CLEC14A) are the other members of this family, with CLEC14A exhibiting closest homology to endosialin. All family members share the same basic structure with a similar domain architecture (Figure 1.7).

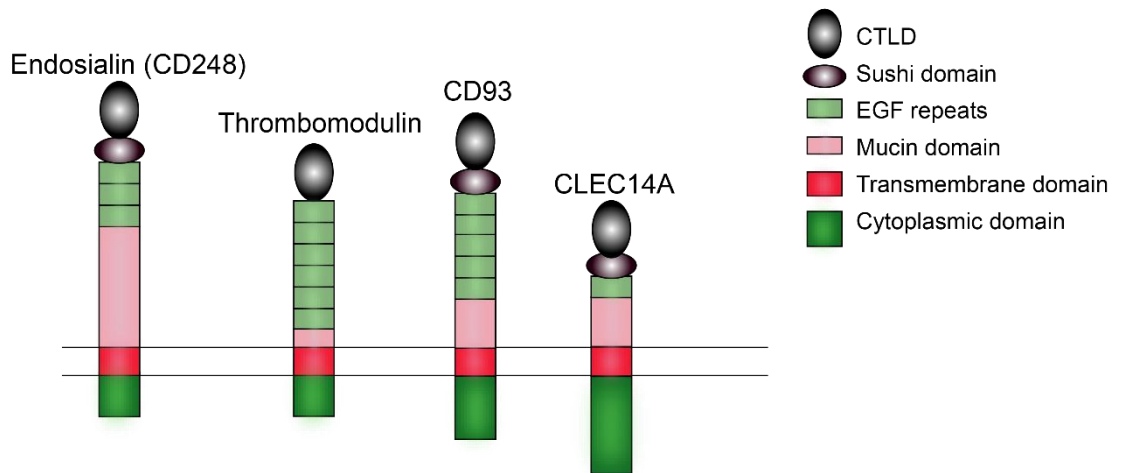


Figure 1. 7 The endosialin family members

Endosialin (CD248) belongs to Group XIV of the C-type lectin-like domain (CTLN)-containing protein family, along with thrombomodulin, CD93 and CLEC14a. Each family member has a single CTLN, a sushi domain, one or more EGF repeats and a heavily glycosylated mucin-like region of varying size followed by a transmembrane domain and a cytoplasmic domain.

CLEC14A is described as an endothelial-specific protein (Mura *et al.* 2012), whereas thrombomodulin and CD93 have been identified on the cell surface of multiple other cell types (Khan *et al.* 2019). The most studied protein of the C-type lectin family XIV is thrombomodulin, which has roles in many biological systems including coagulation, angiogenesis and inflammation (Loghmani and Conway 2018). High expression of thrombomodulin in tumours also correlates with a good prognosis (Hanly *et al.* 2005). Like thrombomodulin, CD93 is believed to have multiple roles which include the maintenance of endothelial cell junctions and regulation of the inflammatory response (Khan *et al.* 2019). However, conversely to thrombomodulin, high expression of CD93 in tumours correlates with poor prognosis (Langenkamp *et al.* 2015).

CLEC14A and endosialin remain the least studied members of the C-type lectin family XIV, with the functions of these proteins remaining largely unknown. It has been suggested that both CLEC14A and endosialin have roles in angiogenesis and, specifically, that they may be important for mediating interactions between vascular cell types. This thesis will focus on endosialin and the function of endosialin will be discussed in more detail on Section 1.3.3.

1.3.2 *Endosialin expression*

1.3.2.1 *Endosialin-expressing cell types*

Endosialin was initially identified as a cell surface protein expressed by vascular endothelial cells in tumour tissue (Rettig *et al.* 1992). A subsequent serial analysis of gene expression (SAGE) screen identified endosialin as the most highly upregulated transcript in human colorectal tumour endothelial cells when compared to normal tissue endothelial cells, resulting in endosialin being known as tumour endothelial marker 1 (TEM1) (Croix *et al.* 2000). In 2004 Brady *et al.* reported the expression of endosialin on α -SMA-positive cells, leading to the endothelial-specific expression of endosialin being brought into question (Brady *et al.* 2004). It has since been demonstrated that the marker

used to isolate endothelial cells in the study by Croix *et al.* (CD146) is also expressed by perivascular cells, thus contamination from these perivascular cells may be responsible for the mistaken identification of endosialin as a protein predominantly expressed by the endothelium (MacFadyen *et al.* 2005). Further to this, using endosialin-specific monoclonal antibodies (mAb) generated by immunising mice with human fibroblasts, our laboratory demonstrated that human umbilical vein endothelial cells (HUVECs) do not express endosialin in either their normal or pro-angiogenic state (MacFadyen *et al.* 2005). The authors conclusively show that endosialin is not expressed by CD31-positive endothelial cells, but rather by fibroblasts and perivascular cells and this has since been supported by additional reports (MacFadyen *et al.* 2005; MacFadyen *et al.* 2007; Simonavicius *et al.* 2008).

Endosialin expression has also been identified in the naïve CD8⁺ population of human T-cells, although this was not apparent in the equivalent murine cells (Hardie *et al.* 2011). In human naïve CD8⁺ T-cells, endosialin is reported to be one of the genes with the highest level of enriched expression when compared to other T-cell types (proteinatlas.org). This finding has yet to be confirmed by subsequent studies, thus further work will be required to understand and characterise this expression.

1.3.2.2 *Endosialin expression in embryonic and adult tissues*

During murine embryonic development endosialin is expressed at a high level by mesenchymal cells in various tissues (Rupp *et al.* 2006; MacFadyen *et al.* 2007). The most notable endosialin expression in the embryo is found in the stroma around the developing hair follicles where strong immunohistochemical (IHC) staining is observed. Additional areas of strong endosialin staining are in the developing brain vasculature, lungs and mesangial cells of the kidneys, with most other organ systems remaining negative (Rupp *et al.* 2006; MacFadyen *et al.* 2007). In the new-born mouse, these positive areas of endosialin expression persist, although the level of expression is

significantly lower. Importantly, endosialin expression is reduced further in the adult mouse; only low levels of endosialin are observed in the lungs, kidneys and the skin and its expression is restricted to stromal fibroblasts, with little or no expression on normal tissue pericytes (MacFadyen *et al.* 2007). One notable exception to the loss of endosialin expression in normal adult tissues is the female uterus, which demonstrates high levels of endosialin expression even in adulthood (Rupp *et al.* 2006). While these studies confirm that the endosialin expression observed in mice during development is largely lost by adulthood, it is important to note that not all organs were examined. Expression of endosialin in a wider range of normal adult mouse tissue will be investigated in this thesis (Chapter 3.2.3).

The pattern of endosialin expression in normal human tissue has also been examined at the mRNA level. Utilising eNorthern gene expression profiles, it was demonstrated that endosialin mRNA can be detected at low levels in all investigated tissue (Dolznig *et al.* 2005). Expression of endosialin mRNA was most notable in the normal breast, uterus, bladder and skin. IHC analysis confirmed the expression of the endosialin protein in the uterus, however other organs of notable mRNA expression were not examined by IHC. The liver and prostate were confirmed as endosialin-negative by IHC (Opavsky *et al.* 2001; Dolznig *et al.* 2005). Importantly, the expression pattern of endosialin in human tissues is largely recapitulated in the normal adult mouse. Interestingly, the bladder was identified as having a higher level of endosialin mRNA expression when compared to other normal human tissues. However, endosialin protein expression in the bladder was not assessed in the adult mouse (Dolznig *et al.* 2005; Rupp *et al.* 2006; MacFadyen *et al.* 2007).

Taken together these data demonstrate that endosialin expression at the protein level is low or absent in adult murine and human tissues, despite some evidence for *CD248* being transcribed in various human tissues to low or moderate levels. Crucially,

where endosialin expression was detected in normal adult tissues, the expression level was low compared to the level observed in developing tissues.

1.3.2.3 *Endosialin expression in tumour tissue and other disease pathologies*

As previously mentioned, endosialin was initially identified as a protein expressed by tumour vasculature (Rettig *et al.* 1992). Since then, our laboratory has demonstrated unambiguously that endosialin is expressed by tumour-associated pericytes in breast cancers (MacFadyen *et al.* 2005) and gliomas (Simonavicius *et al.* 2008). Further, Rouleau and colleagues analysed 250 human cancer specimens covering 20 cancer subtypes for endosialin expression. In all endosialin-positive carcinomas, endosialin expression was observed almost exclusively in the pericyte compartment of the vasculature, with endosialin-positive stromal cells also present in some specimens (Rouleau *et al.* 2008). An equivalent pattern of endosialin expression was detected in mouse xenografts (Rettig *et al.* 1992; Rupp *et al.* 2006). It is now widely accepted that endosialin expression in most solid tumours is restricted to fibroblasts and tumour-associated pericytes.

In carcinomas, with the exception of bladder carcinoma, endosialin expression is mostly absent in the malignant cells. In the case of sarcoma, however, up to 89% of samples displayed endosialin-positive tumour cells (Rouleau *et al.* 2008; Thway *et al.* 2016) and endosialin expression correlated with disease grade (Rouleau *et al.* 2011). Further to this, endosialin-positive tumour cells were observed in metastatic lesions, suggesting malignant sarcoma cells can retain endosialin expression after dissemination, although only a small cohort of samples was tested (Rouleau *et al.* 2011).

As well as in tumour tissue, increased endosialin expression has been reported in other disease settings, particularly in fibrosis and inflammation. An increase in endosialin expression has been observed in splenic enlargement (Lax *et al.* 2007), renal fibrosis (Smith *et al.* 2015), hepatic fibrosis (Mogler *et al.* 2015; Wilhelm *et al.* 2016),

pulmonary fibrosis (Bartis *et al.* 2016) rheumatoid arthritis (Maia *et al.* 2010) and atherosclerosis (Hasanov *et al.* 2017). In all reports, genetic deletion of endosialin was associated with a reduction in fibrotic/inflammatory phenotypes, suggesting a role for endosialin in the establishment of these pathologies.

1.3.2.4 *Regulators of endosialin expression*

To date there are three factors attributed to regulating endosialin expression: hypoxia, cell confluency and TGF- β signalling. The former was demonstrated by Ohradanova and colleagues who showed that endosialin expression is upregulated by the transcription factor hypoxia-inducible factor-2 α (HIF2 α) in hypoxic conditions. HIF2 α activates the endosialin promoter both directly through binding to a hypoxia response element at a distal part of the promoter and indirectly by cooperating with Ets-1 and binding the proximal region of the endosialin promoter (Ohradanova *et al.* 2008). It has also been reported that endosialin is upregulated *in vitro* when cells reach confluency (Opavsky *et al.* 2001). This confluency-induced upregulation of endosialin is mediated via the transcription factor specificity protein 1 (SP1). Supporting the role of hypoxia in regulating endosialin expression, binding of SP1 to the proximal promoter of endosialin is partly induced by pericellular hypoxia in the confluent cultures (Ohradanova *et al.* 2008). Finally, investigation into the mechanisms underlying endosialin downregulation in adult tissues demonstrated that TGF- β was able to suppress endosialin mRNA and protein levels in cultured fibroblasts and vascular smooth muscle cells. This was attributed to transcriptional downregulation through the canonical Smad 2/3 pathway. Interestingly, CAFs and tumour cells were resistant to this downregulation (Suresh Babu *et al.* 2014).

1.3.3 *Endosialin Function*

1.3.3.1 *Endosialin in development and cellular signalling*

To explore the function of endosialin, endosialin knock-out (KO) mice were generated (Nanda *et al.* 2006). Surprisingly, given the high levels of endosialin expression observed during embryonic development, the endosialin KO mice were viable, healthy and exhibited no sign of any developmental defects. Histopathological examination of organ systems from both developing and adult mice revealed no abnormalities in tissue structure or organisation. Moreover, there were no obvious phenotypic differences between endosialin wild-type (WT) and KO adult mice. These data suggest that there are compensatory mechanisms which allow endosialin KO mice to develop normally and also support the consensus that endosialin has a non-essential role in normal adult tissue.

Subsequent to this original study, it was reported that endosialin KO mice have femora and tibiae with superior mechanical properties when compared to their WT counterparts. This was attributed to increased trabecular bone formation by osteoblasts with attenuated sensitivity to PDGF signalling (Naylor *et al.* 2012). These data suggest a role for endosialin in regulating the maturation of osteoblasts and subsequent bone formation via PDGF signalling pathways. Earlier reports also acknowledged a role for endosialin in PDGF signalling. Tomkowicz and colleagues reported reduced PDGF-BB-dependent proliferation in endosialin-deficient human pericytes when compared to WT controls (Tomkowicz *et al.* 2010). PDGF-BB is a known pericyte growth factor secreted by endothelial cells which signals via PDGFR- β on pericytes. Subsequent signalling results in pericyte proliferation and recruitment to new vascular structures (Hellstrom *et al.* 1999). Tomkowicz and colleagues were able to demonstrate that endosialin knock-down (KD) in human pericytes did not affect the surface expression of PDGFR- β or its ability to be phosphorylated in response to PDGF-BB stimulation. However, endosialin KD resulted in a significant decrease in extracellular signal-regulated protein kinase (ERK) 1/2 phosphorylation and *c-Fos* upregulation in response to PDGF-BB stimulation, suggesting a role for endosialin in propagating this signalling pathway downstream of

PDGFR- β (Tomkowicz *et al.* 2010). It has been suggested that endosialin interacts with the PDGF signalling pathway via its cytoplasmic domain, as fibroblasts lacking the endosialin cytoplasmic domain demonstrated impaired PDGF-BB-mediated migration (Maia *et al.* 2011).

Endosialin has also been reported to be upregulated on fibroblasts during wound healing and to potentially facilitate the wound healing process by modulating PDGF signalling (Hong *et al.* 2019). In agreement with previous studies, endosialin KD *in vitro* resulted in diminished PDGF-BB-induced ERK-1/2 phosphorylation in cultured fibroblasts. In this study, KD of endosialin was also associated with a decrease in PDGFR- α expression and IHC staining of wounded tissue demonstrated some colocalisation of endosialin and PDGFR- α . In male mice with 8 mm punch wounds, endosialin KO resulted in a significantly decreased rate of wound healing (Hong *et al.* 2019). These data suggest that endosialin expression is necessary for efficient wound healing and this may be due to the role of endosialin in PDGF signalling. However, it should be noted that contrasting wound healing results have been published in female mice with 6 mm punch wounds, with endosialin KO mice displaying normal wound healing (Nanda *et al.* 2006). Although the reason for this discrepancy is not clear, it may potentially be attributed to differences in gender or initial wound size.

Taken together, these results suggest that endosialin influences the PDGF signalling cascade upstream of ERK-1/2 phosphorylation, either by influencing PDGFR- α expression or acting downstream of PDGFR- β . However, it is not clear how the cytoplasmic domain of endosialin might mediate interaction with this pathway. It may be that the endosialin cytoplasmic domain interacts directly with proteins in the signalling cascade but, equally, endosialin may influence the pathway indirectly through regulation of other proteins involved in the signalling cascade. The cytoplasmic domain of endosialin contains three potential phosphorylation sites, as well as a PDZ domain, a domain associated with protein interactions (Lee and Zheng 2010). Therefore, it is

possible that the cytoplasmic domain of endosialin may be involved in signalling interactions.

Despite these reports that genetic deletion or KD of endosialin perturbs PDGF signalling in pericytes, it would be expected that endosialin-deficient pericytes might not be recruited to vascular structures as efficiently. However, our laboratory has demonstrated no significant difference in pericyte recruitment and coverage of vascular structure in both developing tissues and established tumour tissues (Simonavicius *et al.* 2012; Viski *et al.* 2016).

As well as mediating signalling downstream of PDGF, endosialin has been implicated in TGF- β signalling. KD of endosialin in human pericytes *in vitro* resulted in a reduction in TGF- β -induced α -SMA upregulation. Furthermore, treatment with an anti-endosialin antibody *in vivo* resulted in a striking reduction in α -SMA-positive pericytes associated with tumour vasculature (Rybinski *et al.* 2015). As previously discussed in Section 1.3.2.4, there is some evidence that TGF- β downregulates endosialin expression. Therefore, it is possible that endosialin is involved in a negative feedback loop to control TGF- β signalling, where signalling is limited by TGF- β -mediated downregulation of endosialin, a potential activator of the pathway. Further investigation is warranted to delineate the role of endosialin in TGF- β signalling. Of particular interest are the mechanisms (direct or indirect) by which endosialin is interacting with the TGF- β and PDGF signalling pathways.

1.3.3.2 *Endosialin in angiogenesis*

Although no phenotypic differences are found between healthy tissues from endosialin WT and KO mice, endosialin-deficient tumours have been reported to have an increased number of microvessels (Nanda *et al.* 2006; Simonavicius *et al.* 2008; Viski *et al.* 2016). This suggests a role for endosialin in tumour angiogenesis, which is

supported by the evidence for hypoxia-induced expression of endosialin, as lack of oxygen is an important driver of angiogenesis (Opavsky *et al.* 2001).

Studies involving retinal and aortic ring outgrowths from endosialin WT and KO mice demonstrated an increase in vessel density in the endosialin KO samples. Rather than an increase in vascular sprouting, this was attributed to a reduction in selective vessel regression, as demonstrated by a decrease in the number of collagen IV-positive, endomucin-negative sleeves and supported by the observation that culture with a soluble endosialin-Fc construct enhances endothelial cell apoptosis (Simonavicius *et al.* 2012). Further, observation of growing microvessels in the human telencephalon revealed that endosialin-positive pericytes associate with immature angiogenic vessels (Virgintino *et al.* 2007). Interestingly, the authors demonstrate that endosialin and NG2 double-positive pericytes are only found around the initial segment of the microvessel which also displays CD31-positive endothelial cells, whereas any distal pericyte projections are solely NG2-positive. Taken together, these results suggest that endosialin likely interacts, directly or indirectly, with the endothelial cells of angiogenic vessels and that this interaction mediates vascular pruning.

In support of endosialin being involved in pericyte-endothelial cell interactions, it was subsequently reported by Khan and colleagues that endosialin binds the vascular basement membrane protein multimerin-2 (MMRN2), secreted exclusively by endothelial cells (Khan *et al.* 2017). MMRN2 is an elastic microfibril interfacier (EMILIN) family extracellular matrix protein of ~ 500 kDa comprising a signal sequence followed by an N-terminal EMI domain, a central coiled coil region and a C-terminal C1q-like domain (Figure 1.8A) (Hayward *et al.* 1995; Sven Christian *et al.* 2001). MMRN2 is able to bind all members of the group XIV C-type lectins, with the exception of thrombomodulin. Interestingly, it was shown that CLEC14A and CD93 are able to bind to the MMRN2⁴⁹⁵⁻⁶⁷⁴ fragment, whereas endosialin binds the distinct MMRN2¹³³⁻⁴⁸⁶ fragment. Further to this, MMRN2 was able to bind CLEC14A and endosialin simultaneously (Khan *et al.*

2017). Both MMRN2 and CLEC14A have been described as regulators of angiogenesis, with CLEC14A being reported as pro-angiogenic (Mura *et al.* 2012; Lee *et al.* 2017) and MMRN2 being reported as both pro-angiogenic and angiostatic (Lorenzon *et al.* 2012; Zanivan *et al.* 2013; Colladel *et al.* 2016; Khan *et al.* 2017). As discussed previously, endosialin was demonstrated to play a role in selective vessel regression and vascular pruning (Simonavicius *et al.* 2012). Conversely, CLEC14A has been shown to promote endothelial cell migration and angiogenic sprouting (Noy *et al.* 2015). These opposing roles for endosialin and CLEC14A in vascular patterning may provide an explanation as to why MMRN2 is reported as both pro- and anti-angiogenic; it may be that the three proteins form an intricate angiogenesis-regulating system (Figure 1.8B).

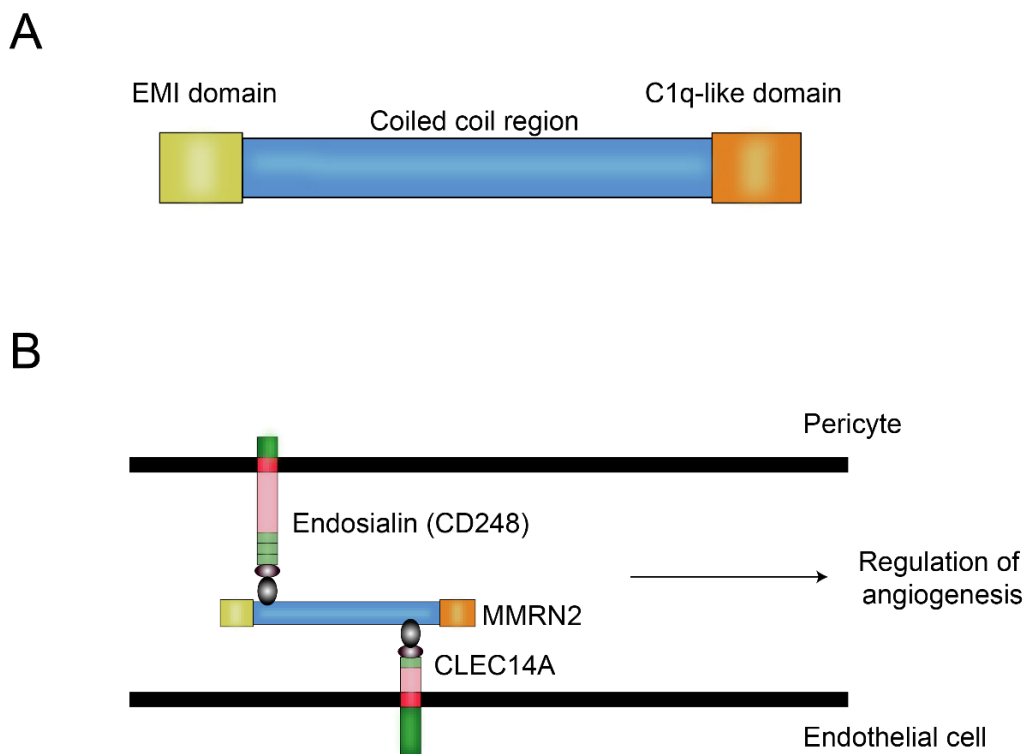


Figure 1. 8 Multimerin 2 (MMRN2) structure and proposed function

(A) MMRN2 structure. The MMRN2 protein comprises a N-terminal EMI domain, a central coiled coil region and a C-terminal C1q-like domain. **(B)** Hypothesis of endosialin (CD248), MMRN2 and CLEC14a interaction. MMRN2 is able to bind endosialin expressed by pericytes and CLEC14a expressed by endothelial cells both singly and simultaneously and the three proteins may form an intricate angiogenesis regulating system.

1.3.3.3 *Endosialin in tumour angiogenesis and growth*

As previously discussed in Section 1.3.2.3, endosialin expression is upregulated on tumour vasculature when compared to the normal tissue. Interestingly, a similar expression pattern was observed for MMRN2 and CLEC14A, with levels of both proteins higher in tumour-associated vessels compared to normal vessels (Zanivan *et al.* 2013). KO mice have been generated for endosialin, MMRN2 and CLEC14A and the subcutaneous growth of a number of tumour types have been assessed in these KO mice (Noy *et al.* 2015; Viski *et al.* 2016; Pellicani *et al.* 2020). Compared to WT controls, Lewis lung carcinoma (LLC) tumour growth was impaired in CLEC14A KO mice, a phenotype which was also observed by blocking the interaction between CLEC14A and MMRN2 (Noy *et al.* 2015). Conversely, an impairment of tumour growth was not observed in endosialin or MMRN2 KO mice (Viski *et al.* 2016; Pellicani *et al.* 2020). Interestingly, a vascular phenotype was observed in all tumours; CLEC14A KO tumours displayed decreased microvessel density (Noy *et al.* 2015) and, conversely, both endosialin and MMRN2 KO tumours exhibited an increased microvessel density (Viski *et al.* 2016; Pellicani *et al.* 2020). These results support the findings of the respective *in vitro* and *ex vivo* studies that highlight opposing roles for CLEC14A and endosialin in vascular patterning and further suggest these proteins form a complex angiogenesis-regulating system in developing tumours.

To date, studies on the functional role of endosialin have focussed on its upregulated expression on tumour pericytes. However, in solid tumours, endosialin expression is also detected on CAFs. Recent single cell sequencing analysis of CAFs, isolated from tumours of the MMTV-PyMT mouse breast cancer model, demonstrated that CAFs may be categorised into spatially distinct sub-populations: vascular CAFs, matrix CAFs and developmental CAFs. Endosialin was found to be characteristic of the vascular CAFs, which were found to have originated from the perivascular location (Bartoschek *et al.* 2018). This suggests that endosialin-positive CAFs that are not

associated with the vasculature may have originated from the perivascular compartment and migrated into the tumour stroma. MMRN2 is secreted exclusively into the vascular basement membrane, therefore, endosialin-expressing CAFs that are not positioned proximally to vascular structures in the tumour will not see MMRN2. However, other members of the EMILIN family, EMILIN-1, EMILIN-2, and potentially MMRN1, have a wider stromal distribution in tumour tissue (proteintlas.org 2020). It would be of interest to determine whether these MMRN2 family members can also serve as endosialin ligands.

1.3.3.4 *Endosialin in metastasis*

Although in the majority of tumour models studied endosialin depletion does not impair primary tumour growth, there are reports of endosialin depletion affecting distant site metastasis. Nanda and colleagues implanted HCT116 human colorectal carcinoma cells orthotopically in mice and monitored metastasis. Here they observed a significant decrease in distant site metastasis to the peritoneum and liver in endosialin KO mice compared to WT controls (Nanda *et al.* 2006). Our laboratory has reported equivalent results in the spontaneously metastatic 4T1 breast carcinoma and LLC models (Viski *et al.* 2016). Tumour cells were implanted subcutaneously and allowed to grow for 30 days, or primary tumours were resected after 9 days and mice were culled on day 93 or prior for health reasons. In both circumstances, metastatic burden in the lungs was significantly reduced in endosialin KO mice compared to WT controls. Subsequently, it was determined that endosialin was important for tumour cell intravasation, as no difference in lung metastatic burden was observed when tumour cells were injected directly into the circulation, via the tail vein, in endosialin WT and KO mice. Further to this, blood cultures from the spontaneously metastatic models revealed a reduced number of circulating tumour cells in endosialin KO mice. A role for endosialin in tumour cell intravasation was also supported by data from an *in vitro* transmigration assay, in which endosialin-depleted 10T½ pericyte-like cells reduced the movement of 4T1 tumour

cells across a sEND endothelial cell layer when compared to 10T $\frac{1}{2}$ WT controls (Viski *et al.* 2016).

Taken together, these data suggest that endosialin may be important for optimal vascular patterning in developing tumour tissues that allows for efficient metastasis. It has been demonstrated that tumours with impaired pericyte recruitment have reduced vessel patency and diminished distant site metastasis (Chantrain *et al.* 2004; Bielenberg and Zetter 2015). Therefore, a similar effect may be observed in the absence of functional endosialin on the pericyte cell surface. It is also possible that endosialin interacts, directly or indirectly, with the tumour cells, promoting their migration across the endothelial cell layer. To date, only one endosialin ligand associated with tumour cells has been identified, Mac2-BP/90K. Mac2-BP/90K is a protein secreted by tumour cells and the interaction between endosialin and Mac2-BP/90K has been suggested to inhibit the adhesion of tumour cells to fibroblasts, thereby mediating repulsive positioning signals between the tumour and stromal cells (Becker *et al.* 2008). This repulsive force may aid in pushing tumour cells through the vascular basement membrane and into the circulation, although the extent that Mac2-BP/90K expressing tumour cells are found in close proximity to endosialin-positive cells in tumours is unclear. Therefore, further work is warranted to establish whether the Mac2-BP/90K-endosialin interaction contributes to endosialin function in tumours and specifically its pro-metastatic effects.

1.3.3.5 Soluble endosialin

Soluble endosialin has been detected in the serum of colorectal cancer patients where it was detected at higher concentrations than in the serum from healthy individuals. The authors also noted that the concentration of endosialin in the serum was significantly associated with tumour stage and correlated with overall survival (Pietrzyk and Wdowiak 2020) However, another study reported no difference in the levels of endosialin in the serum of colorectal cancer patients compared to healthy controls

(O'Shannessy *et al.* 2016; Pietrzyk and Wdowiak 2020). At this time, it is not clear whether the detection of endosialin in the serum is due to proteolytic cleavage or the detection of membrane vesicles released from damaged or dying cells into the serum. It is plausible that endosialin could be cleaved from the cells surface as all other members of the group XIV C-type lectins are cleaved (Lohi *et al.* 2004; Bohlson *et al.* 2005; Noy *et al.* 2016). It is currently not known whether this soluble endosialin has a physiological function and if so, what that might be.

1.3.4 Targeting Endosialin

As endosialin is only expressed at low levels in normal adult tissues and becomes upregulated in tumours and other pathologies, it is considered as a potential candidate for targeted therapy.

1.3.4.1 Endosialin targeting with MORAb-004 (Ontuxizumab)

Endosialin was originally identified by immunising a mouse with human fibroblasts, which gave rise to the FB5 mAb, which recognises human endosialin (Rettig *et al.* 1992). Since then, a collaboration has been established between the authors of this study and Morphotek to develop a humanised mAb from FB5, known as MORAb-004 or Ontuxizumab. *In vivo* testing in a human endosialin knock-in mouse model inoculated subcutaneously with murine B16-F10 melanoma cells demonstrated a significant reduction in tumour growth in Ontuxizumab treated animals when compared to isotype controls. This result was also recapitulated in the same model inoculated with LLC tumours (Rybinski *et al.* 2015). Strikingly, Ontuxizumab treatment in an experimental metastasis model of B16-F10 melanoma resulted in a 70% reduction in lung deposits (Rybinski *et al.* 2015), a result which contrasts with data published by our laboratory in a 4T1 mammary tumour experimental metastasis model, where no difference in lung tumour burden was seen in WT and endosialin KO mice (Viski *et al.* 2016). These

contrasting findings could be due to differences in using a therapeutic antibody compared to using a mouse model which is endosialin-deficient. Conversely, Ontuxizumab treatment was associated with an increased number of microvessels, which supports observations by our laboratory (Viski *et al.* 2016). Ontuxizumab was also found to cause endosialin internalisation and thus, expression of endosialin on the cell surface of pericytes was largely absent. This was concurrent with a decrease in α -SMA expression and depolarisation of pericytes (Rybinski *et al.* 2015).

The first-in-human phase I trial for Ontuxizumab was conducted in the United States between 2009 and 2011 (Diaz *et al.* 2015). In this trial 36 adult patients with treatment refractory, extra-cranial solid tumours were given escalating doses of Ontuxizumab. The maximum tolerated dose was found to be 12 mg/kg and the main adverse effects observed were fatigue, headache, pyrexia, chills and nausea which never exceeded grade 3 in severity. Of the 32 evaluable patients in this study, 56% had stable disease and the median progression free survival was 8.4 weeks. Four patients displayed a minor decrease in tumour size, with the maximum observed decrease being 21%. IHC analysis of diagnostic biopsies revealed that 3 of the 4 patients with tumour regression had high tumour endosialin expression pre-treatment. As biopsies were not taken post-treatment, it was not possible to assess whether endosialin expression was reduced by Ontuxizumab treatment (Diaz *et al.* 2015). The safety profile and potential anti-tumour activity of Ontuxizumab observed in this study led to the initiation of phase II studies in metastatic melanoma (D'Angelo *et al.* 2018), metastatic colorectal carcinoma (Grothey *et al.* 2018) and soft tissue sarcoma (Jones *et al.* 2019). Although Ontuxizumab was well tolerated in all of these studies, no significant differences in progression free or overall survival were observed in any study. Two additional phase I studies have been conducted in paediatric solid tumours (Norris *et al.* 2018) and gastric cancer and hepatocellular carcinoma (Doi *et al.* 2019). Again, Ontuxizumab was well tolerated in

both studies, however it was only the latter that reported any anti-tumour response, with 33.3% of hepatocellular carcinomas displaying tumour shrinkage (Doi *et al.* 2019).

Taken together, these results demonstrate that Ontuxizumab shows little clinical benefit across a range of cancer patient cohorts. The reason behind the disappointing results reported in these studies is not clear at this time. However, it is important to note that there is no data indicating that the FB5 monoclonal antibody has biological activity beyond promoting ligand internalisation. For example, it not known whether FB5 can block the interaction of endosialin with its well characterised ligand MMRN2 (see Section 1.3.2.3). Further, the level of endosialin expression in tumour tissues post-treatment was not assessed and so it cannot be determined whether the lack of anti-tumour response was due to an insufficient decrease in endosialin expression. The majority of these studies gave doses close to maximum tolerated dose, thus further increasing the dose of Ontuxizumab is not a viable solution. There are currently no further clinical trials for Ontuxizumab registered (ClinicalTrials.gov 2020).

1.3.4.2 *Endosialin targeting with antibody-drug conjugates*

The tumour-specific expression of endosialin makes endosialin a good target for the guided therapy of drugs with systemic toxicities. A number of studies have been published investigating the potential of endosialin as a target for antibody-drug conjugate (ADC) therapy. The first of these studies examined shikonin-loaded poly (lactic-co-glycolic acid) (PLGA) nanoparticles coated with anti-endosialin single chain variable fragment (scFv). These nanoparticles were able to interact with and be internalised by endosialin-positive MS1 cells, resulting in enhanced cytotoxicity when compared to uncoated nanoparticles or free drug (Matthaiou *et al.* 2014). No further work has been reported with this conjugate to date.

Since this study, more comprehensive antitumour studies have been reported utilising various endosialin antibody conjugation systems. Mesoporous silica

nanoparticles coated with anti-endosialin scFv for targeted delivery of bevacizumab, a humanised anti-VEGF monoclonal antibody, have demonstrated endosialin-specific cytotoxicity in an endosialin-positive tumour cell line, superior to that observed with uncoated nanoparticles or free drug *in vitro* (Zhang *et al.* 2015). Further to this, three anti-endosialin ADCs have been tested *in vivo* for antitumour activity in sarcoma and neuroblastoma. The first utilises an endosialin-targeting scFv conjugated to monomethylauristatin E, a microtubule-targeting agent. In the endosialin-positive A-673 Ewing's sarcoma and SK-N-AS neuroblastoma mouse models the ADC was well tolerated. Moreover, targeting of the endosialin-positive tumour cells resulted in a prolonged anti-tumour response following ADC treatment that translated into superior overall survival for the ADC treated mice compared to the unconjugated antibody treatment group (Rouleau *et al.* 2015). The remaining two ADCs, an endosialin scFv conjugated to saporin (Guo *et al.* 2018) and a potent duocarmycin derivative (Capone *et al.* 2017), have displayed anti-tumour effects in the SJSA-1 osteosarcoma model.

These data suggest that endosialin presents a good target for ADC therapy in sarcomas and potentially neuroblastomas and other subsets of endosialin-expressing tumours. Further work is required to assess the suitability of these ADCs for clinical use and to determine whether their efficacy extends beyond these mesenchymal tumour types where endosialin is expressed by the tumour cells to carcinoma where endosialin expression is restricted to the tumour vasculature.

1.3.4.3 *Alternative clinical uses for endosialin targeting*

A number of radiolabelled variants of endosialin antibodies have been generated to assess the status of both endosialin and the tumour vasculature *in vivo*. Two of these are radiolabelled variants of Ontuxizumab, the endosialin targeting antibody deemed safe in phase I and II clinical trials. To generate the Ontuxizumab variants the antibody was either iodinated with iodine¹²⁵ and iodine¹²⁴ (Chacko *et al.* 2014) or labelled with

zirconium⁸⁹ (Lange *et al.* 2016). Both radiolabelled Ontuxizumab variants demonstrated tumour-specific pooling and were determined to be useful tools for assessing endosialin status *in vivo*. An additional study was published recently utilising the endosialin scFv that was generated by Guo and colleagues for the ADC discussed previously (Guo *et al.* 2018). The authors radiolabelled scFv78-Fc with indium¹¹¹ and assessed its biodistribution in both RD-ES Ewing's sarcoma and SK-N-AS neuroblastoma tumours. In both models the radiolabelled scFv pooled in the tumour, with some pooling also observed in the liver (Cicone *et al.* 2020). These studies suggest that radiolabelled endosialin antibodies may be useful clinical tools for determining patient endosialin status in the future, thus helping to identify patients who may benefit from endosialin-targeted therapies. Alternatively, as endosialin serves as a marker of tumour vasculature, radiolabelled Ontuxizumab may also be useful for investigating tumour vascular perfusion.

1.4 CAR T-cell therapy

1.4.1 Cancer Immunotherapy

Cancer immunotherapy describes the adaptation and manipulation of the immune system to prevent, control or eliminate cancer (CancerResearchInstitute 2020). This is an emerging field within cancer research, with many new and innovative approaches being rapidly developed. The first documented use of immunotherapy in cancer can be attributed to William B. Coley in 1891 who, after recognising that a cancer patient had gone into spontaneous remission after developing erysipelas, a streptococcal skin infection, injected an attenuated version of the streptococcal organism into patients with inoperable bone and soft tissues sarcomas. Injection of 'Coley's Toxin' led to remission in some cancer patients, with Coley predicting that the patient's stimulated immune system in response to infection was key to tumour regression (McCarthy 2006). This concept of activating the patient's own immune system to attack

the tumour is the basis for immunotherapies today, with further cancer vaccination strategies being developed, alongside antibody-based therapies and immune checkpoint therapy. In this thesis, I will focus on chimeric antigen receptor (CAR) T-cell therapy, which utilises the host's own cytotoxic T-cells to generate genetically altered CAR T-cells that are able to target cells expressing specific antigens.

1.4.2 CAR T-cell design, development & production

1.4.2.1 CAR T-cell generations

In the physiological setting, cytotoxic T-cells express a T-cell receptor (TCR) on their cell surface, which recognises a single, specific antigen. When these T-cells encounter a cell expressing that antigen, a dual signalling process occurs. First the TCR binds its antigen, which is presented on the cell surface by major histocompatibility complex (MHC) molecules. This interaction primes the T-cell for response and is followed by a secondary signal generated by the binding of co-stimulatory molecules on the surface of the target cell and the T-cell. Together, these signals result in the activation of the T-cell and the release of a cytotoxic load which leads to the death of the antigen-presenting cell (Smith-Garvin *et al.* 2009) (Figure 1.9A).

CAR T-cells are cytotoxic T-cells that have been genetically modified to express a CAR construct in place of the natural TCR, which allows the T-cells to recognise and act against cells expressing the target of interest. CAR constructs consist of three main components, an ectodomain, a transmembrane domain and an endodomain (Dotti *et al.* 2014). The endodomain is most commonly made up of the T-cell activation molecule CD3 ζ , either in the presence or absence of other co-stimulatory molecules such as CD28 and 4-1BB. The ectodomain contains a spacer, the scFv portion of an antibody against the desired target, and a signal peptide. Upon encountering an antigen-presenting cell, the scFv portion of the CAR is able to bind to its target antigen; this in turn leads to changes in the conformation of the CAR linker, phosphorylation of CD3 ζ immunoreceptor

tyrosine-based activation motifs (ITAMs) and activation of the T-cell. The death of the antigen-presenting cell is subsequently triggered by release of cytokines and other cytotoxic substances. Importantly, CAR T-cell-induced cell death, unlike that induced by an unmodified cytotoxic T-cell, triggers the subsequent death of the antigen-presenting cell without the need for MHC antigen presentation or cell surface co-stimulatory molecules, which are often not expressed on the surface of tumour cells (Dotti *et al.* 2014) (Figure 1.9B).

The first CAR T-cells were generated in the lab of Zelig Eshar at the Weizmann Institute of Science in Israel in 1989 (Gross *et al.* 1989). The CAR constructs described by the authors are known as first generation CARs. First generation CAR constructs are the simplest form of CAR, with only a CD3 ζ molecule present in their endodomain (Figure 1.10). Although these CAR T-cells elicited cytotoxic functions *in vitro* following activation, they lacked activation, persistence and killing efficacy *in vivo* (Brocker and Karjalainen 1995). In 1998, Finney *et al.* and Krause *et al.* applied the knowledge of the dual signalling that is required during a physiological cytotoxic T-cell response to develop second generation CAR T-cells, which have a co-stimulatory molecule alongside CD3 ζ , arranged in tandem in the CAR endodomain (Figure 1.10). Both second generation CAR T-cells described by the authors incorporated a co-stimulatory CD28 molecule in the endodomain, which showed improved efficacy when compared to first generation CAR T-cells (Finney *et al.* 1998; Krause *et al.* 1998). Other costimulatory molecules such as 4-1BB, OX40, DAP10/12 and inducible T-cell costimulator (ICOS) have also been included in subsequent second generation CAR T-cells (Finney *et al.* 2004; Brentjens *et al.* 2007; Milone *et al.* 2009). In 2002, Michael Sadelain's team generated the first effective second generation, tumour cell-targeting CAR T-cells. These CAR T-cells were directed against prostate-specific membrane antigen (PSMA), an antigen that is often overexpressed by prostate carcinomas, and were able to survive, proliferate and kill prostate cancer cells *in vitro* (Maher *et al.* 2002). Despite the promising results observed

with PSMA-directed CARs, another CAR T-cell target would dominate the field the following year, CD19. This will be discussed in detail in Section 1.4.3.

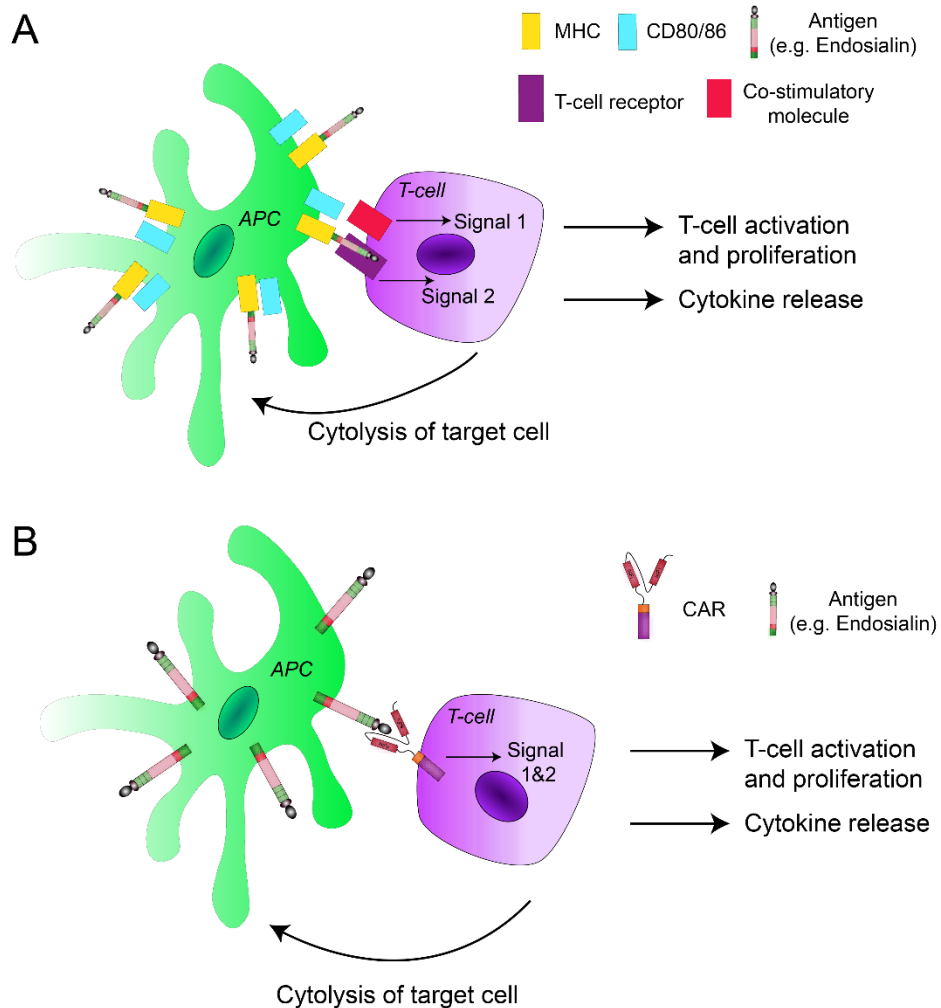


Figure 1. 9 Classic T-cell and CAR T-cell killing

(A) Classic T-cell killing. The antigen-presenting cell (APC) presents antigens (e.g. Endosialin) on the cell surface via major histocompatibility complex (MHC) presentation. The T-cell receptor (CD3ζ) binds the target antigen, resulting in signal 1 which primes the T-cell for response. A second signal is generated by the binding of co-stimulatory molecules on the antigen-presenting cell and T-cell surface. Together, signal 1 and 2 results in T-cell activation, cytokine release and cytolysis of the antigen-expressing cell. **(B)** CAR T-cell killing. The scFv portion of the CAR recognises and binds the target antigen resulting in conformational changes in the CAR. Subsequently, signals 1 and 2 from the T-cell receptor molecule CD3ζ and co-stimulatory molecules, respectively, are generated in the CAR endodomain, resulting in T-cell activation, cytokine release and cytolysis of the antigen-expressing target cell. CAR T-cell killing is possible without MHC antigen presentation or co-stimulatory molecule expression by the target cell, both of which are frequently absent on malignant cells.

Following the success of second generation CARs, it was hypothesised that the addition of another co-stimulatory molecule would further increase the efficacy of CAR T-cells. Subsequently, CAR T-cells were engineered to incorporate multiple co-stimulatory molecules, such as CD28 and 4-1BB together alongside CD3 ζ in the endodomain, and a new generation of CARs was developed, termed third generation CAR T-cells (Figure 1.10). Surprisingly, multiple studies have reported that third generation CAR T-cells offer little additional antitumour benefit when compared to second generation CAR T-cells (Till *et al.* 2012; Gomes da Silva *et al.* 2016; Enblad *et al.* 2018), although the addition of 4-1BB has been demonstrated to enhance CAR T-cell persistence (Milone *et al.* 2009; Byrd *et al.* 2018). The mechanisms by which 4-1BB enhances CAR T-cell persistence are not yet fully understood, however it has been demonstrated that this enhancement requires NF κ B and tumour necrosis factor (TNF) receptor-associated factors (Li *et al.* 2018). Owing to this, focus for clinical development was placed on second generation CAR T-cells and this will be discussed further in Section 1.4.3. Beyond this, there has been considerable focus on the development of new generations of CAR T-cells with enhanced properties that elicit a stronger and more specific anti-tumour response. This will be discussed further in Section 1.4.7.

1.4.2.2 CAR T-cell production

To date, the majority of CAR T-cell treatments are autologous, with the T-cells used for CAR T-cell generation being isolated from the patient. The manufacturing process begins with a collection of PBMCs from the patient via leukapheresis. T-cells are selected from the apheresis product and activated *ex vivo* using cell-based or bead-based activation methods. Activated T-cells are then genetically transduced with the CAR construct via viral transduction or the transposon/transposase system and expanded by co-culture with artificial antigen-presenting cells or by feeding the cells in a bioreactor. Once the appropriate number of desired transduced CAR T-cells has been generated, CAR T-cells undergo a series of quality checks before being transfused back

into the original patient (Wang and Rivière 2016) (Figure 1.11). The development of allogeneic CAR T-cells that utilise T cells from universal donors may provide advantages over autologous CAR T-cell therapy, and this an active area of research. Allogeneic CAR T-cells will be discussed further in Section 1.4.7.4. All CAR T-cells described in the following Section, 1.4.3, were generated by the autologous method described above.

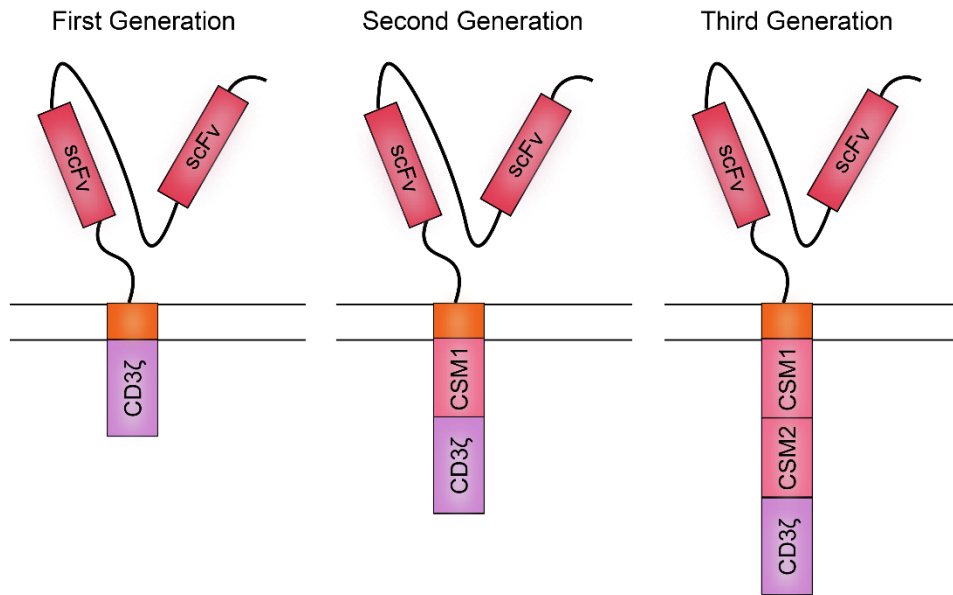


Figure 1. 10 Early CAR generations

All CAR generations have a signal peptide, scFv portion and linker molecule in the ectodomain, followed by a transmembrane domain. In the endodomain, first generation CARs have only the T-cell receptor CD3ζ, second generation CARs have a single co-stimulatory molecule (CSM) and CD3ζ and third generation CARs have multiple costimulatory molecules and CD3ζ.

1.4.3 FDA approved CAR T-cell therapies

To date, all FDA approved CAR T-cell therapies are directed against haematological malignancies, with the majority targeting CD19. As CAR T-cells are infused directly into the blood, they can access circulating malignant cells relatively easily. Targeting solid tumours with CAR T-cells has thus far proven considerably more challenging and this will be discussed further in Section 1.4.5.

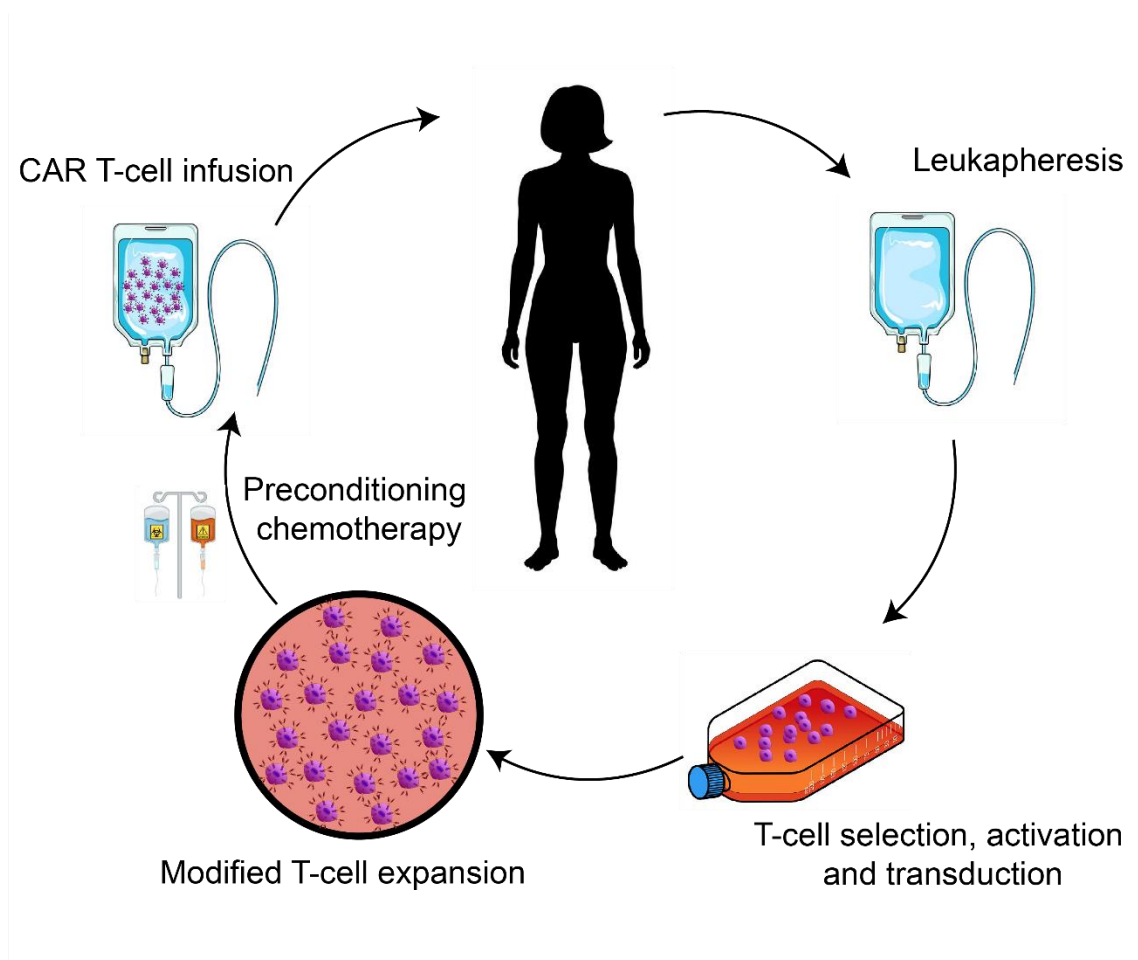


Figure 1. 11 The CAR T-cell production process

Patients undergo leukapheresis to retrieve peripheral blood mononuclear cells (PBMCs) for CAR T-cell generation. T-cells are isolated from the apheresis product, activated using cell-based or bead-based methods and transduced to express the CAR construct. CAR T-cells are then expanded in culture to the desired number. When the CAR T-cell product has passed quality checks and is ready for infusion, patients begin preconditioning chemotherapy to achieve lymphodepletion and aid CAR T-cell engraftment. Finally, CAR T-cells are infused into the patient intravenously.

1.4.3.1 *Kymriah (tisagenlecleucel)*

Kymriah (a.k.a tisagenlecleucel, CTL019, CART-19) is a second generation CAR T-cell targeting CD19, a B-cell lineage-specific protein that is expressed on most malignant B-cells, as well as normal B-cells (Scheuermann and Racila 1995). The Kymriah story begins with Carl June's group at the University of Pennsylvania in 2009. In initial studies, Milone and colleagues used primary human T-cells to generate CD19-

targeting CAR T-cells expressing either CD28 or 4-1BB costimulatory molecules in the endodomain. Direct comparison of *in vitro* activity demonstrated little difference between the two CAR T-cells, with both activating specifically and producing cytokines. However, *in vivo* testing in a primary human pre-B acute lymphoblastic leukaemia (ALL) model revealed superior persistence and antitumour activity of the 4-1BB-containing CAR T-cells (Milone *et al.* 2009). The significant antitumour activity of the 4-1BB-containing CAR T-cells *in vivo*, coupled with a lack of observed treatment-associated toxicities, led to an initial phase 1 clinical trial being conducted (Kalos *et al.* 2011; Porter *et al.* 2011). The three patients that participated in this trial had advanced chemotherapy-resistant chronic lymphocytic leukaemia (CLL) with high tumour burden and extensive bone marrow infiltration. Patients received lymphodepleting chemotherapy before dosing with 1.4×10^7 - 1.1×10^9 CAR T-cells in a split dose regimen (10%, 30% and 60%) over three days to monitor for CAR T-cell-associated toxicities. The CAR T-cells expanded in the blood and persisted for at least 6 months as determined by quantitative polymerase chain reaction (qPCR) analysis. Strikingly, two patients demonstrated complete remission with no malignant cells detected for up to 10 months post-CAR T-cell infusion. The final patient achieved partial remission lasting greater than 8 months. Peak CAR T-cell expansion correlated with the onset of clinical toxicity which included fever and rigors. All toxicities developed between 7 and 12 days post-T-cell infusion and were short-term and reversible (Kalos *et al.* 2011). After demonstrating the effectiveness of these CD19-targeting CARs in CLL, a further study published in 2013 assessed the use of these CARs, referred to as CTL019 T-cells, in the treatment ALL (Grupp *et al.* 2013). The study consisted of two paediatric patients with refractory and relapsed pre-B cell ALL. The first patient, Patient 1, did not receive lymphodepleting chemotherapy prior to CAR T-cell infusion and 1.2×10^7 CAR T-cells/kg bodyweight were administered over a three-day split-dosing regimen, as described in the CLL trial (Kalos *et al.* 2011). The second patient, Patient 2, received lymphodepleting chemotherapy followed by a single dose of

1.4×10^6 CAR T-cells/kg bodyweight. In both patients the CTL019 cells expanded and remission of the leukaemia was achieved. Patient 1 was still in complete remission at 11 months post-T-cell infusion, however Patient 2 relapsed 2 months after CTL019 treatment. Blast cells reappeared in the relapsed patient's circulation and these cells were CD19-negative, suggesting the emergence of a CD19 escape variant in this patient. Approaches to circumvent this acquired resistance will be discussed further in Section 1.4.7. Both children experienced a fever 4-6 days post-CAR T-cell infusion and developed a cytokine release syndrome (CRS). Prophylactic allopurinol was administered to prevent tumour lysis syndrome, with Patient 2 presenting with abnormal levels of uric acid, consistent with a mild form of this syndrome. Patient 1 developed a severe CRS and required glucocorticoids and anti-cytokine therapy (Grupp *et al.* 2013).

Treatment with CTL019 CAR T-cells in these two small patient cohorts demonstrated that CTL019 CAR T-cells were tolerated, with any observed toxicities being reversible with clinical intervention. Further, impressive patient responses were observed, with some patients remaining in remission upon study completion. Following this, two phase 1/2a clinical trials were established (Maude *et al.* 2014; Schuster *et al.* 2017). These studies recruited both paediatric and adult patients with relapsed or refractory B cell-ALL or follicular lymphoma and the patients were treated with lymphodepleting chemotherapy followed by CTL019 CAR T-cells (up to 5×10^8) as a single or split dose. CAR T-cells expanded in the patients in both studies and remained detectable in the blood for up to 24 months. At 6 months post-CTL019 CAR T-cell infusion, up to 57-63% of patients had achieved complete remission, with 57% of patients remaining progression free at 28.6 months in one trial (Maude *et al.* 2014; Schuster *et al.* 2017). As observed previously, treatment with CTL019 CAR T-cells was associated with CRS and neurological toxicities, however toxicity was reversible in all cases (Maude *et al.* 2014; Schuster *et al.* 2017).

Corroboration of the early phase 1 trial results in this larger cohort of CTL019 CAR T-cell treated patients justified the progression of this therapy through to phase 2 trials. Thus, two large, multicentre trials were established, both of which are ongoing. The first trial, the ELIANA trial, commenced in April 2015 and examines CTL019 CAR T-cell therapy in paediatric patients with relapsed or refractory B-cell ALL and high risk B-cell ALL. A total of 75 patients across 25 study centres have been infused with a single dose of CTL019 CAR T-cells, with a median dose of 1×10^8 CAR T-cells infused (Maude *et al.* 2018). The second phase 2 study is the JULIET trial, which investigates CTL019 CAR T-cell therapy in adult patients with diffuse large B-cell lymphoma (DLBCL). This study commenced in July 2015, with a total of 111 patients over 28 study centres infused with a single dose of CTL019 CAR T-cells, with a median dose of 3×10^8 CAR T-cells (Schuster *et al.* 2018). The majority of patients were lymphodepleted prior to CAR T-cell infusion in both studies. CTL019 CAR T-cells expanded in patients and were detected in the blood for up to 2 years. Objective response rates of 52-81% were observed in these studies, with 59% of patients achieving progression free survival at 12 months in the ELIANA trial (Maude *et al.* 2018). Of those patients who relapsed, the majority presented with CD19-negative disease. CRS and neurotoxicities were common adverse effects associated with CTL019 treatment; CRS was observed in 77% and 58% and neurotoxicities in 40% and 21% of CTL019-treated patients in the ELIANA and JULIET trials, respectively. The interim analyses of these two studies suggest impressive antitumour efficacy of CTL019 CAR T-cells in these patient populations, with up to 81% of patients exhibiting a response. As a result, CTL019 CAR T-cells, marketed as Kymriah (tisagenlecleucel), were granted FDA approval for the treatment of children and young adults with relapsed or refractory B-ALL in 2017 and the treatment of adult patients with DLBCL in 2018 (Seimetz *et al.* 2019).

1.4.3.2 Yescarta (*axicabtagene ciloleucel*)

Like Kymriah, the Yescarta (a.k.a axicabtagene ciloleucel, axi-cel, KTE-C19) story begins with the comparison of two CAR designs. Both CARs contained the scFv of the CD19-targeting FMC63 antibody, to recognise the CD19 antigen, but one CAR was second generation (containing the CD28 signalling domain; FMC63-28z) and the other was third generation (incorporating both the CD28 and 4-1BB signalling domains; FMC63-CD828BBz). Superior transduction efficiency was achieved in human T-cells transduced with the retrovirus encoding the FMC63-28z construct compared to the FMC63-CD828BBz construct. Furthermore, FMC63-28z CAR T-cells displayed greater expansion and cytokine production following stimulation with CD19-expressing CLL cells (Kochenderfer *et al.* 2009). The first and third ITAMs of CD3 ζ have been shown to mediate T-cell apoptosis and so inactivation of CD3 ζ ITAM 1 and 3 in this CAR construct was performed to investigate whether it would enhance the function of these CD19-targeting FMC63-28z CAR T-cells. The CAR T-cells with inactivated first and third ITAMs of CD3 ζ displayed enhanced survival and decreased non-specific activation *in vitro*. The transduction efficiency of T-cells with this modified FMC63-28z CAR was higher than had previously been observed with FMC63-28z, confirming no negative impact on the proportion of T-cells successfully transduced with the modified CAR (J. N. Kochenderfer *et al.* 2010). The superior *in vitro* results observed with this modified CAR led to its selection for further testing. In an intraperitoneal (IP) murine 38c13 lymphoma model, treatment with the modified FMC63-28z CAR T-cells resulted in all animals in the treatment group surviving 140 days post-CAR T-cell infusion, while mice that had either been treated with target irrelevant CAR T-cells or were treatment-naive had 0% survival at this time-point. Interestingly, the survival benefit following FMC63-28z treatment was only observed in mice pre-treated with 5 Gy total body irradiation to enhance CAR T-cell engraftment and dosed with IL-2 alongside CAR T-cell treatment. Long-term survival was also significantly improved in FMC63-28z-treated mice bearing subcutaneous 38c13

tumour masses, which were eradicated by the administration of FMC63-28z CAR T-cells but not irrelevant CAR T-cells (James N. Kochenderfer *et al.* 2010).

The first patient was treated with FMC63-28z CAR T-cells by Kochenderfer and colleagues in 2010 at the National Cancer Institute (NCI) (J. N. Kochenderfer *et al.* 2010). The patient was diagnosed with refractory grade 1 stage IVB CD19⁺ follicular lymphoma. CAR T-cells were generated by transducing patient PBMCs with the FMC63-28z construct, achieving a 64% transduction efficiency. The patient was treated with lymphodepleting chemotherapy before 1×10^8 CAR T-cells were administered intravenously (IV). The next day, a second dose of 3×10^8 CAR T-cells was given and an IL-2 dosing regime was commenced with the patient receiving a dose of IL-2 every 8 hours for a total of 8 doses, to enhance T-cell activity. CAR T-cells expanded in the patient and were detected in the blood from 1 to 27 weeks after CAR T-cell treatment. CT scans revealed an impressive partial remission of the lymphoma for a duration of 32 weeks before progressive CD19⁺ disease was observed in the lymph nodes. The CAR T-cells were well-tolerated by this patient, with the only notable side effect being fever which lasted for two days. The patient was discharged 11 days after the second CAR T-cell dose (J. N. Kochenderfer *et al.* 2010). This first-in-human trial demonstrated that FMC63-28z CAR T-cells were safe when administered at this dose and that treatment with the CD19-targeting CAR T-cells was able to induce partial remission of lymphoma in the first patient for which there was sufficient follow-up for analysis.

Promising first-in human results justified the continuation of FMC63-28z CAR T-cells through clinical trials. A phase 1 study was subsequently conducted with 8 patients diagnosed with relapsed indolent B-cell non-hodgkin's lymphoma (NHL) or CLL (Kochenderfer *et al.* 2012). All patients were given lymphodepleting chemotherapy before receiving a single dose of FMC63-28z CAR T-cells ($0.3-3 \times 10^7$ cells/kg), followed by a course of IL-2 treatment. One patient was treated with a second dose of CAR T-cells 7 months after the initial infusion due to progressive disease. Of the 7 evaluable

patients, 6 patients achieved complete or partial remission that lasted a minimum of 7 months with 2 patients continuing in remission for more than a year at the time of the report. CAR T-cell persistence was varied, with some patients having no detectable CAR T-cells within 20 days and other having readily detectable CAR T-cells for at least 130 days. Toxicity was significant in this study, with FMC63-28z treatment resulting in prolonged B-cell aplasia lasting 6 months or more in 4 patients, as well as hypotension, fever, fatigue, renal failure and obtundation. These toxicities were associated with higher levels of inflammatory cytokines such as TNF α and interferon- γ (IFN- γ). All toxicities peaked by 8 days post-infusion and resolved completely over time (Kochenderfer *et al.* 2012).

With the aim of reducing the acute toxicities observed in the above study, the next cohort of 6 patients with indolent B-cell malignancies were given lower FMC63-28z CAR T-cell doses ($1-5 \times 10^6$ cells/kg) and no post-infusion IL-2. Seven patients diagnosed with refractory DLBCL, the most aggressive form of NHL, were also treated in this study. As before, all patients with indolent B-cell malignancies demonstrated complete or partial remission following FMC63-28z CAR T-cell therapy. Interestingly, the absence of post-infusion IL-2 did not perturb CAR T-cell efficacy, suggesting it is not necessary for FMC63-28z CAR T-cell efficacy. Of the 7 treated DLBCL patients, 4 patients achieved complete remission, 2 patients achieved partial remission and 1 patient had stable disease. As previously, toxicities associated with cytokine elevation as well as some neurotoxicities were observed in the patients, however, all adverse effects were transient and reversible (Kochenderfer *et al.* 2015). Importantly, long-term follow up of treated DLBCL patients demonstrated that eventually 5 out of 7 patients achieved complete remission and 4 of these had durable remission lasting more than 38 months, with none of these 4 cases of lymphoma having relapsed at the time of publication (J. N. Kochenderfer *et al.* 2017).

To further address the toxicities associated with FMC63-28z CAR T-cell therapy, a cohort of 22 patients with relapsed or refractory advanced stage lymphoma were treated. In this study, the patients were pre-treated with lower doses of lymphodepleting chemotherapy, as well as receiving the lower CAR T-cell doses administered in the previous study (J. N. Kochenderfer *et al.* 2017). The authors hypothesised that this amended treatment regime would result in comparable anti-lymphoma effects of the CAR T-cell treatment but with less toxicity, as well as aiding in the clearer evaluation of CAR T-cell efficacy, given the lymphodepleting chemotherapy can also have anti-lymphoma activity. The overall remission rate in this study was 73%, with 55% achieving complete remission. The complete remissions were all ongoing (7-24 months) at the time of the report. As before, CAR T-cells reached peak expansion at a median of 8.5 days and remained detectable for up to 3 months. In this study, remission was associated with a higher CAR T-cell number at peak expansion, while the levels of IL-15 and IL-10 in the serum before CAR T-cell therapy were correlated with peak CAR T-cell number. Overall, treatment-associated toxicity was reduced in this study when compared to those studies conducted previously, although patients with higher numbers of CAR T-cells were more likely to experience adverse effects, particularly neurotoxicity (James N. Kochenderfer *et al.* 2017).

Achieving a reduction in overall toxicity associated with FMC63-28z CAR T-cells led to the establishment of the ZUMA-1 trial, a multicentre phase 1/2 trial spanning 36 study centres, in collaboration with Kite Pharma. The ZUMA-1 trial began in January 2015 and recruited 307 patients with either relapsed or refractory DLBCL, transformed follicular lymphoma, primary mediastinal B-cell lymphoma or high grade B-cell lymphoma. Patients in this trial were pre-treated with the low dose lymphodepleting chemotherapy regime established in the previous study (James N. Kochenderfer *et al.* 2017), before receiving $1-2 \times 10^6$ FMC63-28z CAR T-cells, now known as KTE-C19 CAR T-cells. The initial phase 1 study of the Zuma-1 trial involved 7 patients and reported an

overall remission rate of 71%, with 3 patients remaining in complete remission at 12 months. KTE-C19 CAR T-cells were well tolerated in this cohort with only 1 patient experiencing grade 4 CRS, which was reversible (Locke *et al.* 2017). Therefore, this treatment regimen was deemed safe for further study in phase 2. In this phase 2 study of the Zuma-1 trial, 101 patients were treated with the KTE-C19 CAR T-cell regime and interim analysis revealed an objective response rate of 82%. At 15.4 months post-infusion, 40% of patients had achieved complete remission and overall survival at 18 months was 52%. As previously, higher levels of circulating CAR T-cells were associated with increased response but also with adverse toxicities. Grade ≥ 3 CRS and neurotoxicity was observed in 13% and 28% of patients, respectively and all toxicities were reversible as before (Neelapu *et al.* 2017). Recently, an updated analysis has been published, addressing the long-term safety and efficacy of KTE-C19 CAR T-cells in these patients. The median follow-up was 27.1 months and there was an overall response rate of 83%, with 58% CRs, and a median response duration of 11.1 months. There were few additional reported toxicities at this stage (Locke *et al.* 2019).

The impressive results from the ZUMA-1 trial lead to the FDA approval of KTE-C19 CAR T-cells, marketed as Yescarta, for second-line treatment of DLBCL in October 2017 (Seimetz *et al.* 2019). An additional phase 1/2 trial, known as ZUMA-6, was also established to investigate the efficacy of Yescarta therapy in combination with Atezolizumab, an anti-programmed death-ligand 1 (PD-L1) checkpoint inhibitor. Interim results from this trial are currently awaited (ClinicalTrials.gov 2020).

1.4.3.3 *Abecma (idecabtagene vicleucel)*

Abecma (a.k.a idecabtagene vicleucel, ide-cel, bb2121) is a second generation CAR T-cell that targets B-cell maturation antigen (BCMA), a member of the TNF-receptor superfamily which is expressed at only low levels in normal tissue, but is consistently upregulated on malignant plasma cells from multiple myeloma (MM) patients (Tai *et al.*

2013). Preclinical studies utilising NOD scid gamma (NSG) xenograft models of MM demonstrated that doses of $5-10 \times 10^6$ bb2121 CAR T-cells could effectively induce tumour regression, with bb2121 CAR T-cell treated mice surviving to experiment termination in all cases. This was an improvement over the efficacy of the protease inhibitor bortezomib, a current line of treatment for MM patients in the clinic (Friedman *et al.* 2018). These striking results prompted the recruitment of 33 patients for a phase 1 study. In line with common practice, patients were lymphodepleted with fludarabine and cyclophosphamide prior to treatment with a targeted ide-cel dose of between $50-800 \times 10^6$ CAR T-cells. CAR T-cells expanded in all patients and persisted for up to a year post-transfusion. CRS was observed in 25 patients, however this was never more severe than grade 3 and resolved in all patients. Neurotoxicity and infection was observed in 14 patients each, however, again, these complications were resolved in all patients. The objective response rate of ide-cel treatment was 85%, with 15 patients achieving a complete response. Of those 15 patients, 9 continued to respond with a median follow-up of 11.3 months. Median progression free survival was 11.8 months in this study (Raje *et al.* 2019). The phase 2 study for Abecma, the KarMMa trial, involved 128 patients lymphodepleted with fludarabine and cyclophosphamide and treated with ide-cel at target doses of 150, 300 and 450×10^6 CAR T-cells in 4, 70 and 54 patients, respectively. CRS was observed in 107 patients, mostly at grade 1 or 2, however 7 patients had \geq grade 3 CRS and one patient died from this. A further 3 patients died from ide-cel related adverse events (bronchopulmonary aspergillosis, gastrointestinal haemorrhage and cytomegaloviral pneumonia). At a median follow-up of 13.3 months 94 patients had a response to ide-cel with a complete response or better being observed in 25%, 29% and 39% of patients treated with 150, 300 and 450×10^6 CAR T-cells, respectively. The overall median progression free survival was 8.8 months in this study, extended to 12.1 months in patients treated with a dose of 450×10^6 CAR T-cells (Munshi *et al.* 2021). Abecma was approved by the FDA in March 2021 for the treatment of adult

patients with relapsed or refractory MM after four or more prior lines of therapy, including an immunomodulatory agent, a proteasome inhibitor and an anti-CD38 monoclonal antibody.

1.4.3.4 Tecartus (*brexucabtagene autoleucl*)

Tecartus (a.k.a brexucabtagene autoleucl, KTE-X19) is a second generation CAR T-cell designed to target CD19, similarly to Yescarta and Kymriah. Preclinical evaluation at the NCI demonstrated that these CD19-targeting CAR T-cells were able to eradicate established subcutaneous 38c13 lymphoma in female CH3 mice. This resulted in long-term survival of CAR T-cell treated mice up to 140 days post-T-cell infusion, with all controls being sacrificed due to lymphoma burden within 3 weeks of T-cell infusion (James N. Kochenderfer *et al.* 2010). A phase 1 study was recruited between 2012-2014 to assess the safety and tolerability of KTE-X19 CAR T-cells, with 21 young patients (1-30 years old) with relapsed or refractory ALL or NHL being recruited. After fludarabine and cyclophosphamide lymphodepletion, the maximum tolerated dose was found to be 1×10^6 KTE-X19 CAR T-cells per kg of body weight and at this dose the most severe adverse event observed was grade 4 CRS. CRS was reversible in all patients, however one patient required resuscitation following cardiac arrest. Reversible neurotoxicity occurred in 6/21 patients. Complete response was observed in 66.7% of patients, with an overall survival of 51.6% at a median follow-up of 10 months (Lee *et al.* 2015). Following this initial trial, a phase 1/2 study was recruited between 2016-2018 under the name ZUMA-3. Patients with adult relapsed/refractory B-ALL were lymphodepleted with fludarabine and cyclophosphamide and 23 patients were treated with the previously determined MTD of 1×10^6 KTE-X19 CAR T-cells per kg. No fatal adverse events occurred in this cohort of patients. Grade 3 or higher CRS and neurotoxicity was observed in approximately a third of patients, however this was resolved in all cases. Overall remission rate following 1×10^6 KTE-X19 CAR T-cells per kg was 83% at a median follow-up of 22.1 months, with the median duration of relapse-free survival being

7.7 months (Shah *et al.* 2021). The second phase of this study remains ongoing, however Tecartus was approved by the FDA for treatment of adult patients with relapsed or refractory B-ALL in October 2021.

1.4.3.5 Breyanzi (*lisocabtagene maraleucel*)

Breyanzi (a.k.a lisocabtagene maraleucel, JCAR017) is another second generation CD19-targeting CAR T-cell therapy. Breyanzi can be differentiated from other CD19-targeting CAR T-cell therapies in that it is infused in two separate components: CD4⁺ and CD8⁺ CAR T-cell infusions at a 1:1 ratio. In preclinical studies, a 1:1 ratio of delivered CD4⁺ and CD8⁺ CAR T-cells was shown to improve CAR T-cell expansion and anti-tumour activity when compared to either T-cell component alone. Further, treatment with this CAR T-cell product resulted in the regression of Raji tumours and long-term survival of NSG mice (Sommermeyer *et al.* 2016). As Kymriah and Yescarta, which are also CD19 directed CAR T-cells, are tolerated in the clinic, a large scale phase 1 trial (TRANSCEND) for Breyanzi was recruited between 2016 and 2019 across 14 cancer centres in the USA. Recruited patients were adults with relapsed or refractory large B-cell lymphomas and, of note, were a more diverse cohort in terms of disease subtype than those recruited for the ZUMA-1 and JULIET trials. Following fludarabine and cyclophosphamide lymphodepletion, a dose of between 50-150 x 10⁶ CAR T-cells was delivered to patients. All doses were generally well tolerated with grade 3 or higher CRS and neurological events being observed in 2% and 10% of patients, respectively. However, 1 patient given 50 x 10⁶ CAR T-cells died due to CAR T-cell associated diffuse alveolar damage. At a median follow-up of 18.8 months, complete response was observed in 53% of patients, with a median progression free survival of 6.8 months and median overall survival of 21.1 months (Abramson *et al.* 2020). Breyanzi was approved by the FDA in February 2021 for the treatment of adult patients with relapsed or refractory large B-cell lymphoma after two or more lines of systemic therapy.

1.4.4 *Managing CAR T-cell associated toxicity*

Consideration of CAR T-cell toxicities is an important part of my thesis studies, consequently these are discussed in detail below. Clinical trials for CD19-targeting CAR T-cells revealed two main toxicities: CRS and neurotoxicity. CRS is a systemic inflammatory response that was first described as a toxicity associated with the anti T-cell antibody muromonab-CD3 (OKT3) (Chatenoud *et al.* 1989). Subsequently, CRS has been described as a toxicity associated with many immunotherapies, including checkpoint inhibitors (Rotz *et al.* 2017; Dimitriou *et al.* 2019; Honjo *et al.* 2019). A fever of $\geq 38^{\circ}\text{C}$ is usually the first objective sign of CRS, which is sometimes followed by more severe symptoms (Hay *et al.* 2017). CRS can be categorised into 5 severity grades that range from grade 1, where mild, non-life threatening symptoms like fever, nausea, fatigue and headache are present, to grade ≥ 4 , where there are life-threatening symptoms including organ toxicity and respiratory failure which may result in death (Lee *et al.* 2014). Immune effector cell-associated neurotoxicity syndrome (ICANS) may occur during CRS or after CRS has subsided. Clinical presentation typically includes toxic encephalopathy with speech impairments, aphasia and confusion, however more severe cases involving decreased levels of consciousness, coma, seizure, motor weakness and cerebral oedema have been reported (D.W. Lee *et al.* 2019)

CRS and ICANS are not usually observed with traditional cancer therapies, thus management of these toxicities was not well established in early CD19 CAR T-cell clinical trials. CRS and ICANS were limiting toxicities for both Kymriah and Yescarta, which resulted in the revision of their dosing schedules, however CRS and ICANS remained present in future patient populations (Maude *et al.* 2014; Kochenderfer *et al.* 2015). As these toxicities could not be managed by amended dosing regimens, alternative approaches to directly treat CRS and ICANS have been explored.

1.4.4.1 *Managing Cytokine Release Syndrome (CRS)*

CRS is an inflammatory condition resulting from T-cell activation and expansion, thus higher numbers of circulating CAR T-cells in patients results in more severe CRS (Kalos *et al.* 2011; Shimabukuro-Vornhagen *et al.* 2018). Owing to this, initial attempts to manage CRS turned to anti-inflammatory corticosteroids. Although corticosteroid treatment has been reported to successfully manage CRS (Porter *et al.* 2011; Brentjens *et al.* 2013; Grupp *et al.* 2013), the potential for impaired CAR T-cell efficacy to occur concurrently is of concern. CAR T-cell activation results in the subsequent activation of bystander immune and non-immune cells, such as macrophages and endothelial cells, respectively (Shimabukuro-Vornhagen *et al.* 2018). Activation of these cells results in an elevation in serum cytokines, such as IL-6, IFN- γ , IL-1 and TNF- α , which may be targeted directly to manage CRS (Lee *et al.* 2014). As serum IL-6 levels peaks during maximal T-cell proliferation (Teachey *et al.* 2016), IL-6 targeting was investigated as an approach to managing CRS. Patients suffering severe CRS after T-cell therapy were given tocilizumab, a monoclonal antibody against the IL-6 receptor primarily used to treat arthritis, which resulted in rapid reversal of life-threatening CRS (Grupp *et al.* 2013; Teachey *et al.* 2013). Tocilizumab is now a widely accepted treatment for CRS and is incorporated into many CAR T-cell toxicity management strategies (Le *et al.* 2018).

CRS following CAR T-cell therapy is universally managed via a graded intervention system. Patients with grade 1 CRS typically receive supportive care such as IV fluid hydration and antipyretics. For patients with grade 2 CRS, Tocilizumab is generally administered, with or without accompanying corticosteroids, alongside supportive care. For grade 3 or 4 CRS patients require intensive care, along with administration of a more rigorous Tocilizumab and corticosteroid regime (Neelapu *et al.* 2018).

Patients with CRS may also have concurrent haematological disorders which are more common in patients with severe CRS. These include, but are not limited to, hypotension, coagulopathy and capillary leak (Hay *et al.* 2017). Disseminated intravascular coagulation has been reported in patients with severe CRS which was associated with poor prognosis. When present, it is vital that coagulation disorders are managed alongside CRS, with treatments including platelet transfusion and replacement of coagulation factors (Wang *et al.* 2019).

In a comprehensive analysis of CRS kinetics, Hay and colleagues identified several predictive factors which positively correlated with CRS severity. These included, but were not limited to, bone marrow tumour burden, the number of CD8⁺ CAR T-cells infused and the severity of thrombocytopenia at dosing. These data suggest there are factors that may identify a patient at increased risk of developing CRS. Analysis of these factors prior to CAR T-cell infusion may influence the CAR T-cell treatment regime and the aftercare administered to each patient (Hay *et al.* 2017).

1.4.4.2 *Managing Immune Effector Cell-Associated Neurotoxicity Syndrome (ICANS)*

Although CAR T-cell associated CRS has been well characterised, to date CAR T-cell associated ICANS is less well understood. In most cases, ICANS manifests after the onset of CRS and its incidence has been reported to correlate with CRS severity. ICANS severity also correlates with peak cytokine elevation (Gust *et al.* 2017; Neelapu *et al.* 2017; Santomasso *et al.* 2018). Analysis of cerebrospinal fluid from patients with severe ICANS revealed elevated cytokine, protein and leukocyte concentrations when compared to matched samples taken prior to CAR T-cell therapy, suggestive of increased blood-brain-barrier permeability. CAR T-cells were also detected in the cerebrospinal fluid. Further to this, *in vitro* analysis of human brain pericytes exposed to high concentrations of cytokines associated with CRS revealed an increase in pericyte IL-6 and VEGF secretion, both of which can activate endothelial cells and lead to

increased permeability of the blood-brain-barrier (Gust *et al.* 2017). Taken together these results suggest that the inflammatory phenotype associated with CRS leads to increased blood-brain-barrier permeability which allows the increased infiltration of multiple factors into the central nervous system (CNS). Analysis of brain tissue from patients who experience severe ICANS has confirmed increased cerebral endothelial activation which was paired with evidence of vascular disruption (Gust *et al.* 2017).

As previously discussed, Tocilizumab treatment rapidly resolves CRS in most patients (Grupp *et al.* 2013; Teachey *et al.* 2013). As ICANS is associated with CRS severity, the effect of Tocilizumab treatment on ICANS has been studied. Time to ICANS resolution following Tocilizumab treatment was longer than time to resolution of CRS, suggesting treatment of CRS is important for the resolution of ICANS (Gust *et al.* 2017; Santomasso *et al.* 2018). Recent studies have suggested that macrophage-secreted IL-1 has an important role in CAR T-cell associated toxicity (Giavridis *et al.* 2018). In a murine model of CAR T-cell induced CRS and ICANS, Anakinra, an IL-1 receptor (IL-1R) agonist, abolished both CRS and ICANS (Norelli *et al.* 2018). Therefore IL-1R blockade may present an alternative approach for the concurrent treatment of CRS and ICANS.

ICANS is managed via grade-based intervention similar to that of CRS. Patients with grade 1 or 2 ICANS are primarily managed with supportive care and diagnostic tests to rule out more severe underlying symptoms. Tocilizumab is administered only if CRS occurs simultaneously. Grade 3 ICANS is usually treated with corticosteroids with the patient also receiving supportive and diagnostic care. Grade 4 ICANS usually requires intensive care along with intubation and mechanical ventilation (Neelapu *et al.* 2018). Factors found to be predictive of ICANS severity were similar to those predictive of CRS severity, providing further support for that ICANS presents as a direct consequence of CRS (Gust *et al.* 2017). These data suggest that analyses of these factors prior to CAR T-cell therapy may aid in predicting the ICANS severity grade a patient may develop,

thus allowing for the appropriate consideration and preparation to be made ahead of CAR T-cell treatment.

1.4.4.3 Managing Tumour Lysis Syndrome

Tumour lysis syndrome (TLS) results from rapid tumour cell death leading to the release of intracellular metabolites, such as nucleic acids, proteins, phosphorous and potassium from lysed malignant cells. Elevation of these factors can result in hyperuricemia, hyperkalaemia, hyperphosphatemia, with or without hypocalcaemia and uraemia that may lead to renal failure, arrhythmias, seizures and even death (Cairo *et al.* 2010). TLS post-CAR T-cell infusion has been reported, however incidence is not common and rarely results in fatalities (Neelapu *et al.* 2017; Maude *et al.* 2018). As TLS can occur as a consequence of treatment with other non-immunology anti-cancer agents, TLS treatment regimens have been well established. Patients are treated with intensive care regimes, including increased hydration protocols, administration of rasbcurase, cardiac monitoring and, in more severe cases, renal dialysis (Jones *et al.* 2015). Patients who have a high tumour burden or elevated serum uric acid levels prior to commencing CAR T-cell therapy have a higher risk of developing TLS and thus it is recommended that they should receive prophylactic hydration and allopurinol or rasbcurase (Jones *et al.* 2015; Neelapu *et al.* 2018).

1.4.5 Limitations of CAR T-cell therapy in solid tumours

Despite the success in treating haematological cancers, targeting solid tumours using CAR T-cell therapy has proven difficult. Clinical trials testing a number of solid tumour-targeting CAR T-cells have demonstrated modest results at best (Slovin *et al.* 2013; Beatty *et al.* 2014; Nabil Ahmed *et al.* 2015; Katz *et al.* 2015; Junghans *et al.* 2016; O'Rourke *et al.* 2016). The reasons for the limited success of CAR T-cells in solid tumours are several. First, selecting an appropriate, tumour-specific target can be

problematic as most solid tumours are epithelial in origin. Therefore, many tumour cell antigens will also be expressed in normal epithelial tissue. An example of this is the HER2 antigen which is highly expressed by the HER2⁺ subset of breast cancers. When used clinically for the first time, HER2-targeting CAR T-cells resulted in patient death 5 days post-infusion. This was attributed to on-target, off-tumour toxicity in which the CAR T-cells attacked low level HER2-expressing epithelial cells in the lungs (Morgan *et al.* 2010). HER2-targeting CAR T-cells have since been administered to patients without significant toxicity by using a lower dose with concurrent chemotherapy (N. Ahmed *et al.* 2015). Dose-limiting toxicities observed in patients treated with carboxy-anhydrase-IX (CAIX) targeting CAR T-cells further exemplify the challenge of identifying tumour-specific antigens for CAR T-cell therapy in solid tumours. Patients with metastatic renal cell carcinoma were treated with $0.2-21 \times 10^9$ anti-CAIX CAR T-cells and in subset of patients grade 2-4 liver enzyme disturbances were observed resulting in clinical intervention and termination of treatment. Further investigation revealed CAIX expression on the epithelial cells of the bile ducts and the authors conclude that on-target, off-tumour targeting of these cells is likely to be responsible for the anti-CAIX CAR T-cell associated toxicity observed in this study (Lamers *et al.* 2013). These events demonstrate that CAR T-cell therapy can result in severe normal tissue toxicity, even with low levels of antigen expression, thus highlighting the importance of careful selection and evaluation of tumour-associated antigens for solid tumour CAR T-cell therapy.

On-target, off-tumour toxicity has also been observed in a preclinical study utilising CAR T-cells targeting the GD2 ganglioside antigen, a protein abundant on the surface of neuroblastoma cells. In this study, treatment of neuroblastoma xenografts in mice with anti-GD2 CAR T-cells resulted in lethal CNS toxicity due to extensive CAR T-cell infiltration and proliferation within the brain that ultimately resulted in fatal neuronal destruction (Richman *et al.* 2018). It must be noted, however, that in this study the scFv region of the anti-GD2 CAR T-cells was affinity matured (E101K-14g2a) in an attempt to

improve anti-tumour activity. It has been demonstrated, both by Richman and colleagues and others, that CAR T-cells generated from the E101K-14g2a scFv demonstrate higher tonic signalling and cytokine release in response to GD2⁺ cell lines when compared to the original non-matured scFv (14g2a) (Majzner *et al.* 2018; Richman *et al.* 2018). Preclinical studies utilising anti-GD2 CAR T-cells containing the 14g2a scFv, or the E101K-14g2a scFv in a CAR construct containing a CD28 co-stimulatory molecule in place of 4-1BB, have demonstrated effective tumour-targeting in the absence of neurotoxicity (Long *et al.* 2015; Long *et al.* 2016; Mount *et al.* 2017; Majzner *et al.* 2018). Further, clinical studies treating neuroblastoma patients with anti-GD2 CAR T-cells have shown expansion of anti-GD2 CAR T-cells in patients, without any evidence of neurotoxicity (Heczey *et al.* 2017; Straathof *et al.* 2020). Therefore, these studies demonstrate that GD2 can be targeted safely using CAR T-cells and highlight the need for caution when attempting to improve the anti-tumour activity of CAR T-cells by increasing affinity for their target antigen.

The second hurdle encountered when using CAR T-cells to treat solid tumours is the physical barriers the T-cells face when infiltrating the tumour. Many solid tumours have a dense, fibrotic TME that must be penetrated by the CAR T-cells for them to reach their tumour cell targets (Jiang *et al.* 2017). Further to this, many solid tumours have an aberrant tumour vasculature which also contributes to poor delivery of CAR T-cells to the tumour (Schaaf *et al.* 2018). The barrier to CAR T-cell tumour infiltration may even begin at the vascular wall, where high levels of endothelin B receptor (ET_BR) on the tumour endothelium decrease T-cell adhesion through deregulation of intracellular adhesion molecule 1 (ICAM-1) (Buckanovich *et al.* 2008).

The final hurdle CAR T-cells face in solid tumours is the harsh physical and chemical environment that they must survive and activate in. Many solid tumours secrete immunosuppressive factors and thus have poor T-cell infiltration and survival. This is accentuated by the lack of T-cell chemokines being secreted by the TME, making it

difficult for T-cells to migrate into the tumour to reach the tumour cells (Nagarsheth *et al.* 2017). CAR T-cells directed against ovarian cancer cells have been tested in the clinic, however they demonstrated limited persistence and efficacy, which was attributed to T-cell inhibitory activity in the tumour (Kershaw *et al.* 2006). Further to this, upregulation of T-cell inhibitory enzymes, coupled with the expression of inhibitory receptors on the cell surface of the CAR T-cells, was attributed to a rapid loss of functionality in mesothelin-targeting CAR T-cells (Moon *et al.* 2014). One of the inhibitory receptors that was upregulated on the CAR T-cells was programmed cell death protein 1 (PD-1). PD1, along with a second inhibitory receptor cytotoxic T-lymphocyte-associated protein 4 (CTLA-4), have generated significant interest as immune checkpoint molecules (Leach *et al.* 1996; Freeman *et al.* 2000). In an inflammatory environment, many tumour cells upregulate PD-1 and CTLA-4 ligands, which in turn propagates T-cell suppression. Antibody mediated blockade of these molecules, known as immune checkpoint inhibition, has shown remarkable clinical activity in enhancing T-cell activation and infiltration for the treatment of solid tumours (Seidel *et al.* 2018). Therefore, combination of CAR T-cell therapy with immune checkpoint inhibitors may improve CAR T-cell infiltration and activity in solid tumours (John *et al.* 2013). As well as chemical factors, there are also metabolic factors that suppress CAR T-cell activity within solid tumours. For example, when effector T-cells become activated, they switch from oxidative phosphorylation to glycolysis to allow for faster proliferation (Warburg *et al.* 1958; MacIver *et al.* 2013). However the TME is often depleted of glucose by the tumour cells, which significantly limits T-cell proliferation (Chang *et al.* 2015). These environmental factors make CAR T-cell activation and survival within the tumour a difficult and inefficient process.

Taken together, these hurdles present a significant challenge for taking solid tumour CAR T-cell therapy forward. A vast array of innovative research is now underway in attempt to overcome these limitations and this will be discussed further in Section 1.4.7.

1.4.6 CAR T-cells targeting the tumour stroma

1.4.6.1 Targeting cancer associated fibroblasts

To circumvent the problems associated with targeting the malignant cells of solid tumours, an alternative approach may be to target the tumour stromal cells instead. FAP was the first stromal antigen considered for CAR T-cell therapy. FAP is a type 2 dipeptidyl peptidase that was originally identified in CAFs within human sarcomas (Rettig *et al.* 1988). Subsequently, FAP expression has been identified on CAFs in over 90% of common epithelial cancers and is associated with a poor prognosis (Garin-Chesa *et al.* 1990; Saadi *et al.* 2010). Further to this, FAP is largely absent from normal adult tissue, making it a suitable candidate for targeted cancer therapy (Schuberth *et al.* 2013). The FAP binding monoclonal antibody, sibrotuzumab, has demonstrated little clinical benefit in early phase clinical trials, resulting in no further development (Welt *et al.* 1994; Hofheinz *et al.* 2003; Scott *et al.* 2003). Conflicting pre-clinical results have been reported following depletion of FAP-positive cells *in vivo*, with both decreased (Kraman *et al.* 2010) and increased (Özdemir *et al.* 2014; Rhim *et al.* 2014) growth of PDAC tumours being observed.

Despite conflicting results in the efficacy of depleting FAP-positive tumour-associated cells, FAP-targeting CAR T-cells for the treatment of solid tumours were developed by a number of research groups. However, conflicting reports on the effectiveness of these CAR T-cells in treating solid tumours have been published. The first FAP-targeting CAR T-cell was developed by Tran and colleagues at the NCI (Tran *et al.* 2013). This third generation CAR T-cell contains CD28, 4-1BB and the scFv of the mAb FAP5 which recognises both murine and human FAP. FAP5 CAR T-cells demonstrated FAP specific activity *in vitro*, however this did not translate into significant *in vivo* activity. In a range of murine solid tumour models that were preconditioned with 5 Gy total body irradiation, weak or no antitumour activity was observed upon treatment

with $1-2 \times 10^7$ FAP5 CAR T-cells in both C57BL/6 and BALB/c mice. Furthermore, FAP5 CAR T-cell treatment was associated with severe bone marrow hypocellularity and cachexia in both strains, a phenomenon that was not observed in control mice. This toxicity was attributed to the depletion of FAP-positive bone marrow-derived stem cells (BMSCs) by FAP5 CAR T-cells (Tran *et al.* 2013). Conversely, three second generation FAP-targeting CAR T-cells, from independent groups, have demonstrated antitumour efficacy with the absence of CAR T-cell associated toxicities (Kakarla *et al.* 2013; Schuberth *et al.* 2013; Wang *et al.* 2014). Kakarla and colleagues utilised a CD28 containing CAR T-cell generated with the scFv portion of the anti-FAP monoclonal antibody MO36 which, similarly to FAP5, recognises both murine and human FAP (Kakarla *et al.* 2013). These FAP-targeting CAR T-cells demonstrated FAP specific activation and killing *in vitro*, which was not observed with non-transduced T-cells. In an A549 human lung carcinoma xenograft model, three doses of 1×10^7 FAP-targeting CAR T-cells, alongside IL-2, were administered IV at weekly intervals. Mice that received the FAP-targeting CAR T-cells displayed significantly impaired tumour growth when compared to the non-transduced T-cell-treated group. However, the CAR T-cells did not persist well *in vivo* and eventually disease progression was observed in all animals (Kakarla *et al.* 2013). Similar antitumour effects were observed with second generation CD28-containing FAP-targeting CAR T-cells generated from the scFv portion of sibrotuzumab in a mesothelioma xenograft model (Schuberth *et al.* 2013). To note, in these studies the target for the CAR T-cells are the FAP-positive mesothelioma tumour cells rather than the tumour stroma. In an attempt to enhance the persistence of FAP-targeting CAR T-cells, Wang and colleagues generated 4-1BB second generation FAP-targeting CAR T-cells from a murine specific scFv. FAP-targeting CAR T-cells, but not control T-cells, were able to slow tumour growth by 35-50% in syngeneic mesothelioma and lung carcinoma models. However, as before, CAR T-cells did not persist well and depleted significantly after 10 days. Interestingly, no reduction in tumour growth was

observed following CAR T-cell treatment in NSG mice with mesothelioma tumours (Wang *et al.* 2014). These results contrast with the observations by Schuberth *et al.* who did observe a reduction in tumour growth in immunodeficient mice treated with FAP-targeting CAR T-cells (Schuberth *et al.* 2013). This suggests that FAP may have tumour promoting roles that are both dependent and independent of the immune system.

Following reports of antitumour activity of FAP-targeting CAR T-cells in preclinical studies, the first-in-human FAP CAR T-cell was administered in 2015 to a patient diagnosed with malignant pleural mesothelioma. The patient was given 1×10^6 FAP CAR T-cells via pleural effusion, which was well tolerated with no adverse events being recorded (Pircher *et al.* 2015). To date, no follow up to this study has been registered and there are no other clinical trials registered utilising single-targeted FAP CAR T-cells (ClinicalTrials.gov 2020).

1.4.6.2 Targeting the tumour vasculature

A small number of CAR T-cells targeting antigens associated with the tumour vasculature have been developed. CAR T-cells targeting VEGFR-2 have been designed by Steven Rosenberg's group at the NCI (Chinnasamy *et al.* 2010). Direct comparison between first, second (CD28 only) and third (CD28 and 4-1BB) generation CAR T-cells revealed that superior *in vitro* activation and target cell killing was achieved with second and third generation CAR T-cells when compared to first generation CAR T-cells, with second and third generation CAR T-cells comparable one another, with the third generation CAR T-cells demonstrated increased persistence *in vivo* as determined by flow cytometry analysis of treated tumours. In a C57BL/6 syngeneic B16-F10 melanoma model, third generation VEGFR-2-targeting CAR T-cells significantly impaired tumour growth and improved tumour free survival, with doses up to 2×10^7 CAR T-cells being well tolerated. However, comparable experiments in BALB/c mice bearing CT26 or RENCA tumours resulted in severe and fatal toxicity. Interestingly, this toxicity was

attributed to an increased number of CD4⁺ CAR T-cells in the T-cell population isolated from BALB/c mice, as treatment with 2×10^7 purified CD8⁺ CAR T-cells was well tolerated in these mice. Further, C57BL/6 mice treated with 2×10^7 purified CD4⁺ CAR T-cells experienced severe toxicity (Chinnasamy *et al.* 2010). These results suggest that a higher CD4⁺ CAR T-cell population could be associated with CAR T-cell toxicity, however a higher CD8⁺ CAR T-cell population was associated with CRS in patients (Hay *et al.* 2017), thus the composition of the transduced T-cell population should be considered in both preclinical and clinical studies. Despite the promising preclinical activity of VEGFR-2-targeting CAR T-cells, no antitumour response was observed in a phase 1 trial consisting of 24 patients with metastatic melanoma treated with CD8⁺ only VEGFR-2-targeting CAR T-cells, resulting in study termination (ClinicalTrials.gov 2020). Since these results were reported, an additional second generation (CD28) VEGFR-2-targeting CAR T-cell has been designed which contains only the variable domain of the heavy chain (VHH) from an anti-VEGFR-2 mAb. Thus far, this CAR T-cell has demonstrated specific activation and cytotoxicity *in vitro*, however it is yet to be tested in *in vivo* models (Hajari Taheri *et al.* 2019). The approach of using smaller, nanobody CAR constructs will be discussed further in Section 1.4.7.1.

Recently, the integrin-like cell surface protein tumour endothelial marker 8 (TEM8) was identified as a potential tumour vascular target for CAR T-cell therapy (Byrd *et al.* 2018). TEM8 was originally identified by St Croix and colleagues as a marker of colorectal cancer endothelium, in the SAGE screen that identified endosialin as TEM1 (Croix *et al.* 2000). Similarly to endosialin KO mice (see Section 1.3.3.1), TEM8 KO mice exhibit no defects in development or wound healing (Cullen *et al.* 2009), however a number of studies have reported impaired primary tumour growth in TEM8 KO mice (Nanda *et al.* 2004; Fernando and Fletcher 2009; Chaudhary *et al.* 2012). Therefore, CAR T-cells targeting TEM8 were developed by Byrd and colleagues at the NCI (Byrd *et al.* 2018). Similar to VEGFR-2-targeting CAR T-cells, third generation (CD28 and 4-1BB)

CAR T-cells against TEM8 persisted longer *in vivo* when compared to second generation (CD28 only) CAR T-cells. Third generation TEM8 CAR T-cells induced tumour regression in both syngeneic and patient derived xenograft (PDX) models of TNBC and this regression was attributed to the destruction of tumour-associated vascular structures. Further, in a LMD231 metastatic TNBC model, TEM8-targeting CAR T-cells limited metastasis to the bone and the brain, resulting in 100% survival at day 50 in the CAR T-cell-treated group compared to 30% survival in the non-transduced T-cell-treated group. TEM8-targeting CAR T-cells were well tolerated in this study with no signs of on-target/off-tumour toxicity observed. However, this toxicity testing was carried out in immunodeficient mice where the toxicities likely do not manifest to the same extent, for example due to lack of functional macrophages which were previously established to have an important role in CAR T-cell-mediated toxicities (Giavridis *et al.* 2018; Byrd *et al.* 2018).

Taken together, these results suggest that targeting the tumour vasculature with CAR T-cells presents a promising alternative approach for the treatment of solid tumours, however care should be taken to avoid CAR T-cell related and on-target, off-tumour toxicities. The antitumour efficacy and tolerability of CAR T-cells targeting the tumour vascular target endosialin will be investigated in this thesis.

1.4.7 Next Generation CAR T-cells

Next generation CAR T-cells encompass a range of CAR T-cell designs that were developed with a common aim: to overcome the limitations associated with solid tumour directed CAR T-cell therapy. Approaches have been taken to improve the infiltration, specificity, activation and persistence of CAR T-cells, as well as to limit their toxicity. Although these CAR T-cells are yet to be evaluated clinically, many designs have shown promising result in preclinical studies.

1.4.7.1 *Enhancing CAR T-cell migration and tumour infiltration*

Efficient T-cell migration and infiltration into the tumour tissue relies on a complex tumour-chemokine signalling network, in which factors secreted by the tumour cells interact with T-cell chemokine receptors to regulate T-cell migration (Chow and Luster 2014). Therefore, one approach to improve CAR T-cell infiltration is to co-express a cognate chemokine receptor on the CAR T-cell surface that can promote T-cell migration. CCL2 is a T-cell attracting chemokine that is readily secreted by neuroblastoma cells *in vivo* (Craddock *et al.* 2010). Co-expression of the CCL2 receptor CCR2b on the surface of GD2-targeting CAR T-cells resulted in improved CAR T-cell infiltration and tumour regression in established murine subcutaneous SK-N-AS neuroblastoma tumours (Craddock *et al.* 2010). Similar results have also been observed with the co-expression of CCR4 (Di Stasi *et al.* 2009), CXCR1 or CXCR2 (Jin *et al.* 2019), the chemokine CCL19 (Adachi *et al.* 2018) and CXCR2 (Whilding *et al.* 2019) on the surface of CAR T-cells targeting CD30, CD70, CD20 and $\alpha\beta 6$, respectively. To develop this approach further, considerations have to be made regarding the heterogeneity of the chemokine network between tumour types and even patients, thus a personalised approach may be necessary (Liu *et al.* 2013; Norton *et al.* 2015). Further, caution should be taken to avoid T-cell recruitment to normal tissues that may result in enhanced CAR T-cell associated toxicity (Hillyer *et al.* 2003).

A second approach to enhance CAR T-cell infiltration is to substitute the entire scFv portion of a mAb for the VHH region, known as a nanobody. Being smaller in size, nanobodies based CARs can reach epitopes more proximal to the target cell surface and they are also more stable and less immunogenic. Nanobodies exhibit antigen affinities comparable to their parental scFv molecule, however nanobody-based CAR T-cells require less construct optimisation than scFv-based CAR T-cells (Xie *et al.* 2019). Nanobody-based CAR T-cell design is a recent development in CAR T-cell biology however despite this a number of nanobody-based CAR T-cells have already been

developed and exhibit promising preclinical activity (An *et al.* 2018; Hassani *et al.* 2019; Xie *et al.* 2019; De Munter *et al.* 2020; Hassani *et al.* 2020). Further research is required to determine whether nanobody-based CAR T-cells have superior properties to conventional CAR T-cells. However, if effective, the use of nanobodies may present a more versatile approach to CAR T-cell design.

1.4.7.2 *Enhancing CAR T-cell activation, proliferation and survival*

As well as hindering the infiltration of CAR T-cells into the tumour, factors secreted by the TME can also suppress the activation, proliferation and survival of CAR T-cells once they are in the tumour tissue. Approaches have been taken to generate CAR T-cells capable of modifying the immunosuppressive TME to a more immune-permissive environment. One approach is to armour the CAR T-cells with a pro-inflammatory cytokine that is constitutively or inducibly expressed and secreted upon CAR T-cell activation. CAR T-cells designed in this manner are referred to as T-cells redirected for universal cytokine mediated killing (TRUCKs) and are often considered as the fourth generation CAR T-cells (Tokarew *et al.* 2019).

CAR T-cells targeting folate receptor α (FR α) expressing ovarian cancer cells have previously been trialled in the clinic, however, these CAR T-cells showed limited persistence and efficacy, which was attributed to T-cell inhibitory activity (Kershaw *et al.* 2006). More recently, CAR T-cells directed against the ovarian cancer antigen mucin (MUC) 16 have been armoured with IL-12, a proinflammatory cytokine that can suppress tumour-induced T-regulatory cell activity (Cao *et al.* 2009), in an effort to improve their persistence and activity. Armouring MUC16-targeting CAR T-cells with IL-12 resulted in significantly enhanced proliferation and cytotoxicity *in vitro* and *in vivo*, alongside an overall reduction in CAR T-cell apoptosis. Further, IL-12 armoured CAR T-cells resisted PD-L1 induced inhibition and demonstrated impressive antitumour activity in a syngeneic model of ovarian peritoneal carcinoma (Koneru *et al.* 2015; Yeku *et al.* 2017). A similar

outcome has been achieved by armouring carcinoembryonic antigen (CEA)-targeting CAR T-cells with IL-18, a cytokine that has previously been shown to activate lymphocytes without severe toxicity in patients (Robertson *et al.* 2008). Armoured CEA-targeting CAR T-cells demonstrated superior proliferation and efficacy to non-armoured CAR T-cells in both pancreatic and lung tumour models, and this was attributed to a decrease in immune suppressive cells in the tumour (Chmielewski and Abken 2017). In addition, armouring with IL-18 improved the expansion and survival of CD19-targeting CAR T-cells (Hu *et al.* 2017).

An alternative to cytokine armouring involves armouring CAR T-cells to secrete immune checkpoint inhibiting antibodies. Armouring both CD19-and MUC16-targeting CAR T-cells with scFvs against PD-1 resulted in enhanced lysis of antigen-positive tumour cells and improved overall survival in murine models of hematologic and ovarian cancer (Rafiq *et al.* 2018). Further, the armoured T-cells were able to induce PD-1 inhibition in both an autocrine and paracrine manner, augmenting their own activation as well as that of endogenous T-cells in the TME. Importantly, immune checkpoint inhibitor-armoured CAR T-cells may represent a safer alternative to CAR T-cell and immune checkpoint inhibitor combination therapy, as the immune checkpoint inhibiting antibodies secreted by the CAR T-cells were shown to remain localised to the tumour, thereby alleviating the systemic toxicities associated with immune checkpoint therapy (Rafiq *et al.* 2018). CAR T-cells targeting human carbonic anhydrase IX armoured with anti-PD-L1 antibodies have also shown promising results in a preclinical model of renal cell carcinoma. Several clinical trials have now been initiated to test the safety and efficacy of CAR T-cells that secrete immune checkpoint inhibitors (ClinicalTrials.gov 2020).

An additional approach to improving the function of CAR T-cells is to eliminate proteins that mediate T-cell death. Ren and colleagues describe a system in which CRISPR/Cas9 gene editing is used to generate CAR T-cells deficient of the endogenous T-cell receptor, human leukocyte antigen (HLA) class I molecule and PD-1. CAR T-cells

engineered by this system demonstrated prolonged survival *in vivo*. Interestingly, this system could be expanded to target four genes, in which expression of the endogenous TCR, HLA-1, PD-1 and CTLA-4 was ablated (Ren *et al.* 2017). Although this quadruple ablation is yet to be tested *in vivo*, CAR T-cells without PD-1 and CTLA-4-mediated immunosuppressive signalling are predicted to demonstrate superior *in vivo* persistence and activation.

1.4.7.3 Limiting CAR T-cell associated toxicity and overcoming therapeutic resistance

1.4.7.3.1 Bi-specific CAR T-cells

As previously discussed, most tumour-associated antigens are not truly tumour-specific resulting in off-tumour toxicities following CAR T-cell therapy. Further, expression of tumour-associated antigens is often heterogeneous within a malignant population, thus therapeutic resistance to the CAR T-cells can develop with the target-negative variants escaping under selective pressure. Of concern, therapeutic resistance has been reported following CD19-targeted CAR T-cell therapy in the clinic (Grupp *et al.* 2013; Maude *et al.* 2014). To address the issue of therapeutic resistance, CAR T-cells that are specific for two antigens have been developed. Multiple bi-specific CAR designs have been evaluated, with dual CAR T-cells, split CAR T-cells and tandem CAR T-cells being the most success approaches to date. Dual CAR T-cells are engineered to co-express two complete CAR constructs on the cell surface, which are identical except for the scFv portions (Figure 1.12A). Dual CAR T-cells may activate upon engagement with either CAR antigen alone or both simultaneously, reducing the likelihood of antigen-negative escape variants emerging (Ruella *et al.* 2016). Similarly, tandem CARs can activate upon binding with one or both antigens, however this design incorporates two scFvs linked together within the same CAR construct (Figure 1.12B), thus only relying on effective signalling via one receptor (Grada *et al.* 2013). Conversely, split CARs rely on the engagement of both antigens for activation as the activation and costimulatory signals are separated on two complementary CARs (Figure 1.12C). This generates a

split signalling approach in which the first scFv is ligated to CD3 ζ and the second scFv is ligated to the costimulatory molecule. Engagement of either scFv alone is therefore insufficient for T-cell activation as a complete activation signal is not provided (Wilkie *et al.* 2012).

Activation in the presence of single or multiple tumour-associated antigens renders both dual CAR and tandem CAR T-cells interesting approaches for confronting CAR T-cell associated therapeutic resistance. In the context of CD19 CAR T-cell resistance, CD123 has been identified as an antigen commonly expressed by CD19-negative malignant cells. T-cells designed to co-express complete CD19- and CD123-targeting CARs were able to lyse cells expressing either antigen and showed increased antitumour efficacy *in vivo* when compared to the single CAR-expressing T-cells (Ruella *et al.* 2016). In addition, dual CAR T-cells that target CD19 and CD22 were designed by Autolus. These dual CAR T-cells, known as AUTO3 CAR T-cells, are currently being investigated in clinical trials for the treatment of paediatric B-ALL. Early reports have revealed an objective response rate of 75% with CRS and ICANS rarely reported above grade 1. Importantly, in relapsed patients, no evidence of CD19 or CD22 antigen loss was observed, suggesting patients may be responsive to continued therapy (Amrolia *et al.* 2018).

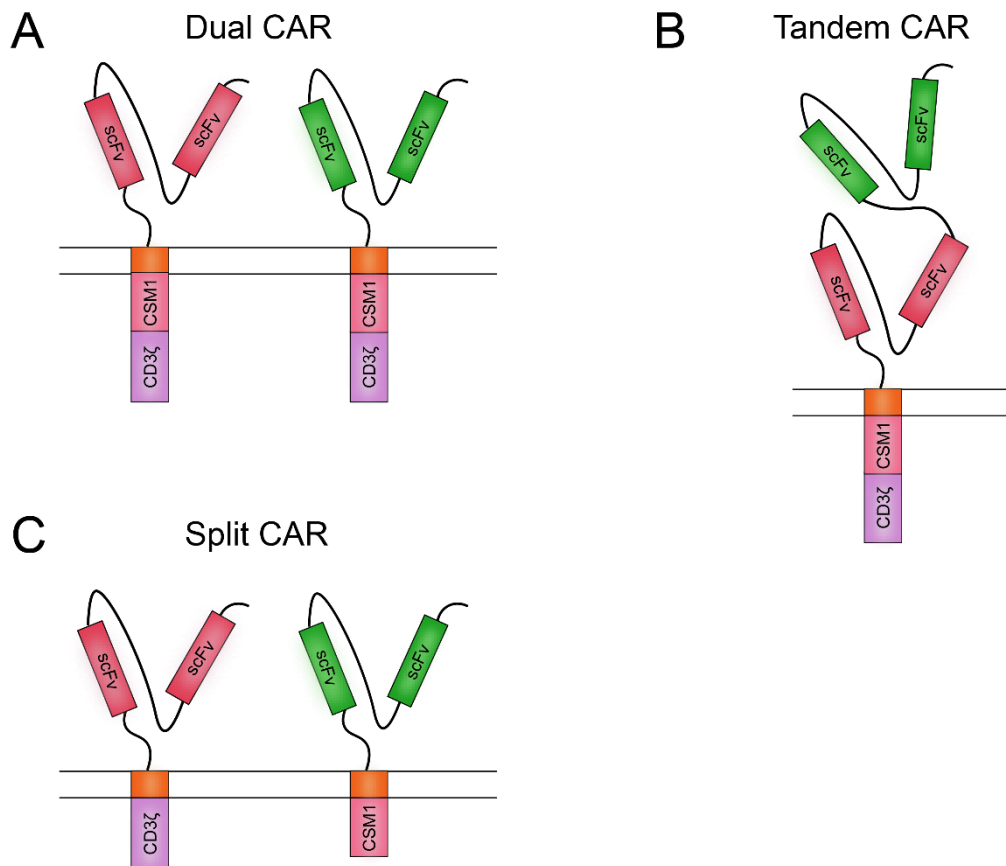


Figure 1. 12 Bispecific CAR T-cells

(A) Dual CAR T-cells simultaneously express two separate second generation CARs against different target antigens. Dual CAR T-cells may be activated by binding to either target antigen alone or both simultaneously. **(B)** Tandem CAR T-cells express a single CAR that has the scFv portion of two different mAbs linked together in its ectodomain. Tandem CAR T-cells may be activated by binding to either target antigen alone or both simultaneously. **(C)** Split CAR T-cells express two complimentary CARs in which one scFv is linked to the T-cell receptor CD3ζ and a different scFv is linked to a co-stimulatory molecule. In this instance, binding of both target antigens is required for T-cell activation.

Tandem CARs offer a more compact design for dual antigen targeting, which does not rely on the efficient transduction of multiple constructs. The concept of tandem CARs was first described by Grada and colleagues (Grada *et al.* 2013), who designed a CAR T-cell that simultaneously targets CD19 and HER2. This proof-of-concept study

demonstrated that tandem CAR T-cells lyse cells positive for either antigen alone, however superior antitumour activity is observed when both CAR targets are expressed by the tumour cells. The antigens HER2 and CD19 are generally associated with different malignancies, thus these CAR T-cells are unlikely to have any clinical benefit. Nevertheless, this study generated substantial interest. T-cells transduced with a tandem CAR engineered to target both CD19 and CD20 demonstrated comparable *in vitro* properties to CD19 single-targeting CAR T-cells, however CD19/CD20 dual-targeting CAR T-cells were able to prevent antigen escape *in vivo*. This translated to improved survival when compared to CD19 single-targeting CAR T-cell treatment (Zah *et al.* 2016). Tandem CARs engineered to target both CD19 and CD20 have also demonstrated increased efficacy and reduced toxicity in high disease burden settings for B-cell malignancies. The superior tolerability of these CAR T-cells was attributed to optimised cell killing with a reduction in cytokine production (Schneider *et al.* 2017).

A unique approach to the tandem CAR design was recently developed by Qin and colleagues (Qin *et al.* 2018) in which the two scFvs are linked in a loop that brings the molecules proximal to one another in the horizontal plane as opposed to the vertical plane. Modifying the scFv linker in this way allowed the CAR construct to recognise both its antigens, CD19 and CD22, with comparable efficiency, which resulted in impressive *in vivo* eradication of ALL cell line xenografts and PDXs from CD19-relapsed patients following treatment with the CAR T-cells (Qin *et al.* 2018). LoopCAR6, the CAR T-cell described here, is now being tested in clinical trials in patients with relapsed or refractory B-ALL or DLBCL (ClinicalTrials.gov 2020). Early phase 1 reports from these trials revealed a dose escalation from $1 \times 10^6/\text{kg}$ to $3 \times 10^6/\text{kg}$ LoopCAR6 resulted in low toxicity, with CRS and ICANS only being reported at grades 1 and 2 in all but one patient (Hossain *et al.* 2018; Schultz *et al.* 2019). There was sufficient time since treatment to report data for 12 ALL patients that were infused with LoopCAR6 (at dose level 1 or 2). All 12 patients achieved an objective response following treatment with LoopCAR6, with

11 out of 12 patients achieving complete remission (Schultz *et al.* 2019). The observed reduction in overall toxicity, alongside impressive and sustained antitumour efficacy, suggests dual-targeting CAR T-cells adopting the described loop design may be superior clinical candidates for the treatment of B-cell malignancies. Further investigation is warranted to confirm whether this dual-targeting approach should be employed in place of the single-targeting strategy currently used in the clinic for B-cell malignancies.

The third class of bi-specific CAR T-cells, split CAR T-cells, were primarily generated to enhance tumour specificity of the CAR in solid tumours. Split CAR T-cells require the engagement of both antigens for complete T-cell activation, which is advantageous as tumour-associated antigens that are not found in close proximity in healthy tissue could be selected as targets, thereby reducing normal tissue toxicity. Conflicting reports on split CAR T-cell efficacy in solid tumours have since been published. Split CAR T-cells designed to target HER2 and MUC1 showed modest cytokine production when co-stimulated and only targeted HER2-positive cells *in vitro* (Wilkie *et al.* 2012). Conversely, split CAR T-cells designed to recognise PSMA and prostate stem cell antigen (PCSA) simultaneously in prostate cancer or mesothelin and FR α simultaneously in ovarian cancer have demonstrated potent anticancer activity *in vivo*. Both of these split CAR T-cells exhibited low or no activity against tumour cells expressing single antigens while displaying potent activity against dual antigen-presenting tumour cells (Kloss *et al.* 2013; Lanitis *et al.* 2013). The increased tumour specificity of these split CAR T-cells is promising in the preclinical setting, however it is yet to be determined whether this will translate into reduced toxicity in the clinic.

1.4.7.3.2 Low affinity CAR T-cells

An alternative approach to limit CAR T-cell associated toxicity is to select a scFv that interacts with its target antigen with a lower affinity, thus reducing CAR T-cell activity in response to low levels of antigen expression. CAR T-cells containing a lower affinity

CD19 scFv have superior tolerability in a phase 1 clinical study, with no patients developing severe CRS (Ghorashian *et al.* 2019). This approach has also shown promise as a strategy to target solid tumours with reduced toxicity. Low affinity CAR T-cells against epidermal growth factor receptor (EGFR) and HER2 have been reported to have reduced activation in the presence of physiological levels of target antigen, whilst maintaining potent antitumour activity (Liu *et al.* 2015). Although in the early stages of development, the approach of substituting the original CAR T-cell scFv molecule for a lower affinity molecule may present an important approach for limiting off-tumour toxicities in the clinic. However, it must be considered that tumour antigen expression is often heterogeneous within a tumour, thus this approach may result in the escape of antigen-low tumour cell variants.

1.4.7.3.3 Inducible CAR T-cell control

CAR T-cell associated toxicities may also be reduced by engineering CAR T-cells so that their number and activity can be controlled *in vivo*. CAR T-cells have been designed to include an activatable “suicide gene” (Casucci *et al.* 2012; Minagawa *et al.* 2016). The most common suicide gene currently used to control T-cell activity is inducible caspase 9, although designs incorporating herpes simplex virus-thymidine kinase (HSV-TK) have also been reported (Bonino *et al.* 1997; Di Stasi *et al.* 2001; Tiberghien *et al.* 2001; Straathof *et al.* 2005). The inducible caspase 9 suicide gene, known as iCasp9, consists of the sequence of a mutated form of the human FK506-binding protein (FKBP2) connected to the gene encoding human caspase 9 with its endogenous caspase activation and recruitment domain deleted. The mutated form of FKBP2 binds with high affinity to a small molecule dimerising agent which results in the dimerisation of iCasp9 and the activation of the mitochondrial apoptotic pathway (Straathof *et al.* 2005; Di Stasi *et al.* 2011). A number of studies have reported this as an effective cell suicide system for adoptive cell transfer therapies, including CAR T-cell therapy, with high levels of CAR T-cell clearance observed within 24 hours (Quintarelli *et al.* 2007; Hoyos *et al.* 2010;

Budde *et al.* 2013; Minagawa *et al.* 2016; Diaconu *et al.* 2017; Stavrou *et al.* 2018; Duong *et al.* 2019).

Although inclusion of a suicide gene in CAR T-cells enables control over associated toxicities, the depletion of CAR T-cell described above is irreversible and may result in disease relapse. To this end, CAR T-cells have been designed that can be more intricately controlled. CAR T-cells with a protease placed between the CAR and a degradation moiety may be controlled by the administration of a protease inhibitor, which results in CAR degradation and decreased expression on the T-cell surface. This approach allows the CAR to be removed from the cell surface without the elimination of the CAR T-cell. Further, ceasing delivery of the protease inhibitor allows CAR expression on the cell surface to resume. Altering the delivered dose of the protease inhibitor therefore can result in more or less CAR expression at the cell surface and thus aid in controlling CAR T-cell associated toxicities. (Juillerat *et al.* 2019). Alternatively, CAR T-cells requiring the administration of a drug to induce CAR expression have also been developed (Wu *et al.* 2015; Sakemura *et al.* 2016; Drent *et al.* 2018; Gu *et al.* 2018). Inducible CAR T-cells have shown antitumour efficacy in solid tumours, as well as haematological malignancies, in preclinical studies (Mata *et al.* 2017).

1.4.7.3.4 CAR T-cell exosomes

An interesting concept explored by Fu and colleagues is the idea of utilising exosomes secreted by CAR T-cells for therapy (Fu *et al.* 2019). Second generation CAR T-cells against both EGFR and HER2 were generated and shown to have antitumour activity *in vivo*. Exosomes from both types of CAR T-cell were isolated and CAR expression was detected on the exosome surface. In multiple breast cancer models, CAR exosomes were found to target tumour cells with a similar efficacy to their parental CAR T-cell, with the exosomes also contain high levels of cytotoxic molecules. Further, CAR exosome activity was not hindered by PD-L1, as the exosomes were PD1-negative,

circumventing PD1-PD-L1-mediated immunosuppression. Importantly, in murine breast cancer models, CAR exosomes were tolerated significantly better than parental CAR T-cells (Fu *et al.* 2019). The striking reduction in treatment-associated toxicity observed in this study indicates that further investigation is warranted to determine if CAR T-cell exosomes provide clinical benefit in patients.

1.4.7.4 Universal CAR T-cells

Whether using early or next generation CAR T-cells, one of the main challenges of CAR T-cell therapy is the time taken and expense incurred to generate a sufficient number of CAR T-cells from patient apheresis products. Therefore, multiple research groups have attempted to develop allogeneic CAR T-cells that may be universally administered to patients in an “off the shelf” approach.

Lymphoma and leukaemia patients often receive an allogeneic haematopoietic stem cell transplant (alloHSCT) as part of their disease treatment. However, progressive malignancy is the leading cause of death in these patients following treatment (Brudno *et al.* 2016). Studies utilising donor cells originally intended for alloHSCT to generate CAR T-cells have been reported. Patients with disease that had progressed after alloHSCT received allogeneic CD19-targeting CAR T-cells generated from their respective donors. The allogeneic CAR T-cells were tolerated with no cases of graft-versus-host-disease (GVHD) reported. Eight out of 20 patients responded to therapy, which is a poorer overall response rate than that observed with conventional autologous CD19-targeting CAR T-cells. However, it must be noted that this is a small cohort of patients and it not directly comparable to the large-scale studies carried out with autologous CD19-targeting CAR T-cells (Cruz *et al.* 2013; Kochenderfer *et al.* 2013; Brudno *et al.* 2016).

In autologous CAR T-cell therapy, CAR T-cells are generated from patient PBMCs. Therefore, a superior approach may be to generate allogenic CAR T-cells from

healthy donor PBMCs. To do so, donor PBMCs must be rendered less immunogenic and this can be achieved by the elimination of the endogenous TCR (Torikai *et al.* 2012). In a proof-of-principle study, Torikaki and colleagues knocked out the endogenous TCR via a zinc finger nuclease system and the resulting CD19-targeting CAR T-cells were unresponsive to TCR stimulation. Further, the CD19-targeting ability of these CAR T-cells was preserved *in vitro* (Torikai *et al.* 2012). Since this study, methods involving transcription activator-like effector nucleases (TALENs), megaTAL and CRISPR/cas9 mediated KO have been used to eliminate endogenous TCR (Poirot *et al.* 2015; Osborn *et al.* 2016). CD19-targeting CAR T-cells with TCR deletion have shown comparable antitumour activity to standard CD19-targeting CARs in a murine lymphoma model (Poirot *et al.* 2015). However, a direct comparison of TALENs, megaTAL and CRISPR/Cas9 mediated TCR KO suggested that megaTAL and CRISPR/cas9 have superior disruption efficiency to TALENs (Osborn *et al.* 2016). In an alternative approach to TCR KO, the CAR transgene has been directly knocked in into the native TCR locus. CD19-targeting CAR T-cells generated via this method have been reported to perform at least comparably, if not superior to, standard CD19-targeting CAR T-cells *in vivo* (Eyquem *et al.* 2017; Hale *et al.* 2017; MacLeod *et al.* 2017; Ren *et al.* 2017). In addition to using the megaTAL method to eliminate TCR expression for use in allogeneic CAR T-cells, Hale and colleagues describe another potential clinical application for this technique. By inserting the CAR transgene into the CCR5 locus, encoding a human immunodeficiency virus (HIV) co-receptor, CAR T-cells that are resistant to HIV infection can be generated. CCR5-deficient, CD19-targeting CAR T-cells have potential as a therapy in patients with HIV-associated B cell malignancies (Hale *et al.* 2017).

Recently, universal CAR T-cells (UniCARs) have been designed which are T-cells engineered to express a UniCAR that recognises a short peptide motif. The T-cells remain inactive when administered as the target is not available. A targeting molecule (TM) consists of a scFv for the tumour-associated antigen and an antigen motif

recognised by the CAR T-cells. This system therefore requires the presence of the TM for CAR T-cell activation, as the TM binds to the tumour-associated antigen and the UniCARs recognise the TM and are subsequently activated and lyse the tumour antigen-presenting cell (Bachmann 2019) (Figure 1.13). This system allows for universal CAR T-cells to be used across all patients, with the TM being altered depending on the disease and the tumour-associated antigen present. Further, proof-of concept and proof-of-function studies have confirmed TM specific activation of UniCARs (Koristka *et al.* 2014; Cartellieri *et al.* 2015; Cartellieri *et al.* 2016). Importantly, the TMs are rapidly cleared from the peripheral blood. Therefore, this system could offer more controlled CAR T-cell therapy, with the ability to regulate T-cell activity while also allowing for alteration of the tumour-associated antigen target to limit the emergence of resistance (Cartellieri *et al.* 2016; Albert *et al.* 2017). Michael Bachmann's group have since published multiple studies confirming TM-specific activity of the UniCAR system *in vivo*, with comparable efficacy of these UniCAR T-cells to conventional CAR T-cells also demonstrated. Successful targeting of both haematological cancers and solid tumours has been demonstrated in preclinical UniCAR models, with no associated toxicities (Albert *et al.* 2017; Bachmann *et al.* 2017; Feldmann *et al.* 2017; Mitwasi *et al.* 2017; Albert *et al.* 2018; Loureiro *et al.* 2018; Arndt *et al.* 2020).

Additional switchable CAR T-cells based on the same principle as the UniCAR system have also been generated, with the TMs being an scFv for the target antigen linked to either fluorescein isothiocyanate (FITC) or peptide neoepitope (PNE) molecules. Switchable CAR T-cells with TMs directed against the folate receptor or HER2 have shown promising antitumour activity *in vivo*, alongside improved tolerability (Lu *et al.* 2019; Raj *et al.* 2019). Universal CAR T-cell systems provide a more tuneable CAR T-cell approach and have so far been well tolerated in preclinical models, thus translation of these CAR T-cell systems to the clinic will be of considerable interest.

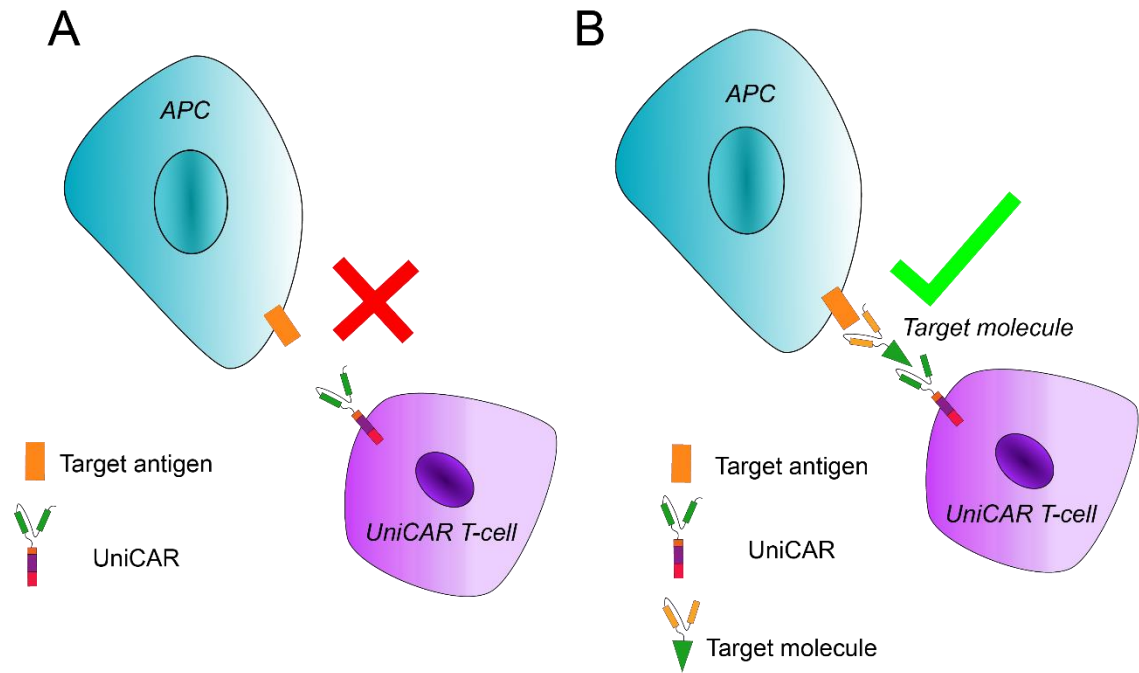


Figure 1. 13 The UniCAR system

The UniCAR system utilises CAR T-cells designed to recognise a short peptide motif and not a physiologically expressed protein. **(A)** UniCAR T-cells cannot be activated when infused alone due to the absence of their target. **(B)** Simultaneous infusion of a target molecule, consisting of an scFv against the target antigen linked to the short peptide motif recognised by the UniCAR T-cells, create a bridge between the target cell and the UniCAR T-cell, resulting in T-cell activation and killing.

1.4.8 CAR T-cells currently in clinical trials

Although CD19-targeting CAR T-cells remain the most widely investigated CAR T-cells worldwide, CAR T-cells directed against a number of other targets are being evaluated in clinical trials. Details of all current active CAR T-cell trials can be found in Table 1.3.

Table 1.3 Active CAR T-cell clinical trials (clinicaltrials.gov)		
CAR T-cell Target	Number of Active Trials	Trial ID(s)
CD19	47	NCT03684889, NCT02443831 NCT03840317, NCT03085173 NCT03434769, NCT04684472 NCT03373071, NCT03302403 NCT02028455, NCT03467256 NCT04416984, NCT03939026 NCT02735291, NCT03327285 NCT02431988, NCT03984968 NCT02601313, NCT01840566 NCT03549442, NCT02659943 NCT00586391, NCT02348216 NCT03265106, NCT03624036 NCT02926833, NCT03620058 NCT01860937, NCT03483103 NCT02706405, NCT03744676 NCT02445248, NCT01683279 NCT01087294, NCT02893189 NCT04014894, NCT03761056 NCT03105336, NCT01815749 NCT04314843, NCT02051257 NCT03144583, NCT00840853 NCT00709033, NCT01318317 NCT02153580, NCT00466531 NCT04276870
BCMA	18	NCT03070327, NCT03288493 NCT03302403, NCT03338972 NCT03602612, NCT03318861 NCT03090659, NCT03548207 NCT03274219, NCT03430011 NCT02658929, NCT04181827 NCT03361748, NCT03549442 NCT02614066, NCT03380039 NCT03716856, NCT03975907
CD30	3	NCT02663297, NCT01316146 NCT01192464
GD2	3	NCT01953900, NCT01822652 NCT00085930
Mesothelin	3	NCT03323944, NCT02414269

		NCT02792114
PSMA	3	NCT03089203, NCT04227275 NCT01140373
CD123	2	NCT02159495, NCT03766126
HER2	2	NCT04903080, NCT00902044
CD22	2	NCT03244306, NCT03620058
CEA	2	NCT03818165, NCT03682744
CD4	2	NCT04712864, NCT03829540
NKG2D	2	NCT03370198, NCT03310008
CD19/CD22 bispecific	2	NCT04034446, NCT03287817
CD19/CD20 bispecific	2	NCT03870945, NCT03019055
MUC16	1	NCT02498912
IL13R α 2	1	NCT02208362
AXL	1	NCT03393936
Lewis Y antigen	1	NCT03851146
ROR2	1	NCT03960060, NCT03393936
CD5	1	NCT03081910
Glypican 3	1	NCT02905188
CLD18	1	NCT03302403
CD20	1	NCT03664635
EGFRvIII	1	NCT05063682
GPRC5D	1	NCT04555551
HER2/PD-L1 bispecific	1	NCT04684459
CD171	1	NCT02311621
GPC3	1	NCT03302403
CD19/BCMA bispecific	1	NCT03879382
CD38	1	NCT03464916

1.5 Project rationale and aims

The upregulation of endosialin in the stroma of multiple solid tumour types and its role in promoting metastasis in solid tumours makes endosialin an interesting antigen for targeted therapy. Clinical trials utilising Ontuxizumab, a monoclonal antibody against endosialin, to target solid tumours have shown limited success, suggesting that using therapeutic antibodies against endosialin is not sufficient.

To date, targeting solid tumours with CAR T-cells has proven challenging, owing to the physical barriers and immunosuppressive environments that they must cross to reach their target tumour cells. Targeting stromal cells proximal to the vasculature may aid in circumventing these issues associated with solid tumour targeting in CAR T-cell

therapy. Endosialin-positive pericytes are closely associated with the tumour vasculature, thus may present good targets for CAR T-cell therapy against solid tumours.

Prior to this PhD, our collaborators, Dr Steven Lee and colleagues at the University of Birmingham designed and generated endosialin-directed CAR T-cells known as Endo3 CAR T-cells.

The overall aims of this PhD were:

- To characterise the specificity of Endo3 CAR T-cells *in vitro*
- To determine the safety and tolerability of Endo3 CAR T-cells *in vivo*
- To assess the efficacy of Endo3 CAR T-cells against multiple preclinical models of cancer.

Chapter 2 Materials and Methods

2.1 Materials

2.1.1 General reagents

H₂O: Central sterile stores department (CSSD).

PBS: 137 mM NaCl, 2mM KCl, 8 mM Na₂HPO₄ 1.5 mM KH₂PO₄ in H₂O. pH adjusted to 7.4 with HCl (CSSD). Stored at 4°C.

Ultra-filtrated (UF) H₂O: CSSD. Stored at 4°C.

Ethanol: CSSD.

2.1.2 Cell culture

4T1-Luc cells: 4T1 mouse mammary carcinoma cell line (ATCC-CRL-2539) engineered to express firefly luciferase.

10T $\frac{1}{2}$ cells: Mouse pericyte-like cells.

AT-3 cells: AT-3 mouse mammary carcinoma cell line derived from C57BL/6 mice.

MRC5 cells: Human fetal lung fibroblasts. ATCC (CCL-171).

MCF7 cells: Human breast cancer cell line. ATCC (HTB-22).

Cell freezing medium: 10% DMSO in FBS (see below). Stored at 4°C.

CellTiter-Glo reagent: Promega (G7570).

Cryovials: Thermo Scientific (363401).

DMEM (Dulbecco's modified Eagle's medium): Invitrogen (41966-029) containing 4.5 g of glucose per litre. Stored at 4°C.

Dimethyl sulfoxide (DMSO): Sigma (D2650).

FBS (foetal bovine serum): Invitrogen (10106-169). Stored at -20°C.

J774a.1 cells: Isacke Lab Stocks

Penicillin/streptomycin: Stock solution stored at -20°C. (1L) benzylpenicillin sodium 12 g, streptomycin sulphate 20 g (CSSD).

Lewis Lung Carcinoma (LLC) cells: mouse lung carcinoma cell line derived from C57BL/6 mice. ATCC (CRL-1642).

RPMI 1640 (Roswell Park Memorial Institute Medium): Thermo Fisher Scientific (22400089).

Tissue culture plastics: All tissue culture plastics were purchased from Falcon.

Trypsin/EDTA: (1L) NaCl 8 g, KCl 0.2 g, Na₂HPO₄ 1.15 g, D-glucose 1 g, KH₂PO₄ 0.2 g, EDTA 0.2 g, Tris 3 g, phenol red (1%) 1.5 mL, trypsin (Difco 1:250) 0.5 g, streptomycin sulphate 0.1 g, benzylpenicillin 0,06 g (CSSD). Stored at -20°C.

2.1.3 Flow cytometry

Control beads: UltraComp eBeads. eBioscience (01-2222-42).

Counting beads: 123count eBeads. Invitrogen (01-1234).

DAPI: 4'6-diamidino-2-phenylindole, dihydrochloride. Invitrogen (D1306).

FACS buffer: 1% FBS in PBS. Stored at 4°C.

FACS tubes: Falcon (352058).

Red blood cell lysing buffer: BD Pharma (555899).

V-bottomed 96-well plates: Costar (3894).

Table 2.1 Antibodies used for flow cytometry

Antibody	Species	Source (Cat. No.)	Dilution
Anti-mouse CD4-PE	Rat	Biolegend (100408)	1:100
Anti-mouse CD8-FITC	Rat	Biolegend (10076)	1:100
Anti-human CD34-APC	Mouse	Biolegend (343608)	1:20

2.1.4 Immunostaining

4% paraformaldehyde in PBS: Paraformaldehyde powder, Sigma (15812-7), was added to PBS to make a 4% weight/volume mixture and dissolved at 50°C on a heated stirrer. pH 7.4.

Antigen retrieval solution: Dako target retrieval solution 10x concentrate, diluted to 1x working solution, Dako (S1699).

Histoclear: Agar Scientific (A2-0105).

Ethanol: 70, 90 & 100% solutions made from CSSD stocks.

Hoechst: Life Technologies (H3570).

Immunofluorescence buffer (IFF): 1% bovine serum albumin (BSA), 2% PBS sterilised using a 20 µm syringe filter. Stored at -20°C.

Prolong Gold antifade reagent: Invitrogen (P36934).

Steamer: Braun pressure steamer.

Table 2.2 Antibodies used for immunofluorescent staining			
Antibody/Marker	Species	Source (Cat. No.)	Dilution
Anti-endosialin (3K2L)	Rat	Isacke Lab	1:500
Anti-endosialin (P13)	Rabbit	Isacke Lab	1:500
Anti-endomucin (V7C7)	Rat	Santa Cruz (sc-65495)	1:1000
Anti-nucleophosmin	Mouse	Invitrogen (32-5200)	1:2000
Alexa488 Anti-rabbit	Goat	Invitrogen (A11034)	1:1000
Alexa555 Anti-rat	Goat	Invitrogen (A21434)	1:1000

2.1.5 Western blotting

4-15% Mini-PROTEAN TGX Precast Protein Gel, 10-well, 30 µL: Bio-Rad (4561083).

Blocking buffer: 5% powdered milk in TBS-T (see below). Made fresh each use.

Enhanced chemiluminescence (ECL) substrate: Clarity Western ECL substrate. Bio-Rad (1705061).

Methanol: VWR Chemicals (85650.320).

Precision Plus Protein Dual Colour Standards: Bio-Rad (161-0374)

Polyvinylidene difluoride (PVDF) membranes: Trans-blot Turbo mini-size LF PVDF membrane. Bio-Rad (1704274).

Radioimmunoprecipitation assay buffer (RIPA) buffer: Sigma (R0278). Stored at -20°C.

Sample buffer: 4x Laemmli sample buffer. Bio-Rad (161-0747).

Trans-Blot Turbo Transfer Stacks: Bio-Rad (10026930).

Tris-buffered saline (TBS): 136.9 mM NaCl, 5 mM KCl, 24.77 mM Tris Base (CSSD).

TBS-T: TBS plus 0.05% Tween 20.

Tween 20: Sigma (P7949).

Table 2.3 Antibodies used for western blotting			
Antibody/Marker	Species	Source (Cat. No.)	Dilution
Anti-endosialin (3K2L)	Rat	Isacke Lab	1:500
Anti- β -actin	Mouse	Sigma (A5441)	1:25000
Anti-rat-HRP	Goat	Abcam (ab205720)	1:5000
Anti-mouse-HRP	Goat	Abcam (ab205719)	1:2000

2.1.6 RNA isolation and RTqPCR

Buffer PKD: Qiagen (1034963).

Nuclease-free water: Invitrogen (AM9938).

Mastermix: Qiagen (201443).

RNeasy FFPE kit: Qiagen (73504).

QiaShredder columns: Qiagen (79656).

Quantitect kit: Qiagen (205311).

Table 2.4 Taqman probes for RTqPCR (Applied Biosystems)			
Probe ID	Gene	Species	Reporter
Mm00547485	<i>Cd248</i>	Mouse	FAM
Mm01201237	<i>Ubc</i>	Mouse	FAM
Mm00437762	<i>B2m</i>	Mouse	FAM

2.1.7 ELISA

Mouse IL-6 ELISA Kit: Abcam (100712).

Mouse IFN- γ ELISA Kit: Abcam (100689).

2.1.8 Cytotoxicity assays

Cyto Tox 96 non-radioactive cytotoxicity assay kit: Promega (G1780).

2.1.9 Generation of Endo3 CAR and Mock T-cells

β -mercaptoethanol: Gibco (31350-010).

BALB/c splenocytes: Isolated from the spleens of 8-10 week old female BALB/c mice.

Blocking buffer: 2% BSA in PBS. Stored at 4°C.

C57BL/6 splenocytes: Isolated from the spleens of 8-10 week old C57BL/6 mice.

Cell strainer (100 μ m): Falcon (352360).

Concanavalin A: Sigma (555899).

Endo3 CAR plasmid: Designed and generated by Dr Steven Lee and colleagues using the MP71 plasmid backbone transferred from The Institute of Experimental Hematology at Hannover Medical School.

Ficoll Paque: GE Healthcare Biosciences (17-5446-02).

Eugene6 Transfection Reagent: Promega (E2691).

Mouse interleukin-2 (mIL-2): Abcam (ab9856).

Mouse interleukin-7 (mIL-7): Peprotech (217-17).

Non-TC treated plates: Falcon (353046)

OptiMEM Reduced Serum Media: Thermo Fisher Scientific (31985062).

pCL-eco plasmid: Packaging plasmid for pCL retroviruses. Gifted by Dr Steven Lee.

Phoenix E cells: Human embryonic retroviral packaging cells. Gifted by Dr Steven Lee.

RetroNectin reagent: Diluted in PBS to a final concentration of 30 µg/mL. Takara (T100B). Used for a maximum of 4 freeze/thaw cycles.

2.1.10 *In vivo studies*

Angiosense 750: Perkin Elmer (NEV10011).

Anti-IL-6R (15A7): BioXcell (BE0047, lot 677718M2).

BALB/c mice (WT): 8-10 week old, female BALB/c mice purchased from Charles River.

BALB/c mice (*Cd248^{-/-}*): 8-10 week old, female *Cd248^{-/-}* (Nanda *et al.* 2006) mice backcrossed for >6 generations onto a BALB/c background and housed at Charles River.

Biopsy punch (6 mm): Medisave (BI2000).

C57BL/6 (WT): 8-10 week old, female C57BL/6 mice purchased from Charles River.

C57BL/6 mice (*Cd248^{-/-}*): 8-10 week old, *Cd248^{-/-}* (Nanda *et al.* 2006) mice backcrossed for >6 generations onto a C57BL/6 background and housed at Charles River.

Cellstor pots: 60 mL 10% neutral buffered formalin. CellPath (BAF-6000-08A).

Cyclophosphamide: Sigma (C3250000).

Endo3 CAR T-cells and mock transduced T-cells: Generated as described in Section 2.2.6.

Isotype control mAb (LTF2): BioXcell (BE0090, lot 707119J1)

Lithium-heparin blood collection tubes: BD Biosciences (365966).

Matrigel: Growth factor reduced. Corning (356231).

NOD scid gamma (NSG) mice: 8-10 week old, female NSG mice purchased from Charles River.

X-ray irradiation machine: AGO (HS MP1 controller, HS 320 cabinet).

2.2 Methods

2.2.1 Cell culture

Cell culture. Adherent cells were cultured at 37°C in a tissue culture incubator with humidified air, supplemented with 5% CO₂. Cells were cultured in DMEM supplemented with 10% FBS and 0.5% penicillin/streptomycin, unless otherwise stated. Cells were cultured in tissue culture flasks and passaged when 80-90% confluent.

T-cell culture: T-cells were cultured at 37°C in a tissue culture incubator with humidified air, supplemented with 5% CO₂. T-cells were cultured in RPMI, supplemented with 10% FBS and 0.5% penicillin/streptomycin

Frozen storage of cells. Adherent cells were detached from flasks using trypsin/EDTA, resuspended in culture medium and pelleted by centrifugation at 700g for 5 min. T-cells were pelleted by centrifugation at 700g for 4 min. Cells were resuspended in freezing medium and 1 mL of cell suspension was added to cryovials. Vials were placed at -80°C for at least 24 h before transfer to liquid nitrogen for long-term storage.

2.2.2 Western blotting

Cell were lysed on ice in 50-100 µL RIPA buffer for 30 min before being centrifuged in an Eppendorf microfuge at 13,200 rpm for 30 min at 4°C. Supernatants were transferred to a new tube and sonicated for 2 x cycles of 30 seconds. Protein concentrations were measured using a Direct Detect Infrared Spectrometer. 10-30 µg of protein per sample was diluted in sample buffer and samples were boiled at 95°C for 5 min.

Separation was performed according to manufacturer's instructions on a 4-15% Mini-PROTEAN TGX Precast Protein Gel and transferred on to a methanol washed PVDF membrane using a Protean 3 Transblot machine. The membrane was blocked in blocking buffer for 1 h and probed with primary antibody overnight at 4°C followed by an HRP-conjugated secondary antibody for 1 h at RT at specified dilutions (Table 2.3) in blocking buffer. Membranes were developed in ECL solution for 3 min and visualised using a ChemiDoc MP Imaging System.

2.2.3 *In vivo studies*

All *in vivo* studies were performed under UK Home Office Project License P6AB1448A granted under the Animals (Scientific Procedures) Act 1986. All studies were performed at The Institute of Cancer Research (Establishment Licence, X702B0E74 70/2902). Ethical permission was granted by the Institute of Cancer Research "Animal Welfare and Ethical Review Body" (AWERB). Animals were housed in IVC type cages which are run under negative airflow. Mice were housed in groups of 2-5, had food and water ad libitum and monitored daily by ICR Biological Services Unit staff. Animal holding rooms were maintained at a temperature of 21°C ± 2°C, a humidity of 55% ± 10% and on a 12 h light, 12 h dark cycle, as recommended by the Home Office Code of Practice. In all cases, animals were culled if the primary tumour reached a mean diameter of >17 mm and before the maximum allowable mean diameter of 18 mm was reached or if signs of ill health were close to limits (see health scoring criteria below).

Tumour growth studies: 8-10 week old wild-type (Charles River, UK) female BALB/c, NSG or C57BL/6 mice were inoculated subcutaneously on the flank with 4T1-Luc or AT-3 cells (2.5×10^5) in PBS. Tumour volume and body weight was measured bi-weekly following tumour cell inoculation. 4T1 tumour-bearing mice were sacrificed 13-20 days post-tumour cell injection and AT-3 tumour-bearing mice were sacrificed 16-21 days post-tumour cell injection.

Validation of lymphodepletion strategies: Wild-type BALB/c or C57BL/6 mice were subjected to 5 Gy x-ray or caesium whole-body irradiation or BALB/c mice were administered with 150 mg/kg cyclophosphamide via intraperitoneal injection. 24 h later, mice were bled via the tail vein and venous blood was analysed via flow cytometry for lymphocyte populations.

In vivo characterisation of anti-IL-6R (15A7): 8-10 week old wild-type (Charles River, UK) female BALB/c mice were inoculated subcutaneously on the flank with 4T1-Luc cells (2.5×10^5) in PBS. Tumour volume and body weight was measured bi-weekly following tumour cell inoculation. Mice were administered with 25 mg/kg anti-IL-6R (15A7) or isotype control (LTF2) mAb via intraperitoneal injection on day 12 post-tumour cell injection and with 12.5 mg/kg/day on days 13-17 post-tumour cell injection. Mice were sacrificed 22 days post-tumour cell inoculation.

Wound healing immunotherapy studies: 8-10 week old wild-type (Charles River, UK) female BALB/c mice were given 6 mm punch wounds through the dorso-lateral skin and wounds were allowed 4 days to begin healing. Mice were subjected to 5 Gy caesium irradiation 18 h before being injected via the tail vein with 2.5×10^6 Endo3 CAR T-cells or HBSS vehicle alone. Mice were provided with Dietgel from the before day T-cell injection to study termination. Circulating CAR T-cell numbers were monitored via tail vein bleeding 7 days post-T-cell infusion, during which up to 100 μ L of blood was collected, immediately heparinised and kept on ice for up to 1 h. Mice were sacrificed 10 days post-T-cell injection and wounded skin and control non-wounded skin was collected and formalin fixed.

Tumour directed CAR T-cell-studies: 8-10 week old wild-type (Charles River, UK) or *Cd248*^{-/-} female BALB/c, C57BL/6 or NOD scid gamma (NSG) mice were inoculated subcutaneously on the flank with 4T1-Luc cells (2.5×10^5 in PBS), AT-3 cells (2.5×10^5 in PBS), LLC cells (5×10^5 in 50:50 PBS:Matrigel) or left tumour-naïve. Tumour volume

and body weight was measured bi-weekly following tumour cell inoculation. After 10-12 days (4T1), 14 days (LLC) or 16 days (AT-3) mice were sorted into groups with comparable tumour burden. Tumour-bearing BALB/c and C57BL/6 mice received 4-5 Gy total body x-ray or caesium irradiation. NSG mice were not irradiated. Where stated, mice were given Dietgel and daily intraperitoneal hydration injections of 200-400 μ L water thereafter. After 18 h, mice were injected via the tail vein with $2.5-7.5 \times 10^6$ transduced Endo3 CAR T-cells or mock-transduced T-cells. Where stated, mice were given an intraperitoneal injection of 25 mg/kg anti-IL-6R (15A7) or isotype control (LTF2) mAb the day before T-cell injection and 12.5 mg/kg of the same mAb on the day of T-cell injection and days 1-7 post-T-cell injection. Circulating CAR T-cell numbers were monitored via tail vein bleeding at stated time points following T-cell infusion, during which up to 100 μ L of blood was collected, immediately heparinised and kept on ice for up to 1 h. Where stated, a subset of animals were injected via the tail vein with 150 μ L AngioSense 750 fluorescent imaging agent 6 days post-T-cell injection and subjected to IVIS imaging at 750/780nm 24 h later. At necropsy, blood was collected via cardiac puncture, immediately heparinised and kept on ice for up to 1 h. Blood samples were centrifuged in an Eppendorf microfuge at 13,200 rpm for 3 min and the serum supernatant was collected and stored at -80°C . Lungs were removed, inflated with formalin, formalin-fixed and paraffin-embedded. Primary tumours were removed, weighed *ex vivo* and isolated tissues were formalin-fixed. Other organs were also collected and formalin-fixed.

Health scoring criteria: In CAR T-cell experiments animals were given a health score based on behaviour and appearance. These are defined in Table 2.5.

Table 2.5 Mouse health scoring criteria	
Health score	Definition
0	Healthy, no signs of ill health
-1	Some evidence of piloerection, behaviour normal
-2	Obvious piloerection and some weight loss, behaviour normal
-3	Obvious piloerection, some weight loss and subdued behaviour (hunching, squinting, malaise) Close to licence threshold and require culling.

Tumour growth rate calculation: The rate of growth for each individual tumour was calculated by plotting log(tumour volume) over time and performing a simple linear regression analysis, where the slope value represents the rate of growth (Karp *et al.* 2020).

2.2.4 Histology

Formalin-fixed tissues were embedded in paraffin wax and 3-4 µm sections were cut by the Breast Cancer Now (BCN) Histopathology facility. Lung metastasis and primary tumour necrosis was quantified manually from H&E stained sections provided by the BCN Histopathology facility.

2.2.5 Immunostaining

Cells were plated on 13 mm glass coverslips and cultured for at least 24 h prior to fixation in 4% paraformaldehyde for 30 min. Formalin-fixed, paraffin-embedded (FFPE) sections were deparaffinised, re-hydrated via immersion in a gradient of ethanol solutions (100-70%) followed by immersion in water and antigen retrieved in DAKO antigen retrieval solution in a pressure cooker for 30 min. Sections were allowed to cool for 30 min. Coverslips or antigen-retrieved sections were washed twice with PBS and once with IFF. Coverslips or sections were then incubated with primary antibody at a specified dilution in IFF (Table 2.2) for 40 min at room temperature or at 4°C overnight, respectively. Coverslips or sections were washed 3 x 5 min with PBS before being incubated with the

appropriate conjugated secondary antibody in IFF for 40 min at room temperature. Coverslips/sections were washed 3 x 5 min with PBS containing Hoechst (1:10,000) or DAPI (1:10,000) before being rinsed in PBS and mounted with Prolong Gold reagent. Low power images were obtained from Hamamatsu NanoZoomer scans, high power images were obtained with a Leica SP8 confocal microscope.

Quantification of endosialin-positive and endomucin-positive tissue area: ImageJ software was used to determine the endosialin-positive area of tissue sections stained for endosialin using a secondary antibody conjugated to Alexa 488 by colour thresholding in the hue range of 74-109 and saturation 0-255. Endomucin-positive area of tissue sections stained for endomucin using a secondary antibody conjugated to Alexa 555 was determined by colour thresholding in the hue range 20-50 and saturation 0-255. Brightness was set based on the mock controls of the image set. Only viable tissue areas were quantified. Percent positive area was calculated as (endosialin-positive area/total tumour area) x 100.

2.2.6 Generation of Endo3 CAR and Mock T-cells

Generation of retrovirus-containing and mock supernatants: Phoenix E cells were seeded into 175 cm² flasks at a density of 1×10^7 cells in antibiotic-free DMEM supplemented with 10% FCS and incubated for 24 h at 37°C. Each 175 cm² flask was transfected with 12 µg of Endo3 plasmid DNA, 12 µg of pCL-eco plasmid DNA, 120 µL Fugene6 transfection reagent and 3480 µL OptiMEM Reduced Serum Media in 13 mL antibiotic-free DMEM, prior to incubation at 37°C. Mock transduction was performed using OptiMEM alone. After 18 h media was changed for 21 mL of fresh antibiotic-free DMEM and flasks were incubated for a further 24 h at 37°C. Retrovirus-containing and mock phoenix E supernatants were harvested, passed through a 45 µm filter and centrifuged at 400g for 5 min to remove any contaminating phoenix E cells.

Isolation and activation of mouse splenocytes: 8-10 week old female BALB/c or C57BL/6 mice were culled and spleens were removed and placed in sterile bijoux vials containing 5 mL T-cell media. Cells were harvested by passing each spleen through a 100 μ m cell strainer and washed in RPMI. Cells were resuspended in 10 mL red blood cell lysis buffer and incubated for 4 min at room temperature. Cells were washed in T-cell media, counted and adjusted to a concentration of 3×10^6 cells/mL. Concanavalin A and mIL-7 were added to activate the T-cells at a final concentration of 2 μ g/mL and 1 ng/mL, respectively. Additionally, 50 μ M 2-mercaptoethanol was added to splenocytes and cells were incubated at 37°C for 48 h, with 2-mercaptoethanol being added again at 24 h.

Transduction of mouse splenocytes: Non-tissue culture treated 6-well plates were coated with 2 mL 30 μ g/mL RetroNectin reagent for 3 h at room temperature or overnight at 4°C. Plates were blocked for 30 min with 2 mL 2% BSA/PBS solution and washed with 4 mL/well PBS. Plates were then centrifuged with 2 mL/well retrovirus-containing or mock supernatants at 2000g at 32°C for 2 h. Supernatants were removed and wells washed with PBS. Splenocytes were added to wells at a concentration of 1×10^6 cells/mL to a total density of $3\text{-}3.5 \times 10^6$ cells/well, in T-cell media containing 100 U/mL mIL-2. Plates were centrifuged at 700g for 5 min followed by a 24 h incubation at 37°C. Cells were then collected and purified using a Ficoll Paque density gradient, washed in T-cell media and frozen in freezing media. T-cells were kept at -80°C for a minimum of 24 h before being transferred to liquid nitrogen storage. Cryopreserved T-cells were used for all *in vitro* and *in vivo* experiments.

2.2.7 Flow cytometry

For analysis of transduced Endo3 CAR T-cells, $2.5\text{-}5 \times 10^5$ Endo3 CAR or Mock T-cells were plated into 96-well v-bottom plates. For analysis of circulating Endo3 CAR T-cells in mouse blood samples, up to 30 μ L of whole tail vein blood was plated into 96-well v-bottom plates and red blood cells were lysed in 200 μ L red blood cell lysis buffer for 4

min at 37°C for two cycles. All samples were washed once in 200 µL FACS buffer before being incubated at 4°C for 30 min with directly conjugated antibodies against CD4, CD8 and human CD34 at specified dilutions in FACS buffer (Table 2.1), or in FACS buffer alone. Fluorescence minus one (FMO) controls were created by abrogating a single antibody. Compensation controls were prepared simultaneously by adding 1 µL of each antibody to a drop of control beads. Samples were washed in FACS buffer and stained with DAPI (1:10,000) or FACS buffer alone at 4°C for 5-10 min. A final wash in FACS buffer was performed before samples were transferred to FACS tubes containing 300 µL FACS buffer. Finally, 50 µL counting beads were added to each tube and samples were analysed using a BD LSR II flow cytometer. Data analysis was performed using Flow Jo v10 software. Absolute cell counts were calculated as follows: absolute count (cells/mL) = [(cell count x counting bead volume)/(counting bead count x cell volume) x counting bead concentration] x 1000.

2.2.8 RNA extraction and RTqPCR analysis

RNA was extracted from FFPE tumour sections using the RNeasy FFPE kit. Briefly, sections were deparaffinised and scraped into 75 µL Buffer PKD and mixed by vortexing. Two sections were combined to give a total of two sections in 150 µL Buffer PKD. RNA was then extracted according to RNeasy FFPE kit instructions. RNA was eluted in 30 µL nuclease-free water, and the RNA concentration was determined using the Nanodrop-8000 spectrophotometer. cDNA was produced by reverse transcribing 500 ng of RNA using the Qiagen Quantitect kit, according to the manufacturer's instructions. Quantitative PCR reactions were performed on the Applied Biosystems QuantStudio6 Real-time PCR system using 11.25 ng cDNA in 4.5 µL volume, 5 µL 2x qPCR mastermix and 0.5 µL Taqman Gene Expression Assay probes for mouse endosialin or housekeeping controls (Table 2.4), with all reactions being performed in triplicate. Relative quantification was achieved using the QuantStudio6-Flex Real-time PCR

software with the endogenous controls *Ubc* and *B2m* used to perform normalisation, and all expression data was normalised to highest mock T-cell treated control.

2.2.9 Cell viability assays

To assess Endo3 CAR T-cell efficacy, target cells and T-cells were cultured alone or at defined effector:target ratios in co-culture in T-cell media or DMEM (target cells alone) for 18-84 h in 96-well plates. T-cells were removed with 3 cycles of PBS washes before 80 μ L of T-cell media with 20 μ L of CellTiter-Glo reagent was added to each well. Plates were agitated gently for 5 min at room temperature before luminescence was read at 450nm on a Victor X machine. The average read-out from target cells cultured alone was defined as 100% viability. Viability of target cells from co-cultures was calculated per well as follows: [(value for target cells from co-culture/average target cell alone) *100].

2.2.10 Enzyme-linked immunosorbent assay (ELISA)

All reagents, samples and standards were prepared and assayed according to the manufacturer's instructions. Briefly, samples and standards were incubated on the assay plate for 2.5 h at room temperature, 1x biotinylated IL-6 or IFN- γ detection antibody was added for 1 h at room temperature, followed by 1x HRP-streptavidin for 45 min at room temperature and finally TMB One-Step Substrate Reagent for 30 min at room temperature in the dark. Wash steps were performed in between each reagent. The reaction was stopped with Stop Solution and absorbance per well was read immediately at 450 nm on a Victor X machine.

2.2.11 Cytotoxicity assays

T-cell cytotoxicity was determined by measuring lactate dehydrogenase (LDH) concentration in the supernatants of T-cell-target cell co-cultures using the Cyto Tox 96 non-radioactive cytotoxicity assay according to manufacturer's instructions. Briefly, T-

cells and target cells were co-cultured in 96-well plates at defined effector:target cell ratios in T-cell media for 24-84 h. Control wells containing T-cells or target cells alone were used to determine the spontaneous LDH release of effector and target cells alone. Additional control wells containing target cells alone were treated with lysis solution 45 min prior to measurement of LDH to determine the maximum LDH release of target cells. Wells containing T-cell media alone or T-cell media plus lysis solution were used to determine assay background. To determine LDH concentration, 50 μ L supernatant was transferred to a new 96-well plate and 50 μ L of Cyto Tox 96 reagent was added to each well. Plates were incubated at room temperature whilst being protected from light and after 30 min 50 μ L of stop solution was added to each well. Absorbance was immediately read at 490 nm on a Victor X machine. Percent cytotoxicity was calculated as follows: % cytotoxicity = [(experimental – effector spontaneous – target spontaneous)/(target maximum-target spontaneous)] x 100.

2.2.12 Statistical analysis

Statistics were performed using GraphPad Prism 8 or 9 software. Unless otherwise stated, all comparisons between two groups were made using two-tailed, unpaired Student's *t*-test. If the analysis did not pass normality testing (Shapiro-Wilk test), groups were analysed by Mann-Whitney *U*-test. When more than two groups were compared, one-way ANOVA analysis was performed with Tukey's test for multiple comparisons. If the analysis did not pass normality testing (Shapiro-Wilk test), groups were analysed by Kruskal-Wallis test with Dunn's test for multiple comparisons. If multiple groups with a second variable were compared e.g. tumour-bearing or tumour-naïve, a two-way ANOVA followed by Sidak post-hoc testing was performed. If multiple groups with a second and third variable were compared e.g. tumour-bearing or tumour-naïve, Cd248^{WT} or CD248^{KO}, a three-way ANOVA followed by Tukey's test for multiple comparisons was performed.

Chapter 3 Generation of Endo3 CAR T-cells and validation of endosialin as a CAR T-cell target

3.1 Introduction

CAR T-cell therapy has delivered striking results in the treatment of haematological cancers such as B-cell malignancies and ALL (Maude *et al.* 2018; Locke *et al.* 2019). However, to date, treatment of solid tumours with CAR T-cells has proven challenging, as discussed in Chapter 1.4.5. An alternative approach to targeting the tumour cells of solid cancers is to target the cells of the TME. This approach circumvents the need for CAR T-cells to penetrate deep within the tumour, thus removing some of the physical barriers that the CAR T-cells must navigate. To date, several CAR T-cells targeting antigens of the TME have been developed, including CAR T-cells against FAP, VEGFR-2 and TEM8, with mixed results *in vivo* that have yet to translate into clinical efficacy (Chinnasamy *et al.* 2010; Kakarla *et al.* 2013; Schuberth *et al.* 2013; Tran *et al.* 2013; Wang *et al.* 2014; Byrd *et al.* 2018).

The transmembrane glycoprotein endosialin (CD248) has been reported, by our laboratory and others, to be expressed at low levels in normal adult tissues (Rupp *et al.* 2006; MacFadyen *et al.* 2007). However, in multiple solid tumours, including breast cancer and glioblastoma, endosialin is upregulated on tumour-associated pericytes and fibroblasts (Rettig *et al.* 1988; MacFadyen *et al.* 2005; Rouleau *et al.* 2008; Simonavicius *et al.* 2008). Further, by comparing endosialin wild-type (Cd248^{WT}) and knock-out (Cd248^{KO}) mice, our laboratory has previously demonstrated that stromal endosialin expression in breast cancer is required for efficient metastatic dissemination (Viski *et al.* 2016). These characteristics identify endosialin as a promising antigen for targeted CAR T-cell therapy.

This Chapter provides validation of endosialin as a CAR T-cell target and evaluates the use of syngeneic mouse models of breast cancer for preclinical testing of endosialin-targeting Endo3 CAR T-cells.

3.2 Results

Prior to the start of this project, the mAb 3K2L was generated by immunising rats with an Fc construct containing the mouse endosialin N-terminal globular domains (MacFadyen *et al.* 2007; Simonavicius *et al.* 2012). Based on mAb 3K2L, the laboratory of Dr Steven Lee (University of Birmingham) generated the Endo3 CAR construct described below and produced the initial Endo3 and mock transfected BALB/c and C57BL/6 CAR T-cells for use in this project. T-cells were frozen, transferred to the ICR by dry ice transportation and immediately stored in liquid nitrogen until use *in vivo*.

3.2.1 mAb 3K2L recognises mouse and human endosialin

In the clinic, CAR T-cell therapy may be associated with adverse events, with the most common manifestations being CRS and neurotoxicity, as discussed in Chapter 1.4.4. Because of this, assessing the toxicity profile of CAR T-cells in an immunocompetent setting at the preclinical level is important. Further, it is challenging to identify a truly tumour-specific antigen in the context of solid tumours, therefore it is also important to evaluate potential on-target, off-tumour toxicities for a given CAR T-cell target.

In this thesis, Endo3 CAR T-cell therapy is evaluated in the context of three syngeneic immunocompetent models of mouse cancer: 4T1 tumours in BALB/c mice and AT-3 or LLC tumours in C57BL/6 mice. In the syngeneic setting all cells, both normal and cancerous, are of mouse origin and thus the CAR T-cell therapy under evaluation must recognise its target antigen in the mouse form.

To confirm the specificity of mAb 3K2L, of which the scFv portion is utilised in the Endo3 CAR construct, mouse pericyte-like 10T $\frac{1}{2}$ cells were subjected to western blot analysis (Figure 3.1A) and immunostaining (Figure 3.1 B). Mouse 4T1 and AT-3 tumour cells and human MRC5 fibroblast and MCF7 tumour cells were also analysed via both methods to (a) confirm endosialin expression was absent on tumour cells and (b) determine if 3K2L was also able to recognise human endosialin. As expected, 3K2L successfully recognises mouse endosialin on 10T $\frac{1}{2}$ cells and indeed also recognises human endosialin on MRC5 fibroblasts. Both 4T1 and MCF7 tumours cells are found to be endosialin-negative, as expected, however a sub-population of AT-3 cells demonstrate endosialin-positive immunostaining *in vitro*. This population is, however, sparse and western blot analysis reveals minimal detection of endosialin protein in AT-3 lysates when compared to 10T $\frac{1}{2}$ or MRC5 cells.

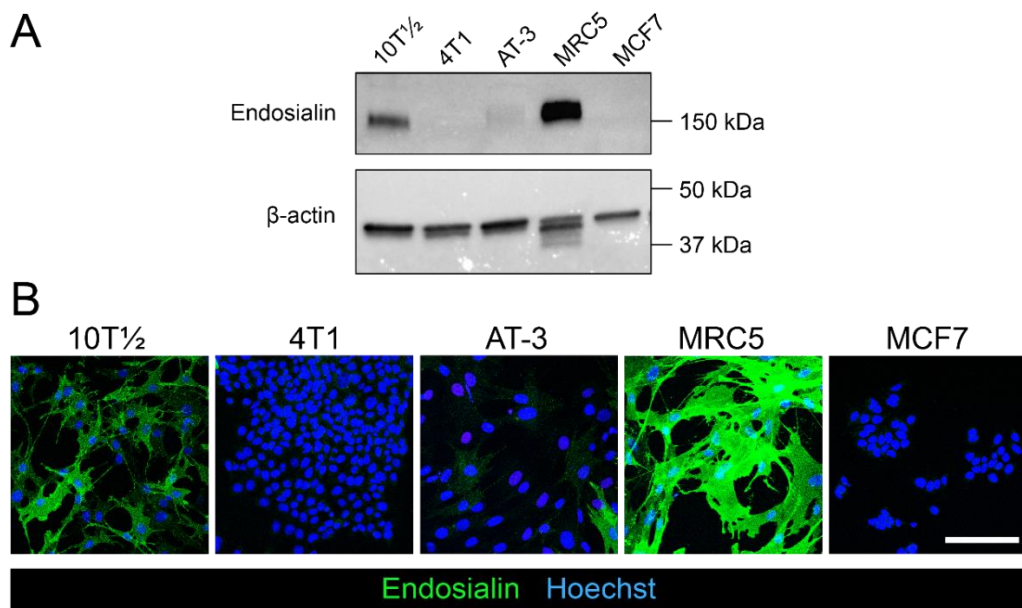


Figure 3. 1 mAb 3K2L recognises mouse and human endosialin

(A) Mouse 10T $\frac{1}{2}$, 4T1 and AT-3 and human MRC5 and MCF7 cell lysates were resolved by SDS-PAGE under non-reducing conditions and subject to western blotting with the anti-endosialin mAb 3K2L, followed by HRP-conjugated anti-rat Ig. β -actin was detected as a loading control. **(B)** Confocal images of fixed cells stained for endosialin with the mAb 3K2L (green). Nuclei were counterstained with Hoechst (blue). Representative images are shown. Scale bar = 125 μ m.

3.2.2 *Endo3 CAR is transduced with high efficiency into mouse T-cells*

Second generation CAR T-cells have irrefutably been shown to have superior characteristics when compared to first generation CAR T-cells (Finney *et al.* 1998; Krause *et al.* 1998; Finney *et al.* 2004; Brentjens *et al.* 2007; Milone *et al.* 2009), with third generation CAR T-cells demonstrating little additional benefit to those of the second generation (Till *et al.* 2012; Gomes da Silva *et al.* 2016; Enblad *et al.* 2018) (see Chapter 1.4.2.1). Our collaborators, Dr Steven Lee and colleagues, developed a second generation endosialin-targeting CAR T-cell, utilising the scFv portion of the endosialin-specific rat mAb 3K2L (MacFadyen *et al.* 2007; Simonavicius *et al.* 2012). The CAR portion of the Endo3 CAR construct contains a signal peptide, the scFv portion of mAb 3K2L, a linker region and the signalling domains of the human co-stimulatory molecule CD28 and the human T-cell receptor molecule CD3 ζ . The construct also contains a truncated version of human CD34 (hCD34) alongside a 2a self-cleaving peptide (Figure 3.2). This allows the simultaneous expression of truncated hCD34 alongside the Endo3 CAR, which facilitates the identification of Endo3 CAR T-cells within mouse samples.

Initial studies carried out in Dr Steven Lee's laboratory demonstrated that the Endo3 CAR construct could be successfully transduced into mouse and human T-cells. In this thesis, early *in vivo* studies were performed using BALB/c or C57BL/6 Endo3 CAR T-cells and mock transduced T-cells generated by our collaborators, however later studies utilise T-cells that I generated in our laboratory. In both laboratories, Endo3 CAR T-cells were successfully generated (Figure 3.3A,B) with a consistently high transduction efficiency (>80%) in both BALB/c and C57BL/6 T-cells (Figure 3.4). As will be indicated in relevant sections of this thesis, Endo3 CAR T-cells produced in Birmingham and at the ICR behave comparably in the experiments performed during this PhD (see Chapter 4).

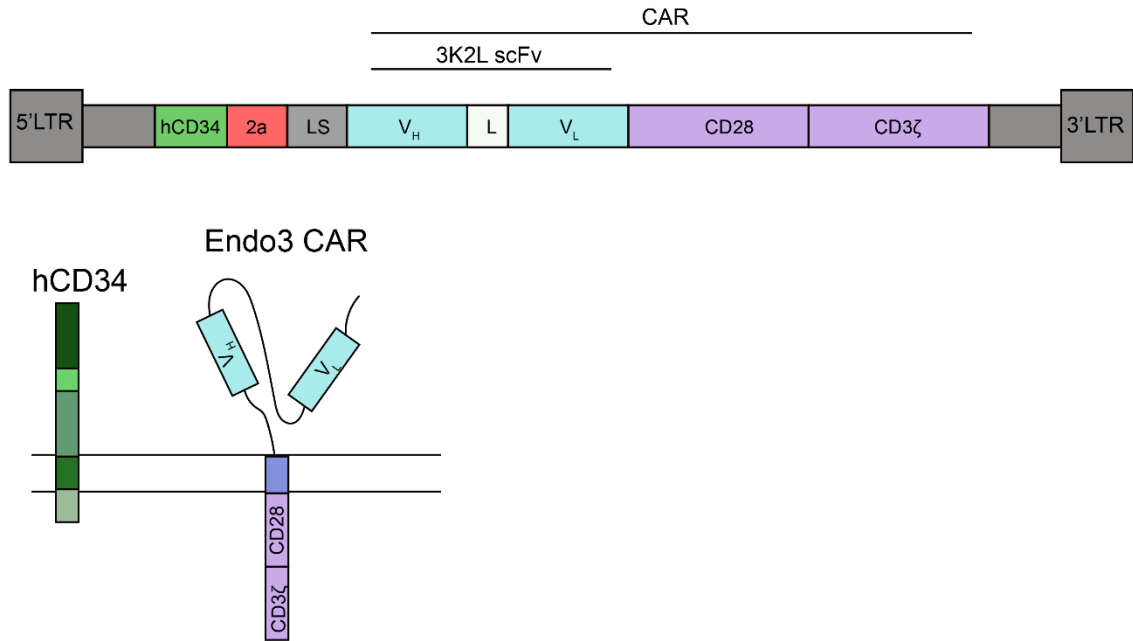


Figure 3. 2 Endo3 CAR construct

Diagram of the Endo3 CAR construct.

The Endo3 CAR contains a signal peptide, the single-chain variable fragment (scFv) portion of the rat anti-endosialin mAb 3K2L, a linker, the cytoplasmic domains of the human co-stimulatory molecule CD28 and the human T-cell receptor molecule CD3 ζ . The construct also contains truncated human CD34 co-expressed via a 2a self-cleaving peptide to allow identification in mouse samples.

3.2.3 Endosialin is upregulated in tumour tissue compared to normal tissues

An important consideration when evaluating CAR T-cell therapies is whether the target antigen of the CAR T-cells is expressed on cells of the normal tissues. On-target, off-tumour toxicities may result in clinical complications, and in severe cases, patient morbidity, as observed after patient transfusion with HER2-targeting CAR T-cells due to on-target, off-tumour targeting of lung epithelial cells (Morgan *et al.* 2010).

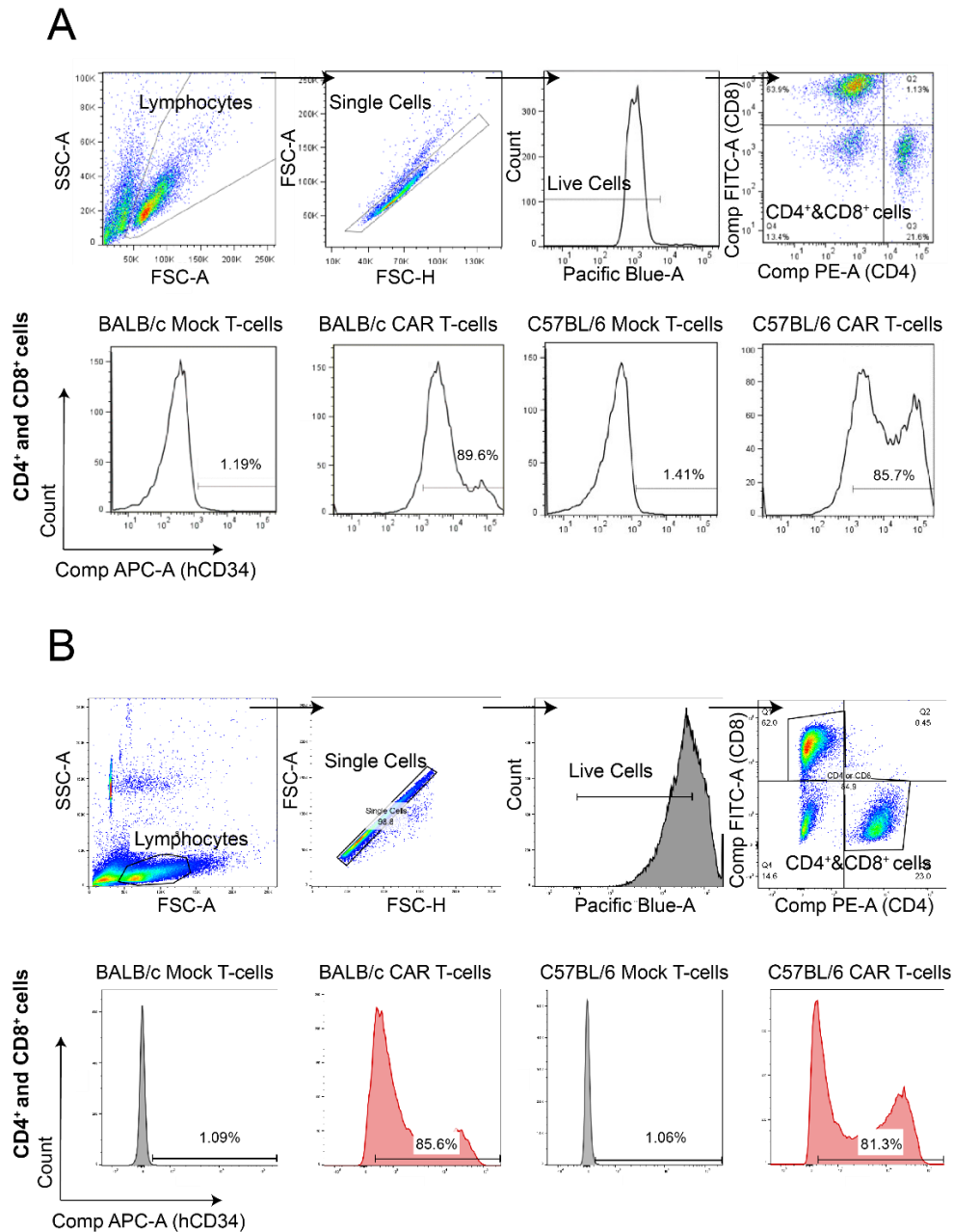


Figure 3. 3 Transduction of Endo3 CAR construct into BALB/c and C57BL/6 T-cells

Mock and Endo3 CAR transduced T-cell populations produced by **(A)** Dr Steve Lee and colleagues and **(B)** as part of this PhD project at the ICR, were analysed in the respective institutes by flow cytometry to evaluate Endo3 CAR transduction efficiency. Forward scatter area (FSC-A) and side scatter area (SSC-A) were used to gate out debris. FSC-A and forward scatter height (FSC-H) were used to gate out doublets. DAPI was used to gate out dead cells. The resulting live single cells were visualised in FITC (CD8) and PE (CD4) channels to identify CD8⁺ and CD4⁺ T-cells. CD4⁺ and CD8⁺ T-cells were subsequently visualised in the APC (hCD34) channel to identify hCD34⁺ Endo3 CAR T-cells and to confirm the absence of hCD34 in mock transduced T-cells.

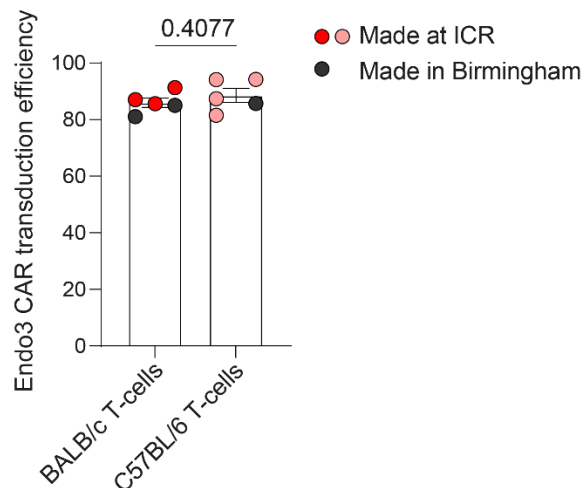


Figure 3. 4 Transduction efficiency of Endo3 CAR construct into BALB/c and C57BL/6 derived T-cells

BALB/c or C57BL/6 Endo3 CAR T-cell populations were determined using the gating strategy shown in Figure 3.3. Each data point represents the transduction efficiency of a single batch of T-cells ($100\text{-}250 \times 10^6$ Endo3 CAR T-cells produced per batch). Red and pink data points represent Endo3 CAR T-cells generated at the ICR as part of this thesis. Grey data points represent Endo3 CAR T-cells generated by Steven Lee and colleagues at the University of Birmingham. Data shows mean \pm SEM. Unpaired Student's *t*-test.

Consequently, the expression pattern of endosialin in the normal tissues of BALB/c (Figure 3.5) and C57BL/6 (Figure 3.6) mice was explored. In both strains, endosialin-positive cells are observed in the skin, brain, adipose tissue, the bladder, connective tissue of the lungs and stomach and in the heart muscle wall. As expected, and as previously reported by our laboratory and others, high levels of endosialin expression are observed on CAFs and pericytes closely associated with endomucin-positive endothelial cells, but not the endothelial cells or tumour cells within AT-3 and 4T1 tumours grown in C57BL/6 and BALB/c mice, respectively (Figure 3.7). 4T1 tumours were also grown in NSG mice for experiments described in Chapter 7 and the restricted pattern of tumour-associated endosialin expression is the same as in 4T1 tumours in immunocompetent mice (Figure 3.7). Of note, the architecture of the AT-3 and 4T1 tumours is distinct with AT-3 tumours containing tumour nests with few infiltrating CAFs surrounded by a well-established vasculature while 4T1 tumours

display a more disorganised vasculature and abundant infiltrating CAFs. Direct comparison of endosialin expression in the normal BALB/c skin and subcutaneous 4T1 tumour tissue reveals endosialin-positive fibroblasts in both tissues, however a strongly increased endosialin level in the cells associated with the endomucin-positive vasculature is observed in 4T1 tumours (Figure 3.8).

Taken together, these results confirm previous reports that endosialin is upregulated in and around the tumour tissue in mouse mammary cancers (MacFadyen *et al.* 2005). However, low levels of endosialin expression in some normal tissue could still result in on-target, off-tumour toxicity associated with Endo3 CAR T-cell therapy, therefore these organs were monitored closely in all *in vivo* experiments during this PhD.

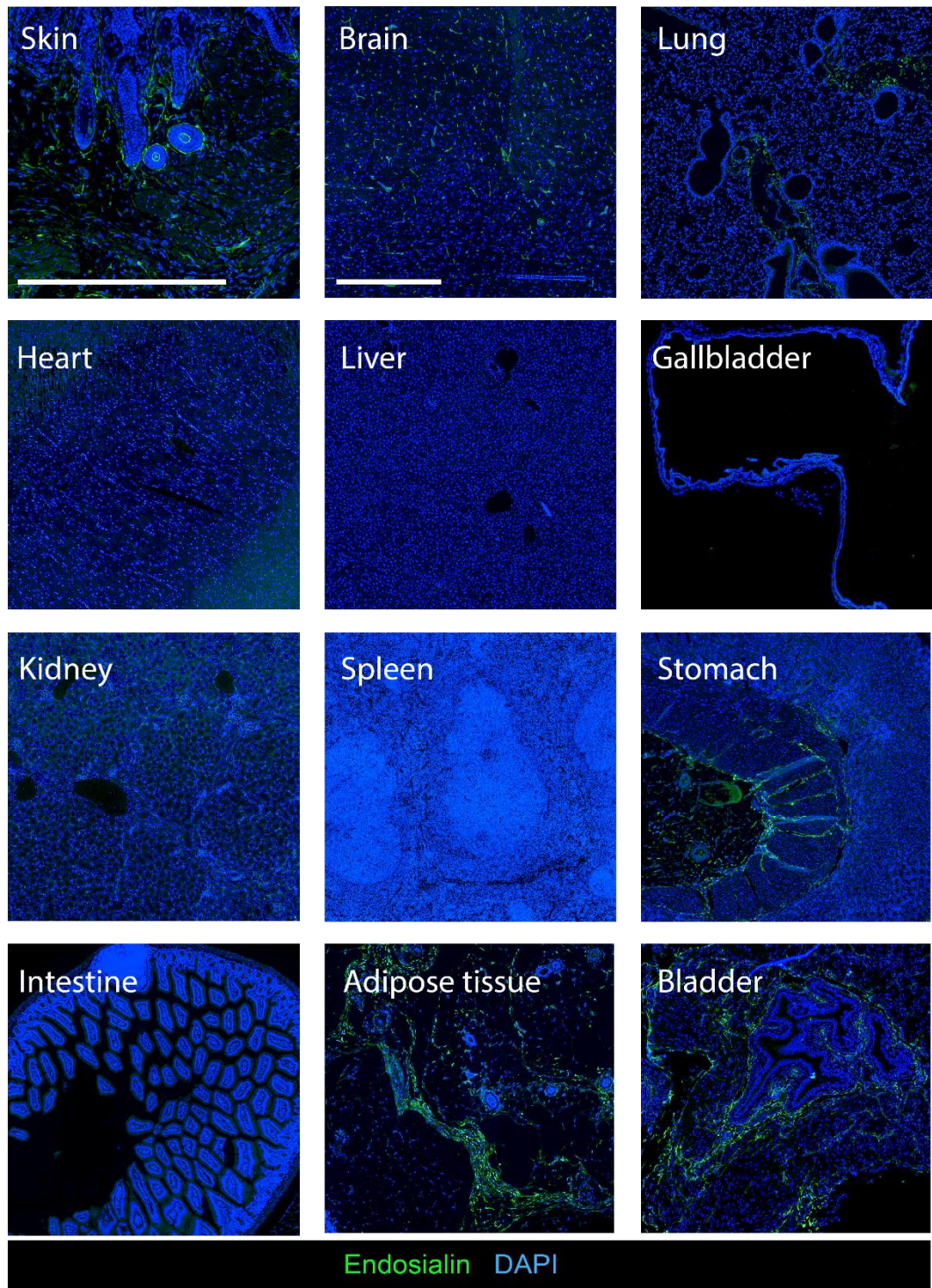


Figure 3. 5 Endosialin expression in the healthy, adult BALB/c mouse

Tissues from 8 week old, non-tumour bearing BALB/c mice (n=2) were formalin-fixed, paraffin-embedded (FFPE). Tissue sections were stained for endosialin (green). Nuclei were counterstained with DAPI (blue). Slides were scanned on a Hamamatsu NanoZoomer. Representative images from the same mouse are shown. Scale bars = 500 μ m (skin 2x higher magnification than all other tissues).

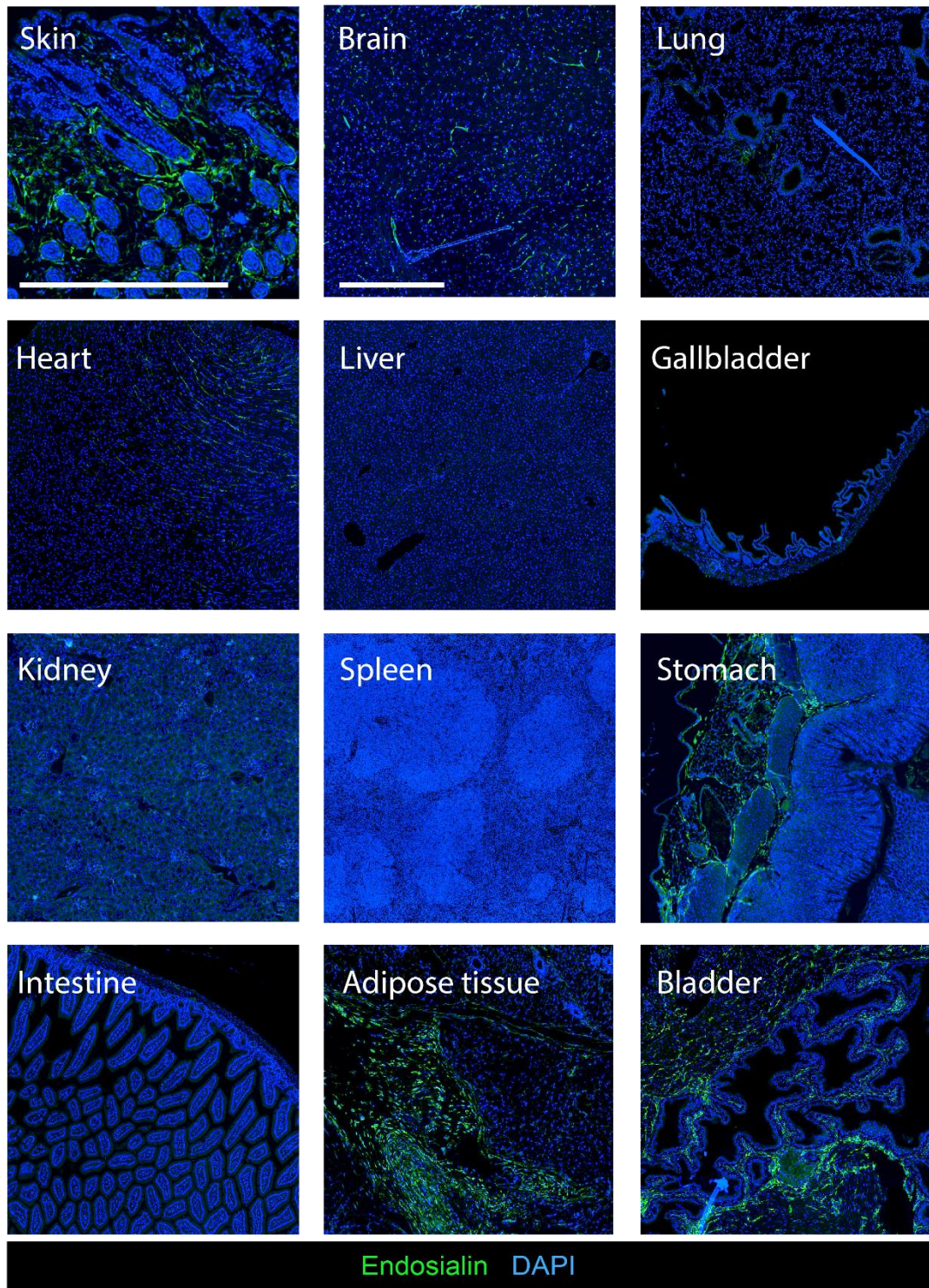


Figure 3. 6 Endosialin expression in the healthy, adult C57BL/6 mouse

Tissues from 8 week old, non-tumour bearing C57BL/6 mice (n=2) were formalin-fixed, paraffin-embedded (FFPE). Tissue sections were stained for endosialin (green). Nuclei were counterstained with DAPI (blue). Slides were scanned on a Hamamatsu NanoZoomer. Representative images from the same mouse are shown. Scale bars = 500 μ m (skin 2x higher magnification than all other tissues).

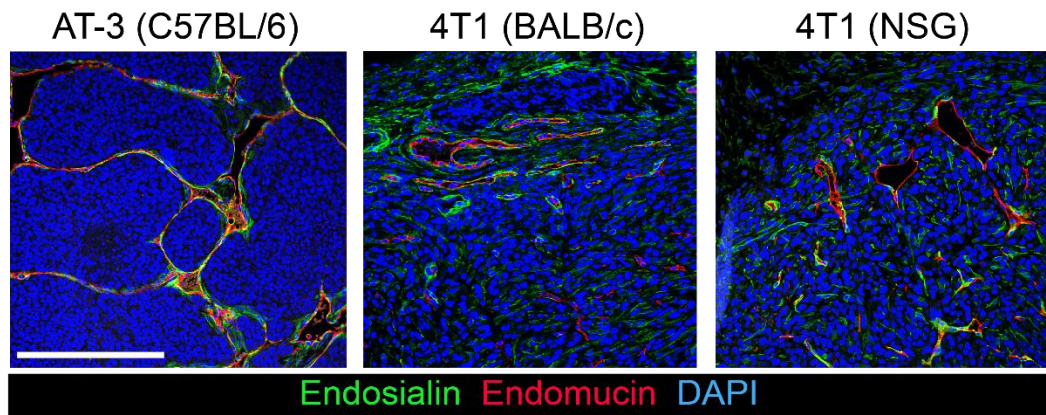


Figure 3. 7 Endosialin expression in syngeneic mouse models of breast cancer

Immunostaining of an AT-3 tumour grown for 29 days in a C57BL/6 mouse (left), a 4T1 tumour grown for 15 days in a BALB/c mouse (centre) and a 4T1 tumour grown for 13 days in an NSG mouse (right). Tumour cells were injected at a density of 2.5×10^5 cells. All mice were aged 8-10 weeks at the time of tumour cell injection. Confocal images of formalin-fixed, paraffin-embedded (FFPE) sections stained for endosialin (green) and the endothelial cell marker endomucin (red). Nuclei were counterstained with DAPI (blue). Representative images of $n=3$ tumours per group are shown. Scale bar = 250 μm .

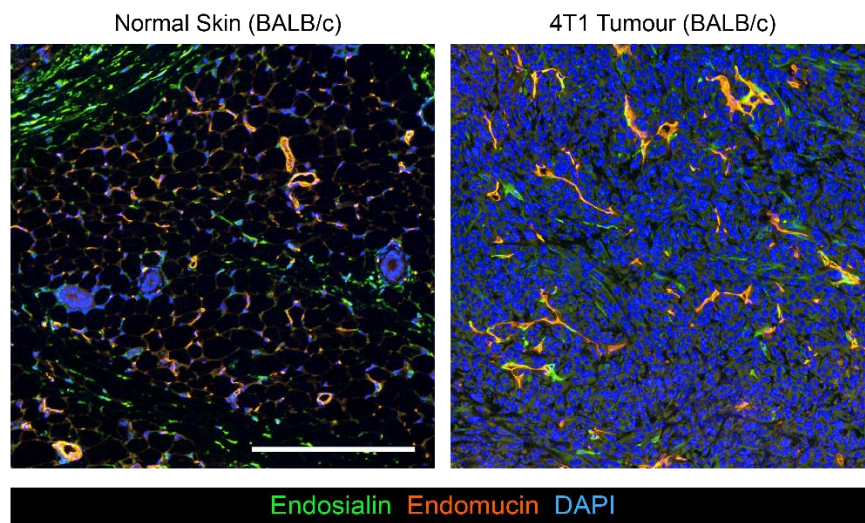


Figure 3. 8 Direct comparison of endosialin expression in normal skin and 4T1 tumour tissue

Skin from a non-tumour bearing 8-10 week old BALB/c mouse (left) and a 4T1 tumour grown in an age-matched BALB/c mouse (right) were formalin-fixed, paraffin embedded (FFPE). Tissues were stained for endosialin (green) and endomucin (red). Nuclei were counterstained with DAPI (blue). Slides were scanned on a Hamamatsu NanoZoomer. Representative images of $n=3$ mice per group are shown. Scale bar = 250 μm .

3.2.4 *Endosialin expression in human breast cancer*

To address the clinical relevance of the findings in this Chapter, the expression of endosialin in human breast cancer stroma was explored. Staining of a human invasive breast cancer microarray, carried out previously in our laboratory, reveals endosialin expression on perivascular cells in 184 out of 219 (84%) and on CAFs in 147 (67%) of the cores, with no expression on tumour cells apart from rare metaplastic tumours (Figure 3.9A). This finding is further supported by single cell sequencing data performed by Wu and colleagues (Wu *et al.* 2021) of a primary breast cancer dissociated into distinct cell types, which shows endosialin (*CD248*) expression is largely restricted to the perivascular cells and CAFs with no expression on tumour cells or other stromal components (Figure 3.9B). Comparison of endosialin expression in microdissected breast tumour stroma and normal adjacent breast tissue stroma, carried out by Finak and colleagues (Finak *et al.* 2008), demonstrates significantly higher levels of *CD248* mRNA in the tumour stroma (Figure 3.9C), further supporting previous findings that endosialin is expressed at low levels in healthy adult tissue, but upregulated in the tumour stroma. Importantly, single cell sequencing data, accessed via the Human Protein Atlas, of normal breast, skin and adipose tissue reveals low levels of endosialin expression on pericytes in these tissues. The pericyte markers NG2, desmin and α -SMA were used to identify pericyte populations within the determined clusters. It must be noted however, that higher levels of endosialin expression are found on fibroblasts in these tissues, with fibulin-1, collagen, type 1, alpha 1 and lysyl oxidase homolog 1 being used to identify fibroblast populations within the determined clusters (Figure 3.10).

Taken together, these data provide further evidence of upregulated endosialin expression in the tumour stroma, especially on the perivascular cells, and support the clinical relevance of endosialin as a CAR T-cell target.

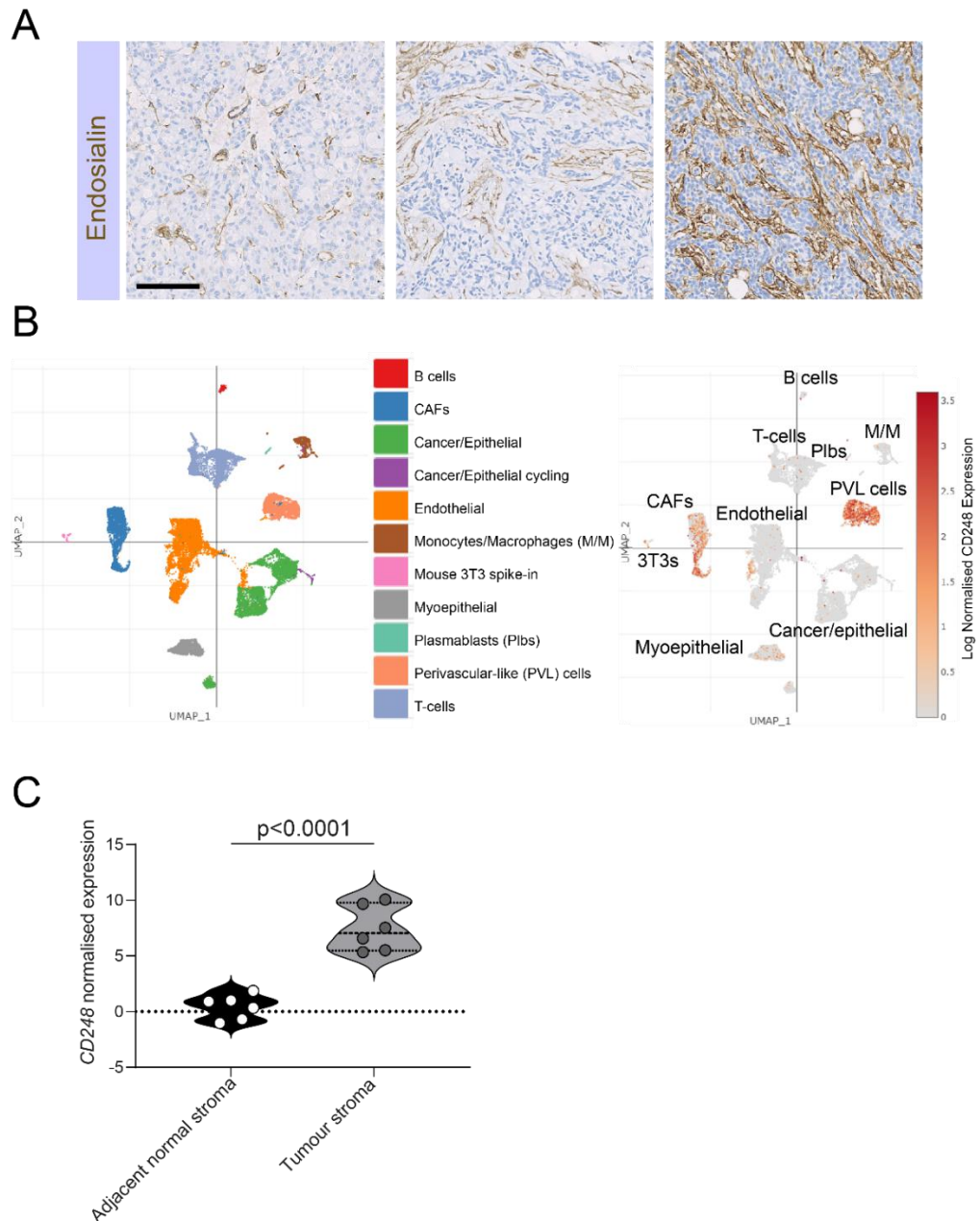


Figure 3. 9 Endosialin expression in human breast cancer

(A) Formalin-fixed, paraffin-embedded (FFPE) human invasive breast cancer tumour microarray (TMA) stained for endosialin. Slides were scanned on a Hamamatsu NanoZoomer. Representative images of invasive breast cancer with endosialin staining predominantly restricted to the pericytes (left panel), CAFs (middle panel) and both pericytes and CAFs (right panel) are shown. Scale bar = 100 μ m. **(B)** Endosialin (*CD248*) expression in different cell types dissociated from 26 primary human breast cancers. Re-analysed data from single cell RNA sequencing conducted by Wu and colleagues (Wu *et al.* 2021) **(C)** Comparison of endosialin expression in six matched cases of microdissected breast tumour stroma and normal adjacent stroma. Re-analysed data from microarray analysis conducted by Finak and colleagues (Finak *et al.* 2008). Paired Student's *t*-test.

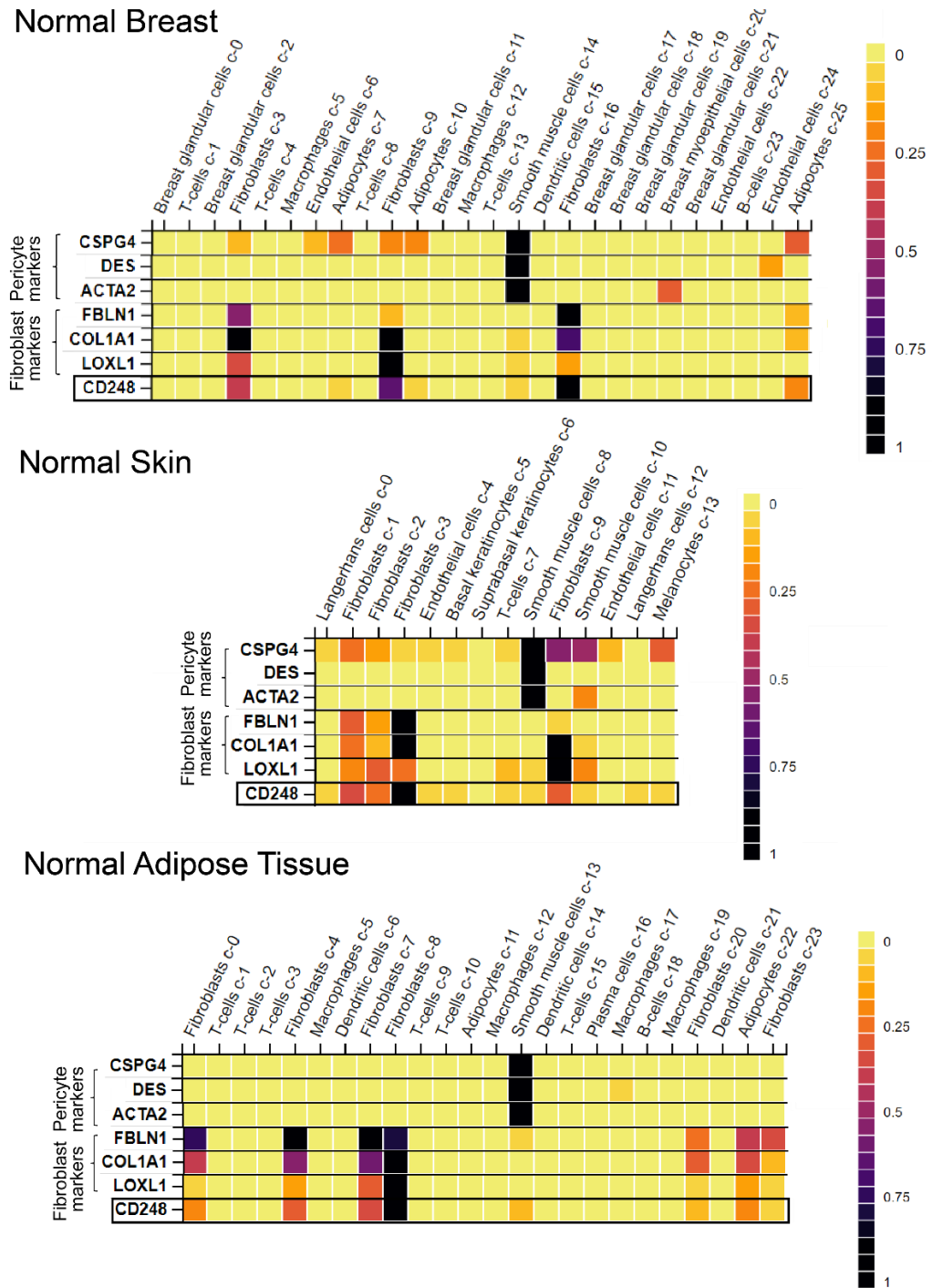


Figure 3. 10 Endosialin expression in normal human tissues

Endosialin (*CD248*) expression in different cell types dissociated from normal human breast (upper), skin (centre) and adipose tissue (lower). NG2 (*CSPG4*), desmin (*DES*) and α -SMA (*ACTA2*) are used to identify pericyte populations. Fibulin-1 (*FBLN1*), collagen, type 1, alpha 1 (*COL1A1*) and lysyl oxidase homolog 1 (*LOXL1*) are used to identify fibroblast populations. Colour scales normalised per row for each individual gene. Data from single cell RNA sequencing conducted by Karlsson and colleagues (Karlsson *et al.* 2021). Expression panels retrieved from Human Protein Atlas [proteinatlas.org](https://www.proteinatlas.org).

3.3 Discussion

3.3.1 *Endo3 CAR is transduced with high efficiency into mouse T-cells*

Whilst successful transduction of human T-cells with CAR constructs has been widely reported in the literature, the transduction of mouse T-cells is less well documented. Of those reports detailing mouse T-cell transduction with CAR constructs, the range of transduction efficiencies of 2nd generation or higher CAR T-cells is 40-80% (James N. Kochenderfer *et al.* 2010; Fu *et al.* 2013; Wang *et al.* 2014), likely due to suboptimal methodologies or reagents. In this thesis, the method for mouse T-cell transduction described in Chapter 2.2.9 was provided by our collaborator Dr Steven Lee and consistently achieved >80% transduction efficiency, with the highest observed transduction efficiency being 94.2%. This is in agreement with recent data reported by Lanitis and colleagues who achieved >80% CAR transduction efficiency of mouse T-cells using a similar method of retroviral transduction (Lanitis *et al.* 2020). Interestingly, Lanitis and colleagues continue to culture their transduced CAR T-cells for 7 days post-transduction in the presence of hIL-7/IL-15, which results in significant CAR T-cell expansion without compromising CAR T-cell viability. During this PhD, the number of CAR T-cells generated in a single protocol has been a limiting factor for the design of *in vivo* studies. Adopting this additional step following retroviral transduction of Endo3 CAR T-cells may allow for larger cohorts or larger Endo3 CAR T-cell doses in future *in vivo* studies.

3.3.2 *Syngeneic models of breast cancer for Endo3 CAR T-cell evaluation*

The majority of preclinical CAR T-cells studies reported in the literature to date focus on targeting human antigens expressed by tumour cells with human CAR T-cells (Hoyos *et al.* 2010; Lanitis *et al.* 2012; Budde *et al.* 2013). Consequently, the models used are often human tumour xenografts in immunodeficient mice. However, the lack of

endogenous immunity in these models hinders the safety and efficacy evaluation of CAR T-cell products at the preclinical level. Further, targeting human antigens within a mouse host system does not allow for the consideration of on-target, off-tumour toxicities against normal tissues, which may result in severe adverse reaction or even death (Lamers *et al.* 2006; Morgan *et al.* 2010; Tran *et al.* 2013).

Engineering CAR T-cells with a scFv fragment that has the ability to recognise both mouse and human forms of the target antigen allows for preclinical evaluation of a CAR T-cell within the context of a fully competent immune system, as well as the investigation of potential on-target, off-tumour activity, without compromising the clinical translatability of the CAR T-cell. In this Chapter, the mAb 3K2L scFv portion of endosialin-targeting Endo3 CAR T-cells was shown to recognise both mouse and human endosialin, which suggests that Endo3 CAR T-cells can act upon both mouse and human cells expressing endosialin.

Our laboratory has previously reported that endosialin is highly expressed in some normal tissues during embryonic development in mice, but is downregulated by age 10 weeks (MacFadyen *et al.* 2007). Despite being considerably downregulated when compared to embryonic tissue, MacFadyen *et al.* reported low levels of residual endosialin expression on fibroblasts in several organs including the skin, lungs and heart in C57BL/6 mice. In agreement with MacFadyen *et al.* the immunostaining performed in this Chapter in BALB/c and C57BL/6 mice identifies endosialin-positive cells in the lungs, skin and heart, but also in the brain, stomach, adipose tissue and bladder. It must be considered however that the mice analysed in this experiment were aged 8 weeks, therefore further downregulation of expression may take place as the mice age. Unpublished data from our laboratory comparing gene expression in the lungs of young adult mice and aged mice shows a significant decrease in endosialin expression in aged mice (data not shown). As most breast cancers are detected in individuals over the age

of 40, it is not anticipated that endosialin expression in normal tissue would cause on-target, off-tumour toxicity in patients, however, this question will be addressed further in Chapter 4.

It must be noted that the panel of normal tissues immunostained for endosialin in this chapter did not include bone tissue. It has previously been shown that endosialin is expressed by cells of the bone marrow, with high expression being observed on osteoblasts within bone marrow taken from newborn mice (Naylor *et al.* 2012). As previously mentioned in Chapter 1.4.6.1, Tran and colleagues observed severe bone hypocellularity and cachexia following the treatment of tumour-bearing mice with FAP targeting CAR T-cells, which was attributed to targeting of FAP-positive bone marrow-derived stem cells (Tran *et al.* 2013). Therefore, examination of endosialin expression in the bone marrow of adult BALB/c and C57BL/6 mice may be an important addition to the normal tissue cross described in this Chapter.

Reassuringly, direct comparison of normal BALB/c skin and 4T1 tumour tissue revealed increased levels of endosialin-positive staining around the tumour vasculature, and, consistent with previous reports (Rettig *et al.* 1988; MacFadyen *et al.* 2005; Rouleau *et al.* 2008; Simonavicius *et al.* 2008), endosialin expression was restricted to the vascular pericytes and CAFs in both 4T1 and AT-3 tumours.

3.3.3 *Endosialin expression in human breast cancer*

Prior to commencing a long-term study, it is important to confirm the relevance of a proposed CAR T-cell target antigen in the human setting. The data presented in this Chapter confirms the restriction of endosialin expression to CAFs and pericytes in human breast cancers, aside from rare metaplastic breast cancers, and the upregulation of endosialin in the tumour stroma when compared to normal breast stroma. Specifically, endosialin is notably expressed by perivascular cells in human breast cancer, but not by

perivascular cells in normal human breast, skin and adipose tissue. This concurs with the results observed when comparing mouse mammary carcinoma and normal skin tissues. It must be considered, however, that the normal human breast, skin and adipose tissue have endosialin-expressing fibroblasts in the stroma. Because of this, patients would require monitoring for on-target, off-tumour affects in the clinic if treated with Endo3 CAR T-cell therapy.

In summary, the work presented in this Chapter demonstrates that the 3K2L mAb recognises both mouse and human endosialin, that the Endo3 CAR construct can be successfully transduced into both BALB/c and C57BL/6 T-cells and that the syngeneic tumour models used in this thesis are suitable for assessing the efficacy of CAR T-cells targeting cells of the tumour microenvironment. The next Chapter will describe the experiments performed to demonstrate the specificity and efficacy of Endo3 CAR T-cells.

Chapter 4 *In vitro* and *in vivo* characterisation of Endo3 CAR T-cells

4.1 Introduction

Endosialin is as a promising antigen for targeted anti-tumour therapy in breast cancer, owing to its upregulated expression in the tumour stroma. In Chapter 3.2.1, the endosialin specific mAb 3K2L, of which the scFv portion is utilised in Endo3 CAR T-cells, was shown to recognise both mouse and human endosialin. In turn, this suggests that Endo3 CAR T-cells have the potential to bind and kill both mouse and human cells expressing endosialin. The syngeneic 4T1 and AT-3 mouse models of breast cancer were identified in Chapter 3.2.3 as suitable preclinical models to test Endo3 CAR T-cells as they both develop an established vascular network and endosialin expression is restricted to the stromal compartment in both models.

Owing to the success of CD19-targeting CAR T-cell therapy for the treatment of haematological cancers, preclinical strategies for investigating novel CAR T-cell designs remain largely based on the clinical strategies of Kymriah and Yescarta. Currently, both strategies involve prior lymphodepletion of patients, followed by the administration of a single dose of CAR T-cells. Patients are subsequently monitored for up to 4 weeks for adverse reactions following T-cell injections (J. N. Kochenderfer *et al.* 2017; Maude *et al.* 2018; Schuster *et al.* 2018). Previous reports have demonstrated that a lymphodepletion step aids in the engraftment and expansion of CAR T-cells (Muranski *et al.* 2006; Dudley *et al.* 2008; Heczey *et al.* 2017), thus lymphodepleting patients prior to CAR T-cell therapy is currently standard practice. As discussed in Chapter 1.4.4, CAR T-cell therapy may be associated with CRS or ICANS, thus patient monitoring post-T-cell injection for signs of toxicity is crucial.

In this Chapter, the activity, specificity and tolerability of Endo3 CAR T-cells are investigated both *in vitro* and *in vivo*, with an *in vivo* therapeutic strategy for testing Endo3 CAR T-cell therapy being developed based on current clinical practices.

4.2 Results

4.2.1 Endo3 CAR T-cells exhibit target-specific activity *in vitro*

As previously discussed, the *in vivo* studies described in this thesis utilised mock transduced and Endo3 CAR T-cells generated by either our laboratory or the laboratory of Dr Steven Lee. All BALB/c studies described in this thesis utilise BALB/c T-cells produced by Dr Steven Lee's laboratory. All C57BL/6 studies described in this thesis utilise C57BL/6 mock transduced and Endo3 CAR T-cells generated by our laboratory. The activity of BALB/c and C57BL/6 derived T-cells produced by Dr Steven Lee's laboratory and C57BL/6 derived T-cells that I produced is explored in this Section.

Upon activation, cytotoxic T-cells release a number of cytokines and other factors into their surrounding environment, including TNF- α , IL-2 and IFN- γ (Andersen *et al.* 2006). To assess the specificity of Endo3 CAR T-cell activation *in vitro*, both mouse (10T $\frac{1}{2}$) and human (MRC5) endosialin-positive stromal cell lines were used as target cells alongside mouse (4T1 or AT-3) and human (MCF7) endosialin-negative tumour cell lines. Target cells were co-cultured with either BALB/c (generated in the Dr Steven Lee's laboratory) or C57BL/6 (generated in our laboratory) derived mock or Endo3 CAR T-cells at various effector:target ratios. Culture supernatants were analysed via IFN- γ ELISA at 24 h post-T-cell addition. As expected, IFN- γ levels are higher in supernatants derived from BALB/c (Figure 4.1A) and C57BL/6 (Figure 4.1B) Endo3 CAR T-cell co-cultured with endosialin-positive 10T $\frac{1}{2}$ and MRC5 cells, with only background levels of IFN- γ detectable in co-cultures with endosialin-negative 4T1, AT-3 and MCF7 cells. Mock T-cells produce only low levels of IFN- γ in the presence of all target cell lines. Of note,

C57BL/6 derived Endo3 CAR T-cells release higher levels of IFN- γ after the 24 h incubation period than BALB/c Endo3 CAR T-cells.

To assess Endo3 CAR T-cell mediated killing of target cell lines, BALB/c and C57BL/6 T-cells were removed from co-cultures by washing with PBS 84 and 24 h after addition, respectively. BALB/c T-cell co-cultures were extended to 84 h due lack of visible cell death at 24, 48 or 72h (data not shown). After washing, cell viability was assessed by addition of CellTiter-Glo reagent, which quantifies the presence of ATP. Percent viability of endosialin-positive 10T $\frac{1}{2}$ and MRC5 cells co-cultured with BALB/c (Figure 4.2A) and C57BL/6 (Figure 4.2B) Endo3 CAR T-cells is significantly reduced at effector:target ratios of 5:1 or greater, when compared to 10T $\frac{1}{2}$ and MRC5 cells co-cultured with mock T-cells. In contrast, 4T1, AT-3 and MCF7 cell viability is unaffected by the presence of Endo3 CAR T-cells.

To confirm that C57BL/6 derived T-cells produced by Dr Steven Lee's laboratory behave comparably to those produced by our laboratory, their batch of mock transduced and Endo3 CAR T-cells were subjected to the same IFN- γ and target cell viability analysis as above. The Birmingham CAR T-cells produce IFN- γ (Figure 4.3A) and kill target cells (Figure 4.3B) in a comparable manner to those produced in our laboratory in the presence of endosialin-positive 10T $\frac{1}{2}$ and MRC5 cells. Again, only low levels of IFN- γ are produced in the presence of endosialin-negative AT-3 and MCF7 cells and the viability of both tumour cell lines is unaffected by co-culture with Endo3 CAR T-cells.

In summary, these data demonstrate that both BALB/c and C57BL/6 Endo3 CAR T-cells are able to activate in the presence of and kill both mouse and human cell lines in an endosialin-specific manner *in vitro*, and that CAR T-cells produced in Birmingham and at the ICR behave in a comparable manner in *in vitro* assays.

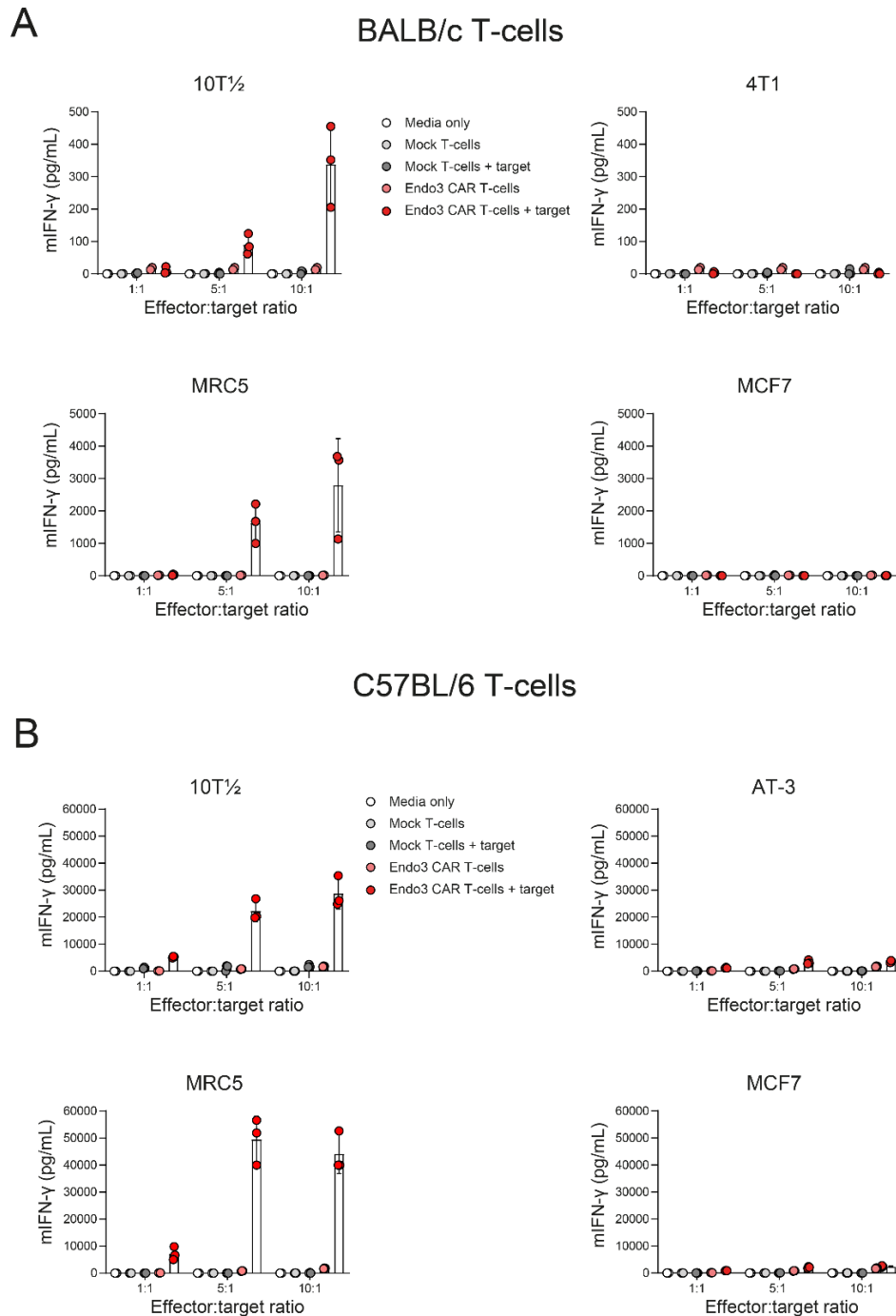


Figure 4. 1 IFN- γ release by mock transduced and Endo3 CAR T-cells co-cultured with target cell lines

Target cells (mouse 10T $\frac{1}{2}$ pericyte-like, 4T1 tumour and AT-3 tumour cells, and human MRC5 fibroblasts or MCF7 tumour cells) were seeded at 1000-5000 cells per well in 96 well plates, depending on growth rate. T-cells were added 24 h after target cell seeding. IFN- γ production by **(A)** BALB/c and **(B)** C57BL/6 derived mock transduced T-cells or Endo3 CAR T-cells when cultured for 24 h alone or with target cells at various effector:target ratios. Each data point represent one well. Data shows mean \pm SD. The displayed results are representative of 3 independent experiments.

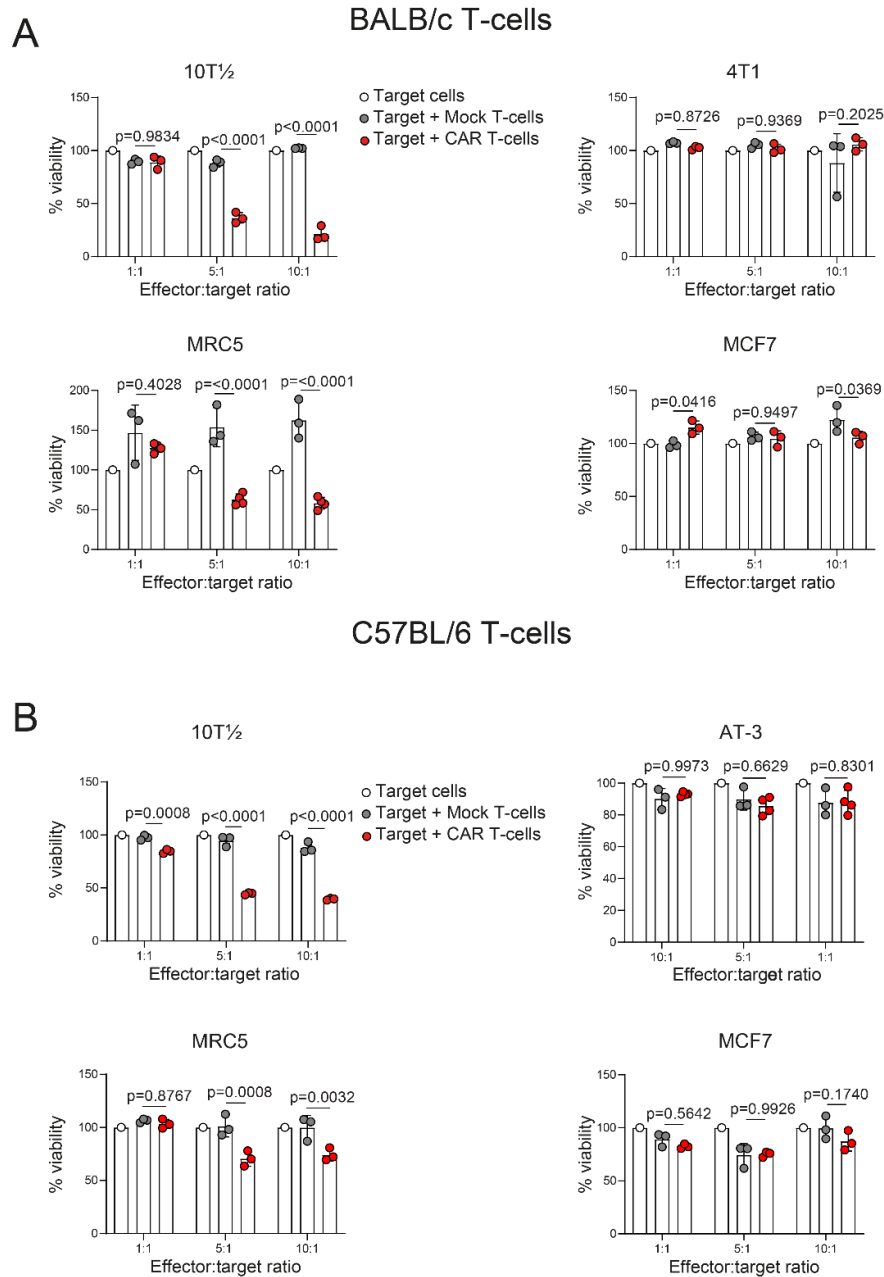


Figure 4. 2 Viability of target cell lines co-cultured with mock transduced or Endo3 CAR T-cells

Target cells (mouse 10T $\frac{1}{2}$ pericyte-like, 4T1 tumour and AT-3 tumour cells, and human MRC5 fibroblasts or MCF7 tumour cells) were seeded at 1000-5000 cells per well in 96-well plates, depending on growth rate. T-cells were added 24 h after target cell seeding. T-cells were washed off 24-84 h after addition and target cell viability was measured by quantifying the presence of ATP via CellTiter-Glo viability assay. Target cell viability of cells incubated with **(A)** BALB/c and **(B)** C57BL/6 derived mock transduced and Endo3 CAR T-cells. The average read-out from target cells cultured alone were defined as 100% viability, viability of target cells from co-culture wells was calculated as a percentage of the target cells alone. Each data point represents one well. Data shows mean \pm SD. Two-way ANOVA. The displayed results are representative of 3 independent experiments.

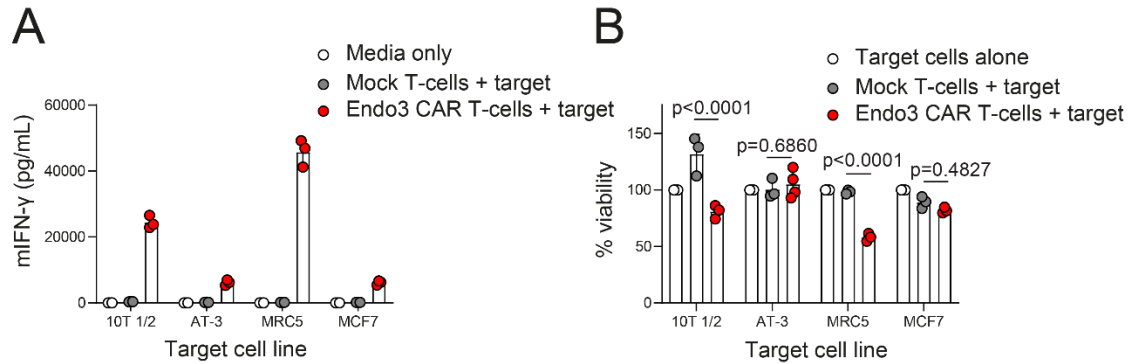


Figure 4. 3 *In vitro* validation of C57BL/6 derived Endo3 CAR T-cells generated by Dr Steven Lee's laboratory

Target cells (mouse 10T $\frac{1}{2}$ pericyte-like and AT-3 tumour cells, and human MRC5 fibroblasts or MCF7 tumour cells) were seeded at 1000-5000 cells per well in 96-well plates, depending on growth rate. T-cells were added 24 h after target cell seeding. **(A)** IFN- γ production by C57BL/6 derived mock transduced or Endo3 CAR T-cells when cultured for 24 h alone or with target cells at a 10:1 effector:target ratio. Data shows mean \pm SD. **(B)** Target cell viability 24 h after T-cell addition measured by Cell-Titer-Glo assay. T-cells were washed off prior to addition of Cell-Titer-Glo reagent. Each data point represents one well. Data shows mean \pm SD. Two-way ANOVA.

4.2.2 Optimisation of Endo3 CAR T-cell in vivo therapeutic strategy

Lymphodepletion prior to CAR T-cell infusion has been shown to improve CAR T-cell engraftment and expansion both in the preclinical and clinical setting (Muranski *et al.* 2006; Dudley *et al.* 2008; Heczey *et al.* 2017; Kueberuwa *et al.* 2018a). Clinically, lymphodepletion may be achieved via the administration of lymphodepleting chemotherapy, such as cyclophosphamide, or by radiotherapy (Brentjens *et al.* 2011a; Brentjens *et al.* 2011b), with the former being the most common method of lymphodepletion in patients. It has been reported by Kueberuwa and colleagues that lymphodepletion via 5 Gy whole body irradiation is a more efficient lymphodepletion method in BALB/c mice, with a more sustained level of lymphodepletion being observed (Kueberuwa *et al.* 2018a). Therefore, to investigate this further, the lymphodepleting

effects of cyclophosphamide chemotherapy, whole body x-ray irradiation and whole body caesium irradiation were assessed in BALB/c mice.

The reported maximum tolerated dose of cyclophosphamide in BALB/c mice is 300 mg/kg (Aston *et al.* 2017), with the lymphodepleting dose being reported between 100-200 mg/kg (Huyan *et al.* 2011; Kueberuwa *et al.* 2018a; Kueberuwa *et al.* 2018b). Therefore, a single dose of 150 mg/kg cyclophosphamide was administered IP to three mice, with additional mice subjected to 5 Gy x-ray or caesium irradiation. After 18 h, venous blood was collected via the tail vein and whole blood was prepared for flow cytometry analysis (Figure 4.4A). Blood collected via cardiac puncture from untreated BALB/c mice was used as a control. CD4⁺ and CD8⁺ lymphocytes are significantly depleted by all lymphodepletion methods with no differences observed in lymphodepletion efficiency between the three methods (Figure 4.4B). However, treatment with cyclophosphamide chemotherapy was not tolerated in this experiment and within 24 h of administration mice were culled due to rapid weight loss and ill health. It was therefore concluded that either 5 Gy whole body x-ray or caesium irradiation were preferable methods for lymphodepletion in future experiments utilising BALB/c mice.

As C57BL/6 mice were also utilised for Endo3 CAR T-cell studies in this thesis, the lymphodepleting effects of 5 Gy x-ray irradiation in C57BL/6 mice was investigated. Mice were sacrificed 24 h after receiving 5 Gy x-ray irradiation and blood was collected via cardiac puncture. Blood collected via cardiac puncture from untreated mice was used as a control. Similarly to BALB/c mice, CD4⁺ and CD8⁺ lymphocytes are significantly depleted by 5 Gy x-ray irradiation (Figure 4.4C).

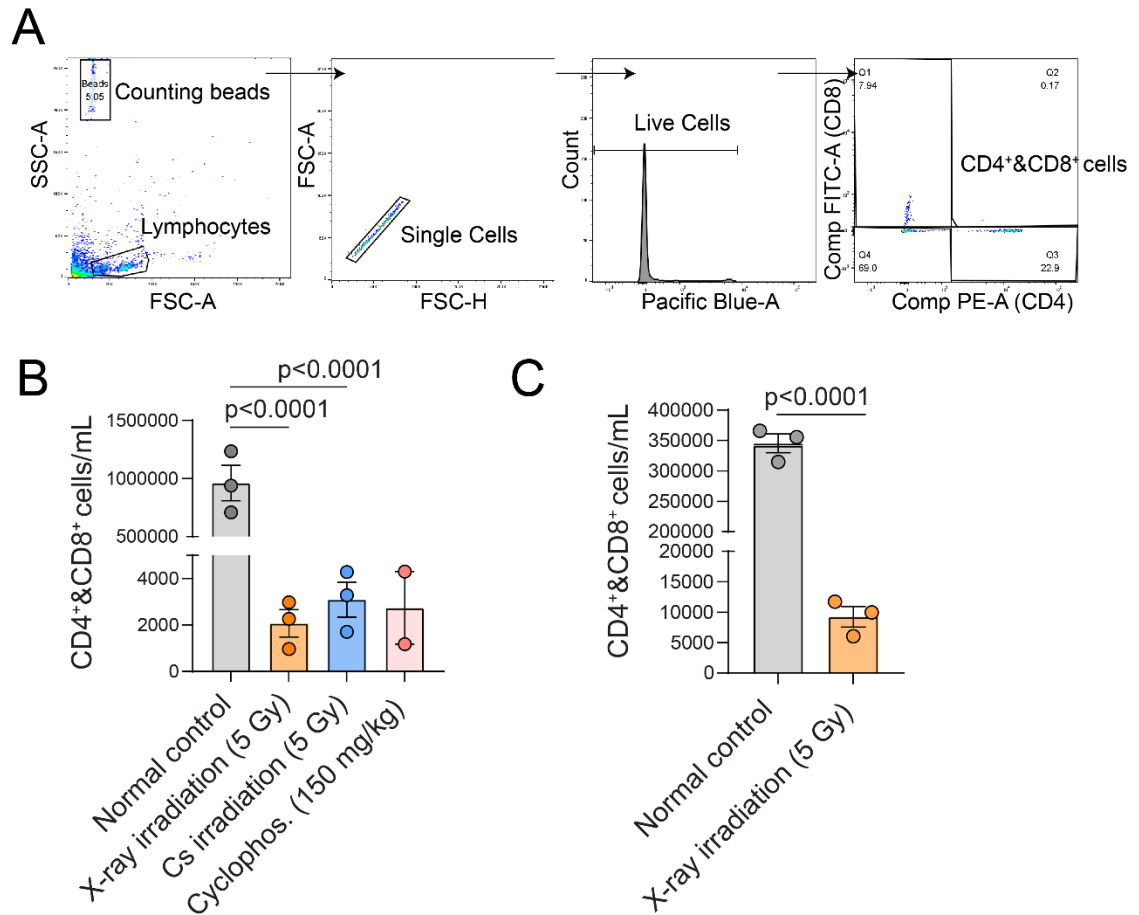


Figure 4. 4 Non-lethal whole body irradiation safely depletes lymphocytes

BALB/c mice were subjected to 5 Gy x-ray ($n=3$) or caesium (Cs) ($n=3$) irradiation or administered IP with 150 mg/kg cyclophosphamide ($n=3$). C57BL/6 mice were subjected to 5 Gy x-ray irradiation. 18 h later venous blood was collected via the tail vein or cardiac puncture. Blood collected from healthy, non-irradiated mice was used as a control ($n=3$). **(A)** Gating strategy used following staining with CD4 and CD8 antibodies. FSC-A and SSC-A were used to gate out debris and non-lymphocyte populations. FSC-A and FSC-H were used to gate out doublets. DAPI was used to gate out dead cells. The resulting live single lymphocytes were visualised in FITC (CD8) and PE (CD4) channels to identify CD8⁺ and CD4⁺ T-cell populations. CD4⁺ and CD8⁺ cells were gated together. Healthy, non-irradiated control samples were used to set gating. **(B)** Total CD4⁺ and CD8⁺ cell counts after irradiation or cyclophosphamide administration in BALB/c mice. Each data point represents one mouse. Data shows mean \pm SEM. Unpaired Student's *t*-tests. **(C)** Total CD4⁺ and CD8⁺ cell counts after 5 Gy x-ray irradiation in C57BL/6 mice ($n=3$). Blood collected from healthy, non-irradiated mice was used as a control ($n=3$) Each data point represents one mouse. Data shows mean \pm SEM. Unpaired Student's *t*-test.

Stromal endosialin expression has previously been shown to play a role in the intravasation step of the metastatic cascade in breast cancer, with *Cd248^{+/+}* mice having increased spontaneous metastasis to the lungs when compared to *Cd248^{-/-}* mice (Viski *et al.* 2016). Therefore, it was hypothesised that the administration of Endo3 CAR T-cells prior to the point of early metastatic spread would be most effective at limiting lung metastasis via the targeted killing of endosialin-positive stromal cells in the tumour.

It has been previously been demonstrated that 4T1 tumours have an established vascular network when they reach approximately 100 mm³ in size (Gregório *et al.* 2016). In the protocols used in our laboratory, 4T1 tumours reach this size at approximately 13 days post-implantation of 2×10^5 tumour cells subcutaneously. To confirm the presence of endosialin-positive stromal cells at this time point, day 13 4T1 tumours were immunostained for endosialin and the endothelial cell marker endomucin (Figure 4.5, left). As expected, endosialin-positive CAFs and pericytes are detected, with positive endomucin staining also confirming the presence of a vascular network. Examination of the lungs of mice 13 days post-4T1 tumour cell implantation reveals an absence of detectable metastatic disease at this time point (Figure 4.5, right).

4.2.3 Endo3 CAR T-cells expand in the circulation of BALB/c mice and deplete endosialin-positive cells in the 4T1 tumour stroma

The strategy to assess the efficacy and tolerability of Endo3 CAR T-cells in *Cd248^{WT}* BALB/c mice is shown in Figure 4.6. In brief, 8 week old female mice were injected subcutaneously on the flank with 4T1-Luc cells, or left tumour-naïve as controls. Tumours were allowed to grow for 13 days to 50-200 mm³ in size. All mice were subjected to 5 Gy whole body x-ray irradiation 18 h before 2.5×10^6 Endo3 CAR T-cells or mock T-cells were injected via the tail vein. Mice were monitored for signs of CAR T-cell associated toxicities following T-cell injection and venous blood was collected 2, 5 and 8 days post-T-cell injection. The original experimental endpoint was set at 16 days

post-T-cell injection, however all animals were culled 8-9 days post-T-cell injection due to ill health in a subset of tumour-bearing, Endo3 CAR T-cell treated mice.

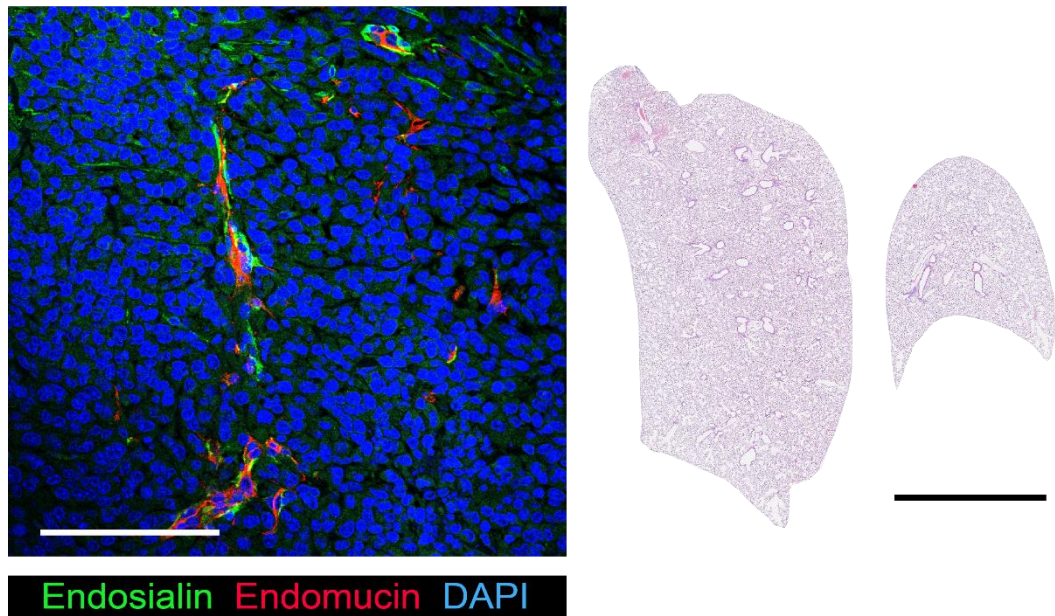


Figure 4. 5 4T1 tumours are vascularised, endosialin-positive and have not metastasised to the lungs at 2-3 weeks post-implantation.

BALB/c mice were injected with 2.5×10^5 4T1 tumour cells and culled 13 days post-tumour cell injection (n=3). Left, representative confocal image of a formalin-fixed, paraffin-embedded (FFPE) section of a 4T1 tumour (286 mm^3) stained for endosialin (green) and the endothelial cell marker endomucin (red). Nuclei were counterstained with DAPI (blue). Scale bar = $125 \mu\text{m}$. Right, representative H&E stained lungs from the same 4T1 tumour-bearing mouse. Scale bar = 2.5 mm.

To monitor circulating CAR T-cell number during the experiment, blood was collected via the tail vein 2, 5 and 8 days post-T-cell injection. On day 2 post-T-cell injection, an insufficient volume of blood was collected from the majority of mice, thus this time point was discarded. This difficulty reoccurred on day 8 post-T-cell injection within the tumour-bearing, Endo3 CAR T-cell treated group of mice, with sufficient blood volumes being collected from only 3 mice. Therefore, only these 3 mice were included in further analysis. Whole bloods were prepared and analysed via flow cytometry, with

Endo3 CAR T-cells being identified as CD4⁺hCD34⁺ or CD8⁺hCD34⁺ cells (Figure 4.7A). Endo3 CAR T-cells are identified in blood from both tumour-bearing and tumour-naïve mice and numbers expand in both subsets of mice. A significant expansion is observed in tumour-bearing mice between 5 and 8 days post-T-cell injection and at 8 days post-T-cell injection Endo3 CAR T-cell numbers are 2.5 fold higher in tumour-bearing mice compared to tumour-naïve mice. Samples from tumour-bearing and tumour-naïve mock T-cell treated mice were analysed as hCD34-negative controls. As mock T-cells do not express hCD34, circulating mock T-cell numbers could not be monitored (Figure 4.7B).

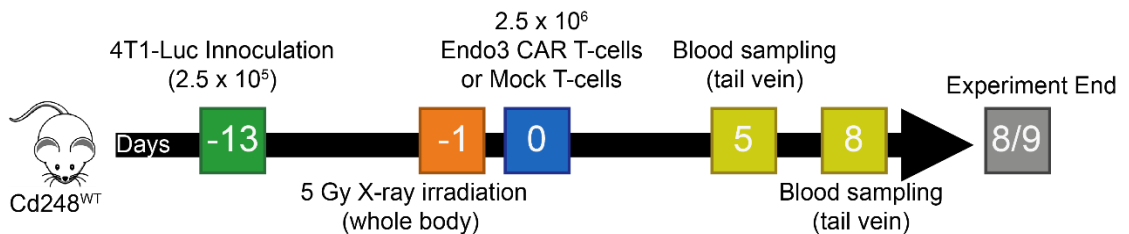


Figure 4. 6 Endo3 CAR T-cell *in vivo* therapeutic strategy for BALB/c mice bearing 4T1 tumours

8 week old endosomal wild-type (CD248^{WT}) BALB/c mice were injected subcutaneously with 2.5 x 10⁵ 4T1-Luc cells or left tumour-naïve. Tumours were allowed to grow for 12 days to 50-200 mm³ volume. All mice were subjected to 5 Gy whole body x-ray irradiation 18 h prior to injection via the tail vein with 2.5 x 10⁶ Endo3 CAR T-cells or mock T-cells (tumour-bearing n=10 per group, tumour-naïve n=2 per group). Venous blood was collected via the tail vein 5 and 8 days post-T-cell injection. A subset of mice (tumour-bearing, n=2 per group) were culled on Day 5. The remaining mice were culled 8-9 days post-T-cell injection due to ill health of tumour-bearing, Endo3 CAR T-cell treated mice (see text).

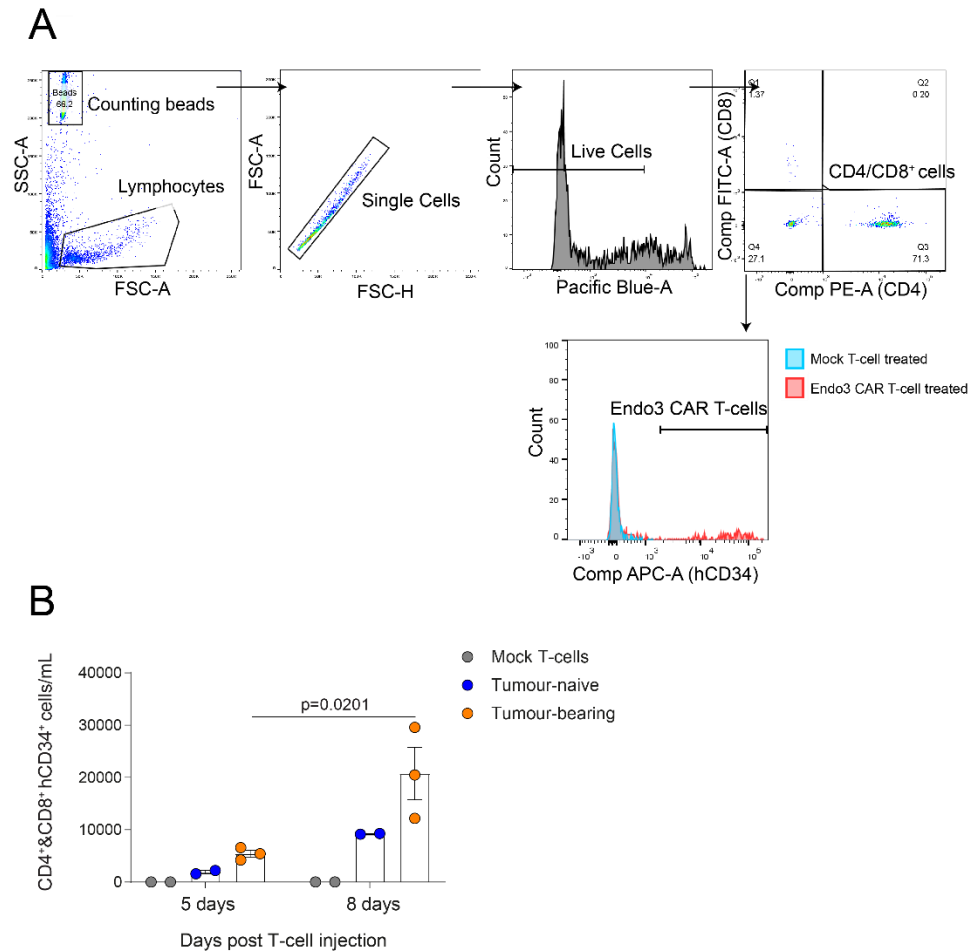


Figure 4. 7 Endo3 CAR T-cells expand in BALB/c mice

Continuation of Figure 4.6. **(A)** Gating strategy used to determine Endo3 CAR T-cell populations. Following staining with CD4, CD8 and hCD34 antibodies, FSC-A and SSC-A were used to gate out debris and non-lymphocyte populations. FSC-A and FSC-H were used to gate out doublets. DAPI was used to gate out dead cells. The resulting live, single lymphocytes were visualised in FITC (CD8) and PE (CD4) channels to identify CD8⁺ and CD4⁺ T-cell populations. CD4⁺ and CD8⁺ cells were gated together and the APC (hCD34) channel was used to identify Endo3 CAR T-cells. Mock T-cell treated controls were used to determine Endo3 CAR T-cell gates. **(B)** Number of circulating CD4⁺hCD34⁺ and CD8⁺hCD34⁺ Endo3 CAR T-cells in venous blood taken from tumour-bearing and tumour-naïve mice 5 or 8 days post-T-cell injection. Blood collected from mock T-cell treated mice were used as negative controls. Each data point represents one mouse. Data shows mean \pm SEM. Two-way ANOVA.

To assess depletion of tumour-associated, endosialin-expressing cells, FFPE sections of 4T1 primary tumours were immunostained for endosialin. An endomucin co-stain was utilised to visualise vascular structures. Endosialin-positive cells are observed

in tumours from both mock T-cell and Endo3 CAR T-cell treated mice culled 5 days post-T-cell injection. As expected, endosialin expressing cells are predominantly in a perivascular location consistent with the upregulated expression of endosialin on tumour pericytes. By contrast, tumours from Endo3 CAR T-cell treated mice culled 8 days post-T-cell injection are largely devoid of endosialin-expressing cells (Figure 4.8). Quantification of endosialin expression in mock T-cell and Endo3 CAR T-cells treated 4T1 tumours by colour thresholding is performed and discussed in Chapter 5.

This initial experiment demonstrates that Endo3 CAR T-cells expand more efficiently in tumour-bearing mice, and this expansion continues to at least 8 days post-T-cell injection. Tumours remain endosialin-positive at 5 days post-T-cell injection, however by 8 days post-T-cell injection tumours are largely endosialin-negative. Therefore, Endo3 CAR T-cells efficiently deplete endosialin-expressing cells in the primary tumour and this depletion occurs following CAR T-cell expansion.

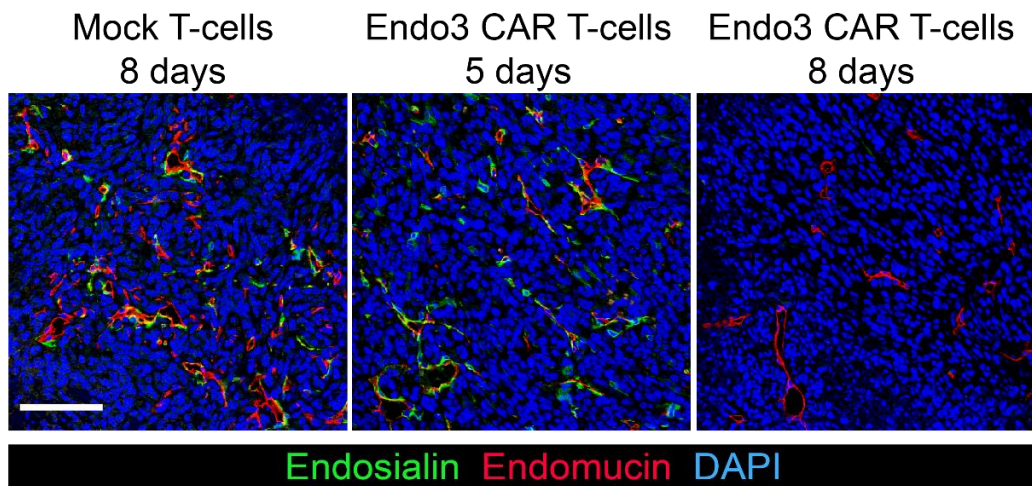


Figure 4. 8 Endo3 CAR T-cells deplete endosialin-positive cells in 4T1 tumours (1)

Continuation of Figure 4.6. Immunostaining of primary tumours from mock T-cell treated or Endo3 CAR T-cell treated mice at 5 (n=2) or 8 days (n=8) post-T-cell injection. Representative confocal immunofluorescence images of formalin-fixed, paraffin-embedded (FFPE) sections stained for endosialin (green) and the endothelial cell marker endomucin (red) are shown. Nuclei were counterstained with DAPI (blue). Scale bar = 150 μ m.

4.2.4 *Endo3 CAR T-cell therapy is associated with toxicity in BALB/c mice but limits metastatic spread of 4T1 tumours*

As discussed in Chapter 1.4.4, CAR T-cell therapy may be associated with adverse toxicities in the clinic, with the most common toxicities being CRS and ICANS (Maude *et al.* 2014; Kochenderfer *et al.* 2015). Post-T-cell injection, mice were monitored for signs of ill health, such as weight loss, malaise and abnormal behaviour. In the study described in Section 4.2.3, all mice experienced weight loss following irradiation and T-cell injection, however mock T-cell treated mice and tumour-naïve mice recover weight over the week following T-cell injection. Conversely, 4T1 tumour-bearing mice treated with Endo3 CAR T-cells do not recover weight and either continue to lose weight or remain at a low weight during the week following T-cell injection (Figure 4.9A). As well as sustained weight loss, tumour-bearing mice treated with Endo3 CAR T-cells show multiple signs of ill health from 5 days post-T-cell injection, including hunching, piloerection and malaise. These symptoms are not observed in tumour-naïve or mock T-cell treated mice. Upon post-mortem dissection, Endo3 CAR T-cell treated tumour-bearing mice are observed to have blackened and enlarged gallbladders, a phenotype that is not present in any other group. Histological examination of gallbladder tissue reveals an accumulation of red blood cells and a thickening of the gallbladder wall in a number of Endo3 CAR T-cell treated tumour-bearing mice (Figure 4.9B). This phenotype is examined further in Chapter 5.

Previously, our laboratory has reported that 4T1 primary tumour growth is not impaired by the genetic deletion of endosialin (Viski *et al.* 2016), but it was feasible that depletion of endosialin-positive cells, as opposed to depletion of the endosialin receptor, may impact tumour growth. To assess whether Endo3 CAR T-cell therapy impacted primary tumour growth, tumour measurements were taken bi-weekly from 6 days post-tumour cell injection. Following T-cell injection, the growth rate of primary tumours from

Endo3 CAR T-cell treated mice shows in comparison to mock T-cell treated tumours, however no significant difference in final tumour volume is observed (Figure 4.9C). To assess lung metastatic burden, lungs were removed upon necropsy and metastatic burden was quantified by manually counting the number of metastatic deposits in the lung H&E stained FFPE sections. Endo3 CAR T-cell treatment is associated with a significant reduction in lung metastasis, with a striking 70% of Endo3 CAR T-cell treated mice having no detectable lung disease (Figure 4.9D).

These results demonstrate that Endo3 CAR T-cell therapy shows potential as a metastasis limiting therapy in the preclinical 4T1 tumour-bearing BALB/c model of breast cancer, however the current regimen is associated with severe toxicity in tumour-bearing mice, which will be further addressed in Chapter 5.

4.2.5 *Endo3 CAR T-cells do not cause toxicity in mice with healing wounds*

As Endo3 CAR T-cell therapy is associated with toxicity in tumour-bearing mice, we sought to investigate whether Endo3 CAR T-cells would cause toxicity in mice with actively healing wounds. It has previously been demonstrated that fibroblasts associated with healing wounds have upregulated endosialin expression (Hong *et al.* 2019) therefore Endo3 CAR T-cells may target these cells. The strategy to assess this hypothesis is outlined in Figure 4.10. In brief, 8-10 week old Cd248^{WT} BALB/c mice were given two 6 mm diameter punch biopsy wounds on the dorso-lateral skin and these were allowed 4 days to begin the healing process. Mice were then subjected to 5 Gy whole body caesium irradiation 18 h prior to being injected via the tail vein with either vehicle only or 2.5×10^6 Endo3 CAR T-cells. Mice were monitored for signs of CAR T-cell associated toxicities following T-cell injection and venous blood was analysed 7 days post-T-cell injection. Mice were culled 10 days post-T-cell injection with no signs of Endo3 CAR T-cell associated toxicity observed. Analysis of venous blood collected 7

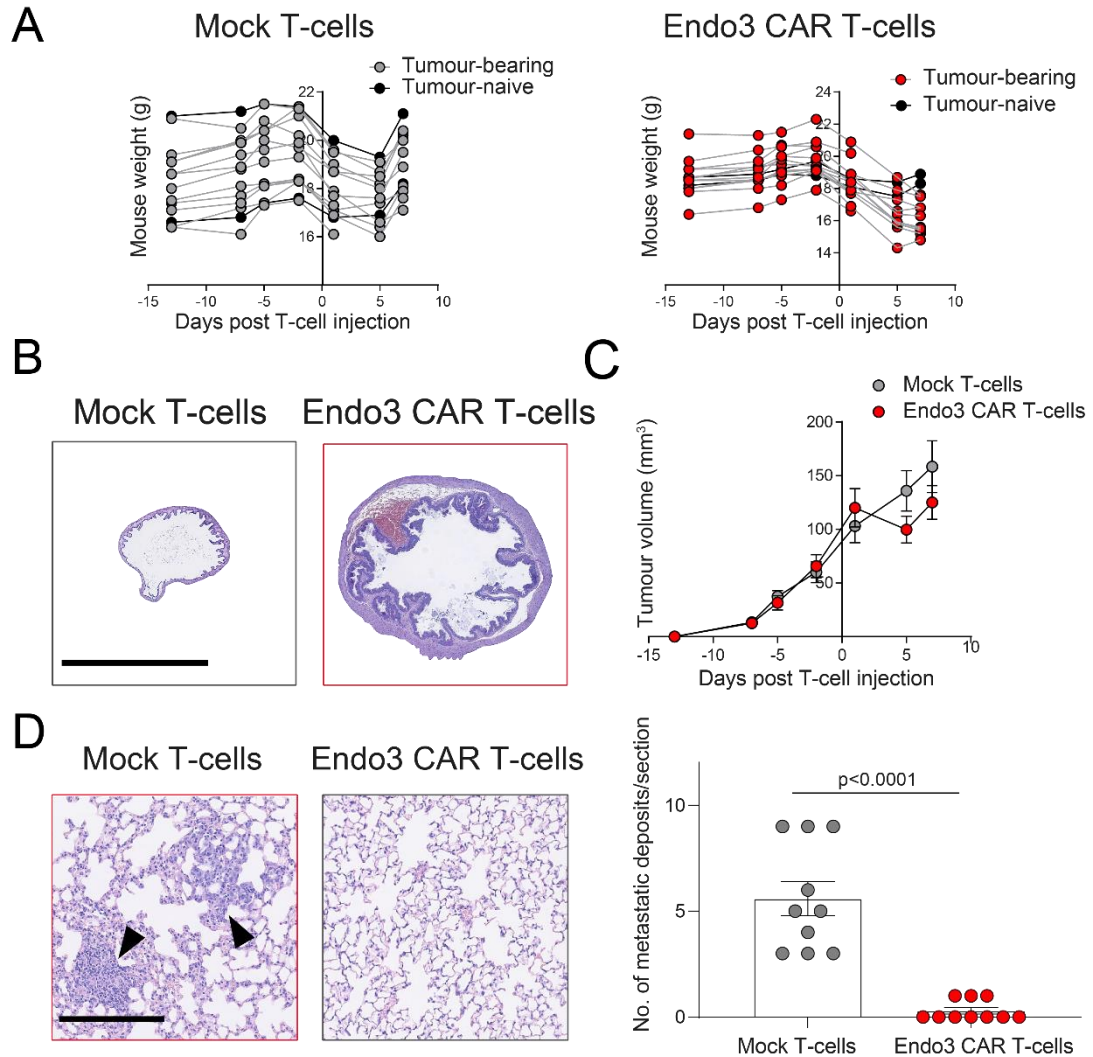


Figure 4.9 Endo3 CAR T-cell therapy limits lung metastasis but is associated with toxicity

Continuation of Figure 4.6. **(A)** Body weights of individual mock T-cell treated and Endo3 CAR T-cell treated mice. Each series represents one mouse **(B)** Representative H&E stained gallbladders showing enlargement and red blood cell pooling within a thickened gallbladder wall in 4T1 tumour-bearing Endo3 CAR T-cell treated mice. Scale bar = 1 mm. **(C)** Tumour growth curves for mock T-cell treated and Endo3 CAR T-cell treated 4T1 primary tumours. Data shows mean \pm SEM for each time point. **(D)** Left, representative H&E stained lungs, arrowheads indicate metastatic deposits. Scale bar = 250 μ m. Right, quantification of spontaneous lung metastasis in mock T-cell treated or Endo3 CAR T-cell treated mice. Metastatic deposits were quantified by manually counting the number of deposits in H&E stained formalin-fixed, paraffin-embedded (FFPE) lung sections. Each data point represents one mouse. Data shows mean \pm SEM. Unpaired Student's *t*-test.

days post-T-cell injection demonstrates low levels of circulating Endo3 CAR T-cells compared with those observed 5-8 days post-T-cell injection in tumour-bearing mice in Section 4.2.3 (Figure 4.11A). As previously, a decrease in body weight is observed in both Endo3 CAR T-cell treated and vehicle only mice following whole body irradiation, however both groups progressively regain body weight from 2 days post-T-cell injection (Figure 4.11B). Importantly, no difference in the rate of wound closure is observed between Endo3 CAR T-cell treated mice and mice administered with vehicle only (Figure 4.11C,D). Further, no evidence of Endo3 CAR T-cell-mediated depletion of endosialin-expressing cells is observed 10 days post-T-cell injection in non-wounded skin (Figure 4.12A) or at the site of the healing wound (Figure 4.12B). Of note, and in agreement with previous reports, an increased presence of endosialin-expressing cells is observed in wounded skin when compared to non-wounded skin in both vehicle treated and Endo3 CAR T-cell treated mice (Figure 4.12A,B).

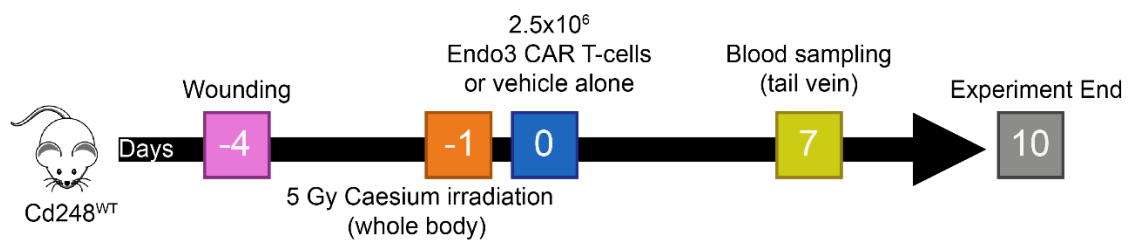


Figure 4. 10 Endo3 CAR T-cell *in vivo* strategy for BALB/c wounded mice

8-10 week old Cd248^{WT} BALB/c mice were given 6 mm punch wounds through the dorso-lateral skin and wounds were allowed 4 days to begin healing. Mice were subjected to 5 Gy caesium irradiation (day -1) 18 h before being injected via the tail vein with 2.5×10^6 Endo3 CAR T-cells or vehicle alone. Mice were provided with Dietgel from day -1 to study termination. Venous blood was collected via the tail vein 7 days post-T-cell injection. Mice were culled 10 days post-T-cell injection. No signs of ill health were present at this time

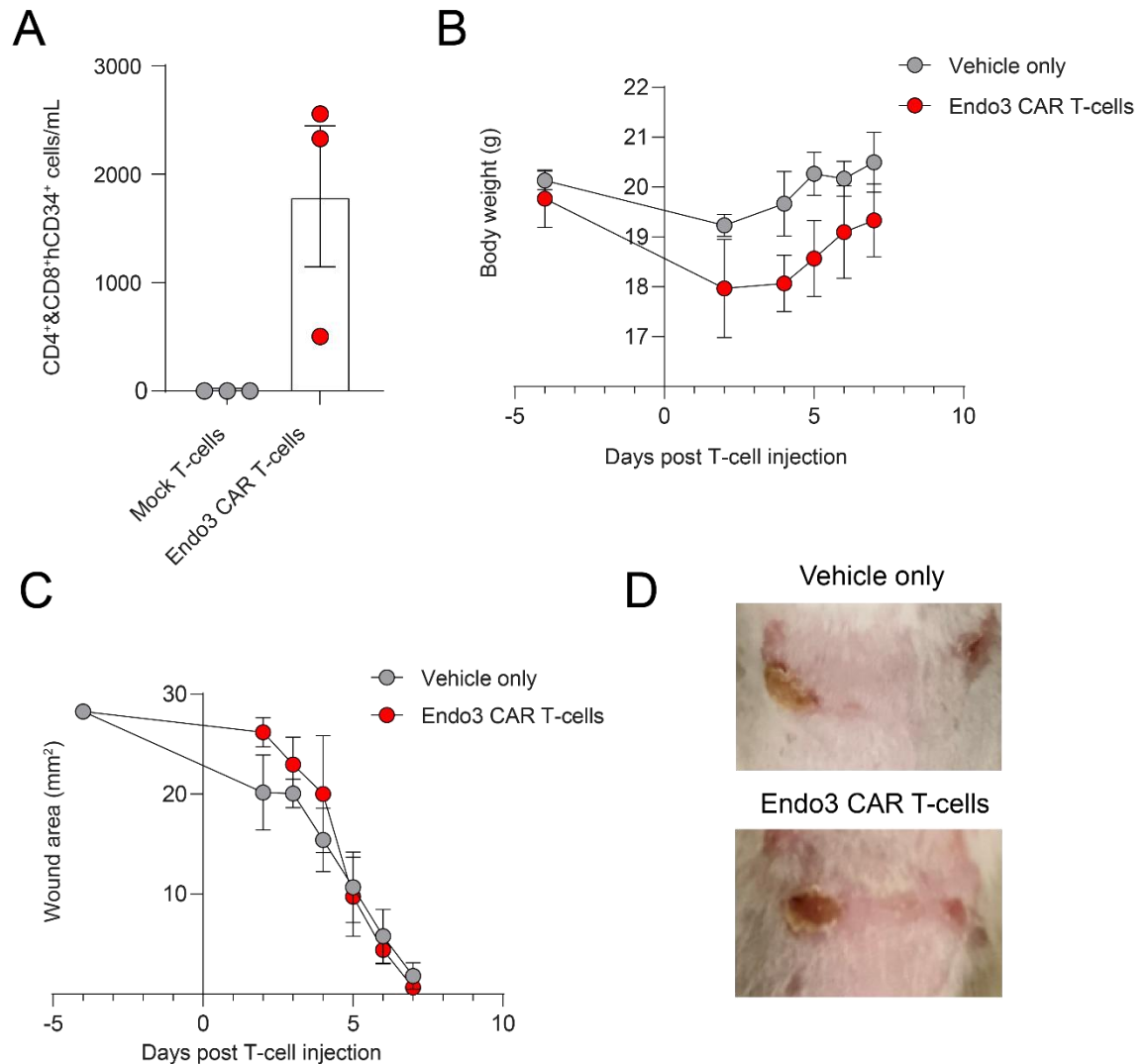


Figure 4. 11 Endo3 CAR T-cells do not affect wound healing or cause toxicity in wounded mice

Continuation of Figure 4.10. **(A)** Number of circulating CD4⁺hCD34⁺ and CD8⁺hCD34⁺ Endo3 CAR T-cells in venous blood taken 7 days post-T-cell injection from Endo3 CAR T-cell treated mice. Samples from mock T-cell treated mice from the study described in Figure 4.6 were used as negative controls. Each data point represents one mouse. Data shows mean \pm SEM. **(B)** Body weights of mice treated with vehicle alone or Endo3 CAR T-cells. Data shows mean \pm SEM. **(C)** Wound area (starting on the day of wounding) of mice subsequently treated with vehicle alone or Endo3 CAR T-cells. Data shows mean \pm SEM. **(D)** Photographs taken 4 days post-T-cell injection of healing wounds on the dorso-lateral skin of mice treated with vehicle alone or Endo3 CAR T-cells. Representative of n=3 mice per group.

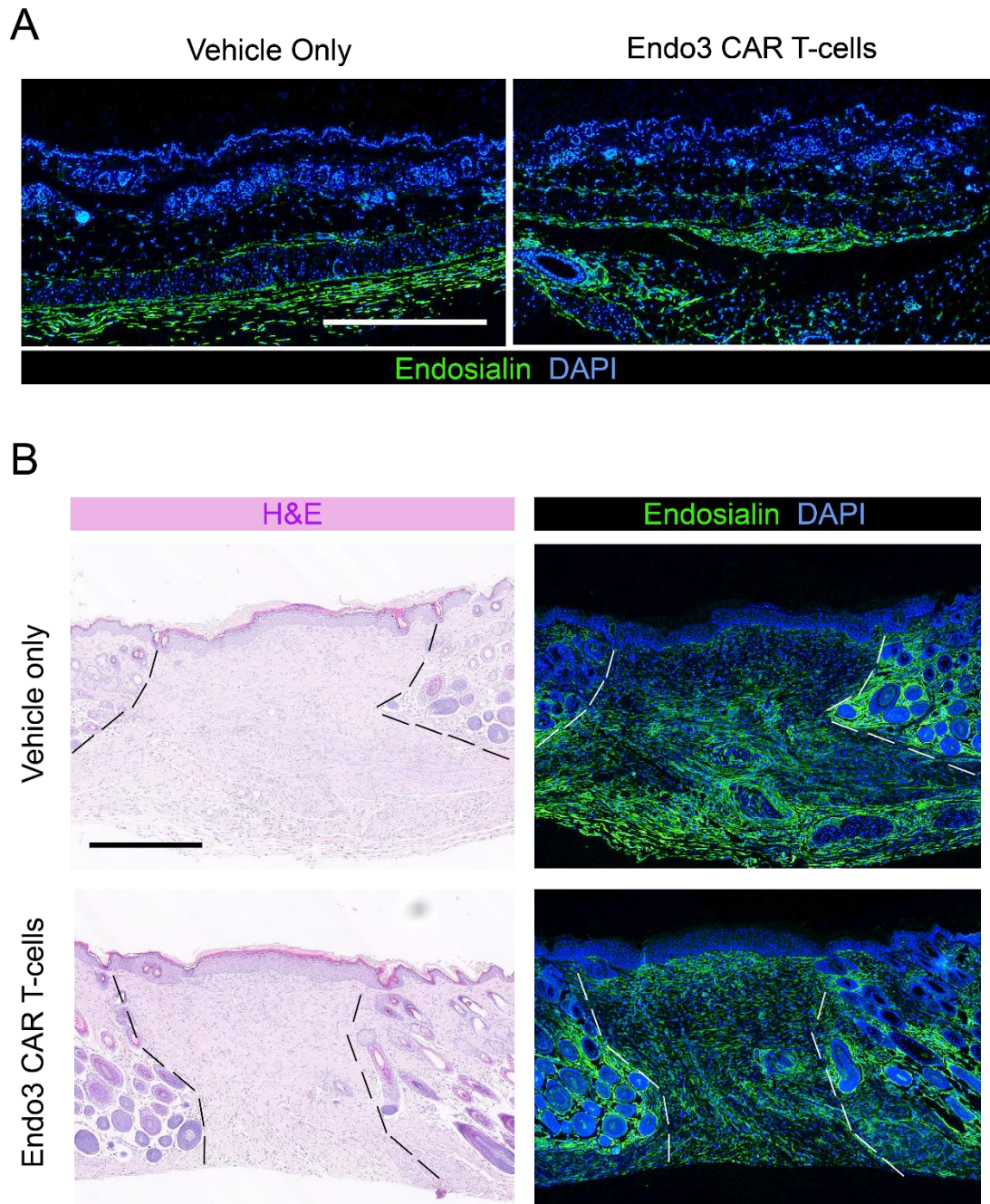


Figure 4. 12 Endo3 CAR T-cells do not deplete endosialin-positive cell in the healing wound

Continuation of Figure 4.10. Non-wounded and wounded skin tissue from vehicle only (n=3) or Endo3 CAR T-cell treated (n=3) mice 10 days post-wounding was formalin-fixed, paraffin-embedded (FFPE) and sectioned. **(A)** Non-wounded skin was immunostained for endosialin (green). Nuclei were counterstained with DAPI (blue). Slides were scanned on a Hamamatsu Nanozoomer. Representative images are shown. Scale bar = 500 μ m. **(B)** Wounded skin was stained with (left) H&E or (right) immunostained for endosialin (green). Nuclei were counterstained with DAPI (blue). Slides were scanned on a Hamamatsu Nanozoomer. Representative images are shown. Scale bar = 500 μ m.

4.3 Discussion

4.3.1 *Endo3 CAR T-cells exhibit endosialin-specific activity in vitro*

To avoid off-target toxicity, it is important that CAR T-cells activate and kill in a target-specific manner. The data presented in this Chapter demonstrate that BALB/c and C57BL/6 derived Endo3 CAR T-cells are activated and kill target cells in an endosialin-specific manner *in vitro*, as determined by IFN- γ ELISA and CellTiter-Glo analysis, respectively. BALB/c Endo3 CAR T-cells appeared to kill more slowly than C57BL/6 CAR T-cells and the levels of IFN- γ release after 24 h of co-culture with target cells are modest when compared to levels released by C57BL/6 Endo3 CAR T-cells. This is likely due to differences in immune activity between T-cells derived from BALB/c and C57BL/6 mice and this will be further explored in Chapter 6. It is likely that supernatants from BALB/c T-cell-target cell co-cultures collected at a later time point would have contained higher levels of IFN- γ , as target cell death was only evident after 84 h of co-culture, however this was not explored in this thesis. Nevertheless, the levels of IFN- γ detected in C57BL/6 Endo3 CAR T-cell co-cultures with target-positive cells were comparable to those reported by others in the literature utilising other CAR T-cell designs (Castella *et al.* 2019; Liao *et al.* 2020; Liu *et al.* 2020). Similarly, C57BL/6 Endo3 CAR T-cells were able to reduce cell viability comparably with other 2nd generation CAR T-cells reported in the literature (Long *et al.* 2015; Hamieh *et al.* 2019), and this was also true of BALB/c Endo3 CAR T-cells when co-cultures were extended to 84 h. It must be considered however that CellTiter-Glo assays determine cell viability by quantifying metabolic activity, therefore target cells with reduced CellTiter-Glo read-out may only have reduced metabolic activity, but not contain more dead cells. Future work may consider a second method of quantifying target cell viability to confirm cell death in the presence of Endo3 CAR T-cells.

Importantly, both strains of Endo3 CAR T-cells were able to activate against and kill both mouse and human cells expressing endosialin. This suggests that Endo3 CAR T-cells have the potential to be directly translated to humans in the clinic, whilst retaining the advantages of being appropriate for use in syngeneic preclinical mouse models.

As discussed in Chapter 4, various batches of Endo3 CAR T-cells and mock T-cell were produced in this PhD, with early batches being produced by our Dr Steven Lee's laboratory in Birmingham and later batches being produced in our laboratory. Batches of T-cells produced by both parties were tested *in vitro* and the results obtained were comparable in all cases.

4.3.2 *Optimisation of Endo3 CAR T-cell in vivo therapeutic strategy*

To investigate Endo3 CAR T-cell efficacy *in vivo*, a preclinical strategy based on current clinical practices, including prior lymphodepletion, was assessed. In contrast with reports by Kueberuwa and colleagues (Kueberuwa *et al.* 2018a), 5 Gy whole body irradiation and cyclophosphamide chemotherapy were found to achieve comparable levels of lymphodepletion in BALB/c mice, however whole body irradiation was determined to be the most appropriate lymphodepletion method, as lymphodepleting doses of cyclophosphamide were not well tolerated by the mice. The reason for this intolerance is unclear, as previous reports utilising the doses used in this study, or higher, have demonstrated tolerance in BALB/c mice (Huyan *et al.* 2011; Aston *et al.* 2017; Kueberuwa *et al.* 2018a; Kueberuwa *et al.* 2018b).

Our laboratory has previously demonstrated that endosialin plays a role in the intravasation step of the metastatic cascade (Viski *et al.* 2016), thus Endo3 CAR T-cell therapy should be delivered prior to early metastatic dissemination. In line with previous reports, 4T1 tumours were found to be well vascularised between the sizes of 50-200 mm³ (Gregório *et al.* 2016) and endosialin-positive stromal CAFs and pericytes were

observed. At 13 post-tumour cell implantation, the lungs from mice bearing 4T1 tumours were free of metastatic disease, as determined by H&E stained FFPE lung sections. It must be considered, however, that a limitation of quantifying metastasis by H&E stains alone is that single mouse tumour cells cannot be detected by this method. Circulating tumour cells have been detected as early as 7 days post-tumour cell implantation in murine models of breast cancer (Ramani *et al.* 2019) and so it is possible that single cells may have begun to enter the lungs at the time points explored in this thesis.

4.3.3 *Endo3 CAR T-cells deplete endosialin-positive cells in the tumour stroma*

Utilising this preclinical strategy for investigating Endo3 CAR T-cell therapy, a pilot study examining the effects of Endo3 CAR T-cells on primary tumour growth and metastasis was performed in the 4T1 syngeneic mouse model of breast cancer, in BALB/c mice. Endo3 CAR T-cells were readily detectable in the venous blood collected at various time points post-T-cell injection. However, difficulties collecting blood were experienced 2 and 8 days post-T-cell injection. Following whole body irradiation, mice may experience radiation sickness which can lead to a decrease in food and water intake and thus dehydration and weight loss (Moccia *et al.* 2010). It has been reported that BALB/c mice are more sensitive to radiation sickness than other strains (Ponnaiya *et al.* 1997). In the study described in Section 4.2.3, up to 13% body weight loss was observed post-irradiation even in mock T-cell treated controls. This suggests that animals may have been suffering from some degree of radiation sickness and this may explain why insufficient blood volumes were collected at 2 days post-T-cell injection. It was considered that it may be necessary to provide animals with nutritional gels and use methods to hydrate animals following irradiation procedures. Such aftercare regimens will be discussed further in Chapter 5. Insufficient blood volume collection from a subset of tumour-bearing Endo3 CAR T-cell treated BALB/c mice at 8 days post-T-cell injection

may also have been due to the ill health of the mice in this group and this will be discussed further below in Section 4.3.4.

Where measurable, the greatest expansion of Endo3 CAR T-cells from 5 to 8 days post-T-cell injection is observed in tumour-bearing mice, likely due to an increased CAR T-cell target density in tumour-bearing mice. A smaller expansion of Endo3 CAR T-cells is observed in tumour-naïve mice, which may be due to general T-cell expansion following lymphodepletion (Williams *et al.* 2007), or low levels of endosialin expression in healthy tissues, as shown in Chapter 3.2.3 and by others (Rupp *et al.* 2006; MacFadyen *et al.* 2007).

Immunostaining of Endo3 CAR T-cell treated primary 4T1 tumours revealed that, whilst little depletion of endosialin-expressing cells was observed 5 days post-T-cell injection, at 8 days post-T-cell injection Endo3 CAR T-cell treated tumours are largely endosialin-negative. This observation aligns with fact that significantly higher number of circulating Endo3 CAR T-cells are detected in the venous blood 8 days post-T-cell injection when compared to 5 days post-T-cell injection in tumour-bearing mice. Whilst a reduction in endosialin-positive staining indicates that the endosialin antigen is not readily detected in 4T1 tumours treated with Endo3 CAR T-cells, suggesting that endosialin-expressing cells have been targeted, it does not confer certainty that endosialin-positive pericytes have been depleted. Future work may consider staining with a pericyte marker, such as NG2, to confirm pericyte depletion post-therapy. Additionally, visualisation of Endo3 CAR T-cells within 4T1 tumours would provide evidence that Endo3 CAR T-cells are able to enter the primary tumour and interact with endosialin-expressing cells. Future work should focus on optimising methods of Endo3 CAR T-cell visualisation in the primary tumours of Endo3 CAR T-cell treated mice.

4.3.4 *Endo3 CAR T-cell therapy has a therapeutic effect in 4T1 tumour-bearing mice but induces toxicity*

The 4T1 murine breast carcinoma model is an attractive syngeneic preclinical model for triple negative breast cancer, as it spontaneously metastasises to the lung, brain, liver and bone, the four most common sites of breast cancer metastasis (Aslakson and Miller 1992; Pulaski and Ostrand-Rosenberg 1998; Eckhardt *et al.* 2005). Our laboratory has previously shown that genetic deletion of endosialin in BALB/c mice significantly reduces the spontaneous metastasis of subcutaneously implanted 4T1 breast carcinoma cells to the lungs (Viski *et al.* 2016). Therefore, at the beginning of this project it was hypothesised that selective depletion of endosialin-expressing cells in 4T1 tumours via the administration of Endo3 CAR T-cells would limit tumour cell metastasis to the lungs.

Data previously published by our laboratory have demonstrated that endosialin knockout has no effect on primary tumour growth in syngeneic mouse models of breast cancer (Viski *et al.* 2016). However, in these experiments endosialin is not expressed by the CAFs and perivascular stromal cells, but the cells remain present in the stroma. As discussed in Section 4.3.3, Endo3 CAR T-cell therapy resulted in the depletion of endosialin-expressing cells in the tumour stroma and in turn this results in the transient slowing of 4T1 primary tumour growth. Evidence of slowed primary tumour growth became apparent between 5-8 days post-T-cell injection, corresponding with a significant expansion in circulating Endo3 CAR T-cells. It has been reported that human CAR T-cells exhibit the most effective tumour cell killing *in vitro* in the first 48 h of co-culture (Anurathapan *et al.* 2014; Park *et al.* 2020) and it has been shown by *in vivo* imaging that human CAR T-cells against haematological targets can traffic to tumour sites and exhibit tumour cell killing within 5 days of administration (Cazaux *et al.* 2019; Minn *et al.* 2019). As discussed in Chapter 1.4.5, CAR T-cells must overcome multiple barriers to

access targets within solid tumours. Although endosialin is expressed by perivascular cells that sit proximally to vascular structures, Endo3 CAR T-cells must still navigate the endothelial barrier and basement membrane to reach their target. This, together with the presence of the endogenous immune system in our syngeneic models, may account for the delay in Endo3 CAR T-cell activity when compared to CAR T-cells targeting haematological cancers.

In 4T1 tumour-bearing mice, Endo3 CAR T-cell treatment results in a striking reduction in metastatic lung deposits, with 70% (7 of 10) of mice having no detectable metastatic disease. All mock T-cell treated control mice had detectable metastatic disease in this study. This suggests that depletion of endosialin-expressing cells in the primary tumour limits metastatic spread in this model. This finding supports data previously published by our laboratory demonstrating reduced spontaneous metastasis of 4T1 tumours to the lungs in endosialin KO mice (Viski *et al.* 2016), however, in this Chapter, Endo3 CAR T-cell therapy resulted in a transient slowing of 4T1 tumour growth, a phenotype not observed in endosialin KO mice bearing 4T1 tumours. This is likely because in endosialin KO mice, the CAFs and pericytes are still present in the tumour but do not express endosialin, whereas following Endo3 CAR T-cell therapy these cells are likely depleted, which may have additional anti-tumour effects. As previously mentioned, in this study the effects of Endo3 CAR T-cell therapy on 4T1 primary tumour growth were modest, however the reduction in spontaneous metastasis to the lungs following Endo3 CAR T-cells therapy was striking. It may be that the depletion of endosialin-positive cells in 4T1 tumours following Endo3 CAR T-cell therapy transiently perturbs the vascular structures through-out the primary tumour, which in turn limits tumour cell intravasation for a period of time, however as areas of viable tumour cells with endomucin-positive structures are observed in Endo3 CAR T-cell treated primary tumours at experiment end, it is likely that either depletion of endosialin-expressing cells does not perturb all vascular structures in the primary tumour or that compensatory

mechanisms to restore the vascular network are established. Endo3 CAR T-cell associated toxicities in BALB/c mice limited the duration of this study, with mice being culled after 22-13 days of tumour growth. To determine whether the effect of Endo3 CAR T-cell therapy on 4T1 spontaneous metastasis to the lung is also transient, it will be important to manage Endo3 CAR T-cell toxicities in BALB/c mice to extend the study duration further to assess the extent of Endo3 CAR T-cell-mediated metastasis limitation. This will be addressed further in Chapter 5.

In this study, Endo3 CAR T-cell therapy was associated with toxicity specifically in 4T1 tumour-bearing mice. Three possible mechanisms for Endo3 CAR T-cell associated toxicity are: CRS triggered by the activation of Endo3 CAR T-cells; on-target, off-tumour activity of Endo3 CAR T-cells in the normal tissues; or off-target activity of Endo3 CAR T-cells. In the clinic, the most commonly reported toxicities are CRS and ICANS. CRS is a systemic toxicity resulting from the activation of CAR T-cells, which in turn release cytokines that activate bystander immune cells such as macrophages and dendritic cells. Activation of these cells result in the release of high levels of multiple cytokines, which leads to a systemic inflammation and if left untreated, damage to multiple organs. Toxicity associated with on-target, off-tumour activity of CAR T-cells results from CAR T-cells homing to and attacking normal tissues that contain cells expressing their target antigen. This can result in severe organ damage either by CAR T-cells killing vital cell populations or by triggering inflammation in vital organs. Off-target CAR T-cell activity can also result in severe organ damage in the same manner as on-target, off-tumour toxicity, however this toxicity results from CAR T-cells recognising and killing cells expressing a non-relevant antigen.

In this Chapter, 4T1 tumour-bearing, Endo3 CAR T-cell treated mice show the first signs of ill health 5 days post-T-cell injection and by 8 days post-T-cell injection some mice required culling. Affected mice appeared piloerect, hunched and lethargic and continued to lose weight or stay at a low weight post-irradiation, whilst mock T-cells

treated and tumour-naïve mice regained a healthy weight. The absence of ill health in mock T-cell treated mice and Endo3 CAR T-cell treated tumour-naïve mice suggest, respectively, that toxicity was not associated with T-cell injection alone and was tumour-specific. Lack of toxicity in tumour-naïve mice suggests that, at the delivered Endo3 CAR T-cell dose, Endo3 CAR T-cells do not cause toxicity by targeting the normal tissues. However, greater levels of circulating Endo3 CAR T-cells were detected in tumour-bearing mice when compared to tumour-naïve mice, thus it is not possible to conclude that Endo3 CAR T-cells do not exhibit on-target, off-tumour activity as this may occur when Endo3 CAR T-cells are circulating at higher levels. On this note, increased levels of circulating Endo3 CAR T-cells in 4T1 tumour-bearing mice may result in greater Endo3 CAR T-cell activation and in turn greater activation of bystander immune cells, resulting in high levels of cytokine release and CRS. Murine models of CRS have been established and the mice demonstrate subdued behaviour, piloerection and continued weight loss in these studies (van der Stegen *et al.* 2013; Giavridis *et al.* 2018). As Endo3 CAR T-cell treated mice displayed similar symptoms, Endo3 CAR T-cell associated toxicity may be due to CRS. In the clinic, a factor for CRS diagnosis is serum levels of various cytokines. To determine whether Endo3 CAR T-cell associated toxicity is likely due to CRS, it is important to interrogate serum cytokines in Endo CAR T-cell treated mice. This will be addressed in Chapter 5. Alongside CRS and on-target, off-tumour toxicity, Endo3 CAR T-cell associated toxicity may be attributed to off-target activity. The study described in this Chapter utilised only Cd248^{WT} mice, thus we were not able to determine whether the observed toxicity is due to off-target activity of Endo3 CAR T-cells. This will be addressed utilising Cd248^{KO} in Chapter 5.

4.3.5 *Endo3 CAR T-cells do not cause toxicity in mice with healing wounds*

The fibroblasts present at the site of a healing wound have previously been shown to upregulate endosialin during the healing process (Hong *et al.* 2019). In agreement

with these reports, comparison of wounded and non-wounded skin in the present study revealed an increased presence of endosialin-expressing cells at the site of the healing wound.

As Endo3 CAR T-cells induce toxicity in 4T1-tumour bearing mice, it is important to investigate whether Endo3 CAR T-cells are capable of causing toxicity in mice with other physiological conditions involving endosialin upregulation. It is plausible that patients in the clinic may have actively healing wounds, thus any toxicity caused by Endo3 CAR T-cells attacking fibroblasts in the healing wound would be problematic. Fortunately, mice with 6 mm dorsolateral wounds administered with 2.5×10^6 Endo3 CAR T-cells, the same dose given to tumour-bearing animals, did not present with signs of Endo3 CAR T-cell associated toxicity up to 10 days post-T-cell administration. At 7 days post-T-cell injection the number of circulating Endo3 CAR T-cells detected in wounded mice was lower than that observed in tumour-naïve mice 8 days post-T-cell injection in Section 4.2.3, suggesting a lack of Endo3 CAR T-cell expansion in the wounded setting. Further, Endo3 CAR T-cell treatment had no effect on the rate of wound closure and there was no evidence that endosialin-expressing cells had been depleted in the healing wound 10 days post-T-cell injection. These results suggest that Endo3 CAR T-cells either do not reach the endosialin-expressing cells in the healing wound or they do not activate in response to these cells. It is plausible that, due to endosialin expression in the tumour being tightly associated with the vasculature but fibroblasts in the healing wound being numerous and not necessarily associated with the vasculature, Endo3 CAR T-cells face additional difficulties to infiltrate the healing wound tissue and access the fibroblasts. Further investigation is required to address this hypothesis.

Chapter 5 Endo3 CAR T-cell activity in BALB/c mice

5.1 Introduction

Managing CAR T-cell associated toxicities remains one of the most significant challenges in treating patients with CAR T-cell therapy. In the clinic, patients are monitored closely following lymphodepletion and CAR T-cell infusion and regimens to maintain patient hydration and monitor cytokine levels are undertaken (Neelapu *et al.* 2018).

In Chapter 4, Endo3 CAR T-cells were shown to have endosialin-specific activity and promising efficacy against 4T1 tumours. However, in 4T1 tumour-bearing mice, but not in non-tumour-bearing or wounded mice, Endo3 CAR T-cell therapy was associated with toxicity. Mice displayed evidence of weight loss and were difficult to collect blood from within 2 days of CAR T-cell injection, which may be a consequence of dehydration. Further, 4T1 tumour-bearing, Endo3 CAR T-cell treated mice began to show signs of ill health from 5 days post-T-cell injection. As discussed in Chapter 1.4.4, CAR T-cell associated toxicities may manifest as a consequence of excessive CAR T-cell activation and cytokine release, rapid tumour lysis, on-target/off-tumour activity in which CAR T-cells attack normal tissues, or off-target activity in which CAR T-cells recognise an inappropriate target (Sun *et al.* 2018). In the previous Chapter, toxicity was not observed in wild-type tumour-naïve mice treated with Endo3 CAR T-cells, suggesting that the observed toxicity was not due to on-target, off-tumour activity.

In this Chapter, Endo3 CAR T-cell activity will be investigated in both Cd248^{WT} and Cd248^{KO} mice, aiming to further characterise Endo3 CAR T-cell associated toxicity, as well as confirm the absence of Endo3 CAR T-cell activity in endosialin-deficient mice. Approaches to limit Endo3 CAR T-cell associated toxicity in 4T1 tumour-bearing mice will also be explored.

5.2 Results

5.2.1 Endo3 CAR T-cell targeting is specific to tumour tissue in Cd248^{WT} mice

The strategy to evaluate Endo3 CAR T-cell activity in both Cd248^{WT} and Cd248^{KO} is shown in Figure 5.1. In brief, 8-10 week old female mice were injected subcutaneously on the flank with 4T1-Luc cells, or left tumour-naïve as controls. Tumours were allowed to grow for 12 days to 50-200 mm³ in size. All mice were subjected to 5 Gy whole body x-ray irradiation 18 h before 2.5 x 10⁶ mock T-cells or Endo3 CAR T-cells were injected via the tail vein. Mice were given water via intraperitoneal injection from day -1 to day 8 and were supplied with Dietgel from day -1 to experiment termination. Venous blood was collected 2, 5 and 8 days post-T-cell injection and mice were monitored for signs of CAR T-cell associated toxicities throughout the study. The experiment was ended 8-9 days post-T-cell injection due to ill health in the Cd248^{WT}, tumour-bearing, Endo3 CAR T-cell treated mice. All Cd248^{WT} mice were culled 8 days post-T-cell injection, Cd248^{KO} mice were culled the next morning 9 days post-T-cell injection.

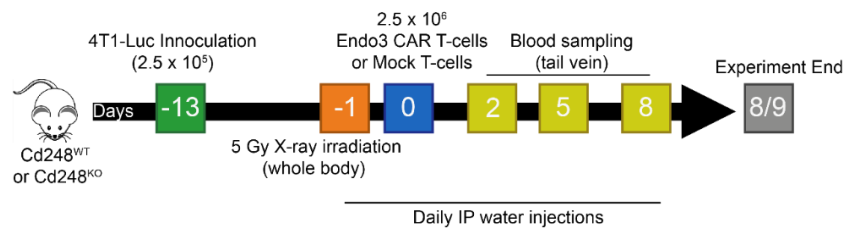


Figure 5. 1 Therapeutic strategy for treating Cd248^{WT} and Cd248^{KO} mice with Endo3 CAR T-cell therapy

8-10 week old endosialin wild-type (Cd248^{WT}) and endosialin knock-out (Cd248^{KO}) BALB/c mice were injected subcutaneously with 2.5 x 10⁵ 4T1-Luc cells or left tumour-naïve. Tumours were allowed to grow for 12 days to 50-200mm³ volume. All mice were subjected to 5 Gy whole body x-ray irradiation 18 h prior to injection via the tail vein with 2.5 x 10⁶ mock T-cells or Endo3 CAR T-cells (Cd248^{WT} tumour-bearing n=5-7 per group, tumour-naïve n=3-4 per group. Cd248^{KO} tumour-bearing n=3 per group, tumour-naïve n=3-4 per group). Animals were given intraperitoneal (IP) hydration injections daily from day -1 to day 8 and supplied with Dietgel from day -1 until experiment termination. Venous blood was collected via the tail vein 2, 5 and 8 days post-T-cell injection. Mice were culled 8-9 days post-T-cell injection due to ill health of Cd248^{WT}, tumour-bearing, Endo3 CAR T-cell treated mice (see text).

Venous blood samples were collected, as previously, to monitor circulating CAR T-cells. Sufficient blood volumes were collected 2, 5 and 8 days post-T-cell injection from at least $n=3$ mice per group, indicating that the hydration strategy used in this study overcame the previous problems with collecting blood 2 days post-T-cell injection. Whole bloods were prepared and analysed by flow cytometry, with Endo3 CAR T-cells being identified as $CD4^+hCD34^+$ or $CD8^+hCD34^+$ cells (Figure 5.2A). Samples from mock T-cell treated mice were analysed as hCD24-negative controls. Endo3 CAR T-cells are identified in blood from both $Cd248^{WT}$ and $Cd248^{KO}$ tumour-bearing or tumour-naïve mice. An expansion of circulating Endo3 CAR T-cells is observed in all groups between days 2 and 5 post-T-cell injection, however a significant expansion between 5 and 8 days post-T-cell injection is only observed in $Cd248^{WT}$, tumour-bearing mice (Figure 5.2B).

To assess depletion of tumour-associated, endosialin-expressing cells in $Cd248^{WT}$ mice, and to confirm the absence of endosialin-expressing cells in $Cd248^{KO}$ mice, FFPE sections of 4T1 primary tumours were immunostained for endosialin. As expected, 4T1 tumours from $Cd248^{KO}$ mice, treated with either mock T-cells or Endo3 CAR T-cells, show no endosialin-positive staining. Endosialin-positive cells are observed in $Cd248^{WT}$ mock T-cell treated tumours and as reported in Chapter 4.2.3, 4T1 tumours from $Cd248^{WT}$ Endo3 CAR T-cell treated mice are largely devoid of endosialin expressing cells (Figure 5.3A,B). To determine whether the depletion of endosialin-positive cells results in a reduction of vascular structures in the viable tumour tissue, 4T1 tumours from $Cd248^{WT}$ mock T-cell treated or Endo3 CAR T-cell treated mice were immunostained for the endothelial cell marker endomucin. A significant decrease in endomucin-positive area is observed in Endo3 CAR T-cell treated tumour when compared to mock T-cell treated controls (Figure 5.3C).

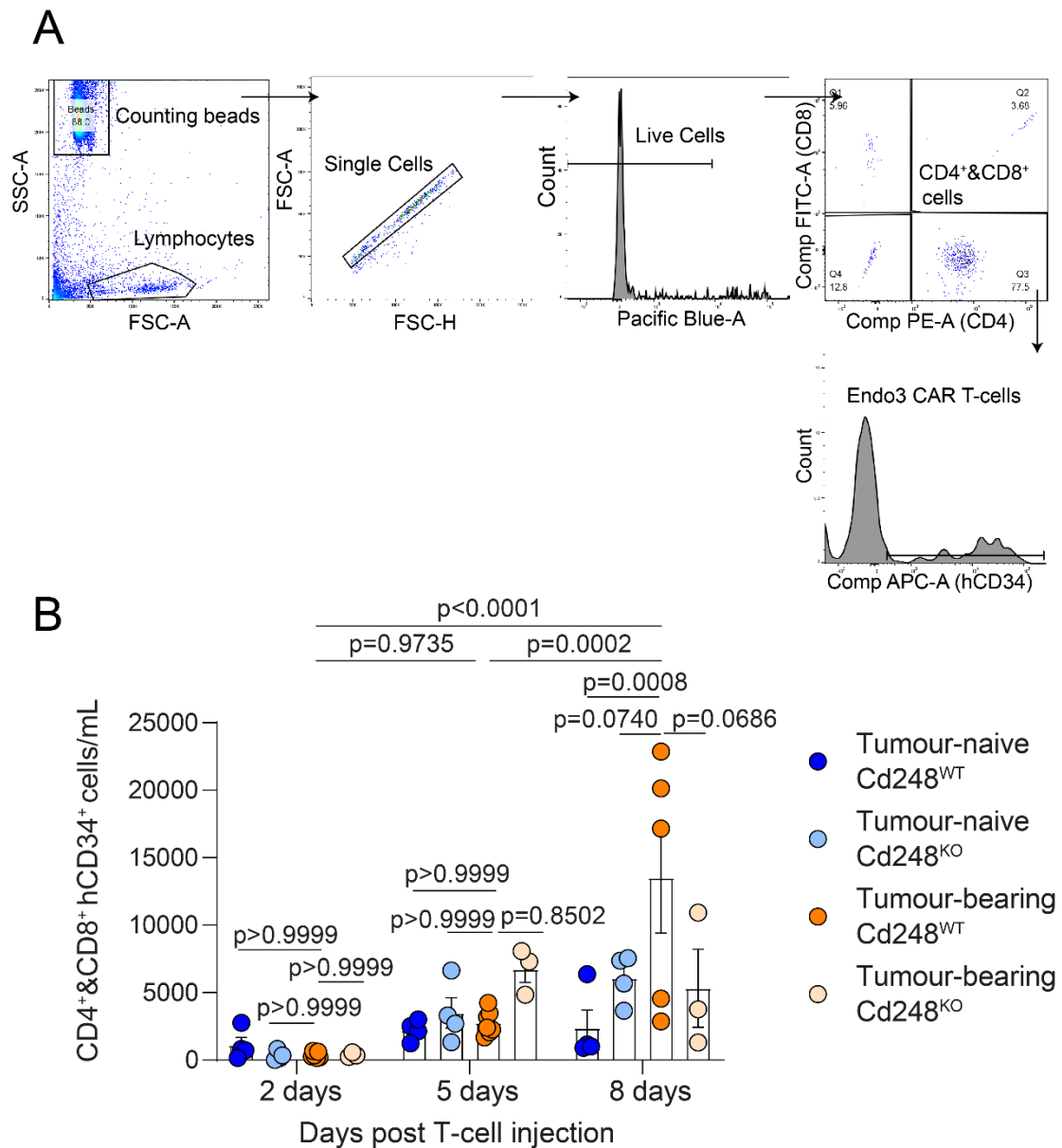


Figure 5. 2 Endo3 CAR T-cell expansion and activity in Cd248^{WT} and Cd248^{KO} mice

Continuation of Figure 5.1. **(A)** Gating strategy used to determine Endo3 CAR T-cell populations. Following staining with CD4, CD8 and hCD34 antibodies, FSC-A and SSC-A were used to gate out debris and non-lymphocyte populations. FSC-A and FSC-H were used to gate out doublets. DAPI was used to gate out dead cells. The resulting live, single lymphocytes were visualised in FITC (CD8) and PE (CD4) channels to identify CD8⁺ and CD4⁺ T-cell populations. CD4⁺ and CD8⁺ cells were gated together and the APC (hCD24) channel was used to identify Endo3 CAR T-cells. Mock T-cell treated controls were used to determine Endo3 CAR T-cell gates. **(B)** Combined number of circulating CD4⁺hCD34⁺ and CD8⁺hCD34⁺ Endo3 CAR T-cells in venous blood taken from Cd248^{WT} or Cd248^{KO}, tumour-bearing or tumour-naïve mice 2, 5 and 8 days post-T-cell injection. Samples from mock T-cell treated mice were used as negative controls. Each data point represents one mouse. Data shows mean \pm SEM. Three-way ANOVA.

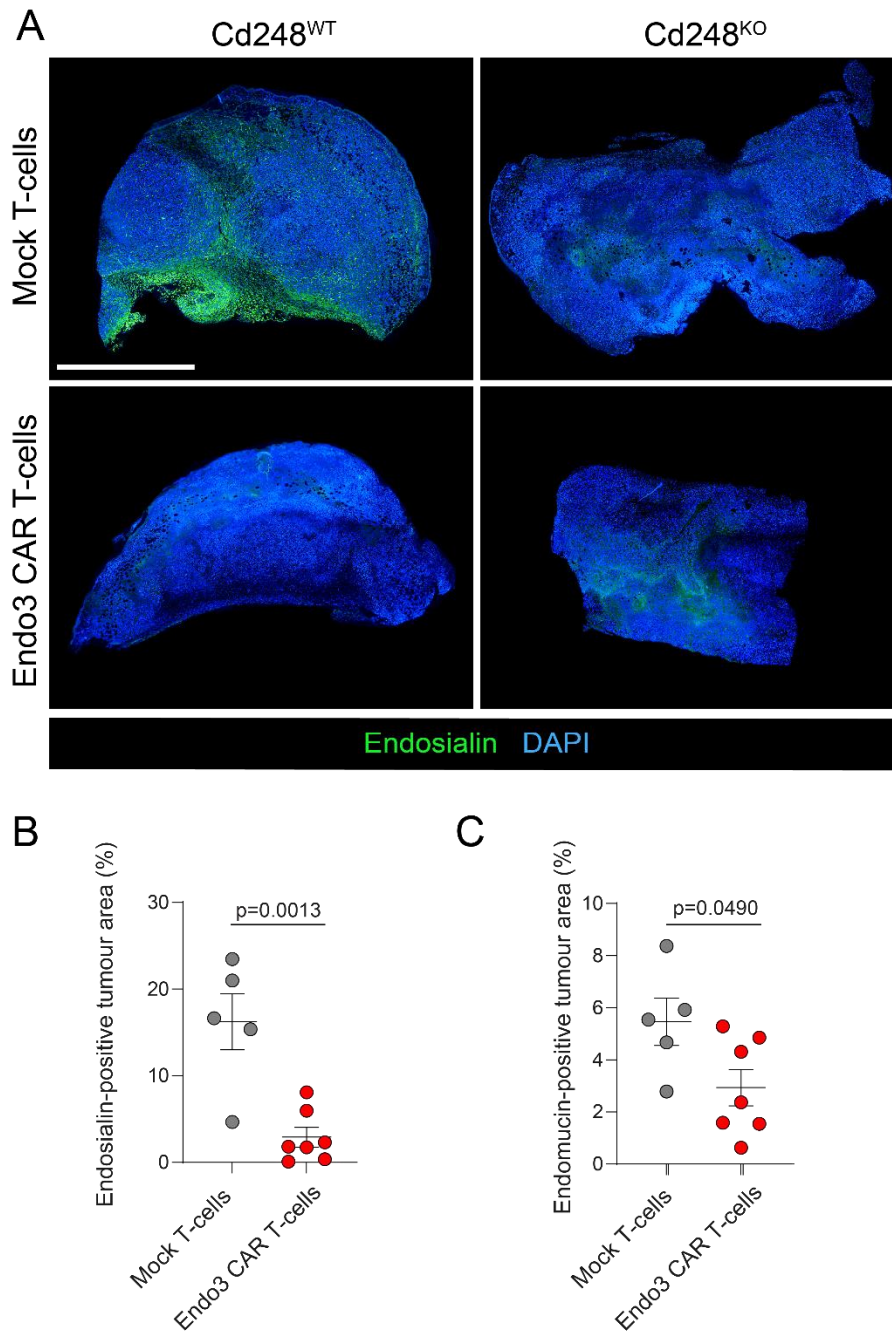


Figure 5. 3 Endo3 CAR T-cells deplete endosialin-positive cells in 4T1 tumours (2)

Continuation of Figure 5.1. **(A)** Primary tumours from Cd248^{WT} or Cd248^{KO} mice treated with mock T-cells or Endo3 CAR T-cells were formalin-fixed, paraffin-embedded (FFPE). Tumour sections were stained for endosialin (green). Nuclei were counterstained with DAPI (blue). Slides were scanned on a Hamamatsu NanoZoomer. Representative images are shown. Scale bar = 1 mm. **(B)** Quantification of endosialin-positive area in 4T1 tumours treated with mock T-cell or Endo3 CAR T-cells. Data shows mean \pm SEM. Unpaired Student's *t*-test. **(C)** Quantification of endomucin-positive area in 4T1 tumours treated with mock T-cell or Endo3 CAR T-cells. Data shows mean \pm SEM. Unpaired Student's *t*-test.

In addition to tumour tissue, FFPE sections of normal bladder and skin tissue from Cd248^{WT} tumour-bearing mice were immunostained for endosialin. As expected, bladder and skin tissue from mice treated with mock T-cells shows a similar pattern of endosialin-expressing cells as was observed in Chapter 3.2.3. This pattern of endosialin-expressing cells in normal tissue is not notably different in mice treated with Endo3 CAR T-cells (Figure 5.4).

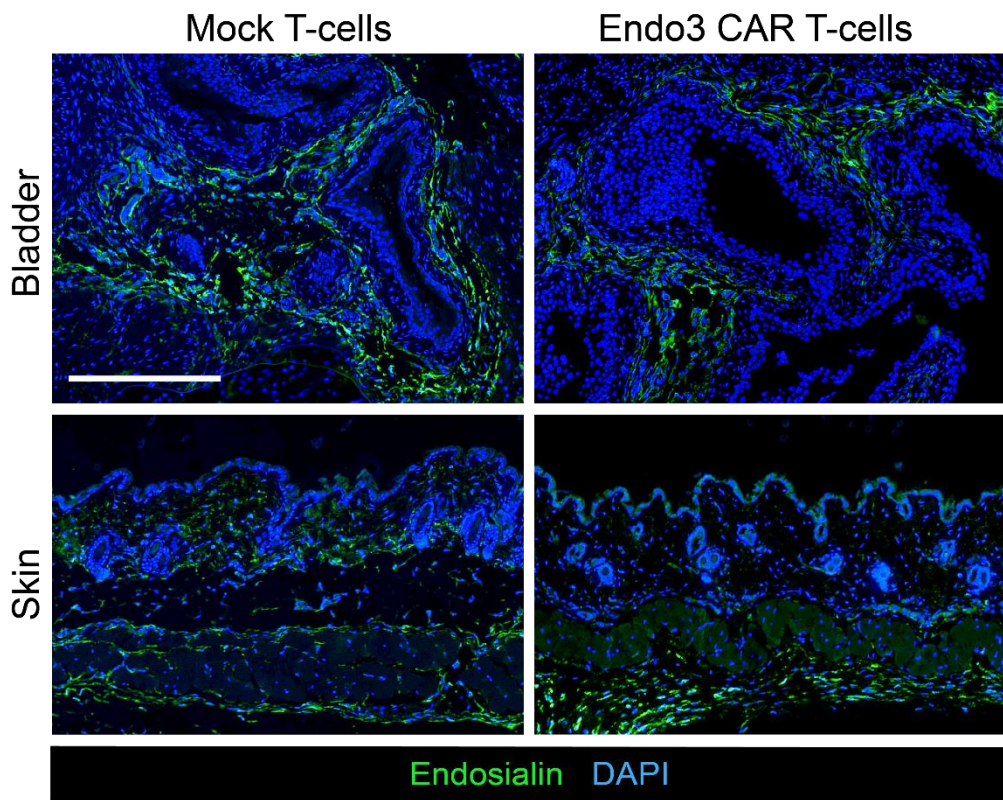


Figure 5. 4 Endo3 CAR T-cells do not deplete endosialin-positive cells in normal tissue

Continuation of Figure 5.1. **(A)** Bladder and skin tissue from Cd248^{WT} tumour-bearing mice treated with mock T-cells or Endo3 CAR T-cells were formalin-fixed, paraffin-embedded (FFPE). Tissue sections were stained for endosialin (green). Nuclei were counterstained with DAPI (blue). Slides were scanned on a Hamamatsu NanoZoomer. Representative images are shown. Scale bar = 250 μ m.

In Chapter 3.2.1 4T1 tumour cells were shown to be endosialin-negative in cell culture and in the present Chapter 4T1 tumours immunostained for endosialin do not show any positive tumour cell staining (Figure 5.3). Therefore, anti-tumour activity against 4T1 tumours would not be expected in Cd248^{KO} mice. Indeed, Endo3 CAR T-cell treatment does not result in decreased tumour volume in Cd248^{KO} mice when compared to Cd248^{KO} mice treated with mock T-cells. As expected, no difference in tumour volume is observed between Cd248^{WT} and Cd248^{KO} mice treated with either mock T-cells or Endo3 CAR T-cells. Additionally, no difference in tumour volume is observed between Cd248^{WT} mice treated with mock T-cells or Endo3 CAR T-cells (Figure 5.5A). However, although no difference is observed in tumour volume, the tumour weights taken at necropsy from Cd248^{WT} mice reveal a trend for decreased weight of tumours taken from Cd248^{WT} mice treated with Endo3 CAR T-cells when compared to Cd248^{WT} treated with mock T-cells. This trend was not observed in Cd248^{KO} mice (Figure 5.5B). To assess whether this discrepancy between tumour volume and tumour weight in Cd248^{WT} mice is due to the presence of dead tissue within the Cd248^{WT} Endo3 CAR T-cell treated tumours, the necrotic tumour area was quantified. Tumours from Cd248^{WT} Endo3 CAR T-cell treated mice have significantly increased necrotic area when compared to Cd248^{WT} mice treated with mock T-cells. A trend is also observed for increased necrotic area in Cd248^{WT} Endo3 CAR T-cell treated mice when compared to Endo3 CAR T-cell treated Cd248^{KO} mice, however this difference is not significant (Figure 5.5C). To visualise these differences in necrotic area, tumours from Cd248^{WT} or Cd248^{KO} mice treated with mock T-cells or Endo3 CAR T-cells were immunostained for nucleophosmin, a ubiquitously expressed nucleolar phosphoprotein that is frequently overexpressed by solid tumour cells (Di Matteo *et al.* 2016). A visible reduction in viable nucleophosmin-positive tumour cells is observed in Cd248^{WT} Endo3 CAR T-cell treated tumours when compared to both Cd248^{WT} mock T-cell treated tumours and Cd248^{KO} tumours treated with either mock T-cells or Endo3 CAR T-cells (Figure 5.5D).

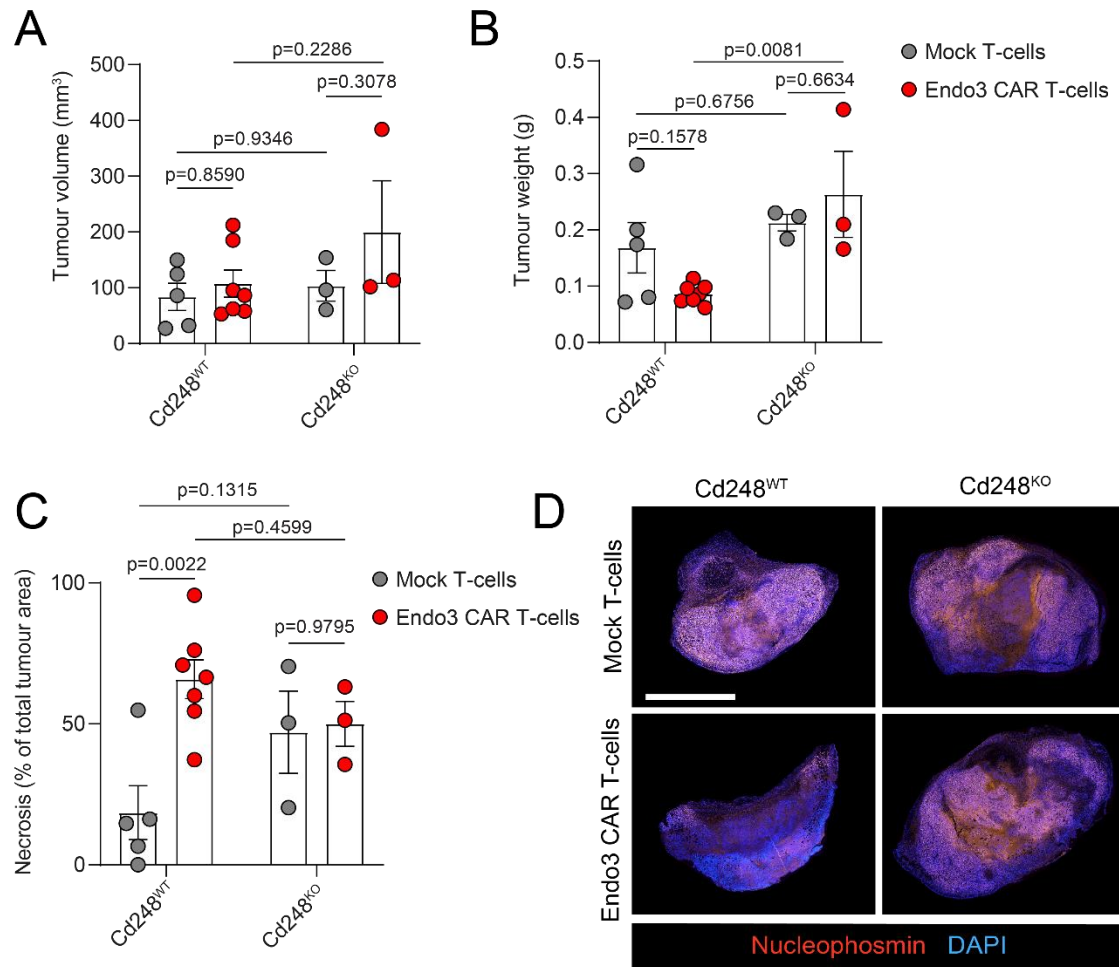


Figure 5.5 Efficacy of Endo3 CAR T-cell therapy against 4T1 tumours in Cd248^{WT} and Cd248^{KO} mice

Continuation of Figure 5.1. **(A)** 4T1 tumour volumes taken at necropsy from Cd248^{WT} or Cd248^{KO} mice treated with mock T-cells or Endo3 CAR T-cells. Data shows mean \pm SEM. Two-way ANOVA. **(B)** 4T1 tumour weights taken at necropsy from Cd248^{WT} or Cd248^{KO} mice treated with mock T-cells or Endo3 CAR T-cells. Data shows mean \pm SEM. Two-way ANOVA. **(C)** Percent necrotic area of 4T1 tumours from Cd248^{WT} or Cd248^{KO} mice treated with mock T-cells or Endo3 CAR T-cells. Necrotic area was determined from H&E stained tumour sections. Data shows mean \pm SEM. Two-way ANOVA. **(D)** 4T1 tumours from Cd248^{WT} or Cd248^{KO} mice treated with mock T-cells or Endo3 CAR T-cells were formalin-fixed, paraffin-embedded (FFPE). Tumour sections were stained for nucleophosmin (red). Nuclei were counterstained with DAPI (blue). Slides were scanned on a Hamamatsu NanoZoomer. Representative images are shown. Scale bar = 2.5 mm.

As previously, lung metastatic burden was assessed by manually counting the number of metastatic deposits in H&E stained lung sections. A significant reduction in lung metastasis is observed between Cd248^{WT} and Cd248^{KO} mock T-cell treated mice, consistent with data published previously by our laboratory (Viski *et al.* 2016). Lung metastasis is further limited in Cd248^{WT} mice receiving Endo3 CAR T-cells compared to both mock T-cell treated Cd248^{WT} mice, consistent with results reported in Chapter 4.2.4, and Cd248^{KO} mice (Figure 5.6).

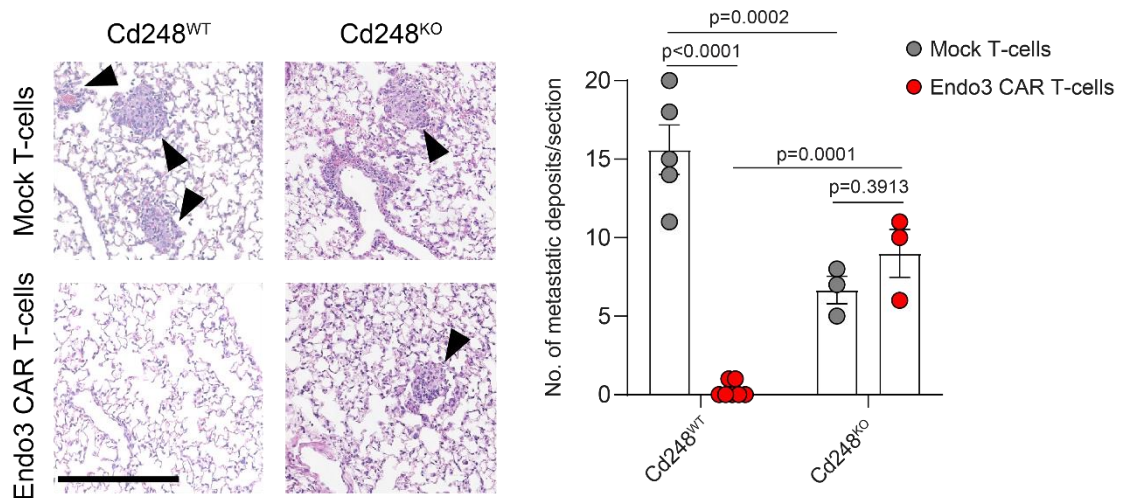


Figure 5. 6 Endo3 CAR T-cells limit 4T1 lung metastasis in Cd248^{WT} but not Cd248^{KO} mice

Continuation of Figure 5.1. Left, representative H&E stained lungs, arrowheads indicate metastatic deposits. Scale bar = 250 μ m. Right, metastatic deposits were quantified by manually counting the number of deposits in H&E stained formalin-fixed, paraffin-embedded (FFPE) lung sections from Cd248^{WT} or Cd248^{KO} mice treated with mock T-cells or Endo3 CAR T-cells. Data shows mean \pm SEM. Two-way ANOVA.

5.2.2 Endo3 CAR T-cell-associated toxicity is target and tumour specific

Consistent with observations described in Chapter 4.2.4, and despite an improved aftercare regimen of Dietgel and water injections, Cd248^{WT} tumour-bearing Endo3 CAR T-cell treated animals develop signs of toxicity from 5 days post-T-cell

injection and their health continues to deteriorate until a number of animals in this group require culling as per the limits of our licence 8 days post-T-cell injection. All other animals in this study show no signs of ill health up to 8-9 days post-T-cell injection (Figure 5.7A). Again, upon necropsy, pale livers with darkened and enlarged gallbladders are observed in Cd248^{WT} tumour-bearing, Endo3 CAR T-cell treated mice, whereas mice in all other groups do not display this phenotype (Figure 5.7B).

As discussed in Chapter 1.4.4., the most common manifestation of toxicity in CAR T-cell treated patients is CRS. CRS may be characterised by an elevation in serum cytokines, including IL-6 (Teachey *et al.* 2013; Pabst *et al.* 2020). Consequently, serum was collected from all animals and analysed for IL-6 levels. The two Cd248^{WT}, tumour-bearing, Endo3 CAR T-cell treated mice that were observed to be in the worst health show the highest serum IL-6 levels, which are at least 2-fold that of all other mice in the study (Figure 5.7C).

5.2.3 *Anti-IL-6R treatment does not alleviate Endo3 CAR T-cell-associated toxicity*

Patients that present signs of CRS post-CAR T-cell therapy in the clinic are administered tocilizumab, an IL-6 receptor (IL-6R) antagonist, as a first line of intervention (Yáñez *et al.* 2019). Tocilizumab acts to block the IL-6R, thus inhibiting IL-6 signalling via this pathway and lessening the inflammatory response. The elevation of serum IL-6 in a subset of Cd248^{WT} tumour-bearing mice indicated that Endo3 CAR T-cell associated toxicity could be due to CRS. If this is the case, treatment with a mouse analogue of tocilizumab, mAb 15A7, should alleviate this toxicity.

Binding of IL-6 to the IL-6R stimulates signalling via the JAK-STAT3 pathways, which results in the phosphorylation of STAT3 (Murray 2007). To confirm 15A7 (anti-IL-6R) successfully blocks IL-6 signalling, phosphorylation of STAT3 was

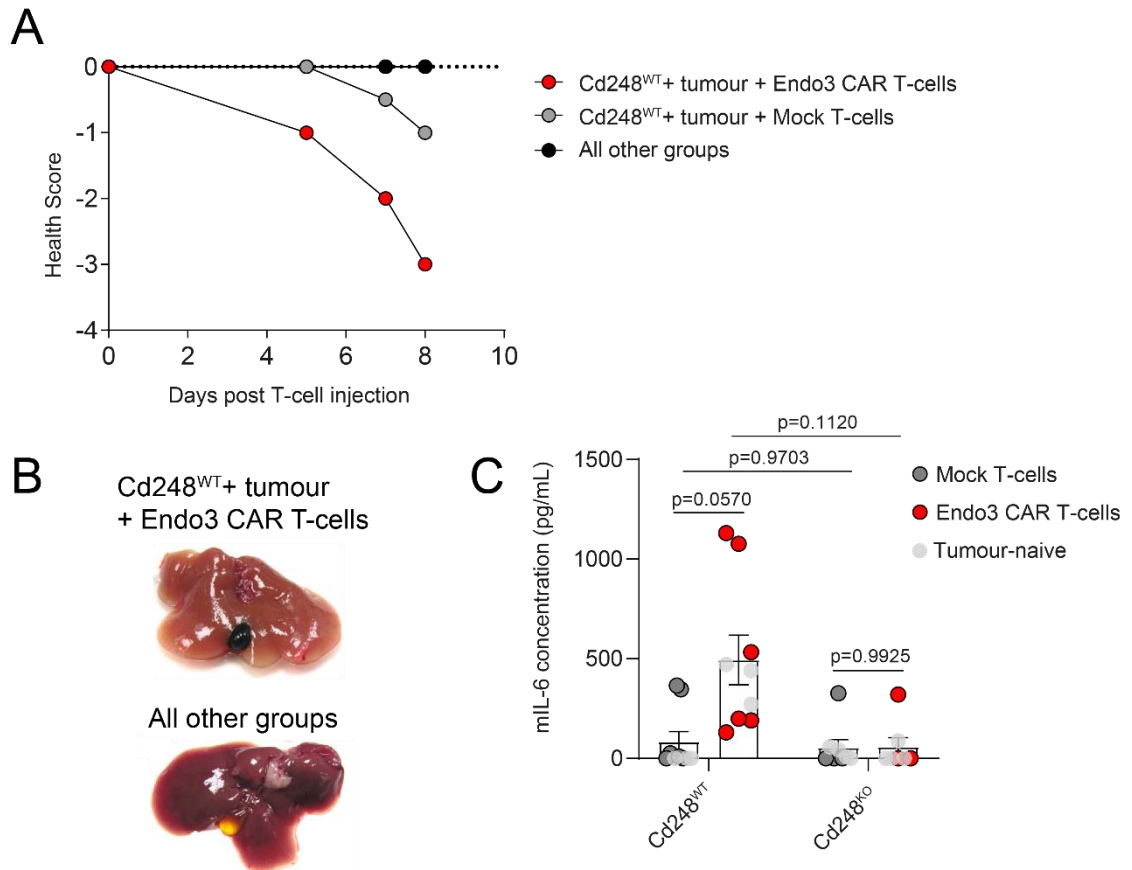


Figure 5. 7 Endo3 CAR T-cell associated toxicity is limited to Cd248^{WT}, tumour-bearing mice

Continuation of Figure 5.1. **(A)** Health score progression of mice in all groups. Animals were monitored closely after T-cell injection and given a health score based on appearance and behaviour (see Section 2.2.3). **(B)** Representative images of liver and attached gallbladders taken at necropsy from Cd248^{WT}, tumour-bearing, Endo3 CAR T-cell treated mice (upper) and all other animals (lower). **(C)** Serum was collected upon necropsy 8-9 days post-T-cell injection and analysed for mIL-6 concentration. Samples were analysed from mock T-cell treated or Endo3 CAR T-cell treated, tumour-bearing (solid circles) or tumour-naïve (grey circles), Cd248^{WT} or Cd248^{KO} mice. Data shows mean \pm SEM. Two-way ANOVA (tumour-naïve mice were excluded from statistical analysis).

examined in J774a.1 macrophage cells treated with media alone, media supplemented with mouse recombinant IL-6 only or media supplemented with mouse recombinant IL-6 and anti-mouse IL-6R or an isotype control mAb that binds keyhole limpet hemocyanin (LTF2). Western blot analysis of J774a.1 cell lysates reveals an absence of

phosphorylated STAT3 (pSTAT3) in cells treated with media alone and increased levels of pSTAT3 when cells are cultured in the presence of recombinant mouse IL-6 (Figure 5.8 A). The level of pSTAT3 is decreased in the presence of anti-IL-6R, but not in the presence of isotype control mAb, suggesting that the anti-IL-6R mAb is indeed acting to block IL-6 binding to the IL-6 receptor (Figure 5.8B).

To determine whether anti-IL-6R treatment alone affects 4T1 tumour growth and metastasis, 8-10 week old female BALB/c mice were injected subcutaneously with 2.5×10^5 4T1-Luc tumours cells and tumours were allowed to grow for 12 days to 50-200mm³ in size. On day 12 post-tumour cell injection, mice were treated with 25 mg/kg anti-IL-6R or isotype control mAb by intraperitoneal injection. For the subsequent 5 days, mice were treated daily with 12.5 mg/kg anti-IL-6R or isotype control mAb via intraperitoneal injection (Figure 5.8C). This treatment regime has previously been reported to be well tolerated in SCID-beige mice (Giavridis *et al.* 2018). Animals were culled 22 days post-tumour cell injection. Bi-weekly tumour measurements reveal that tumour growth is comparable between anti-IL-6R treated and isotype control treated mice (Figure 5.8D). Further, there was no difference in lung metastasis between anti-IL-6R and isotype control mAb treated mice (Figure 5.8E).

The strategy to evaluate the efficacy of anti-IL-6R treatment in alleviating Endo3 CAR T-cell associated toxicity in BALB/c mice is shown in Figure 5.9. In brief, 8-10 week old female mice were injected subcutaneously with 2.5×10^5 4T1-Luc cells and tumours were allowed to grow for 12 days to 50-200mm³ in size. All mice were subjected to 5 Gy whole body caesium irradiation and intraperitoneal injection with 25 mg/kg anti-IL-6R or isotype control mAb 18 h before 2.5×10^6 mock T-cells or Endo3 CAR T-cells were injected via the tail vein. From the day of T-cell injection to 7 days post-T-cell injection, mice were administered daily with 12.5 mg/kg anti-IL-6R or isotype control mAb via intraperitoneal injection. Venous blood was collected 7 days post-T-cell analysis. Animals were culled 8-14 days post-T-cell injection.

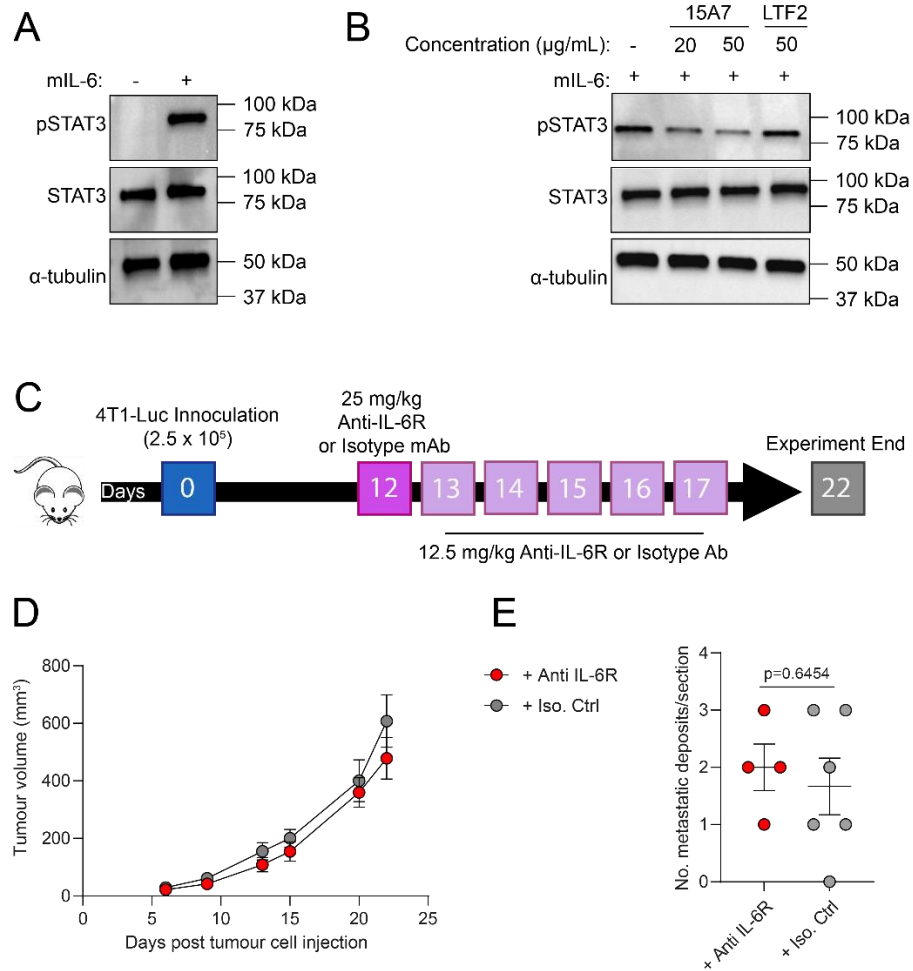


Figure 5. 8 Validation of anti-IL-6R mAb 15A7 and isotype control mAb LTF2

(A) Mouse J774a.1 macrophage cells were plated at 5×10^5 cells per well in 6-well plates and cultured overnight. The next day, media was replaced with serum free media (A) with or without 100 ng/mL recombinant mIL-6 or (B) supplemented with 100 ng/mL recombinant mIL-6 alone or 100 ng/mL recombinant mIL-6 and either 20 or 50 µg/mL anti-IL-6R mAb 15A7 or 50 µg/mL anti-keyhole limpet hemocyanin mAb LTF2 (isotype control). After 30 min, wells were washed with PBS and cell lysates were collected and subject to western blotting with anti-pSTAT3 and anti-STAT3 antibodies, followed by HRP-conjugated anti-rabbit Ig. α-tubulin was detected as a loading control. (C) Experimental strategy for *in vivo* characterisation of anti-IL-6R (15A7) or isotype control (LTF2) mAb treatment. BALB/c mice aged 8-10 weeks were injected subcutaneously with 2.5×10^5 4T1-Luc cells on day 0. Tumours were allowed to grow for 12 days to 50-200 mm^3 in size. Mice were administered with 25 mg/kg anti-IL-6R or isotype control mAb via intraperitoneal injection on day 12 post-tumour cell injection and with 12.5 mg/kg/day on days 13-17 post-tumour cell injection. The experiment was ended on day 22 day. (D) Tumour growth curves for anti-IL-6R (n=4) or isotype control (n=6) mAb treated mice bearing 4T1 primary tumours. Data shows mean \pm SEM for each time point. (E) Metastatic deposits were quantified by manually counting the number of deposits in H&E stained formalin-fixed, paraffin-embedded (FFPE) lung sections from anti IL-6R or isotype control mAb treated mice. Data shows mean \pm SEM. Unpaired Student's *t*-test.

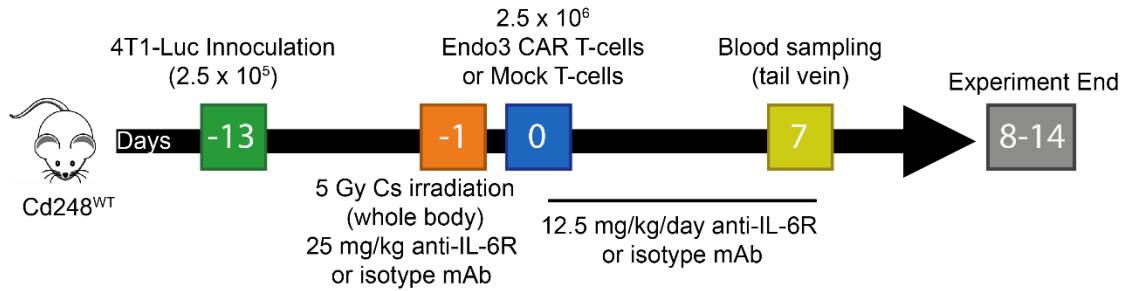


Figure 5. 9 Experimental strategy for investigating Endo3 CAR T-cell and anti-IL-6R co-therapy in BALB/c mice

8-10 week old Cd248^{WT} BALB/c mice were injected subcutaneously with 2.5×10^5 4T1-Luc cells. Tumours were allowed to grow for 12 days to 50-200mm³ volume. All mice were subjected to 5 Gy whole body caesium irradiation and administered with 25 mg/kg anti-IL-6R or isotype control mAb via intraperitoneal injection 18 h prior to injection via the tail vein with 2.5×10^6 mock T-cells or Endo3 CAR T-cells (n=8-10 per group). Mice were given additional intraperitoneal injections of 12.5 mg/kg anti-IL-6R or isotype control mAb on days 0-7 post-T-cell injection. Dietgel was provided to all mice from day -1 to study termination. Venous blood was collected via the tail vein 7 days post-T-cell injection. Mice were culled 8-14 days post-T-cell injection due to ill health of Endo3 CAR T-cell treated mice. Mock T-cell treated mice were culled 8-14 days post-T-cell injection as controls only.

In this study, Endo3 CAR T-cell therapy had a significant effect on tumour growth rate in animals co-treated with isotype control mAb, however this was not observed in animals co-treated with anti-IL-6R mAb (Figure 5.10A). Analysis of CD4⁺&CD8⁺ hCD34⁺ cells in venous blood of mice treated with Endo3 CAR T-cells and anti-IL-6R or isotype control mAb reveals no difference in circulating Endo3 CAR T-cell levels on day 7 post-T-cell injection (Figure 5.10B). To assess the effect of Endo3 CAR T-cell therapy on the tumour vasculature, a subset of three mice per group were injected via the tail vein with AngioSense reagent, a fluorescent macromolecule that pools in the tumour vasculature, and imaged on an IVIS Lumina imaging platform 24 h later. The AngioSense signal from 4T1 tumours treated with mock T-cells is comparable whether co-treated with anti-IL-6R or isotype control mAb. Interestingly, AngioSense signal is reduced in 4T1 tumours

treated with Endo3 CAR T-cells and this effect appears exacerbated by anti-IL-6R co-treatment (Figure 5.10C).

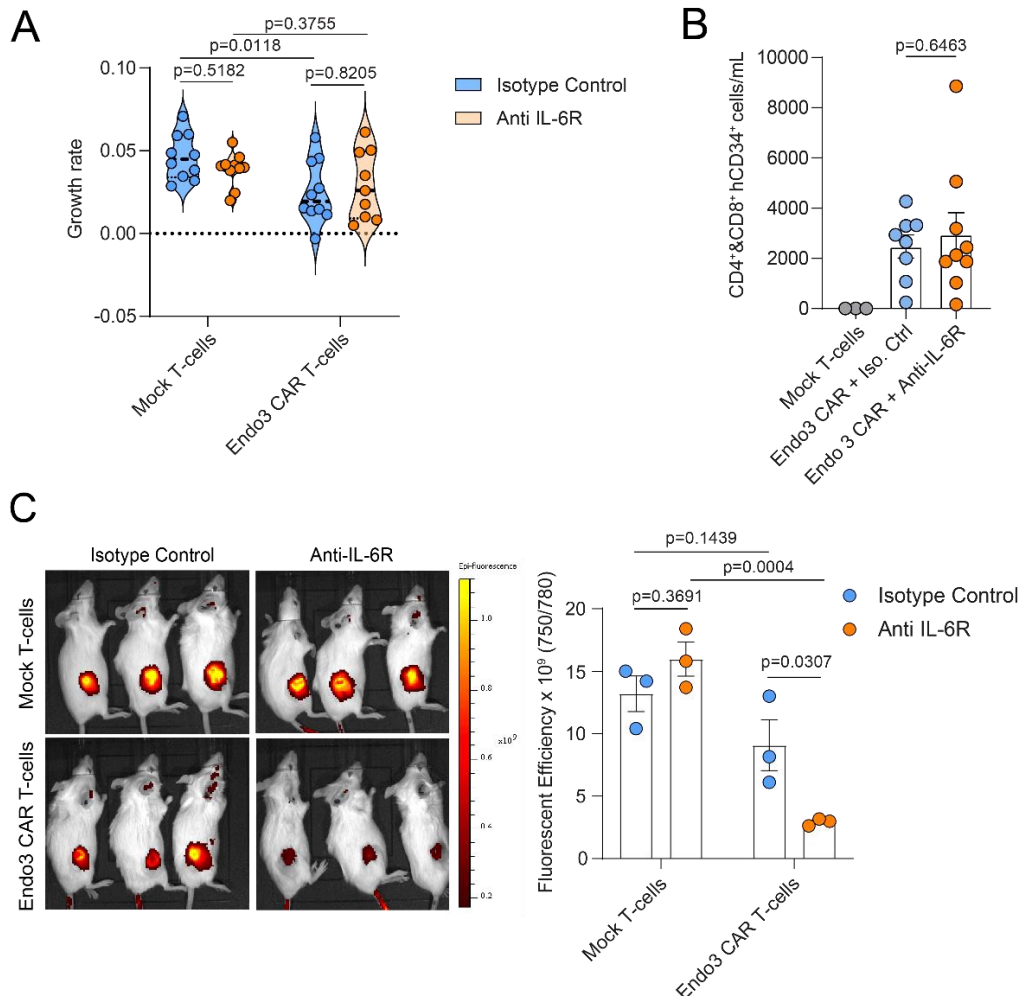


Figure 5. 10 Anti-IL-6R co-therapy does not affect Endo3 CAR T-cell persistence

Continuation of Figure 5.9. **(A)** Tumour growth rates for mock T-cell or Endo3 CAR T-cell treated mice co-treated with anti-IL-6R or isotype control mAb. Data shows mean \pm SEM. Two-way ANOVA. **(B)** Number of circulating CD4⁺hCD34⁺ and CD8⁺hCD34⁺ Endo3 CAR T-cells in venous blood taken 7 days post-T-cell injection from Endo3 CAR T-cell treated mice co-treated with anti-IL-6R or isotype control mAb. Samples from mock T-cell treated mice were used as negative controls. Each data point represents one mouse. Data shows mean \pm SEM. Student's *t*-test. **(C)** 6 days post-T-cell injection, mice were injected via the tail vein with AngioSense reagent ($n=3$ per group, average tumour volumes: mock + isotype control = 452 mm³, mock + anti-IL-6R = 448 mm³. Endo3 + isotype control = 312 mm³. Endo3 + anti-IL-6R = 325 mm³). After 24 h, mice were subjected to IVIS imaging measuring fluorescence at 750/780 nm. Left, images of all mice injected with AngioSense reagent 24 h after injection. Right, quantification of total radiant efficiency measured on an IVIS Lumina imaging system. Data shows mean \pm SEM. Two-way ANOVA.

Tocilizumab treatment has been found to increase free IL-6 in the serum (Nishimoto *et al.* 2008). Therefore, to confirm the anti-IL-6 treatment was working *in vivo*, IL-6 concentration was determined in serum from mock T-cell treated and Endo3 CAR T-cell treated mice co-treated with anti-IL-6R or isotype control mAb. An increase in serum IL-6 is observed in mice co-treated with anti-IL-6R mAb, in both mock T-cell treated and Endo3 CAR T-cell treated mice, when compared to isotype control mAb co-treated mice (Figure 5.11A). This suggests that the anti-IL-6R mAb indeed functions to block the IL-6R *in vivo*. However, despite this, co-treatment of Endo3 CAR T-cells with anti-IL-6R mAb did not result in a survival benefit over mice co-treated with Endo3 CAR T-cells and isotype control mAb and all mice succumbed to the same toxicities as before (Figure 5.11 B). These results indicate that Endo3 CAR T-cell associated toxicity in BALB/c mice cannot be alleviated by classic treatment against CRS.

5.2.4 Multiple low doses of Endo3 CAR T-cells reduce the incidence of, but do not fully alleviate, Endo3 CAR T-cell-associated toxicity

In this Chapter, it has been demonstrated that Endo3 CAR T-cell associated toxicity is not alleviated by co-treatment with anti-IL-6R mAb. Therefore, it is unlikely that Endo3 CAR T-cell associated toxicity is solely due to CRS. In Section 5.2.1, Endo3 CAR T-cell treated tumours in Cd248^{WT} mice were found to be more necrotic than those treated with mock T-cells. Therefore, Endo3 CAR T-cell associated toxicity may be in part due to the rapid death of 4T1 tumour cells leading to TLS, a condition that can be fatal if left untreated (Howard *et al.* 2014). It was hypothesised that separating the Endo3 CAR T-cell treatment regime into 3 smaller doses, amounting to the same overall dose, would alleviate or significantly reduce Endo3 CAR T-cell associated toxicity, whether due to CRS, TLS or a combination of both.

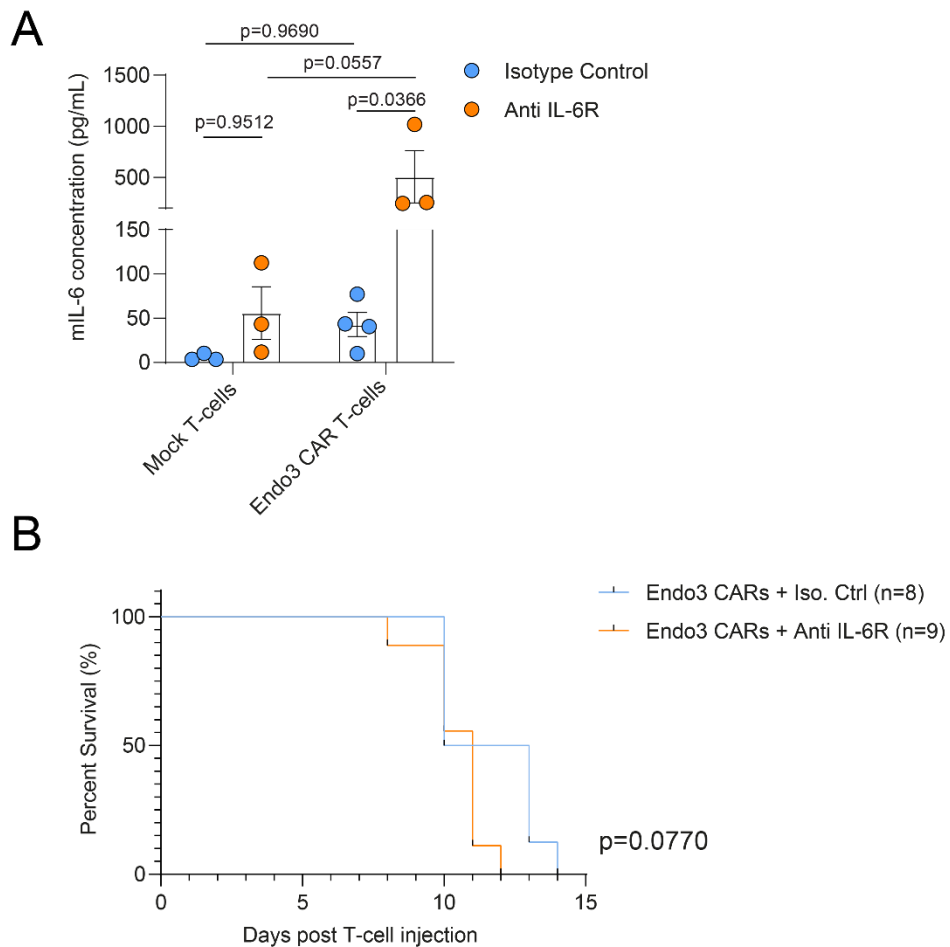


Figure 5. 11 Anti-IL-6R co-therapy does not alleviate Endo3 CAR T-cell associated toxicity in BALB/c mice

Continuation of Figure 5.9. **(A)** Serum concentrations of mIL-6 in mock T-cell or Endo3 CAR T-cell treated mice co-treated with anti-IL-6R or isotype control mAb (n=3-4 per group). Serum was collected upon necropsy 9-11 days post-T-cell injection. Data shows mean \pm SEM. Two-way ANOVA **(B)** Kaplan-Meier survival analysis of Endo3 CAR T-cell treated mice co-treated with anti-IL-6R (n=9) or isotype control (n=8) mAb. Endo3 Car T-cell treated mice were culled when they displayed signs of toxicity. Log-rank test, p=0.0770. Mock T-cell treated mice were culled in groups at the same time as Endo3 CAR T-cell treated mice as controls only.

The strategy to investigate whether multiple lower doses of Endo3 CAR T-cells can alleviate Endo3 CAR T-cell associated toxicity is outlined in Figure 5.12. In brief, Cd248^{WT} female mice were injected subcutaneously with 2.5×10^5 4T1-Luc cells and tumours were allowed to grow for 12 days to 50-200 mm³ in size. Mice were subjected

to 5 Gy whole body x-ray irradiation 18 h before 0.83×10^6 mock T-cells or Endo3 CAR T-cells were injected via the tail vein. Additional doses of 0.83×10^6 mock T-cells or Endo3 CAR T-cells were delivered 5 and 10 days after the initial dose. Mock T-cell treated and Endo3 CAR T-cell treated mice were culled when they approached the severity limits of our licence, whether due to Endo3 CAR T-cell associated toxicity or metastatic lung burden. In contrast to previous studies described in this thesis in which 100% of Endo3 CAR T-cell treated mice were culled due to Endo3 CAR T-cell associated toxicity, only 50% of mice displayed toxicity in the present study. The other 50% of Endo3 CAR T-cell treated mice were culled due to lung metastatic burden. Some mice also had decreased use of one limb as well as laboured breathing. Comparison of survival rate between Endo3 CAR T-cell treated mice that did not show any signs of toxicity and mock T-cell treated mice shows a modest, but non-significant, survival advantage over mock T-cell treated mice (Figure 5.13).

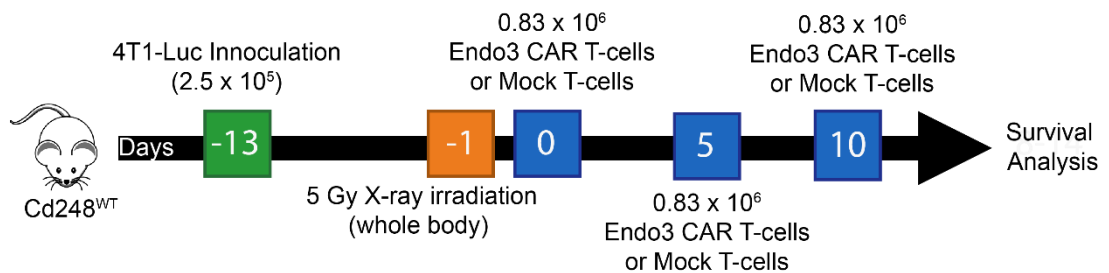


Figure 5. 12 Experimental strategy for investigating multiple low doses of Endo3 CAR T-cell therapy in BALB/c mice

8-10 week old Cd248^{WT} BALB/c mice were injected subcutaneously with 2.5×10^5 4T1-Luc cells. Tumours were allowed to grow for 12 days to 50-200mm³ volume. All mice were subjected to 5 Gy whole body x-ray irradiation 18 h prior to injection via the tail vein with 0.83×10^6 mock T-cells ($n=14$) or Endo3 CAR T-cells ($n=20$). Mice were injected via the tail vein with a further 0.83×10^6 mock T-cells or Endo3 CAR T-cells on 5 and 10 days post-initial T-cell injection. Endo3 CAR T-cell treated mice were monitored for signs of ill health and were culled when signs of toxicity or high lung burden were apparent. Mock T-cell treated mice were culled either as histological controls for Endo3 CAR T-cell treated mice or when high lung burden was apparent.

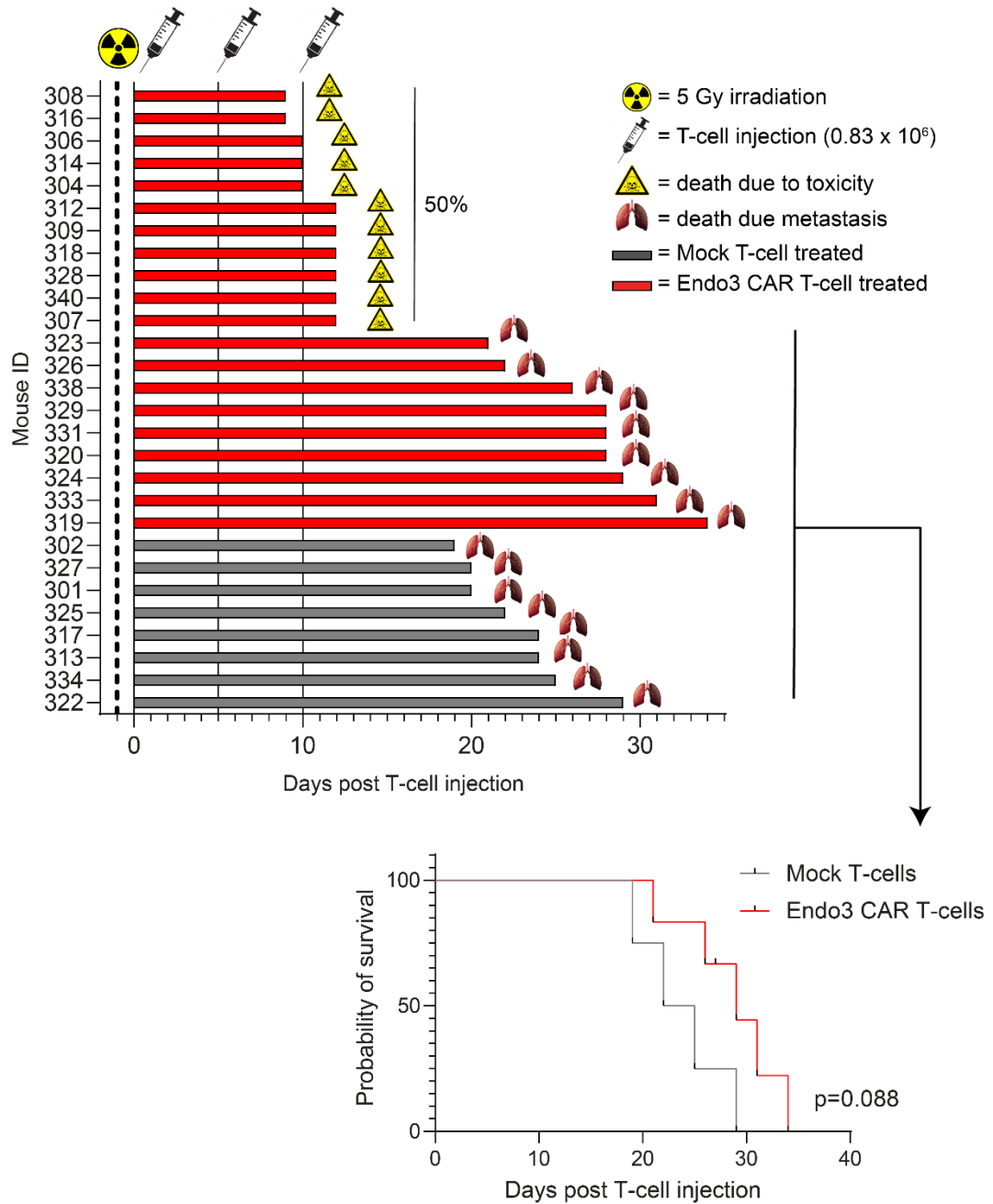


Figure 5. 13 Delivering multiple low doses of Endo3 CAR T-cell therapy alleviates CAR T-cell-mediated toxicity in a subset of BALB/c mice

Continuation of Figure 5.12. Upper panel, individual fates of mice treated with multiple 0.83×10^6 doses of mock T-cells or Endo3 CAR T-cells. $n=5$ Endo3 CAR T-cell treated mice were culled due to ill health before receiving the day 10 dose. $n=6$ Endo3 CAR T-cell treated mice were culled due to ill health 12 days post-initial T-cell injection and $n=6$ mock T-cell treated mice were culled simultaneously for histological comparison (not shown on graph). Lower panel, Kaplan-Meier survival analysis on the remaining mock T-cell treated ($n=8$) and Endo3 CAR T-cell treated ($n=9$). All mice were culled due to ill-health associated with high metastatic burden. Log-rank test, $p=0.088$.

5.3 Discussion

5.3.1 *Endo3 CAR T-cells increase 4T1 tumour necrosis and limit spontaneous metastasis to the lungs in Cd248^{WT} mice*

As seen in Chapter 4, Endo3 CAR T-cell therapy results in a striking decrease in lung metastasis in Cd248^{WT} mice, which is significantly lower than that observed in Cd248^{WT} mock T-cell treated mice and all Cd248^{KO} mice. Interestingly, Cd248^{WT} Endo3 CAR T-cell treated tumours are not different in volume from all other groups, however they are found to weigh less and contain a higher proportion of necrotic tissue. This suggests that Endo3 CAR T-cell therapy results in increased tumour cell death in 4T1 primary tumours. As Endo3 CAR T-cells target endosialin-positive perivascular cells, this may be due to a loss of vascular structures in the tumour, as tumour tissue cannot survive without a sufficient vascular network (Hanahan and Folkman 1996). Indeed, quantification of endomucin-positive cells in 4T1 tumours from Cd248^{WT} Endo3 CAR T-cell treated mice shows decreased endothelial staining when compared to mock T-cell treated controls. A decrease in endomucin-positive vasculature and increase in necrotic tumour tissue also likely contributes to the phenotype for reduced lung metastasis in Cd248^{WT} Endo3 CAR T-cell treated 4T1 tumours.

5.3.2 *Endo CAR T-cells demonstrate no activity or toxicity in Cd248^{KO} mice*

In Chapter 4, a pilot study of Endo3 CAR T-cell therapy against 4T1 tumours revealed that although Endo3 CAR T-cells demonstrated promising anti-tumour activity, therapy was associated with toxicity in tumour-bearing mice. Endosialin knock-out mice develop into adulthood without any obvious defects (Nanda *et al.* 2006) and our laboratory has previously demonstrated that 4T1 primary tumours grow subcutaneously in Cd248^{KO} BALB/c mice at a comparable rate to 4T1 tumours implanted in Cd248^{WT} BALB/c mice (Viski *et al.* 2016). Therefore, to assess the specificity of Endo3 CAR T-cell

activity and toxicity, Endo3 CAR T-cells were administered to both Cd248^{WT} and Cd248^{KO} 4T1 tumour-bearing or tumour-naïve BALB/c mice.

Expansion of Endo3 CAR T-cells in Cd248^{KO} mice is less than that observed in Cd248^{WT} tumour-bearing mice with both tumour-bearing and tumour-naïve Cd248^{KO} mice displaying comparable Endo3 CAR T-cells levels to those observed in Cd248^{WT} tumour-naïve mice. As expected, Cd248^{KO} tumours are confirmed negative for endosialin via immunostaining and Endo3 CAR T-cell therapy does not affect 4T1 tumour growth in Cd248^{KO} mice. Consistent with previous reports by our laboratory (Viski *et al.* 2016), mock treated Cd248^{KO} mice have a significantly decreased number of metastatic deposits in the lungs when compared to mock treated Cd248^{WT} mice. However, the number of metastatic deposits in the lungs of Cd248^{KO} mice is not affected by Endo3 CAR T-cell therapy. Importantly, no evidence of Endo3 CAR T-cell associated toxicity is observed in any Cd248^{KO} mice. These data suggest that Endo3 CAR T-cells do not demonstrate off-target activity and do not function against 4T1 tumour cells themselves, but indeed target stromal endosialin. Interestingly, Cd248^{WT} mice treated with Endo3 CAR T-cells demonstrate a further reduction in lung metastasis when compared to Cd248^{KO} mice treated with mock T-cells. This suggests that depletion of endosialin-expressing cells is more effective at preventing metastasis to the lungs than genetic deletion of the receptor alone.

5.3.3 *Endo3 CAR T-cells demonstrate tumour-specific toxicity and do not attack normal tissues*

Consistent with results reported in Chapter 4, the first Cd248^{WT} tumour-bearing mice treated with Endo3 CAR T-cells succumb to adverse toxicity within 8 days post-T-cell injection in the study presented in Section 5.2.1-2, despite an enhanced aftercare hydration regimen. However, this toxicity is not observed in tumour-naïve mice, suggesting that Endo3 CAR T-cells expand only where tumours are present. This

supports previous reports of endosialin being a tumour stroma-associated antigen (MacFadyen *et al.* 2005).

In Chapter 3, low levels of endosialin expression were found in the BALB/c mouse bladder and skin tissue. Interestingly, immunostaining of these tissues from Cd248^{WT} tumour-bearing Endo3 CAR T-cell treated mice reveals no evidence that endosialin-expressing cells are depleted in the normal tissue. This is in line with results described in Chapter 4.2.5, in which Endo3 CAR T-cells were not found to deplete endosialin-positive fibroblasts in the healing wound, and again this may be due to the additional barriers faced by Endo3 CAR T-cells to navigate beyond cells associated with the vasculature. In mice with actively healing wounds, circulating Endo3 CAR T-cell levels were found to be lower than those observed in Cd248^{WT} tumour-bearing mice and thus the demonstration that Endo3 CAR T-cells do not deplete endosialin-expressing cells in the normal tissue even at higher circulating levels is an important and positive finding.

Upon post-mortem dissection of animals, it was noted that Cd248^{WT} tumour-bearing mice treated with Endo3 CAR T-cells had pale livers and a visibly darkened and enlarged gallbladders, a phenotype that was exclusive to this group. A similar phenotype has been observed in an experimental model of sepsis where a combination of scavenger receptor A knock-out and caecal ligation puncture induced sepsis and resulted in a darkened and enlarged gallbladder (Drummond *et al.* 2012b). The authors of this study report this as comparable to acalculous cholecystitis in humans, which is associated with morbidity and mortality. As endosialin is expressed by perivascular cells, it may be that excessive targeting of vascular pericytes results in vascular breakdown, allowing the infiltration of septic factors into the circulation and resulting in sepsis. Alternatively, severe CRS can be associated with capillary leak syndrome (Lamers *et al.* 2013), therefore the observed liver and gallbladder phenotype may be a direct consequence of CRS mediated leakage of septic factors into the circulation. As discussed in Chapter 4.3.4., CRS is also a common adverse event associated with CAR

T-cell activity and it may be characterised by the elevation of serum cytokines, including IL-6 (Teachey *et al.* 2013; Pabst *et al.* 2020). In the present study, the most unwell Cd248^{WT} tumour-bearing mice had elevated serum levels of IL-6 compared to all other animals in the study. Together with the absence of normal tissue targeting, this suggests that the observed Endo3 CAR T-cell associated toxicity may be due to CRS. Approaches to limit CRS following Endo3 CAR T-cell therapy will be discussed in the following Section.

5.3.4 Endo3 CAR T-cell associated toxicity is not alleviated by anti-IL-6R co-treatment

In Section 5.2.2, a subset of Cd248^{WT} tumour-bearing, Endo3 CAR T-cell treated mice displayed elevated serum IL-6 levels when compared to all other mice in the study. CRS, the most common adverse event associated with CAR T-cell therapy, is characterised by increased concentrations of serum cytokines, including IL-6 (Pabst *et al.* 2020). CRS-like phenotypes have been reported in mice treated with CAR T-cells (Y.G. Lee *et al.* 2019; Sanderson *et al.* 2019) and the symptoms reported in these studies, weight-loss, hunching, piloerection and malaise, align with the symptoms observed in Section 5.2.2. Together with the elevated serum IL-6 levels, these findings suggest that Cd248^{WT} tumour-bearing mice treated with Endo3 CAR T-cells displaying signs of ill health may be suffering from CRS following CAR T-cell injection.

Giavridis and colleagues developed a mouse model of CRS that develops 2-3 days post-CAR T-cell infusion and found that co-treatment with a mouse IL-6R blocking antibody prevents CRS-associated mortality, when compared to co-treatment with an isotype control. In this Chapter, the same anti-IL-6R and isotype control mAbs were utilised according to the same dosing schedule reported by Giavridis and colleagues (Giavridis *et al.* 2018). The anti-IL-6R mAb was batched tested to ensure correct functionality and was indeed found to reduce STAT3 phosphorylation *in vitro* and

increase free serum IL-6 *in vivo*, both of which indicate blockade of IL-6 signalling (Murray 2007; Nishimoto *et al.* 2008). Importantly, anti-IL-6R treatment alone is well tolerated and does not have any effects on 4T1 primary tumour growth or metastasis to the lung. Anti-IL-6R treatment had no effect on Endo3 CAR T-cell persistence in the circulation, which agrees with clinical findings in patients treated with other CAR T-cells and tocilizumab simultaneously (Davila *et al.* 2014; Neelapu *et al.* 2017; Maude *et al.* 2018). However, unfortunately, anti-IL-6R treatment fails to increase survival of Cd248^{WT} tumour-bearing mice treated with Endo3 CAR T-cells. On reflection, the levels of serum IL-6, though elevated in Cd248^{WT} tumour-bearing, Endo3 CAR T-cell treated mice, are still relatively low compared to those reported in mouse models of CRS (Giavridis *et al.* 2018; Norelli *et al.* 2018). This, together with the lack of response to anti-IL-6R treatment, suggests that Endo3 CAR T-cell therapy may not be due solely to CRS.

Interestingly, co-treatment of Endo3 CAR T-cells and anti-IL-6R mAb further reduces the vascular signal from 4T1 tumours after AngioSense administration, when compared to Endo3 CAR T-cells and isotype control treatment. This suggests that anti-IL-6R co-treatment may increase the efficacy of Endo3 CAR T-cells *in vivo*. However, this is contradicted by the fact that anti-IL-6R co-treatment does not enhance the reduction in primary tumour growth rate when compared to Endo3 CAR T-cell and isotype control co-treatment. Further, as Endo3 CAR T-cell therapy is associated with toxicity in 4T1 tumour-bearing BALB/c mice, it could be hypothesised that enhanced anti-tumour activity would result in more severe or rapid toxicity, which was not evidenced in this study. These findings require additional investigation and are not explored further in this thesis.

5.3.5 Multiple low doses of Endo3 CAR T-cells reduces the incidence but does not alleviate Endo3 CAR T-cell-associated toxicity

An additional reported side effect of CAR T-cell therapy, as well as CRS and neurotoxicity, is TLS caused by rapid tumour cell death (Porter *et al.* 2011; Kochenderfer *et al.* 2013). In mice, TLS can present with symptoms that include weight-loss, malaise and piloerection, similarly to CRS (Vogel *et al.* 2010; Zhang *et al.* 2016). In Section 5.2.1, Cd248^{WT} 4T1 tumours treated with Endo3 CAR T-cells were found to be more necrotic than those treated with mock T-cells and in Section 5.2.3 Cd248^{WT} Endo3 CAR T-cell treated tumours were shown to have a decreased vascular signal. Therefore, it is possible that Endo3 CAR T-cell therapy causes a degree of TLS.

It has been demonstrated that lowering the dose of CAR T-cells, or breaking it down into multiple smaller fractions, may reduce CAR T-cell associated toxicities in patients (Porter *et al.* 2011; Frey *et al.* 2016; Pan *et al.* 2017). Therefore, the Endo3 CAR T-cell therapy schedule was revised to 3 smaller doses of 0.83×10^6 Endo3 CAR T-cells, delivered 5 days apart, with the first dose being given 18 h after lymphodepleting irradiation. In contrast to previous studies, in which 100% of Endo3 CAR T-cell treated mice developed toxicity, 50% of mice succumbed to Endo3 CAR T-cell toxicity following the revised schedule. The remaining 50% survived until they became moribund with lung metastasis. However, taking into account only mice that did not present with Endo3 CAR T-cell toxicity, the survival advantage of Endo3 CAR T-cell treatment was modest at best. This is consistent with reports by Porter and colleagues, which demonstrate that lowering the delivered CAR T-cell dose, with or without fractionation, reduces overall response rate to the therapy, despite reducing the number of serious adverse events (Porter *et al.* 2011).

Taken together, these results suggest that, although lowering and fractionating Endo3 CAR T-cell dose reduces the incidence of toxicity, this is not a viable strategy for treatment of 4T1 tumours in BALB/c mice.

Chapter 6 Endo3 CAR T-cell activity in C57BL/6 mice

6.1 Introduction

Despite associated toxicity, Endo3 CAR T-cell therapy demonstrates promising anti-tumour activity against 4T1 tumours in BALB/c mice. It has been previously reported that 4T1 tumour-bearing BALB/c mice are hypersensitive to PD-1/PD-L1 checkpoint blockade immunotherapy, with repeated dosing being fatal in this model (Mall *et al.* 2015). However, hypersensitivity reactions were not observed in C57BL/6 mice bearing B16 melanoma tumours. This suggests that BALB/c mice may be more sensitive to toxicity associated with immunotherapy and therefore it is important to evaluate Endo3 CAR T-cell therapy in a second non-BALB/c model.

In immunotherapy research, C57BL/6 mice are often utilised in the syngeneic setting. The AT-3 tumour cell line is of C57BL/6 origin and was established from the cells of the primary mammary gland carcinoma of the PyMT transgenic mouse model of autochthonous mammary carcinoma (Stewart and Abrams 2007). It has been previously reported that AT-3 cells implanted as subcutaneous tumours spontaneously metastasise to the lungs (Mammadova-Bach *et al.* 2016; Patin *et al.* 2018), making the AT-3 tumour line a suitable second model for evaluating Endo3 CAR T-cell therapy in the context of breast cancer.

Endosialin is not only upregulated in the stroma of breast cancers, but also of multiple other solid tumour types, including lung cancer. The LLC tumour cell line is also of C57BL/6 origin and spontaneously metastasises to the lungs (Yu *et al.* 2014; Hara *et al.* 2017; Kim *et al.* 2017). Further, our laboratory, in collaboration with others, has demonstrated that spontaneous metastasis of subcutaneous LLC tumours to the lungs is significantly reduced in Cd248^{KO} mice when compared to Cd248^{WT} mice (Viski *et al.*

2016). Therefore, the LLC lung cancer model is a suitable model for evaluating Endo3 CAR T-cell therapy in the context of non-breast solid tumours.

This Chapter will therefore investigate Endo3 CAR T-cell tolerability and efficacy in C57BL/6 mice in both the AT-3 mouse breast cancer model and LLC mouse lung cancer model.

6.2 Results

6.2.1 Characterisation of Endo3 CAR T-cell therapy in AT-3 tumour-bearing C57BL/6 mice

To validate the AT-3 model as a suitable model for testing Endo3 CAR T-cell therapy, AT-3 tumour growth, endosialin-expression and early lung metastasis was explored. AT-3 tumours grow slower than 4T1 tumours, reaching approximately 100-200 mm³ by 16 days post-subcutaneous inoculation of 2.5×10^5 tumour cells (Figure 6.1A). Day 16 AT-3 tumours were immunostained for endosialin and the endothelial cell marker endomucin (Figure 6.1B, left) and, similarly to the 4T1 model, AT-3 tumours display positive endosialin staining on CAFs and pericytes and endomucin staining reveals an established vascular network. H&E staining of lungs taken from AT-3 tumour-bearing mice 16 days post-tumour cell implantation also confirms the absence of detectable lung metastasis in the AT-3 model at this time point (Figure 6.1B, right).

Doses of up to 1×10^7 CAR T-cells are frequently delivered systemically and well tolerated in C57BL/6 mice (Chen *et al.* 2019; Rodriguez-Garcia *et al.* 2021; Rousso-Noori *et al.* 2021). To assess the tolerability of Endo3 CAR T-cell therapy in AT-3 tumour-bearing C57BL/6 mice, a pilot study was performed utilising doses of up to 7.5×10^6 Endo3 CAR T-cells. Figure 6.2 outlines the therapeutic strategy for evaluating Endo3 CAR T-cell therapy in AT-3 tumour-bearing mice. Briefly, 8-10 week old female C57BL/6 mice were injected subcutaneously on the flank with 2.5×10^5 AT-3 cells and tumours

were allowed to grow for 16 days to 100-200 mm³ in size. All mice were subjected to 5 Gy whole body x-ray irradiation 18 h before 2.5, 5 or 7.5 x 10⁶ Endo3 CAR T-cells or 7.5 x 10⁶ mock T-cells were injected via the tail vein. As before, mice were monitored for signs of CAR T-cell associated toxicities following T-cell injection and venous blood was collected for analysis 6 and 8 days post-T-cell injection. This experiment ended 20 days post-T-cell injection when the largest tumour reached the maximum allowable size.

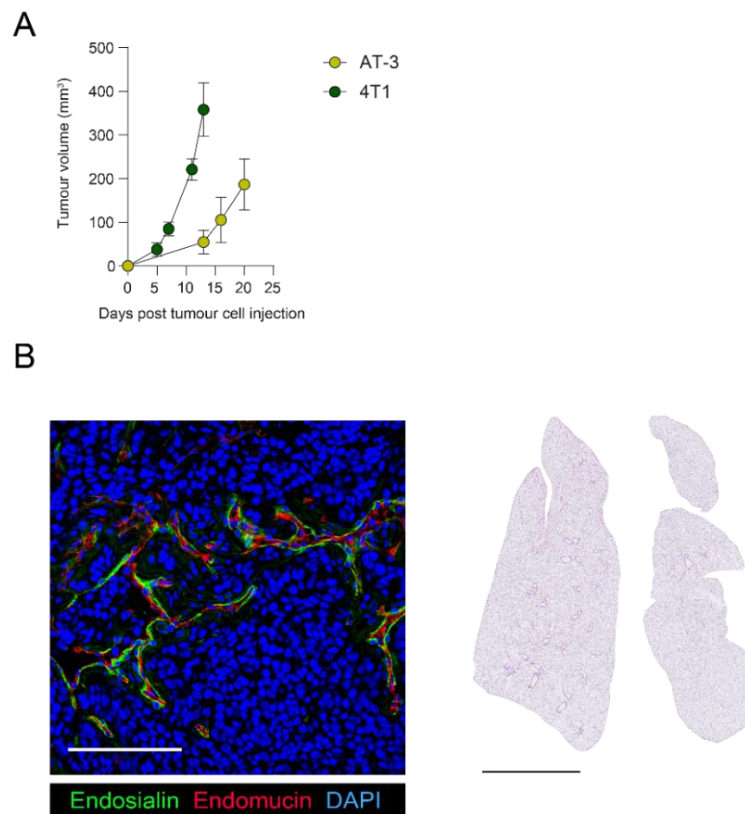


Figure 6. 1 AT-3 tumours are vascularised, endosialin-positive and have not metastasised to the lungs at 2-3 weeks post-implantation.

(A) BALB/c or C57BL/6 mice were injected subcutaneously with 2.5 x 10⁵ 4T1 or AT-3 tumour cells, respectively. Tumour growth curves for 4T1 and AT-3 tumours are shown (n=4-5 per group). Data shows mean ± SEM. **(B)** C57BL/6 mice were injected with 2.5 x 10⁵ AT-3 tumour cells and culled 16 days post-tumour cell injection. Left, representative confocal image of a formalin-fixed, paraffin-embedded (FFPE) section of an AT-3 tumour (50 mm³) stained for endosialin (green) and the endothelial cell marker endomucin (red). Nuclei were counterstained with DAPI (blue). Scale bar = 125 µm. Right, representative H&E stained lungs from the same AT-3 tumour-bearing mouse. Scale bar = 2.5 mm.

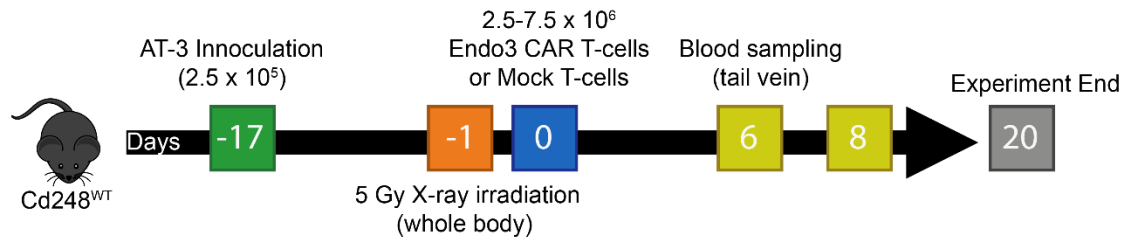


Figure 6. 2 Endo3 CAR T-cell *in vivo* therapeutic strategy for C57BL/6 mice bearing AT-3 tumours

8-10 week old endosialin wild-type (Cd248^{WT}) C57BL/6 mice were injected subcutaneously with 2.5×10^5 AT-3 cells. Tumours were allowed to grow for 16 days to 100-200 mm³ volume. All mice were subjected to 5 Gy whole body x-ray irradiation 18 h prior to injection via the tail vein with 2.5 , 5 or 7.5×10^6 Endo3 CAR T-cells ($n=1$ per group) or 7.5×10^6 mock T-cells ($n=2$). Venous blood was collected via the tail vein 6 and 8 days post-T-cell injection. Mice were culled 20 days post-T-cell injection due to tumours reaching the maximum allowable size in mock T-cell treated mice.

Sufficient volumes of blood were collected for all mice at 6 and 8 days post-T-cell injection for flow cytometry analysis of Endo3 CAR T-cell number (Figure 6.3A). In this model, Endo3 CAR T-cells do not expand, with a decrease in circulating Endo3 CAR T-cells observed 8 days post-T-cell injection when compared to 6 days post-T-cell injection in all dose groups (Figure 6.3B). This decrease in circulating CAR T-cell number is less apparent in the mouse treated with 7.5×10^6 Endo3 CAR T-cells.

Despite the lack of Endo3 CAR T-cell expansion in AT-3 tumour-bearing mice, depletion of endosialin-positive cells in the tumour stroma is still observed in mice dosed with 5 and 7.5×10^6 Endo3 CAR T-cells (Figure 6.4). In the mouse dosed with 2.5×10^6 Endo3 CAR T-cells endosialin-positive staining is comparable with that observed in the mock T-cell treated controls.

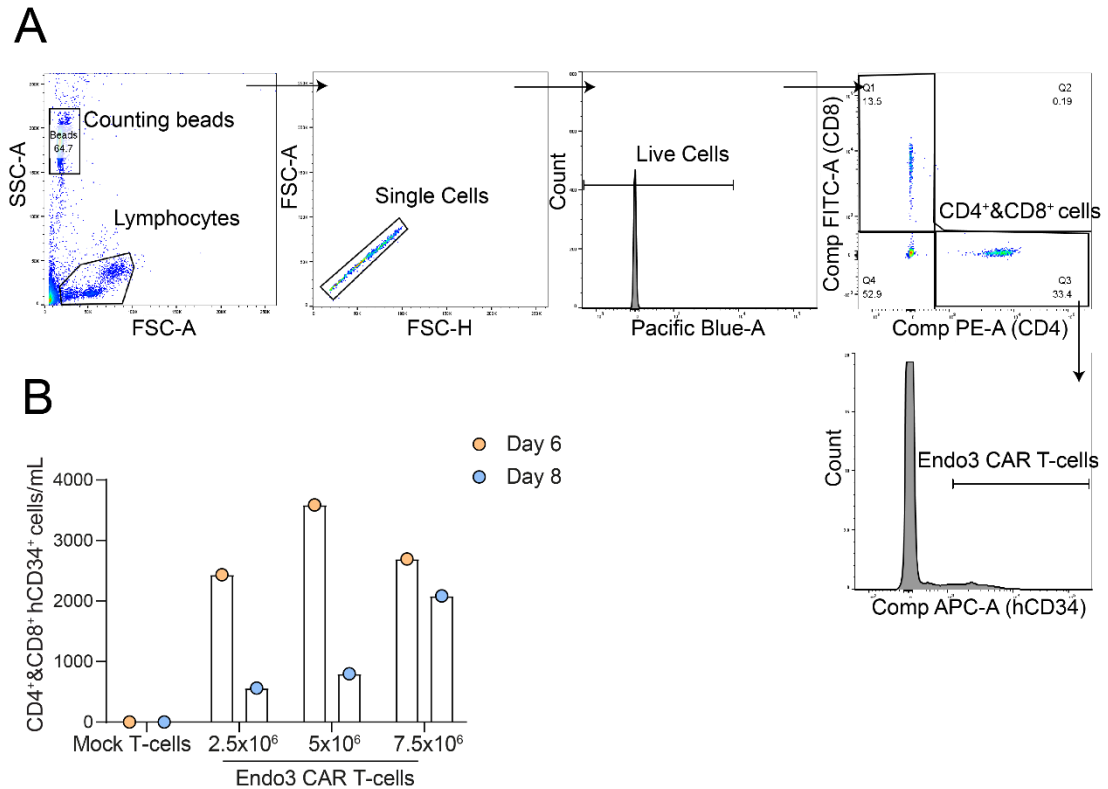


Figure 6. 3 Endo3 CAR T-cells do not expand in C57BL/6 mice

Continuation of Figure 6.2. **(A)** Gating strategy used to determine Endo3 CAR T-cell populations. Following staining with CD4, CD8 and hCD34 antibodies, FSC-A and SSC-A were used to gate out debris and non-lymphocyte populations. FSC-A and FSC-H were used to gate out doublets. DAPI was used to gate out dead cells. The resulting live, single lymphocytes were visualised in FITC (CD8) and PE (CD4) channels to identify CD8⁺ and CD4⁺ T-cell populations. CD4⁺ and CD8⁺ cells were gated together and the APC (hCD34) channel was used to identify Endo3 CAR T-cells. Mock T-cell treated controls were used to determine Endo3 CAR T-cell gates. **(B)** Number of circulating CD4⁺hCD34⁺ or CD8⁺hCD34⁺ Endo3 CAR T-cells in venous blood taken from mice 6 and 8 days post-T-cell injection. Samples from mock T-cell treated mice were used as negative controls. Each data point represents one mouse.

In this pilot study, Endo3 CAR T-cell therapy is not associated with toxicity at any dose. All Endo3 CAR T-cell treated mice maintain a healthy weight until experimental endpoint (Figure 6.5A) and no visual or behavioural signs of ill health are observed, including no observation of abnormal gallbladders upon necropsy and histology (Figure 6.5B). Because of this, the experiment was able to continue until mice reached the

defined end point dictated by the tumour size limits of our licence. In turn, this allowed extended monitoring of tumour growth and metastasis. Continuous measuring of primary tumour volumes from 1 day prior to T-cell injection demonstrates a striking reduction in growth rate in the mouse treated with 5×10^6 Endo3 CAR T-cells when compared to the two mice treated with mock T-cells (Figure 6.5C). The mouse treated with 7.5×10^6 Endo3 CAR T-cells also demonstrates a slight reduction in primary tumour growth, however this is modest compared to that observed in the mouse receiving the 5×10^6 dose. Treatment with 2.5×10^6 Endo3 CAR T-cells has no impact on primary tumour growth in this model when compared to mice treated with mock T-cells.

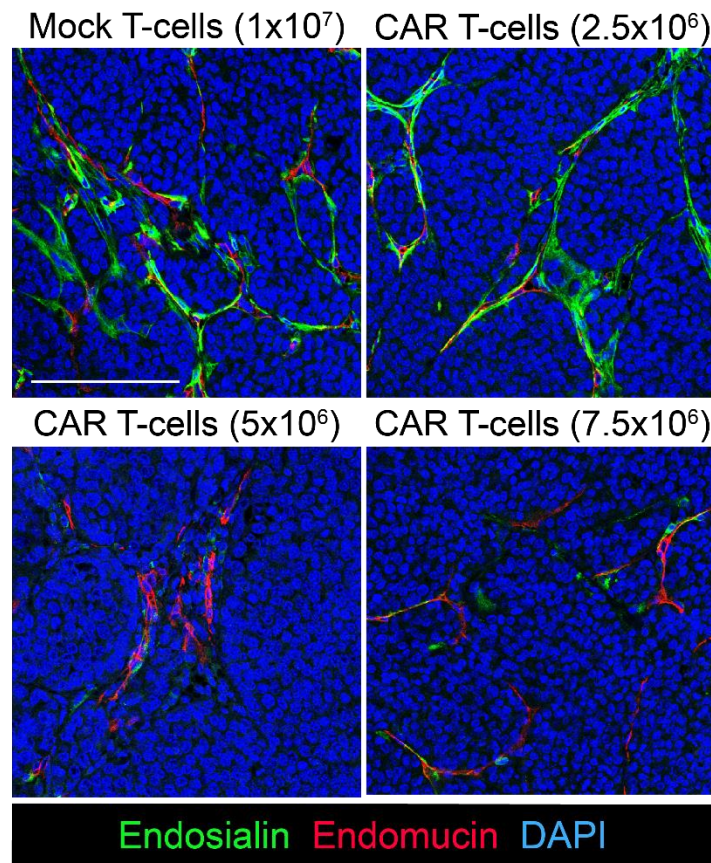


Figure 6. 4 Endo3 CAR T-cells deplete endosialin-positive cells in AT-3 tumours

Continuation of Figure 6.2. Immunostaining of AT-3 primary tumours from mock T-cell treated or Endo3 CAR T-cell treated mice at 20 days post-T-cell injection. Representative confocal immunofluorescence images of formalin-fixed, paraffin-embedded (FFPE) sections stained for endosialin (green) and the endothelial cell marker endomucin (red) are shown. Nuclei were counterstained with DAPI (blue). Scale bar = 75 μ m.

As previously, metastatic burden in the lungs was assessed by manually counting the number of metastatic deposits in H&E stained lung sections. Unexpectedly, mock T-cell treated tumours give rise to few metastatic deposits in the lungs, despite both mock T-cell treated control mice having large primary tumours (Figure 6.5D). The reason for this lack of metastatic burden in the control mice is unclear but may simply reflect the small numbers of animals in the experiment and the inherent variability of tumour growth and metastasis. Quantification of metastatic deposits in the lungs of mice treated with Endo3 CAR T-cells reveals a pattern between tumour size and lung burden, as would be expected, with the mice dosed with 2.5, 5 and 7.5 x 10⁶ Endo3 CAR T-cells having 13, 0 and 1 metastatic deposits, respectively.

As a dose of 7.5 x 10⁶ Endo3 CAR T-cells is tolerated, results in the smallest decrease in circulating CAR T-cells from 6-8 days post-T-cell injection and depletion of endosialin-expressing cells is observed in the AT-3 tumour treated with this dose, all further C57BL/6 studies were dosed with 7.5 x 10⁶ Endo3 CAR T-cells.

6.2.2 Endo3 CAR T-cells do not expand in Cd248^{WT} or Cd248^{KO} AT-3 tumour bearing C57BL/6 mice

In Chapter 3, a subpopulation of endosialin-positive AT-3 tumours cells was observed. To confirm that anti-tumour activity of Endo3 CAR T-cells against AT-3 tumours is due to stroma cell targeting and not tumour cell targeting, and to confirm the results observed in the pilot study described in Section 6.2.1, Endo3 CAR T-cell therapy was administered to Cd248^{WT} and Cd248^{KO} mice. The strategy to treat Cd248^{WT} and Cd248^{KO} mice is outlined in Figure 6.6. Briefly, 8-10 week old female C57BL/6 mice were inoculated subcutaneously on the flank with 2.5 x 10⁵ AT-3 cells or left tumour naive. Tumours were allowed to grow for 16 days to 20-100 mm³ in size. All mice were subjected to 5 Gy whole body irradiation 18 h before being injected with 7.5 x 10⁶ mock T-cells or Endo3 CAR T-cells. Venous blood was collected for analysis 3, 6 and 8 days

post-T-cell injection and mice were culled 20 days post-T-cell injection when the first tumour came close to reaching tumour size limits dictated by our licence.

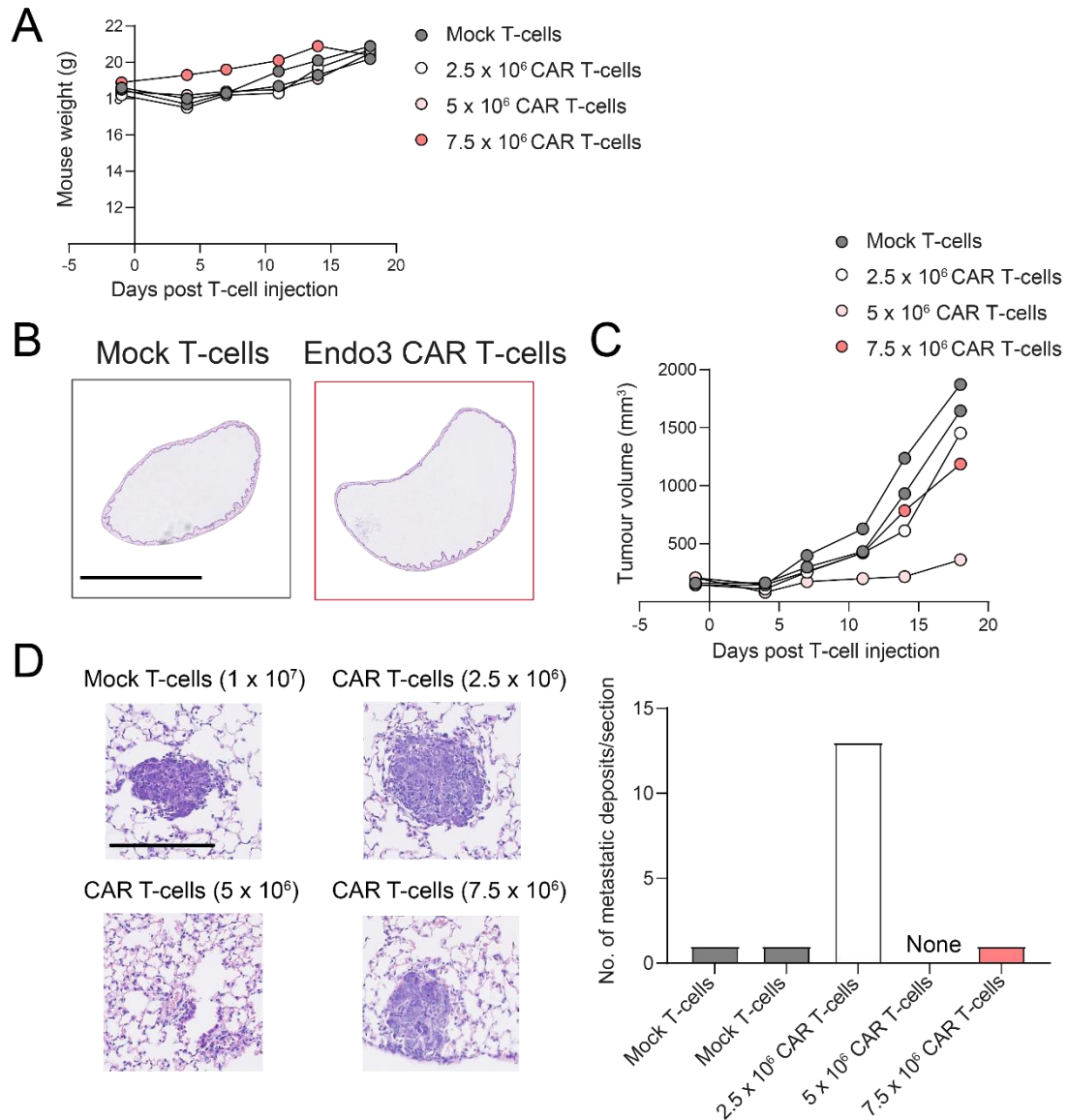


Figure 6. 5 Endo3 CAR T-cell therapy may limit tumour growth in AT-3 tumour-bearing mice without associated toxicity

Continuation of Figure 6.2. **(A)** Body weights of individual AT-3 tumour-bearing mock T-cell or Endo3 CAR T-cell treated mice. **(B)** Representative H&E stained gallbladders from mock T-cell or Endo3 CAR T-cell treated mice. Scale bar = 1 mm. **(C)** Tumour growth curves for individual mice. **(D)** Left, representative images of metastatic deposits from H&E stained lungs. Scale bar = 200 μ m. Right, quantification of spontaneous lung metastasis in mock T-cell treated or Endo3 CAR T-cell treated mice. Metastatic deposits were quantified by manually counting the number of deposits in H&E stained formalin-fixed, paraffin-embedded (FFPE) lung sections.

In all mice, whether Cd248^{WT} or Cd248^{KO}, tumour-bearing or tumour-naïve, circulating Endo3 CAR T-cell levels remain at similar levels at 3, 6 or 8 days post-T-cell injection (Figure 6.7A,B). Levels of circulating Endo3 CAR T-cells are also comparable between all groups at each time point. This suggests that Endo3 CAR T-cells persist, but do not expand in this model up to 8 days post-T-cell injection.

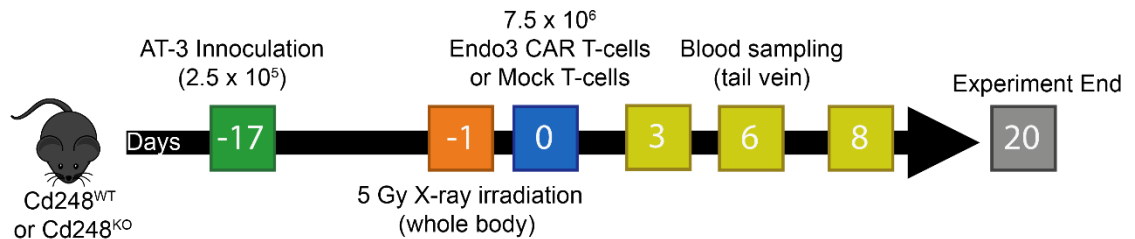


Figure 6. 6 Therapeutic strategy for treating Cd248^{WT} and Cd248^{KO} AT-3 tumour-bearing mice with Endo3 CAR T-cell therapy

8-10 week old endosialin wild-type (Cd248^{WT}) and endosialin knock-out (Cd248^{KO}) C57BL/6 mice were injected subcutaneously with 2.5×10^5 AT-3 cells or left tumour-naïve. Tumours were allowed to grow for 16 days to 20-100mm³ volume. All mice were subjected to 5 Gy whole body x-ray irradiation 18 h prior to injection via the tail vein with 7.5×10^6 mock T-cells or Endo3 CAR T-cells (Cd248^{WT} tumour-bearing n= 12; tumour-naïve, n=2. Cd248^{KO} tumour-bearing, n=4). Animals were supplied with Dietgel from day -1 until experiment termination. Venous blood was collected via the tail vein 3, 6 and 8 days post-T-cell injection. Mice were culled 20 days post-T-cell injection due to the first control tumours reaching maximum allowable size.

6.2.3 *Endo3 CAR T-cells partially deplete endosialin-expressing cells in AT-3 tumours but not in the normal tissue*

To confirm (1) whether Endo3 CAR T-cells are capable of depleting endosialin-expressing cells in the AT-3 tumour stroma and (2) the absence of endosialin-positive staining in AT-3 tumours from Cd248^{KO} mice, tumours from Cd248^{WT} or Cd248^{KO} mock T-cell treated or Endo3 CAR T-cell treated mice were immunostained for endosialin. As expected, no endosialin-positive staining is observed in AT-3 tumours from Cd248^{KO} mice, either treated with mock T-cells or Endo3 CAR T-cells. Evidence of reduced

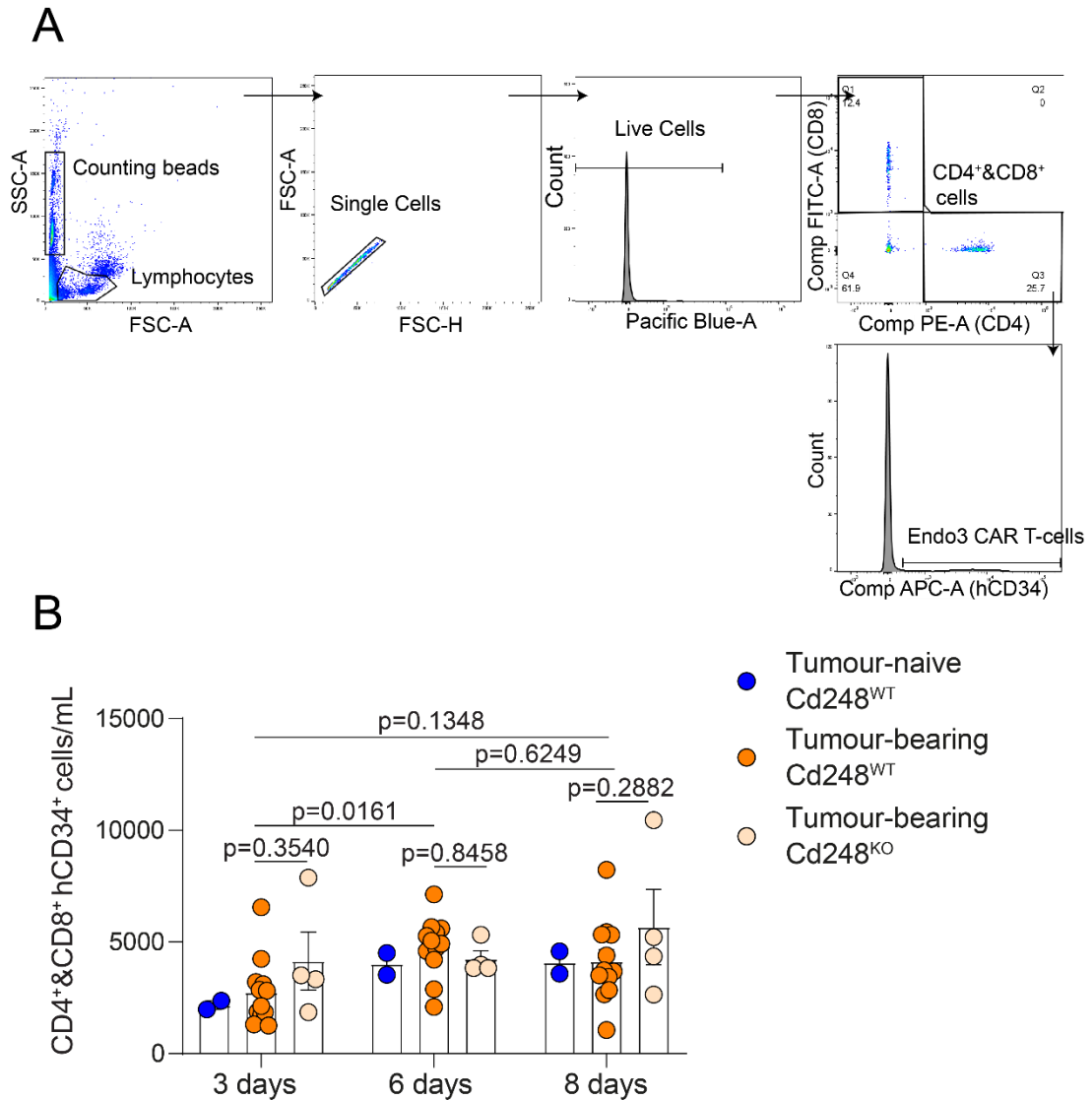


Figure 6. 7 Endo3 CAR T-cell numbers and activity in Cd248^{WT} and Cd248^{KO} AT-3 tumour-bearing mice

Continuation of Figure 6.6. **(A)** Gating strategy used to determine Endo3 CAR T-cell populations. Following staining with CD4, CD8 and hCD34 antibodies, FSC-A and SSC-A were used to gate out debris and non-lymphocyte populations. FSC-A and FSC-H were used to gate out doublets. DAPI was used to gate out dead cells. The resulting live, single lymphocytes were visualised in FITC (CD8) and PE (CD4) channels to identify CD8⁺ and CD4⁺ T-cell populations. CD4⁺ and CD8⁺ cells were gated together and the APC (hCD24) channel was used to identify Endo3 CAR T-cells. Mock T-cell treated controls were used to determine Endo3 CAR T-cell gates. **(B)** Combined number of circulating CD4⁺hCD34⁺ and CD8⁺hCD34⁺ Endo3 CAR T-cells in venous blood taken from Cd248^{WT} or Cd248^{KO}, tumour-bearing or tumour-naïve mice 3, 6 and 8 days post-T-cell injection. Samples from mock T-cell treated mice were used as negative controls. Each data point represents one mouse. Data shows mean \pm SEM. Three-way ANOVA.

endosialin-positive staining is observed in Cd248^{WT} tumours treated with Endo3 CAR T-cells when compared to Cd248^{WT} tumours treated with mock T-cells (Figure 6.8A) and quantification of the endosialin-positive area of Cd248^{WT} AT-3 tumours confirms there is a significant reduction (negating the identified outlier) in endosialin-positive staining in Endo3 CAR T-cell treated tumours (Figure 6.8B). To determine whether Endo3 CAR T-cell treatment affected the presence of endomucin-positive vessels in this model, AT-3 tumours from Cd248^{WT} mice were immunostained for endomucin and the endomucin-positive area was calculated. In this model, Endo3 CAR T-cell treated tumours do not show a decreased endomucin-positive area when compared to mock T-cell treated controls (Figure 6.8C).

As previously, the normal bladder and skin from a random subset of Cd248^{WT} tumour-bearing mice treated with mock T-cells or Endo3 CAR T-cells were collected and immunostained for endosialin as normal tissue controls. No differences in endosialin-expressing cells are observed in either bladder or skin tissue treated with Endo3 CAR T-cells when compared to those treated with mock T-cells (Figure 6.9A). This is confirmed by quantifying the endosialin-positive area of bladder tissue via colour thresholding in the green channel (Figure 6.9B).

6.2.4 Endo3 CAR T-cells limit AT-3 tumour growth in Cd248^{WT} but not Cd248^{KO} mice

To determine whether Endo3 CAR T-cell therapy has an effect on AT-3 primary tumour growth in Cd248^{WT} or Cd248^{KO} mice, tumour volumes were measured bi-weekly from the day before T-cell injection. Final tumour measurements taken on day 20 post-T-cell injection, the day of study termination, and calculated tumour growth rates reveal that Cd248^{WT} tumours treated with Endo3 CAR T-cells are significantly smaller at end point and have a significantly reduced growth rate compared to Cd248^{WT} tumours treated with mock T-cells. Importantly, no difference in AT-3 tumour size or growth rate is

observed between tumours from Cd248^{KO} mice treated with mock T-cells or Endo3 CAR T-cells (Figure 6.10A-C).

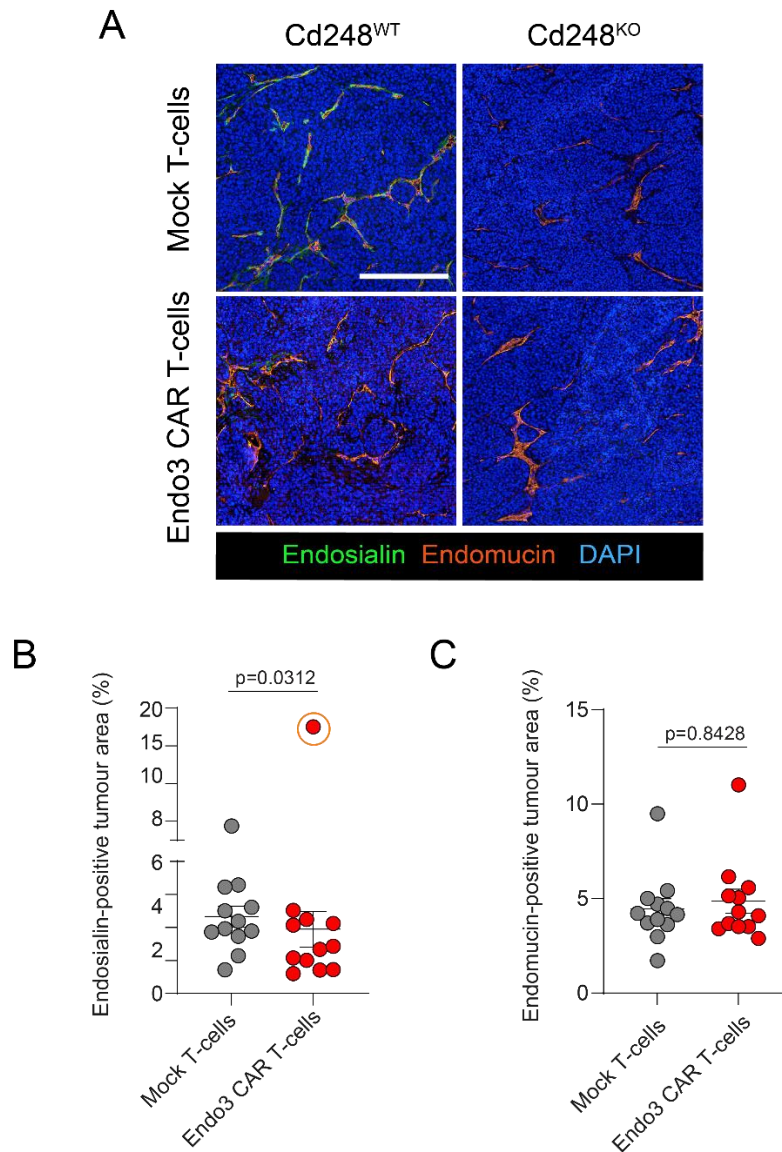


Figure 6. 8 Endo3 CAR T-cells deplete endosialin-positive cells in AT-3 tumours

Continuation of Figure 6.6. **(A)** Primary tumours from Cd248^{WT} or Cd248^{KO} mice treated with mock T-cells or Endo3 CAR T-cells were formalin-fixed, paraffin-embedded (FFPE). Tumour sections were stained for endosialin (green) and the endothelial cell marker endomucin (orange). Nuclei were counterstained with DAPI (blue). Representative confocal images are shown. Scale bar = 250 μ m. **(B)** Quantification of endosialin-positive area in AT-3 tumours treated with mock T-cell or Endo3 CAR T-cells. Data points circled in orange were identified as outliers via the ROUT method and excluded from statistical analysis. Data shows mean \pm SEM. Unpaired Student's *t*-test. **(C)** Quantification of endomucin-positive area in AT-3 tumours treated with mock T-cells or Endo3 CAR T-cells. Data shows mean \pm SEM. Unpaired Student's *t*-test.

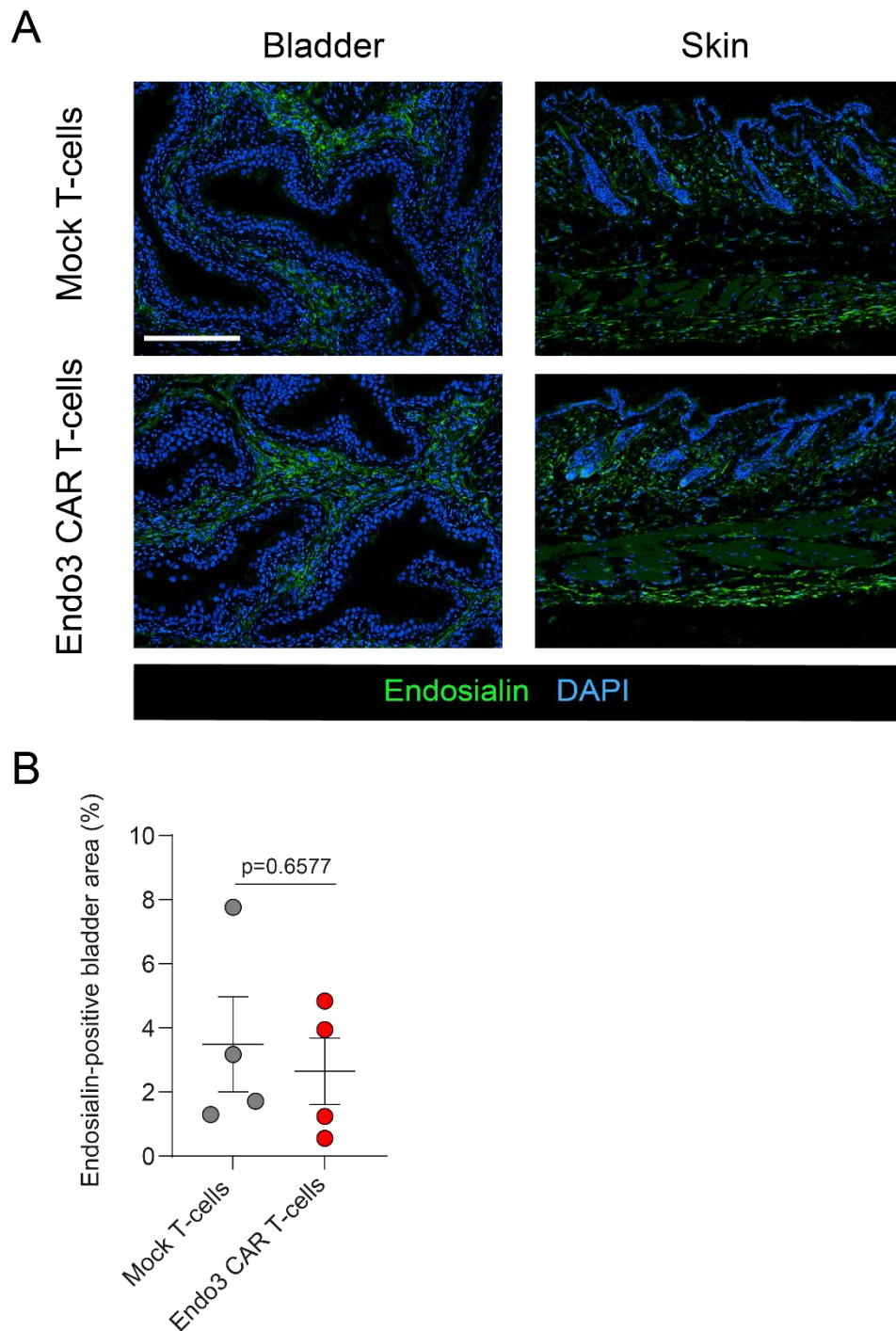


Figure 6. 9 Endo3 CAR T-cells do not deplete endosialin-positive cells in normal tissue in AT-3 tumour-bearing mice

Continuation of Figure 6.6. Bladder and skin tissue from Cd248^{WT} tumour-bearing mice treated with mock T-cells or Endo3 CAR T-cells were formalin-fixed, paraffin-embedded (FFPE). Tissue sections were stained for endosialin (green). Nuclei were counterstained with DAPI (blue). Slides were scanned on a Hamamatsu NanoZoomer. Representative images are shown. Scale bar = 250 μ m. **(B)** Quantification of endosialin-positive area in bladder tissue from AT-3 tumour-bearing mice treated with mock T-cell or Endo3 CAR T-cells. Unpaired Student's *t*-test.

Endo3 CAR T-cell treated Cd248^{WT} 4T1 tumours are significantly more necrotic than mock T-cell treated controls, as demonstrated in Chapter 5. In contrast, AT-3 tumours treated with Endo3 CAR T-cells demonstrate a trend of reduced necrosis when compared to mock T-cell treated Cd248^{WT} mice and Cd248^{KO} mice treated with mock T-cells or Endo3 CAR T-cells. No difference in primary tumour necrosis is observed between mock T-cell treated and Endo3 CAR T-cell treated Cd248^{KO} mice (Figure 6.10D).

In Chapters 4 and 5 4T1 tumour-bearing BALB/c mice treated with 2.5×10^6 Endo3 CAR T-cells were found to have pale livers with darkened and enlarged gallbladders upon necropsy. Consistent with the pilot AT-3 experiment (Figure 6.2 -6.5), this phenotype is not observed (Figure 6.10E), and no other signs of toxicity were noted.

6.2.5 Endo3 CAR T-cells do not limit AT-3 spontaneous metastasis to the lungs

To determine whether Endo3 CAR T-cell therapy is able to limit metastasis to the lung in the AT-3 model, metastatic deposits were manually quantified from H&E stained lung sections. Unexpectedly, no significant difference in the number of metastatic lung deposits is observed between Cd248^{WT} mock T-cell treated or Endo3 CAR T-cell treated mice, despite the Endo3 CAR T-cell treated tumours being smaller. Comparison of metastatic deposits in the lungs of Cd248^{KO} mice treated with mock T-cells or Endo3 CAR T-cells also reveals no significant difference (Figure 6.11)

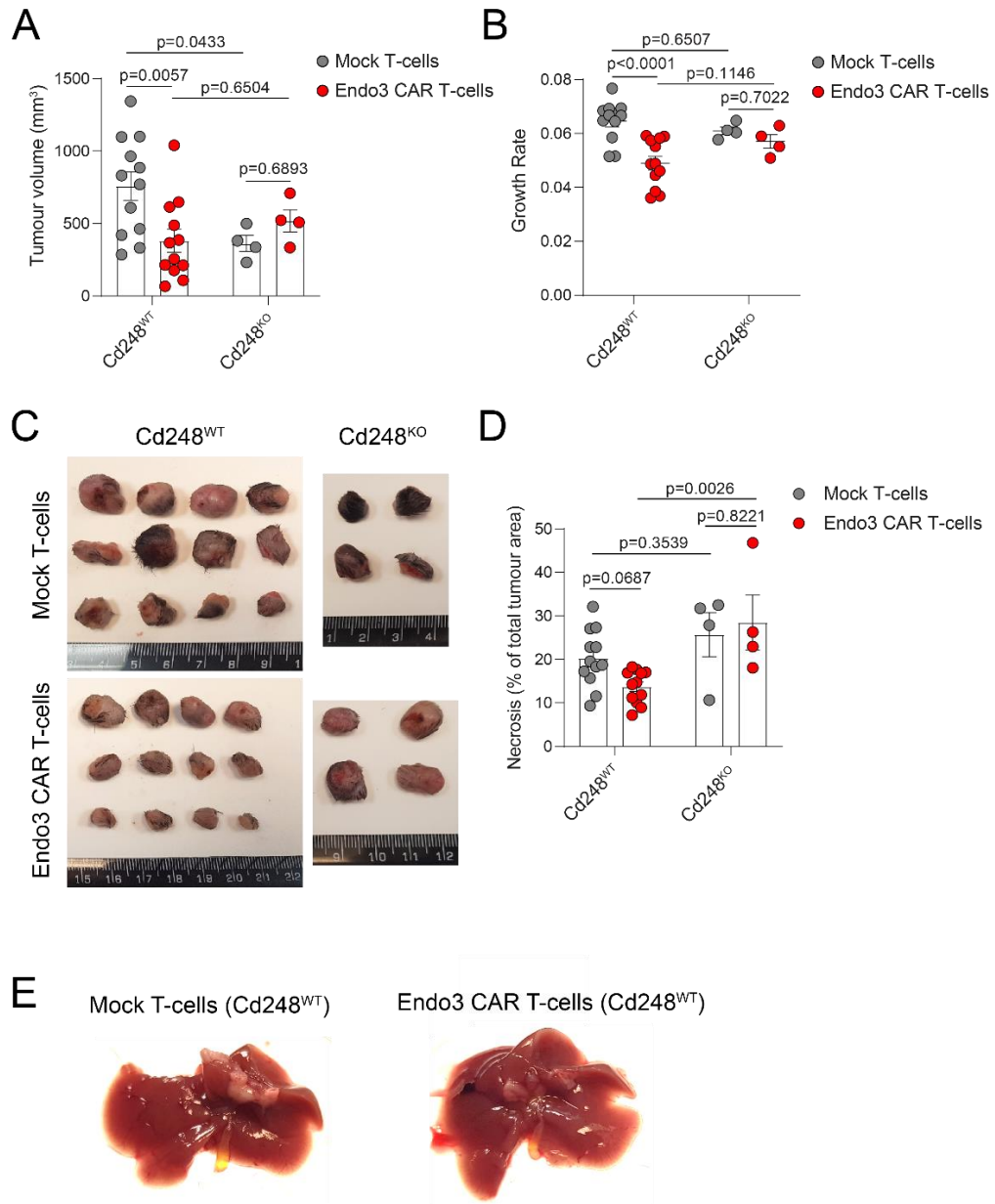


Figure 6. 10 Efficacy of Endo3 CAR T-cell therapy against AT-3 tumours in Cd248^{WT} and Cd248^{KO} mice

Continuation of Figure 6.6. **(A)** AT-3 tumour volumes taken at necropsy from Cd248^{WT} or Cd248^{KO} mice treated with mock T-cells or Endo3 CAR T-cells. Data shows mean \pm SEM. Two-way ANOVA. **(B)** AT-3 tumour growth rates for Cd248^{WT} or Cd248^{KO} mice treated with mock T-cells or Endo3 CAR T-cells. Data shows mean \pm SEM. Two-way ANOVA. **(C)** Photographs of AT-3 tumours from Cd248^{WT} or Cd248^{KO} mice treated with mock T-cells or Endo3 CAR T-cells. **(D)** Percent necrotic area of AT-3 tumours from Cd248^{WT} or Cd248^{KO} mice treated with mock T-cells or Endo3 CAR T-cells. Necrotic area was determined from H&E stained tumour sections. Data shows mean \pm SEM. Two-way ANOVA. **(E)** Representative images of liver and attached gallbladders taken at necropsy from AT-3 tumour-bearing Cd248^{WT} mock T-cell (upper) or Endo3 CAR T-cell (lower) treated mice.

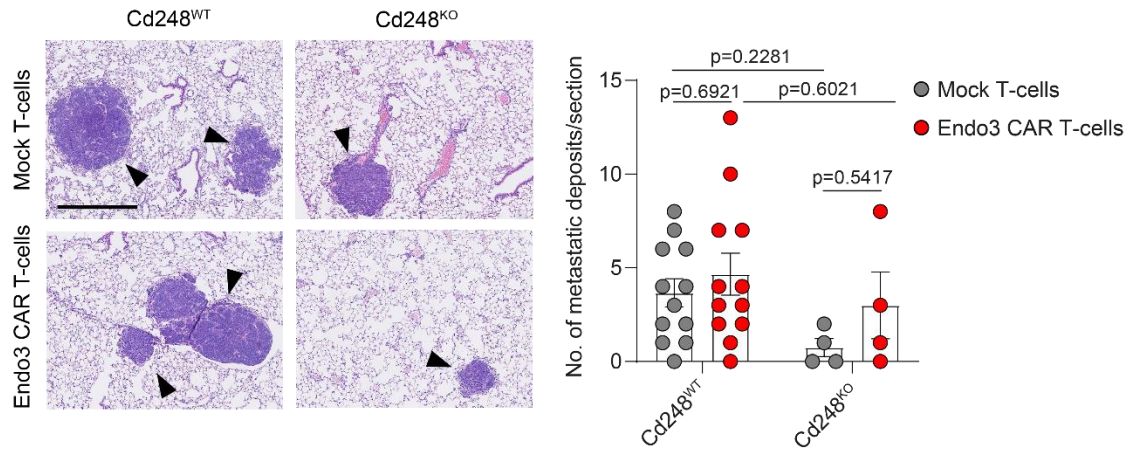


Figure 6. 11 Endo3 CAR T-cells do not limit AT-3 lung metastasis

Continuation of Figure 6.6. Left, representative H&E stained lungs, arrowheads indicate metastatic deposits. Scale bar = 500 μ m. Right, metastatic deposits were quantified by manually counting the number of deposits in H&E stained formalin-fixed, paraffin-embedded (FFPE) lung sections from Cd248^{WT} or Cd248^{KO} mice treated with mock T-cells or Endo3 CAR T-cells. Data shows mean \pm SEM. Two-way ANOVA.

6.2.6 *Endo3 CAR T-cells significantly limit spontaneous metastasis of LLC tumours to the lungs*

Our laboratory, in collaboration with others, has demonstrated that CAFs and pericytes associated with LLC tumours have upregulated endosialin expression and spontaneous metastasis of these tumours to the lungs is significantly limited by genetic deletion of endosialin (Viski *et al.* 2016). Therefore, to investigate whether Endo3 CAR T-cell therapy can limit the spontaneous metastasis of LLC tumours, 8-10 week old female C57BL/6 were injected with 5×10^5 LLC tumour cells, as outlined in Figure 6.12. Tumours were allowed to grow for 14 days to 100-200 mm³ in size. All mice were subjected to 5 Gy whole body irradiation 18 h before being injected via the tail vein with 7.5×10^6 mock T-cells or Endo3 CAR T-cells. A subset of mice were culled on day 0 to examine the primary tumour and lungs at the point of T-cell injection. Venous blood was collected for analysis 6 and 8 days post-T-cell injection and mice were culled 13 days

post-T-cell injection due to tumour ulceration and ill health of multiple animals in both groups.

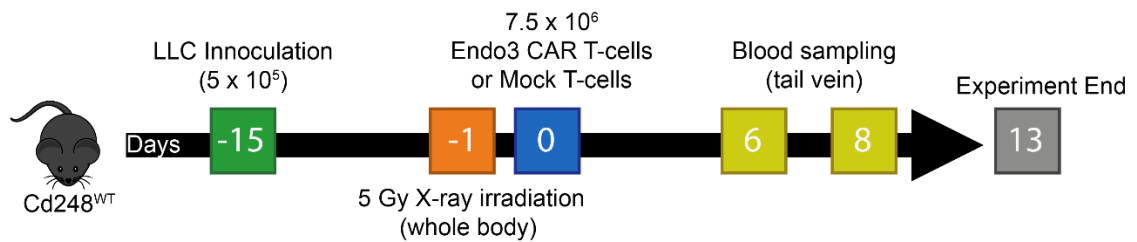


Figure 6. 12 Therapeutic strategy for treating LLC tumour-bearing mice with Endo3 CAR T-cell therapy

8-10 week old endosialin wild-type (Cd248^{WT}) C57BL/6 mice were injected subcutaneously with 5 x 10⁵ LLC cells. Tumours were allowed to grow for 14 days to 100-200mm³ volume. All mice were subjected to 5 Gy whole body x-ray irradiation 18 h prior to injection via the tail vein with 7.5 x 10⁶ mock T-cells or Endo3 CAR T-cells (n=12 per group). Animals were supplied with Dietgel from day -1 until experiment termination. A subset of mice were culled on day 0 to examine primary tumour and lung phenotypes. Venous blood was collected via the tail vein 6 and 8 days post-T-cell injection. Mice were culled 13 days post-T-cell injection due to tumour ulceration in both groups (see text).

Immunostaining of LLC tumours grown for 15 days for endosialin and endomucin confirms the presence of endosialin-positive cells and an established vascular network at the time of T-cell injection (Figure 6.13, left) and examination of H&E stained lungs taken from the same mouse reveals an absence of lung metastasis at this time point (Figure 6.13, right). As observed in Section 6.1.2 with AT-3 tumour-bearing mice, Endo3 CAR T-cells do not expand in LLC tumour-bearing mice from 6 to 8 days post-T-cell injection (Figure 6.14A). No difference in final tumour weight or tumour growth rate is observed between mock T-cell and Endo3 CAR T-cell treated LLC tumours (Figure 6.14B-D). As expected, no abnormal liver or gallbladder phenotype is observed upon necropsy of mock T-cell treated and Endo3 CAR T-cell treated mice (Figure 6.14E). Despite the lack of Endo3 CAR T-cell associated toxicity, multiple mice in both groups developed signs of ill health (malaise, hunching, piloerection) after T-cell injection, with

2 and 3 mice being culled early in the mock T-cell treated and Endo3 CAR T-cell groups, respectively (not included in analysis). It appears that this ill health may be associated with ulceration of the LLC tumour.

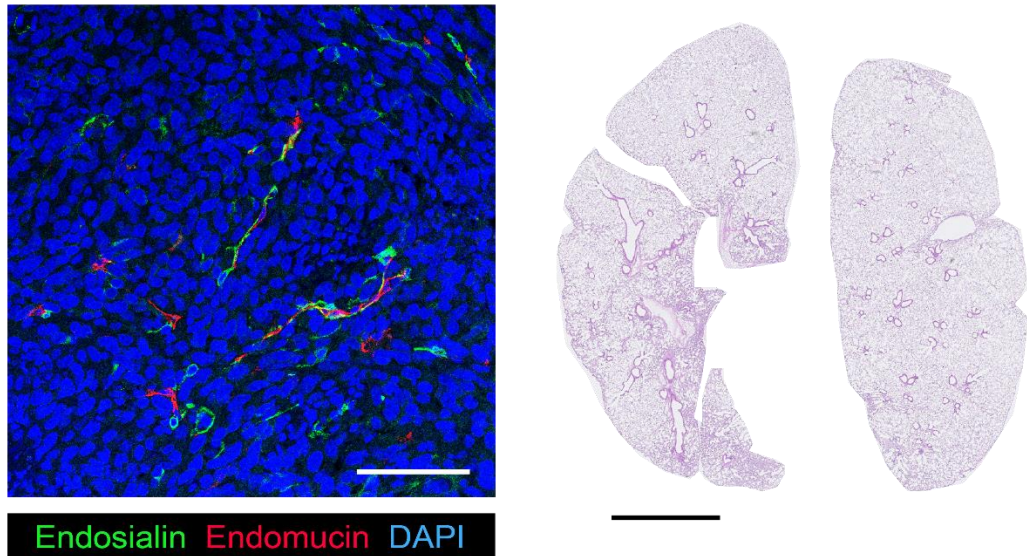


Figure 6. 13 LLC tumours are vascularised, endosialin-positive and have not metastasised to the lungs at 2 weeks post-implantation.

Continuation of Figure 6.12. **(A)** C57BL/6 mice were injected with 5×10^5 LLC tumour cells and culled 15 days post-tumour cell injection. Left, representative confocal image of a formalin-fixed, paraffin-embedded (FFPE) section of an LLC tumour (167 mm^3) stained for endosialin (green) and the endothelial cell marker endomucin (red). Nuclei were counterstained with DAPI (blue). Scale bar = $100 \mu\text{m}$. Right, representative H&E stained lungs from the same LLC tumour-bearing mouse. Scale bar = 2.5 mm .

Metastatic deposits were manually quantified from H&E stained lungs sections. Interestingly, the number of metastatic deposits in the lungs is significantly decreased in Endo3 CAR T-cell treated mice when compared to mock T-cell treated mice (Figure 6.15).

The analysis of this experiment remains ongoing at the time of thesis submission, including endosialin immunostaining of primary tumours and normal tissues.

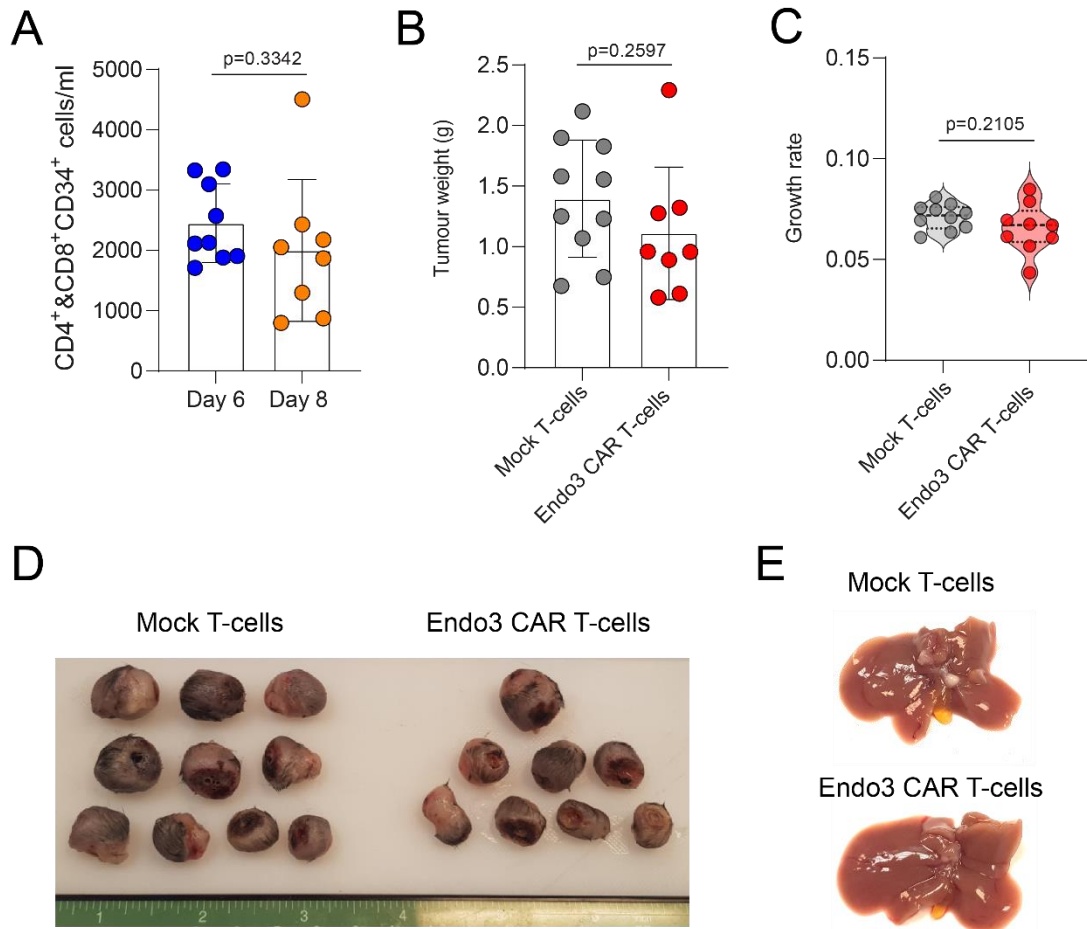


Figure 6.14 Endo3 CAR T-cell numbers and activity in LLC tumour-bearing mice

Continuation of Figure 6.12. **(A)** Number of circulating CD4⁺hCD34⁺ and CD8⁺hCD34⁺ Endo3 CAR T-cells in venous blood taken 6 and 8 days post-T-cell injection from Endo3 CAR T-cell treated mice. Samples from mock T-cell treated mice were used as negative controls. Each data point represents one mouse. Data shows mean ± SEM. Unpaired Student's *t*-test. **(B)** LLC tumour weights taken at necropsy from mice treated with mock T-cells or Endo3 CAR T-cells. Data shows mean ± SEM. Unpaired Student's *t*-test. **(C)** LLC tumour growth rates from mice treated with mock T-cells or Endo3 CAR T-cells. Data shows mean ± SEM. Unpaired Student's *t*-test. **(D)** Photographs of LLC tumours from mice treated with mock T-cells or Endo3 CAR T-cells. **(E)** Representative images of liver and attached gallbladders taken at necropsy from LLC tumour-bearing, mock T-cell treated (upper) and Endo3 CAR T-cell treated (lower) mice.

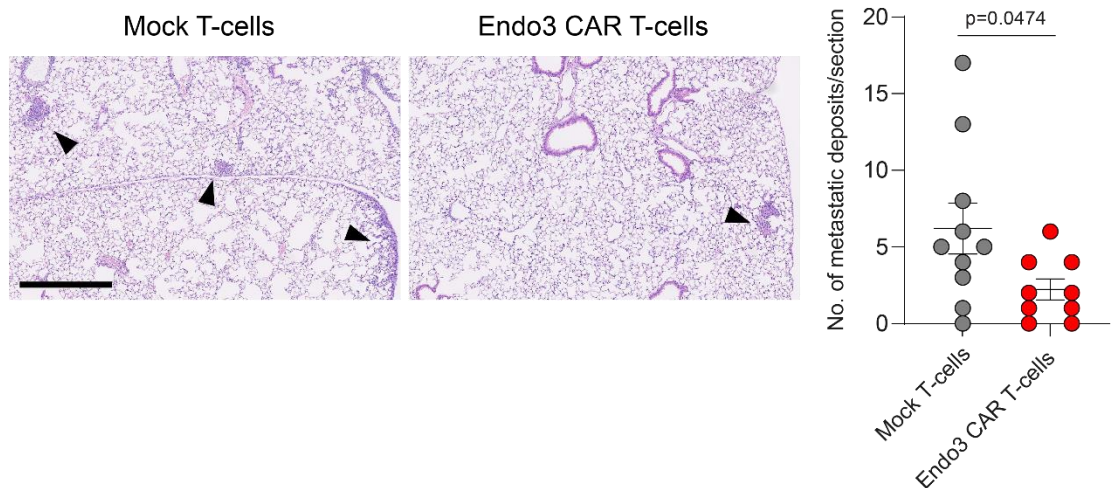


Figure 6. 15 Endo3 CAR T-cells limit metastasis of LLC tumour cells to the lungs

Continuation of Figure 6.12. Left, representative H&E stained lungs, arrowheads indicate metastatic deposits. Scale bar = 500 μ m. Right, metastatic deposits were quantified by manually counting the number of deposits in H&E stained formalin-fixed, paraffin-embedded (FFPE) lung sections from mice treated with mock T-cells or Endo3 CAR T-cells. Data shows mean \pm SEM. Unpaired Student's *t*-test.

6.3 Discussion

6.3.1 *Endo3 CAR T-cells are not toxic in C57BL/6 mice at doses of up to 7.5×10^6 CAR T-cells*

Second generation CAR T-cell products have been safely delivered to C57BL/6 mice bearing various subcutaneous tumours at doses of up to 1×10^7 CAR T-cells (Chen *et al.* 2019; Rodriguez-Garcia *et al.* 2021; Rousso-Noori *et al.* 2021). In line with these reports, Endo3 CAR T-cell doses of up to 7.5×10^6 CAR T-cells are well tolerated in AT-3 and LLC tumour-bearing mice. Tumour-bearing C57BL/6 mice treated with Endo3 CAR T-cells maintain a healthy weight post-T-cell injection, unlike 4T1-tumour bearing mice who lose weight continually following Endo3 CAR T-cell injection. Importantly, no targeting of normal tissues containing endosialin-positive cells is evident even at the

highest dose of 7.5×10^6 Endo3 CAR T-cells. This suggests that Endo3 CAR T-cells do not act in an on-target/off-tumour manner.

Interestingly, Endo3 CAR T-cells do not expand from 6 to 8 days post-T-cell injection in either AT-3 or LLC tumour-bearing C57BL/6 mice. This is in contrast to the significant expansion observed during these time points in 4T1 tumour-bearing BALB/c mice (see Chapters 4 and 5). The reason for this discrepancy between mouse strains is currently unclear, however it may be due to immunological differences between BALB/c and C57BL/6 mice. The key immunological difference between BALB/c and C57BL/6 mice is the innate immune response, with T-cells from C57BL/6 and BALB/c mice preferentially mediating a Th1 and Th2 response, respectively (Mills *et al.* 2000). BALB/c mice also tend to have stronger humoral responses than C57BL/6 mice (Guyach *et al.* 2009).

BALB/c mice have been found to have impaired bacterial clearance following cecal-ligation puncture when compared to C57BL/6 mice, which was accompanied by enhanced systemic inflammation and a significantly decreased survival rate (Watanabe *et al.* 2004). As discussed in Chapter 5.3.3, cecal-ligation puncture in mice can result in sepsis and a similarly darkened, enlarged gallbladder phenotype as observed following Endo3 CAR T-cell therapy in BALB/c mice (Drummond *et al.* 2012a). It is unlikely that Endo3 CAR T-cell therapy results in sepsis by damaging intestinal tissue owing to the lack of endosialin-positive cell targeting in the normal tissue. However, it may be that the endogenous immune response to Endo3 CAR T-cell therapy in BALB/c mice produces greater levels of systemic inflammation than in C57BL/6 mice, resulting in greater toxicity. Alternatively, differences in the endogenous immune systems of BALB/c and C57BL/6 mice may result in composition differences of their respective Endo3 CAR T-cell products. This will be explored in the next Chapter.

6.3.2 *Endo3 CAR T-cells limit AT-3 primary tumour growth but not metastasis to the lung*

In Chapters 4 and 5, we demonstrated a mild effect of Endo3 CAR-T cell treatment on 4T1 primary tumour growth that was not reproducibly significant between experiments, with CAR-T-cells eliciting other effects on the primary tumour such as increasing necrosis and reducing endothelial cell staining in the remaining viable tumour tissue. In contrast, in both the pilot and larger scale AT-3 tumour studies described in this Chapter, administration of Endo3 CAR T-cell therapy results in a significantly reduced growth rate of AT-3 tumours in Cd248^{WT} mice when compared to those treated with mock T-cells at doses of 5×10^6 Endo3 CAR T-cells or higher. Further, AT-3 tumours from Cd248^{WT} mice demonstrate a trend of reduced necrosis and no difference in endothelial staining when compared to mock T-cell controls, despite a significant reduction in endosialin-positive staining. The discrepancy in primary tumour phenotype between 4T1 and AT-3 tumours following Endo3 CAR T-cell therapy is currently unknown and requires further investigation. However, one explanation may be differences in tumour architecture. As discussed in Chapter 3, AT-3 tumours have a well-organised vascular network with many large vessels surrounding tumour cell nests whereas 4T1 tumours have a more disorganised vascular network with more microvessels within the tumour core characteristic of a chaotic network. It may be that depleting endosialin-positive cells has a greater effect on the stability of smaller, less established blood vessels, which in turn results in oxygen deprivation and necrosis of the tumour tissue. In tumours with larger, well-organised vessels, depletion of endosialin-positive cells may be sufficient to perturb the efficiency of the vascular network, resulting in slowed tumour growth, but not to cause vascular collapse and necrosis in the tumour tissue.

An alternative hypothesis is that the lack of Endo3 CAR T-cell expansion in AT-3 tumour-bearing mice results in a transient effect on the primary tumour that is not sustained sufficiently enough to cause continued disruption to the primary tumour vasculature. Examining the number of Endo3 CAR T-cells reaching and persisting in the primary tumour model may aid in elucidating the differences in Endo3 CAR T-cell activity against 4T1 and AT-3 tumours. Unfortunately, as Endo3 CAR T-cells do not incorporate a tag that can be imaged *in vivo*, nor has a suitable antibody for visualising the truncated form of hCD34 co-expressed by Endo3 CAR T-cells in FFPE sections been identified, it was not possible to examine the location of Endo3 CAR T-cells post-injection. It is possible, however, to identify Endo3 CAR T-cells via flow cytometry analysis so future work may look at dissociating tumour tissue from 4T1 and AT-3 tumours at multiple time points post-T-cell injection to examine Endo3 CAR T-cell infiltration density by flow cytometry. In both 4T1 and AT-3 tumour-bearing mice, evidence of slowed primary tumour growth becomes apparent between 5-8 days post-T-cell injection. Flow cytometry analysis of dissociated tumour tissue over time would also allow for examination of how long it takes for Endo3 CAR T-cells to reach the tumour after infusion and whether this sits within the 5-8 days post-T-cell injection window.

In Chapter 3 immunostaining and western blotting of AT-3 tumour cells revealed a small subset of endosialin-positive AT-3 cells. To ensure that the efficacy of Endo3 CAR T-cells against AT-3 tumours is due to stromal cell targeting and not targeting of this tumour cell subset, AT-3 tumour-bearing Cd248^{KO} mice were also treated with mock T-cells or Endo3 CAR T-cells. No differences in AT-3 tumour growth rate are observed between mock T-cell treated and Endo3 CAR T-cell treated Cd248^{KO} mice. This agrees with data reported in 4T1 tumour-bearing Cd248^{KO} mice and demonstrates that Endo3 CAR T-cell efficacy is indeed associated with activity against stromal cell populations.

In contrast to results reported in 4T1 tumour-bearing mice, Endo3 CAR T-cell therapy did not limit the spontaneous metastasis of AT-3 tumours to the lungs in Cd248^{WT}

mice. This is a surprising result considering the significant effect on AT-3 primary tumour growth. As Endo3 CAR T-cell therapy did not result in increased necrosis or reduced endothelial cell staining in Cd248^{WT} AT-3 tumours, it is likely that the absence of difference in spontaneous metastasis to the lungs can be attributed to an insufficient effect on the vascular network. Although a reduction in endosialin-positive staining is observed in Cd248^{WT} Endo3 CAR T-cell treated tumours, Endo3 CAR T-cells do not expand in this model and thus likely exhibit a short term effect on the primary tumour. Future work may investigate greater or multiple doses of Endo3 CAR T-cells in this model.

6.3.3 Endo3 CAR T-cells do not limit LLC primary tumour growth but suppress metastasis to the lung

Previous reports have identified endosialin as an upregulated protein in the stroma of a wide variety of solid tumours, such as glioblastoma, lung cancer and colorectal cancer (Nanda *et al.* 2006; Simonavicius *et al.* 2008; Viski *et al.* 2016). To determine whether Endo3 CAR T-cell therapy could be used to target other cancer types, the LLC mouse lung cancer model was utilised. The same therapeutic strategy was applied to LLC tumours as was applied to AT-3 tumours, with a dose of 7.5×10^6 Endo3 CAR T-cells being delivered. In contrast to results obtained from the AT-3 model, Endo3 CAR T-cell therapy results in only modest slowing of LLC primary tumour growth, however a significant decrease in lung metastasis is observed. This is likely due to architectural differences in the vascular network of LLC tumours when compared to AT-3 tumours. The LLC tumour vasculature is similar to that observed in 4T1 tumours (Viski *et al.* 2016) which may explain why a significant reduction in lung metastasis is observed in this model. However, the Endo3 CAR T-cell associated reduction in LLC lung metastasis is less striking than that observed in the 4T1-BALB/c model. Endo3 CAR T-cells do not expand in LLC tumour-bearing mice from 6 to 8 days post-T-cell injection,

thus it may be that Endo3 CAR T-cells initially deplete endosialin-positive cells and limit metastatic spread, however as Endo3 CAR T-cell numbers begin to decrease this effect is lessened. In contrast, Endo3 CAR T-cells do expand in 4T1 tumour-bearing mice and these mice are sacrificed at an earlier time point due to toxicity. Together, these factors may explain why a more striking reduction in metastatic disease is observed in Endo3 CAR T-cell treated mice bearing 4T1 tumours. Therefore, a better Endo3 CAR T-cell treatment strategy in LLC tumour-bearing mice may be to deliver multiple doses over a number of days.

Alternatively, like the differences in toxicity, the differences in efficacy against metastatic disease in LLC tumour bearing-mice compared to 4T1 tumour-bearing mice may also be due to differences in the composition of the BALB/c and C57BL/6 CAR T-cell product. This will be discussed in the next Chapter.

At the time of writing, the analysis of the LLC study remains ongoing. It will be important to investigate the presence of endosialin-positive cells in mock T-cell and Endo3 CAR T-cell treated LLC tumours from this experiment to confirm the observed difference in lung metastasis is due to endosialin-targeting. Further, it will be interesting to compare the endosialin-positive area in Endo3 CAR T-cell treated LLC tumours with Endo3 CAR T-cell treated AT-3 and 4T1 tumours. Endo3 CAR T-cell treated 4T1 tumours exhibited a greater reduction in endosialin-positive area when compared to mock T-cell controls than Endo3 CAR T-cell treated AT-3 tumours. As the efficacy against LLC tumour metastasis was a middle-ground between that observed in 4T1 tumours and AT-3 tumours, it will be interesting to see whether this is also true of the endosialin-positive area post-therapy.

Chapter 7 Comparing BALB/c and C57BL/6 derived Endo3 CAR T-cells

7.1 Introduction

In Chapters 4 and 5 Endo3 CAR T-cell therapy was associated with fatal toxicity in 4T1 tumour-bearing BALB/c mice. However, conversely, in Chapter 6 treatment with Endo3 CAR T-cells did not result in toxicity in AT-3 or LLC tumour-bearing C57BL/6 mice. The reasons for this strain dependent difference in toxicity are unclear. In Chapter 5, strategies to alleviate Endo3 CAR T-cell toxicity in tumour-bearing BALB/c mice, including anti-IL-6R treatment and multi-dosing at lower CAR T-cell numbers, were unsuccessful. Therefore, examining the differences between BALB/c and C57BL/6 mice may provide useful insights into the cause of Endo3 CAR T-cell associated toxicity.

Immunologically, C57BL/6 and BALB/c mice are quite different. It has previously been reported that C57BL/6 and BALB/c mice preferentially mediate a Th1 and Th2 innate immune response, respectively and that BALB/c mice may have stronger humoral responses than C57BL/6 mice (Mills *et al.* 2000; Guyach *et al.* 2009). Therefore, Endo3 CAR T-cell toxicity observed in tumour-bearing BALB/c mice may be due to immunological differences in the BALB/c Endo3 CAR T-cell product, differences in the interaction of the endogenous immune system with Endo3 CAR T-cells in BALB/c mice, or a combination of both.

This Chapter will examine the composition and behaviour of Endo3 CAR T-cells derived from BALB/c or C57BL/6 splenocytes, including comparison of their function against 4T1 tumours in immunodeficient mice.

7.2 Results

7.2.1 *CD4⁺:CD8⁺ T-cell ratio in BALB/c and C57BL/6 derived Endo3 CAR T-cells*

It has been reported that mouse CD4⁺ and CD8⁺ CAR T-cells function differently *in vivo* (Kägi *et al.* 1994; Stalder *et al.* 1994), therefore the CD4⁺:CD8⁺ ratio of BALB/c and C57BL/6 Endo3 CAR T-cells was analysed via flow cytometry. Interestingly, BALB/c Endo3 CAR T-cells have a CD4⁺:CD8⁺ ratio of ~75:25% (Figure 7.1A), whereas C57BL/6 Endo3 CAR T-cells have the opposite CD4⁺:CD8⁺ ratio of ~25:75% (Figure 7.1B).

7.2.2 *BALB/c derived Endo3 CAR T-cells show delayed killing in vitro*

In Chapter 4, *in vitro* co-culture experiments demonstrated that Endo3 CAR T-cells activate and kill target cells in an endosialin-specific manner. T-cell activation assays in Chapter 4 were analysed at 24 h post-T-cell addition and it was noted that BALB/c derived Endo3 CAR T-cells release less IFN- γ than C57BL/6 derived Endo3 CAR T-cells after 24 h of co-culture. Therefore, to determine whether BALB/c Endo3 CAR T-cells exhibit delayed cytotoxicity when compared to C57BL/6 Endo3 CAR T-cells, BALB/c or C57BL/6 mock T-cells or Endo3 CAR T-cells were co-cultured with endosialin-positive mouse 10T $\frac{1}{2}$ cells for 24 or 84 h at various effector:target ratios. After 24 h of co-culture, C57BL/6 Endo3 CAR T-cells exhibit significant cytotoxicity against 10T $\frac{1}{2}$ cells when compared to mock T-cells (Figure 7.2A). In contrast, BALB/c Endo3 CAR T-cells are not cytotoxic to 10T $\frac{1}{2}$ cells after 24 h of co-culture (Figure 7.2B). However, if co-culture is extended to 84 h, BALB/c Endo3 CAR T-cells exhibit significant cytotoxicity against 10T $\frac{1}{2}$ cells when compared to mock T-cells (Figure 7.2C). These data suggest that BALB/c derived Endo3 CAR T-cells have a delayed cytotoxic response to endosialin expressing cells.

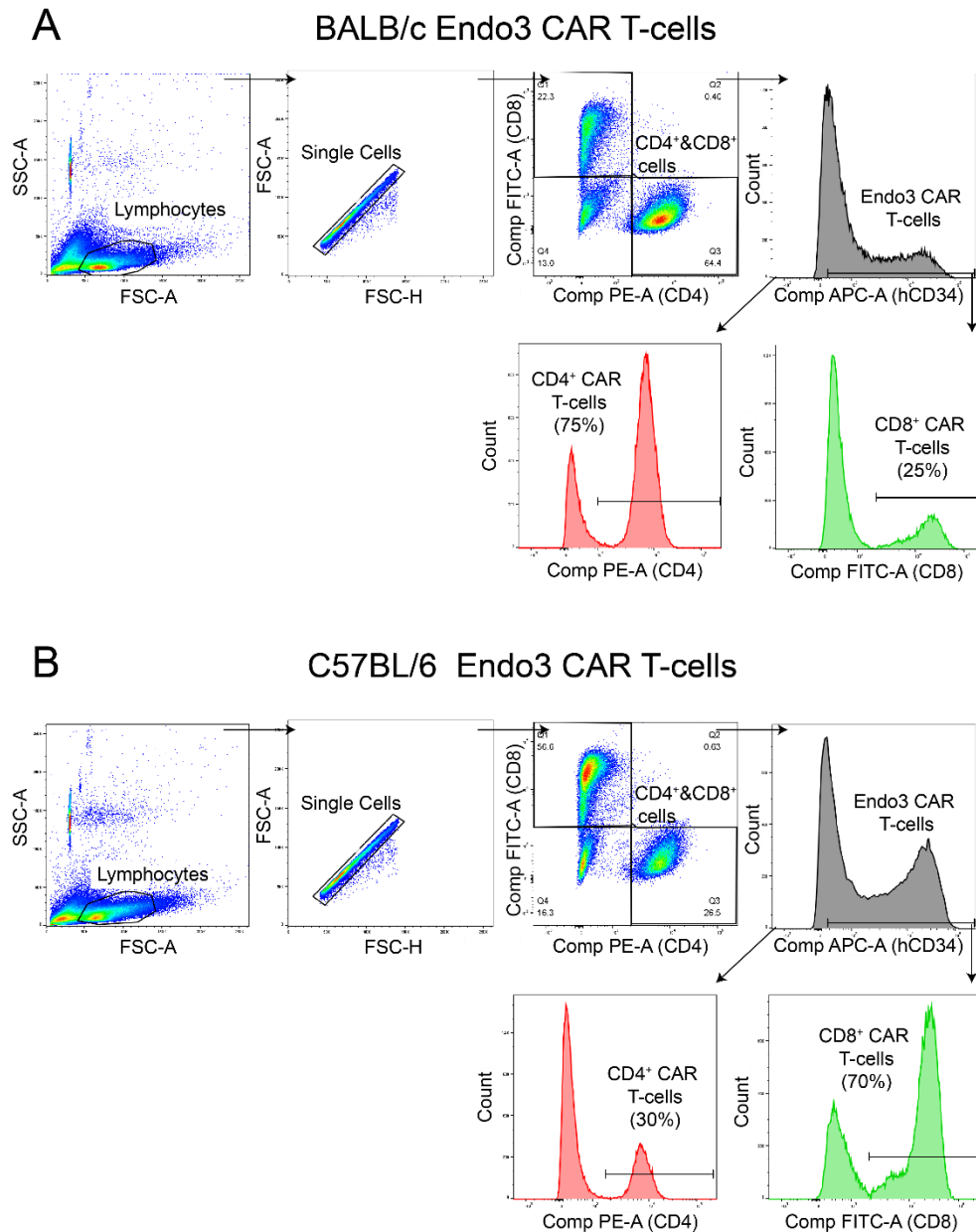


Figure 7. 1 BALB/c and C57BL/6 derived Endo3 CAR T-cells have different CD4⁺:CD8⁺ ratios

Gating strategy used to determine CD4⁺ and CD8⁺ Endo3 CAR T-cell populations in **(A)** BALB/c and **(B)** C57BL/6 derived Endo3 CAR T-cells. Following staining with CD4, CD8 and hCD34 antibodies, FSC-A and SSC-A were used to gate out debris and non-lymphocyte populations. FSC-A and FSC-H were used to gate out doublets. The resulting single lymphocytes were visualised in FITC (CD8) and PE (CD4) channels to identify CD8⁺ and CD4⁺ T-cell populations. CD4⁺ and CD8⁺ cells were gated together and the APC (hCD34) channel was used to identify Endo3 CAR T-cells. Mock T-cell treated controls were used to determine Endo3 CAR T-cell gates. Endo3 CAR T-cells were then inspected in the PE (CD4) or FITC (CD8) channels separately to obtain a CD4⁺ and CD8⁺ population percentage.

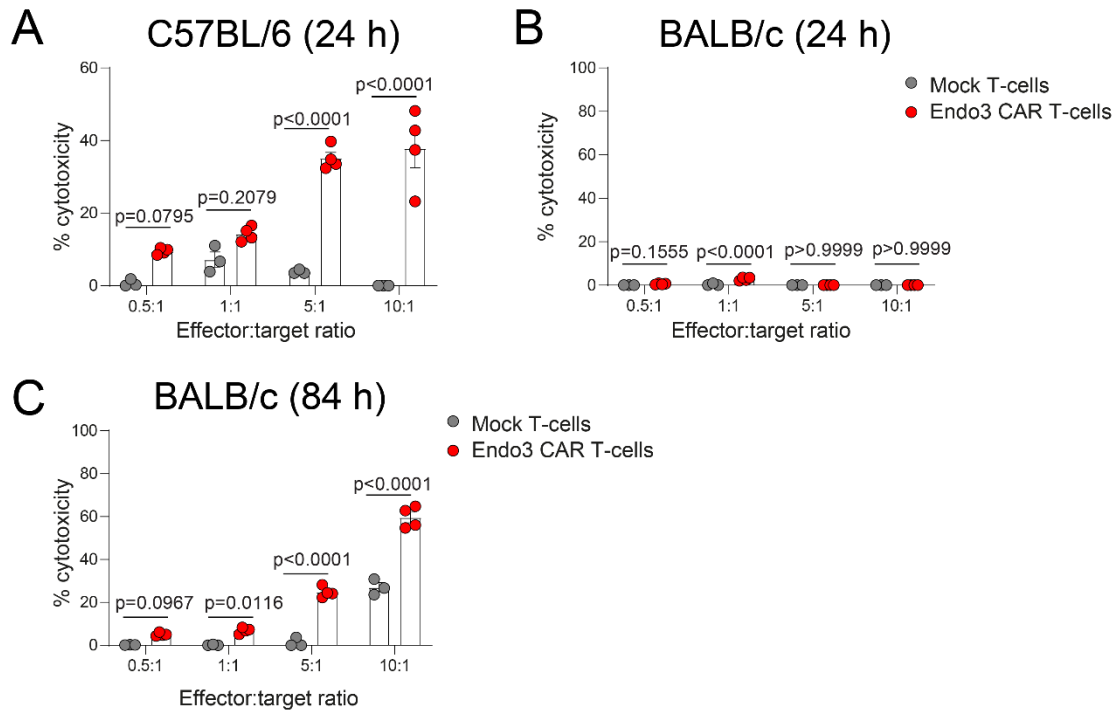


Figure 7. 2 BALB/c and C57BL/6 derived Endo3 CAR T-cell cytotoxicity

Mouse 10T $\frac{1}{2}$ pericyte-like cells were seeded at 2000 cells per well in 96-well plates and mock T-cells or Endo3 CAR T-cells were added after 24 h. After a further 24 h (**A,B**) or 84 h (**C**) of co-culture, cytotoxicity was determined using the Cytotox 96 non-radioactive cytotoxicity assay. Data shows mean \pm SEM. Two-way ANOVA.

7.2.3 C57BL/6 Endo3 CAR T-cells limit 4T1 metastasis, whereas BALB/c Endo3 CAR T-cells are non-toxic but display no efficacy in NSG mice

To establish whether 4T1 tumours grow and metastasise at comparable rates in NSG and BALB/c mice, 2.5×10^5 4T1 tumour cells were injected into NSG or BALB/c mice subcutaneously on the flank. 4T1 tumours grew more rapidly in NSG mice when compared to BALB/c mice, reaching the desirable size range for T-cell injection of 100-200 mm³ approximately 10 days post-tumour cell injection (Figure 7.3A). Examination of 4T1 tumours at 13 days post-T-cell injection, the day 0 time point for BALB/c Endo3 CAR T-cell experiments, reveals a comparable endosialin staining pattern to that observed in 4T1 tumours from BALB/c mice (Figure 7.3B, left). However, H&E staining of lungs taken

from 4T1 tumour-bearing NSG mice 13 days post-T-cell injection reveals small micrometastases at this time point (Figure 7.3B, right). Therefore, it was decided that NSG mice bearing 4T1 tumours would be treated with Endo3 CAR T-cells after 10 days of tumour growth, when the primary tumour size is comparable to that observed in BALB/c mice and to reduce the likelihood of micrometastases being present in the lungs at the time of T-cell injection.

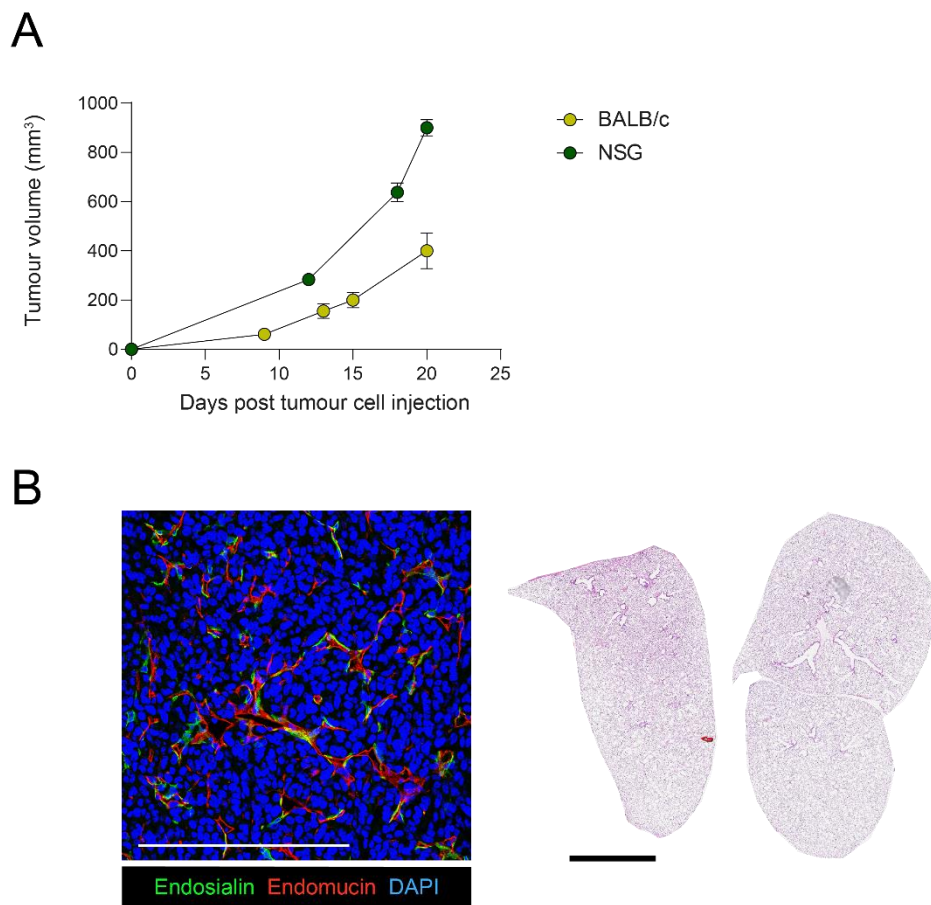


Figure 7. 3 4T1 tumours grow and metastasise more rapidly in NSG mice

(A) BALB/c or NSG mice were injected subcutaneously with 2.5×10^5 4T1. Tumour growth curves for 4T1 tumours are shown ($n=5-6$ per group). Data shows mean \pm SEM. **(B)** NSG mice were injected with 2.5×10^5 4T1 tumour cells and culled 13 days post-tumour cell injection. Left, representative confocal image of a formalin-fixed, paraffin-embedded (FFPE) section of a 4T1 tumour (331 mm^3) stained for endosialin (green) and the endothelial cell marker endomucin (red). Nuclei were counterstained with DAPI (blue). Scale bar = $250 \mu\text{m}$. Right, representative H&E stained lungs from the same 4T1 tumour-bearing NSG mouse. Scale bar = 2.5 mm .

To compare the efficacy of BALB/c and C57BL/6 derived Endo3 CAR T-cells *in vivo*, 4T1 tumours were established in NSG mice by injecting 2.5×10^5 tumour cells subcutaneously on the flank, as outlined in Figure 7.4. As NSG mice are immunodeficient, mice were not irradiated prior to T-cell injection. 10 days after 4T1 inoculation, mice were injected via the tail vein with 2.5×10^6 BALB/c or C57BL/6 derived Endo3 CAR or mock T-cells. Mice were provided with Dietgel from day -1 to study termination. Venous blood was collected for analysis 6 and 8 days post-T-cell injection and mice were sacrificed 12 or 16 days post-T-cell injection. All mice were sacrificed due to tumour size or evidence of lung burden.

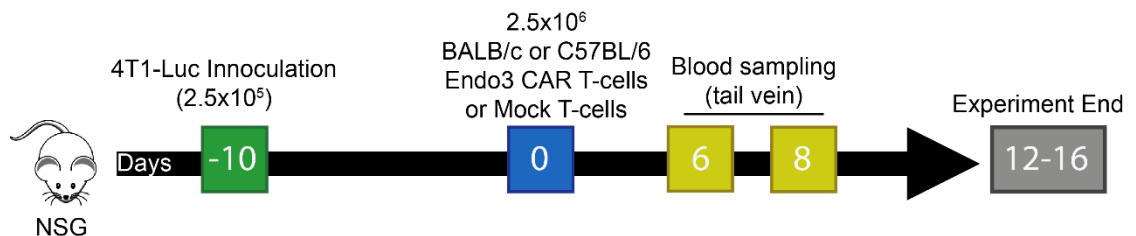


Figure 7. 4 *In vivo* therapeutic strategy for comparing BALB/c and C57BL/6 derived Endo3 CAR T-cells simultaneously

8-10 week old NOD scid gamma (NSG) mice were injected subcutaneously with 2.5×10^5 4T1-Luc cells. Tumours were allowed to grow for 13 days to 100-200 mm³ in volume. Mice were injected via the tail vein with 2.5×10^6 BALB/c or C57BL/6 derived mock T-cells (BALB/c derived n=3, C57BL/6 derived n=3) or Endo3 CAR T-cells (BALB/c derived n=6, C57BL/6 derived n=6). Mice were supplied with Dietgel from day -1 to study termination. Venous blood was collected on day 6 and 8 post-T-cell injection and mice were culled 12 or 16 days post-T-cell injection due to tumour size or lung burden.

No differences in primary tumour growth are observed between mock T-cell or Endo3 CAR T-cell treated mice whether derived from BALB/c or C57BL/6 T-cells (Figure 7.5A,B). Analysis of venous blood collected 6 and 8 days post-T-cell injection reveals a comparable number of circulating Endo3 CAR T-cells in mice injected with BALB/c or C57BL/6 Endo3 CAR T-cells at both time points. A trend for expansion between day 6 and 8 post-T-cell injection is observed in both BALB/c and C57BL/6 Endo3 CAR T-cell

treated mice, however this is not significant in those injected with either T-cell strain (Figure 7.5C). Of note, BALB/c and C57BL/6 Endo3 CAR T-cells remain majority CD4⁺ (CD4⁺:CD8⁺ = 75.3:24.7%) and CD8⁺ (CD4⁺:CD8⁺ ratio= 24.6:75.4%), respectively (Figure 7.5D). Importantly, no evidence of Endo3 CAR T-cell associated toxicity is observed in any animal, with all mice being culled due to tumour or metastatic burden and no abnormalities in liver or gallbladder appearance upon necropsy (Figure 7.5E).

As before, tumours were immunostained for endosialin to examine the targeting of tumour-associated endosialin-positive cells. No evidence of substantial endosialin-positive cell depletion is observed by visual inspection of immunostained tumour sections (Figure 7.6A), however RTqPCR analysis of RNA isolated from FFPE tumour sections reveals a decrease in endosialin expression in C57BL/6 Endo3 CAR T-cell treated tumours, albeit insignificant when compared to mock T-cell treated controls (Figure 7.6B).

To examine spontaneous metastasis of 4T1 tumours to the lung, mice were culled at either 12 or 16 days post-T-cell injection to ensure comparable primary tumour sizes and H&E stained lung sections from mock T-cell treated, BALB/c or C57BL/6 Endo3 CAR T-cell treated mice were quantified manually (Figure 7.7A). Mock T-cell treated mice were not differentiated by strain due to imbalance in number culled at each time point. Comparison of the percentage of lung tissue occupied by metastatic disease reveals a significant decrease in lung metastatic burden between mock T-cell treated mice and C57BL/6, but not BALB/c, Endo3 CAR T-cell treated mice (Figure 7.7B, left). To determine whether this difference was due to a lower number of deposits or smaller metastases, indicative of reduced dissemination to the lungs and targeting of the deposits at the secondary site, respectively, the number of metastatic deposits per section were counted manually and the average deposit area was determined. A significant reduction in the number of deposits is observed in C57BL/6 Endo3 CAR T-cell treated mice when compared to mock T-cell treated mice. Again, no difference is

observed when comparing BALB/c Endo3 CAR T-cell treated mice to mock T-cell treated mice (Figure 7.7B, centre). In contrast, the average metastatic deposit area is not significantly different between mock T-cell and C57BL/6 Endo3 CAR T-cell treated mice, nor between mock T-cell and BALB/c Endo3 CAR T-cell treated mice (Figure 7.7B, right).

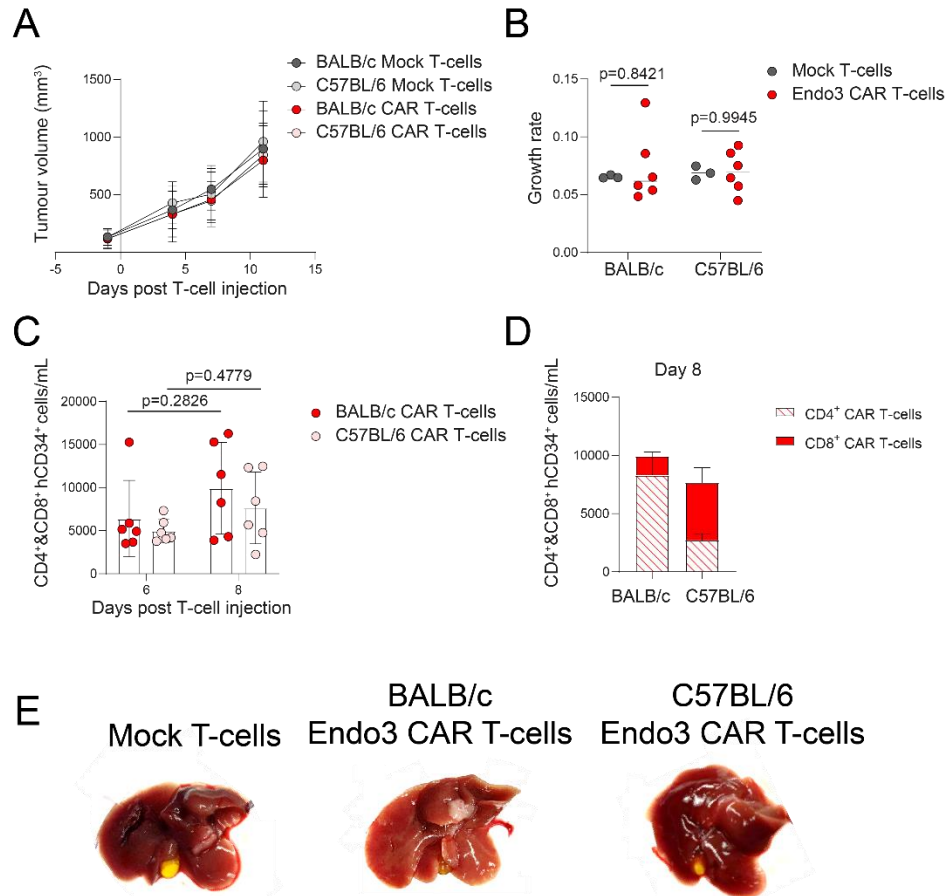


Figure 7. 5 No toxicity or efficacy against 4T1 tumours is observed in NSG mice treated with BALB/c or C57BL/6 derived Endo3 CAR T-cells

Continuation of Figure 7.4. **(A)** Tumour growth curves for mice treated with BALB/c or C57BL/6 derived mock T-cells or Endo3 CAR T-cells. Data shows mean \pm SEM. **(B)** 4T1 tumour growth rates for NSG mice treated with BALB/c or C57BL/6 derived mock T-cells or Endo3 CAR T-cells. Data shows mean \pm SEM. Two-way ANOVA. **(C)** Combined number of circulating CD4⁺hCD34⁺ and CD8⁺hCD34⁺ Endo3 CAR T-cells in venous blood taken 6 and 8 days post-T-cell injection. Samples from mock T-cell treated mice were used as negative controls. Each data point represents one mouse. Data shows mean \pm SEM. Two-way ANOVA. **(D)** Breakdown of CD4⁺ and CD8⁺ Endo3 CAR T-cells detected in the circulation of NSG mice treated with BALB/c or C57BL/6 derived Endo3 CAR T-cells. Data shows mean \pm SEM. **(E)** Representative images of liver and attached gallbladders taken at necropsy from NSG mice treated with mock T-cells, BALB/c derived Endo3 CAR T-cells or C57BL/6 derived Endo3 CAR T-cells.

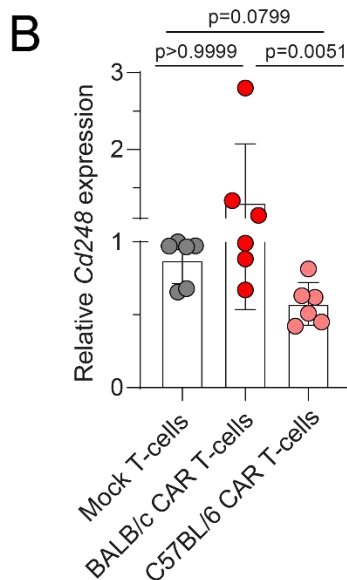
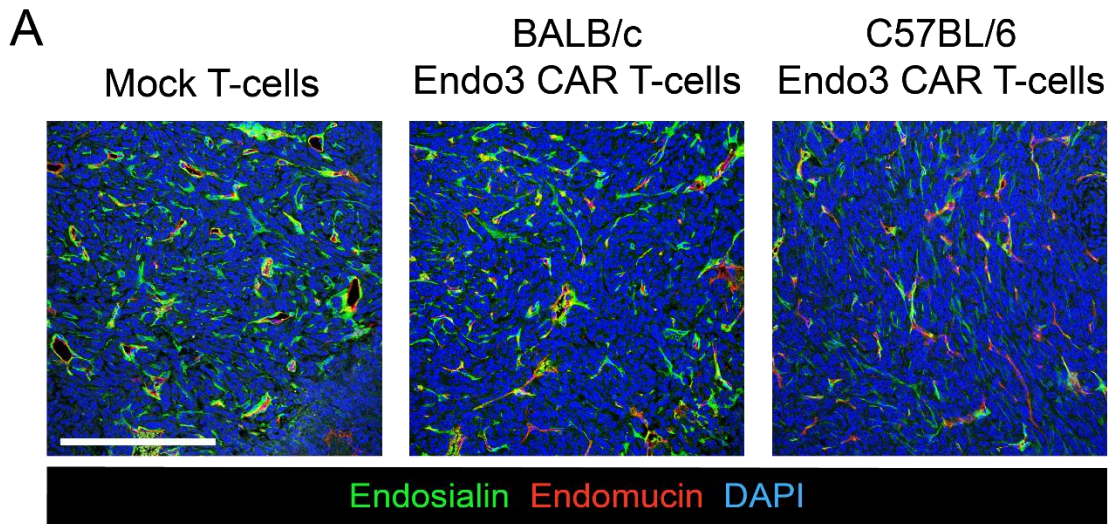


Figure 7. 6 C57BL/6 derived Endo3 CAR T-cells may deplete endosialin-positive cells more effectively than BALB/c derived Endo3 CAR T-cells in NSG mice

Continuation of Figure 7.4. **(A)** 4T1 tumours from NSG mice treated with mock T-cells, BALB/c derived Endo3 CAR T-cells or C57BL/6 derived Endo3 CAR T-cells were formalin-fixed, paraffin-embedded (FFPE). Tissue sections were stained for endosialin (green) and endomucin (red). Nuclei were counterstained with DAPI (blue). Slides were scanned on a Hamamatsu NanoZoomer. Representative images are shown. Scale bar = 250 μ m. **(B)** RNA was isolated from FFPE sections of 4T1 tumours treated with mock T-cells, BALB/c derived Endo3 CAR T-cells or C57BL/6 derived Endo3 CAR T-cells. Relative *Cd248* expression was determined by qPCR analysis. *Ubc* was used to normalise *Cd248* values. Data shows mean \pm SEM. One-way ANOVA.

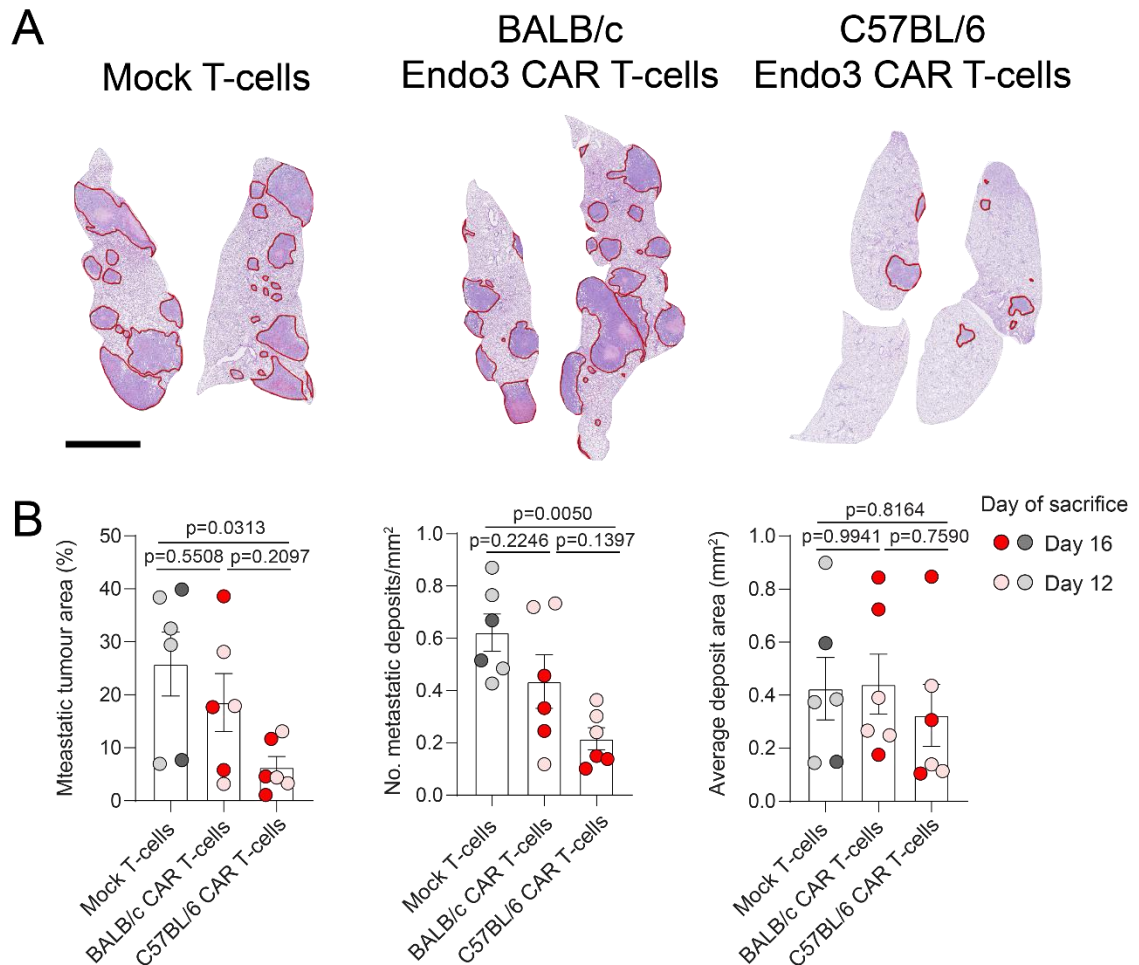


Figure 7. 7 C57BL/6 derived Endo3 CAR T-cells limit 4T1 lung metastasis but BALB/c derived Endo3 CAR T-cells have no effect in NSG mice

Continuation of Figure 7.4. **(A)** Representative H&E stained lungs taken from mock T-cell, BALB/c derived Endo3 CAR T-cell or C57BL/6 derived Endo3 CAR T-cell treated 4T1 tumour bearing mice culled 16 days post-T-cell injection. Red outlines indicate metastatic deposits. Scale bar = 2.5 mm. **(B)** Mice were sacrificed either 12 or 16 days post-T-cell injection to ensure comparable primary tumour sizes. Lung tumour burden was assessed by manually quantifying the percent metastatic tumour area (left), number of deposits per mm² (centre) or average deposit area (right) from H&E stained formalin-fixed, paraffin-embedded (FFPE) lung sections taken from mice treated with mock T-cells, BALB/c derived Endo3 CAR T-cells or C57BL/6 derived Endo3 CAR T-cells (n=6 per group). All mock T-cell treated mice were treated as one group. Data shows mean \pm SEM. One-way ANOVA.

7.3 Discussion

7.3.1 BALB/c and C57BL/6 Endo3 CAR T-cells behave differently *in vitro*

In Section 7.2.1, BALB/c and C57BL/6 derived Endo3 CAR T-cells were found to consist of CD4⁺ and CD8⁺ heavy T-cell populations, respectively. This is in agreement with several other studies published examining BALB/c and C57BL/6 lymphocyte populations (Chen *et al.* 2002; Pinchuk and Filipov 2008). It has previously been reported that CD4⁺ T-cells take longer to develop effector properties *in vitro* than CD8⁺ T-cells (Kaech *et al.* 2002; Hildemann *et al.* 2013). In agreement with this, co-culture of endosialin-positive 10T $\frac{1}{2}$ cells with CD8⁺ heavy C57BL/6 Endo3 CAR T-cells results in significant cytotoxicity after 24 h, however no significant cytotoxicity is observed in 10T $\frac{1}{2}$ co-cultures with CD4⁺ heavy BALB/c Endo3 CAR T-cells after 24 h. Evidence of BALB/c Endo3 CAR T-cell induced cytotoxicity is only observed after 84 h of co-culture with 10T $\frac{1}{2}$ cells.

The delay in cytotoxic activity of BALB/c Endo3 CAR T-cells may be due to differences in cytotoxic pathways utilised by CD4⁺ and CD8⁺ cytotoxic lymphocytes in the mouse system. CD4⁺ cytotoxic lymphocytes most frequently kill via the Fas/Fas ligand pathway, whereas CD8⁺ lymphocytes release perforin and granzyme molecules to kill the target cell (Kägi *et al.* 1994; Stalder *et al.* 1994). Lymphocytes are capable of storing and releasing cytotoxic granules rapidly, however low quantities of Fas Ligand are stored in lymphocytes, thus new ligand must be generated to facilitate the cytotoxic event, which is a slower process (Russell and Ley 2002).

Delayed killing by CD4⁺ Endo3 CAR T-cells may explain the differences in Endo3 CAR T-cell tolerability observed between tumour-bearing BALB/c and C57BL/6 mice. Slower target cell killing results in endosialin molecules being accessible to Endo3 CAR T-cells for longer, thus allowing for longer periods of CAR T-cell stimulation, activation

and proliferation. As a result, this may explain the higher levels of Endo3 CAR T-cell expansion observed in tumour-bearing BALB/c mice, which in turn results in greater systemic inflammation and toxicity.

7.3.2 BALB/c Endo3 CAR T-cells are non-toxic but display no efficacy in NSG mice, whereas C57BL/6 Endo3 CAR T-cells limit 4T1 metastasis

NSG mice are immunodeficient animals, with the majority of white blood cell populations being absent or defective. Because of this, NSG mice may be infused with CAR T-cells derived from any strain of mouse. 4T1 tumours were grown in NSG mice and treated with either BALB/c or C57BL/6 derived Endo3 CAR T-cells to (1) determine whether BALB/c Endo3 CAR T-cells are toxic in the absence of the endogenous immune system and (2) directly compare the efficacy of BALB/c and C57BL/6 Endo3 CAR T-cells against the same tumour model.

Interestingly, treatment with BALB/c derived Endo3 CAR T-cells did not result in expansion of the CAR-T cells to levels previously seen or toxicity in 4T1 tumour-bearing NSG mice. This suggests that the endogenous immune system in BALB/c mice is key in mediating Endo3 CAR T-cell antitumour effects and associated toxicity. In the classical immune response, CD4⁺ T-cells are helper cells that recognise antigens expressed by antigen-presenting cells and secrete cytokines to engage other immune cells and it has previously been reported that CD4⁺ CAR T-cells are more effective at stimulating the host immune system than CD8⁺ CAR T-cells (Boulch *et al.* 2021). Therefore, CD4⁺ CAR T-cells may also exhibit helper functions and stimulate other immune cells, such as dendritic cells and macrophages, to become active. NSG mice have absent or defective lymphoid cells and myeloid cells with the exception of neutrophils and monocytes, therefore, the absence of BALB/c Endo3 CAR T-cell associated expansion and toxicity in NSG mice suggests that in the syngeneic setting expansion and toxicity is driven by Endo3 CAR T-cells over-engaging with lymphoid and myeloid populations, which in turn

results in lethal systemic inflammation. Further, BALB/c mice are polarised towards a Th2 innate immune response, whereas C57BL/6 mice are polarised towards a Th1 innate immune response (Mills *et al.* 2000). Excessive Th2 response results in the overactivation of humoral immunity, including activation of mast cells, eosinophils and dendritic cells. In turn this can result in hypersensitivity which can be fatal if untreated. Therefore, BALB/c specific Endo3 CAR T-cell toxicity may be due to excessive triggering of the endogenous Th2 response.

As no toxicity is observed following treatment of tumour-bearing C57BL/6 mice with Endo3 CAR T-cells containing majority CD8⁺ CAR T-cells, it would be interesting to investigate whether selecting C57BL/6 Endo3 CAR T-cells for CD4⁺ CAR T-cells recapitulates the same toxicities observed in BALB/c mice. In the same context, selecting BALB/c Endo3 CAR T-cells for CD8⁺ CAR T-cells and assessing tolerability of this population alone in tumour-bearing BALB/c mice would be an interesting strategy to examine in future work.

Although no differences in primary tumour growth or Endo3 CAR T-cell persistence are observed in BALB/c and C57BL/6 derived Endo3 CAR T-cell treated mice, CD4:CD8 CAR T-cell ratios remain *in vivo* and C57BL/6 derived Endo3 CAR T-cells appear to be more efficacious. Spontaneous metastasis of 4T1 tumours to the lungs is significantly decreased in mice treated with C57BL/6, but not BALB/c, derived Endo3 CAR T-cells and this is due to a decrease in the number of metastatic deposits rather than decreased deposit outgrowth. Previous work by our laboratory has demonstrated that endosialin plays a role in the intravasation step of the metastatic cascade and not in extravasation and colonisation of the secondary site (Viski *et al.* 2016). This finding is supported by the fact that Endo3 CAR T-cells limit the number of metastatic deposits in the lung but not size of their outgrowth.

Interestingly, in the immunocompromised setting, no significant depletion of endosialin-positive cells is observed in 4T1 primary tumours following treatment with either BALB/c or C57BL/6 derived Endo3 CAR T-cells. However, in 4T1 tumours treated with C57BL/6 Endo3 CAR T-cells, there is a trend for decreased endosialin-expression when compared to BALB/c Endo3 CAR T-cell or mock T-cell treated 4T1 tumours. One hypothesis for this observation is that, again, BALB/c derived Endo3 CAR T-cells are limited by the absence of endogenous immune populations and thus have no effect on tumour-associated endosialin-expressing cells, whereas C57BL/6 derived Endo3 CAR T-cells are active within the primary tumour, however in the absence of the endogenous immune system are only able to exhibit a minor effect on endosialin-expressing cells, suggesting that C57BL/6 Endo3 CAR T-cells too rely on interactions with the endogenous immune system to effectively target, deplete and clear endosialin-expressing cells within the primary tumour. Alternatively, the dose of C57BL/6 derived Endo3 CAR T-cells delivered in this study may have been too low to affect primary tumour growth. In Chapter 6, pilot studies utilising C57BL/6 derived Endo3 CAR T-cells against AT-3 tumours in C57BL/6 mice demonstrated that a dose of 2.5×10^6 Endo3 CAR T-cells was not sufficient to perturb AT-3 tumour growth, but doses of 5×10^6 or higher did decrease primary tumour growth rate. For direct comparison of BALB/c and C57BL/6 derived Endo3 CAR T-cells, it was important to deliver the same dose in 4T1 tumour-bearing NSG mice, however future studies may consider treating with higher doses in this setting to determine whether this would result in greater anti-tumour efficacy of C57BL/6 derived Endo3 CAR T-cells.

The apparent loss of BALB/c Endo3 CAR T-cell efficacy in the immunodeficient setting suggests that the endogenous immune system plays an important role in mediating Endo3 CAR T-cell response in BALB/c mice. It has been reported that, although CD4⁺ CAR T-cells are more effective at stimulating the host immune response, CD8⁺ T-cells are more efficient at target cell killing (Boulch *et al.* 2021). Therefore, with

BALB/c Endo3 CAR T-cells being a majority CD4⁺ T-cell population, a bystander effect in which endogenous immune cells engage in the CAR T-cell response is required in BALB/c mice, whereas in C57BL/6 mice Endo3 CAR T-cells rely less on this same effect.

A limitation of the studies carried out in this thesis is the lack of Endo3 CAR T-cell detection *in vivo* or in *ex vivo* tissues. The Endo3 CAR construct does not include a tag that allows bioluminescent imaging and a suitable antibody for identifying Endo3 CAR T-cells via truncated human CD34 in FFPE sections was not identified during this PhD. As previously mentioned in Chapter 4.3.3, visualisation of Endo3 CAR T-cells within the primary tumour of our syngeneic models would provide further evidence that Endo3 CAR T-cells reach and attack tumour-associated endosialin-expressing cells. In the immunodeficient setting, it would be of interest to determine whether the lack of BALB/c Endo3 CAR T-cell efficacy is due to Endo3 CAR T-cells not reaching their target cells within the primary tumour, and in the same context, whether C57BL/6 Endo3 CAR T-cells demonstrate greater tumour penetration in this setting. Future work may focus on alternative methods of Endo3 CAR T-cell visualisation, such as trailing anti-hCD34 antibodies on frozen tumour sections or by dissociating primary tumours and subjecting them to flow cytometry analysis for hCD34⁺ cells. Additionally, it may be of interest to interrogate endogenous immune cell populations in our syngeneic models to gain a deeper understanding of which cells of the endogenous immune system are important bystanders to BALB/c Endo3 CAR T-cell activity.

Further investigation is warranted to determine the role of the endogenous immune system and the CAR T-cell CD4⁺:CD8⁺ ratio in BALB/c specific Endo3 CAR T-cell efficacy and associated toxicity. At the time of writing, ongoing experiments are being carried out to characterise this further.

Chapter 8 Final discussion and future directions

Advances in T-cell engineering in recent decades have facilitated research into CAR T-cell therapy for the treatment of cancers. Engineering T-cells to express a CAR construct allows the redirecting of T-cell populations against a cancer-specific antigen and CAR T-cells have the advantage of recognising the target antigen and killing the antigen expressing cell in the absence of MHC molecules, which are often not present on the surface of cancer cells. To date, only CAR T-cells directed against targets upregulated by haematological malignancies have been approved for clinical use and designing CAR T-cells that are effective against solid tumours remains a major challenge in the field at present.

As discussed in Chapter 1.4.7 various approaches to improve CAR T-cell persistence, survival and infiltration into solid tumours have been investigated. An alternative approach to improve solid tumour targeting is to target cells of the TME instead of the harder to reach tumour cells. As CAR T-cells are infused intravenously, the most accessible cells upon reaching a malignant mass are those associated with the vasculature. Endosialin is a cell surface protein that is upregulated on tumour-associated pericytes, cells that are tightly associated with the tumour vasculature, with only low levels of expression in normal healthy tissue (MacFadyen *et al.* 2005; MacFadyen *et al.* 2007; Simonavicius *et al.* 2008). Therefore, endosialin represents a novel target for CAR T-cell therapy and for targeting the tumour vasculature.

The overall objective of this PhD was to investigate the potential of endosialin-targeting CAR T-cells against the progression of solid tumours, with three overall aims. First, to characterise the specificity of endosialin-targeting Endo3 CAR T-cells *in vitro*. Data presented in this thesis demonstrate the specific activation and target cell killing of Endo3 CAR T-cells in the presence of endosialin-positive cell lines, both of mouse and human origin.

Second, to determine the safety and tolerability of Endo3 CAR T-cells *in vivo*. Administration of Endo3 CAR T-cells resulted in strain dependent Endo3 CAR T-cell associated toxicity in tumour-bearing BALB/c mice, with no toxicity observed in tumour-bearing C57BL/6 mice or non-tumour bearing mice of either strain. Further, no toxicity was observed when BALB/c Endo3 CAR T-cells were delivered to tumour-bearing immunodeficient NSG mice, suggesting a role for the endogenous immune system in BALB/c Endo3 CAR T-cell associated toxicity.

Finally, to assess the efficacy of Endo3 CAR T-cell therapy in multiple preclinical models of cancer. It was shown that treatment with Endo3 CAR T-cells resulted in a depletion of tumour-associated endosialin-expressing cells and a slowing of primary tumour growth in preclinical models of solid tumours. In tumours with a more aberrant vasculature, Endo3 CAR T-cell therapy also limited metastatic spread to the lungs.

Together, the data presented in this thesis support the hypothesis that Endo3 CAR T-cell therapy has the potential to limit solid tumour growth and metastasis by ablating tumour-associated endosialin expressing cells. Previous studies have reported conflicting results of tumour response to pericyte-ablating therapies (Xian *et al.* 2006; Cooke *et al.* 2012), however in the studies described in thesis, pericyte ablation was only associated with slowed and never accelerated tumour progression. This will be discussed further in Section 8.2.

8.1 Targeting endosialin as a novel CAR T-cell approach

The major limitation of CAR T-cell therapy for solid tumours is the arduous journey CAR T-cells face to reach the malignant cells, both in terms of physical barriers and immunosuppressive environments. Targeting cells tightly associated with the vasculature represents an approach that reduces the physical barriers to only that of the endothelial cell layer and the vascular basement membrane without needing to navigate

the immunosuppressive environment of the tumour mass. Solid tumours may be categorised broadly into 'immune hot' and 'immune cold' tumours, with the latter having little infiltration of immune cells due to the extremely immunosuppressive TME. Immune cold tumours are generally not responsive to immunotherapy (Appleton *et al.* 2021). Studies reported in this thesis demonstrate that Endo3 CAR T-cells are effective against immune cold, immune checkpoint-resistant 4T1 tumours (Mosely *et al.* 2017), which is an encouraging finding.

An additional benefit of targeting endosialin-positive cells in the TME is the relative genetic stability of these cells when compared to tumour cells. An important challenge identified clinically in patients treated with FDA approved CD19-targeting CAR T-cells is the emergence of CD19-negative subpopulations of cancer cells that escape CAR T-cell killing and result in disease progression (Grupp *et al.* 2013; Maude *et al.* 2014). As CAFs and pericytes are genetically stable compared to tumour cells, it is less likely that escape variants would emerge in response to Endo3 CAR T-cell therapy.

Previous work by our laboratory and collaborators has shown that TNBCs implanted into endosialin KO mice metastasise significantly less than those implanted into endosialin WT mice (Viski *et al.* 2016), therefore identifying endosialin as an interesting target for the prevention of TNBC metastasis. TNBCs account for approximately 15% of diagnosed breast cancers in the UK (CRUK 2022), and are typically of high grade with greater metastatic potential. Within the first 5 years of diagnosis, up to 40% of TNBC patients will relapse with metastatic disease. In a study by Kassam and colleagues, the median survival of patients with metastatic TNBC was 13.3 months (Kassam *et al.* 2009). As TNBCs are more proliferative and are often larger in size than other breast cancer subtypes, the first line of therapy is often neoadjuvant chemotherapy to reduce the size of the tumour prior to surgery. However, recent reports suggest that this neoadjuvant chemotherapy may promote metastatic dissemination (Karagiannis *et al.* 2017). Endo3 CAR T-cell therapy may offer an alternative or

compliment to neoadjuvant chemotherapy as it shows promising preclinical activity in both limiting the size of TNBCs and hindering metastatic spread. In a subset of patients with TNBC, the individual cannot have surgery due to other health conditions preventing them from receiving anaesthesia. The prognosis for these patients is worse than those with operable TNBC and thus Endo3 CAR T-cell therapy may present an interesting option for controlling tumour growth and limiting metastatic spread in these patients. Additional advantages of CAR T-cell therapy over conventional chemotherapy include the short duration of inpatient care required for delivery and monitoring and the fact that they are a 'living drug' capable of persisting in the body long term. Studies have reported detectable CAR T-cells in the body up to 130 days post-infusion (Kochenderfer *et al.* 2012). Therefore, Endo3 CAR T-cells may be capable of attacking relapses in patients if they also contain endosialin-positive cells. This is an area that requires further exploration to gain knowledge and understanding of the specific long term benefits of Endo3 CAR T-cell therapy.

Endosialin is also upregulated in the stroma of less superficial cancers that require much more invasive and risky surgery. One such example is lung cancer, which can involve the removal of an entire lung in severe cases. Further, metastatic lung cancer has a 5 year survival rate of <5% (CRUK 2022). Treatment of mice bearing subcutaneous LLC lung tumours with Endo3 CAR T-cells resulted in a modest reduction in LLC tumour growth but a significant reduction in metastasis to the lungs. The dose of 7.5×10^6 Endo3 CAR T-cells was well tolerated in this model and thus higher doses, or multiple doses given over time, may be considered going forward to further improve this efficacy. As survival rates associated with secondary lung cancer are poor, Endo3 CAR T-cell therapy represents a promising therapy for the prevention of lung cancer metastasis.

Simultaneously to the work carried out in this thesis, groups at the Ludwig Institute for Cancer Research in Lausanne, Switzerland were also examining the potential of endosialin-targeting CAR T-cell therapy. A recent study published by Fierle

and colleagues described the investigation of three second generation (CD28 containing) endosialin-targeting CAR T-cells with scFv components differing to the 3K2L scFv utilised in Endo3 CAR T-cells (Fierle *et al.* 2021). In this study, CAR T-cells were successfully transduced into human T-cells, however all three CAR T-cells showed only modest activity *in vitro*. Co-culture of each of these endosialin-targeting CAR T-cells with human endosialin-positive cells lines resulted in a supernatant IFN- γ concentration of <10,000 pg/mL, as determined by IFN- γ ELISA assays. In this thesis, where significant target cell death was observed, co-culture of mouse Endo3 CAR T-cells with mouse endosialin-positive cells resulted in IFN- γ concentrations up to 6-fold higher than those reported by Fierle and colleagues. Further, work done by our collaborators has demonstrated that human Endo3 CAR T-cells co-cultured with human endosialin-positive cells release between 30-40,000 pg/mL into the supernatant (Lee Laboratory, unpublished data). This suggests that Endo3 CAR T-cells are more efficiently activated than those reported by Fierle and colleagues, however no *in vivo* data was reported so it is not possible to compare how this translates to anti-tumour efficacy. CAR T-cell efficacy may be affected by the structure and affinity of the scFv used in the CAR construct (Fujiwara *et al.* 2020), therefore it may be that the characteristics of our scFv 3K2L are more suited to CAR T-cell engineering than those of Fierle and colleagues.

To date, few TME-targeting CAR T-cells have been developed and evaluated. At the preclinical level, the most promising TME-targeting CAR T-cells thus far are VEGFR-2-targeting CAR T-cells (Chinnasamy *et al.* 2010), however only one clinical trial has been carried out utilising these CAR T-cells against metastatic melanoma, but this was terminated as no objective response were observed. Data has since been published suggesting that VEGFR-2 CAR T-cells compete with VEGF-A for receptor binding and that co-administration of an anti-VEGF-A antibody may improve VEGFR-2 CAR T-cell efficacy (Lanitis *et al.* 2021). At the time of writing, no clinical trials utilising VEGFR-2 CAR T-cells, or any other TME specific CAR T-cells are active (ClinicalTrials.gov 2020).

Therefore, Endo3 CAR T-cells could represent the first TME-targeting CAR T-cells to show efficacy in human patients, however further work is required to optimise Endo3 CAR T-cell dosing and safety profile before translation into human patients.

Although Endo3 CAR T-cells have been evaluated in the context of stromal cell targeting in this thesis, Endo3 CAR T-cells may also be considered for tumour cell targeting. Solid tumours containing malignant cells of a mesenchymal lineage or that have differentiated into a mesenchymal phenotype, such as soft tissue sarcomas (Rouleau *et al.* 2008; Thway *et al.* 2016) or metaplastic breast cancers (Isacke Lab, unpublished data), have been shown to contain endosialin-positive tumour cells. The five year survival rate for soft tissue sarcoma and metaplastic breast cancers are 55% and 56-78%, respectively (Nelson *et al.* 2015; Tadros *et al.* 2021; CRUK 2022). Therefore, both of these cancers represent an area of clinical need for improved therapies. As previously discussed, targeting the malignant cells in a solid tumour mass is more challenging than targeting cells associated with the vasculature, however future work should investigate the suitability of Endo3 CAR T-cells for tumour cell targeting and next generation engineering may be considered to enhance Endo3 CAR T-cell function in this setting.

8.2 Endosialin blockade vs pericyte ablation

The identification of endosialin as a tumour specific antigen resulted in the development of the anti-endosialin blocking mAb MORAb-004, more commonly known as Ontuxizumab. However, clinical activity of Ontuxizumab was modest at best when administered to patients diagnosed with a range of solid tumours (Diaz *et al.* 2015; D'Angelo *et al.* 2018; Grothey *et al.* 2018; Norris *et al.* 2018; Doi *et al.* 2019; Jones *et al.* 2019). These results suggest that blockade of the endosialin protein is not sufficient to hinder tumour progression. However, it must be considered that no work was done to demonstrate efficient Ontuxizumab binding in patient tumours. Further, these studies

aimed to target endosialin expressed by tumour cells, not stromal cells. To date, the reasons for endosialin upregulation on malignant cells are not well understood. One hypothesis is that tumour cells expressing endosialin are of mesenchymal lineage and thus express endosialin solely as a by-product of their origin. If this hypothesis is correct, then it may be speculated that endosialin expressed by tumour cells serves no function and thus blockade of tumour cell expressed endosialin would be of little consequence.

Identification of an endosialin ligand in the vascular basement membrane by Khan and colleagues facilitated important insights into the function of endosialin expressed by stromal cells closely associated with the tumour vasculature. MMRN2, a matrix protein secreted by endothelial cells into the vascular basement membrane, is able to bind endosialin whilst also simultaneously binding CLEC14A or CD93, proteins expressed on the endothelial cell surface (Khan *et al.* 2017). Endosialin has been shown to play a role in selective vessel regression and vascular pruning (Simonavicius *et al.* 2012), whereas CLEC14A has been reported to promote endothelial cell migration and angiogenic sprouting (Noy *et al.* 2015). Interestingly, MMRN2 has been shown to be both a pro-and anti-angiogenic protein (Lorenzon *et al.* 2012; Zanivan *et al.* 2013; Colladel *et al.* 2016; Khan *et al.* 2017). This suggests that endosialin, MMRN2 and CLEC14A may form an intricate angiogenesis-regulating system and that blockade of endosialin with Ontuxizumab in this context may be more efficacious than blockade of endosialin expressed by tumour cells spatially distant from the vascular basement membrane.

It has been demonstrated that tumours grown in endosialin KO mice have an increased number of microvessels and decreased number of large vessels when compared to those grown in endosialin WT mice (Viski *et al.* 2016). This suggests that endosialin plays a role in promoting vascular stability and maturation. Therefore, an alternative approach to blocking endosialin is to ablate endosialin expressing cells completely to perturb the stability of the associated vessels, thus disrupting the vascular supply to the tumour.

CAR T-cells directed against endosialin represent a therapeutic approach to ablate endosialin expressing cells. In this thesis, Endo3 CAR T-cell therapy successfully depleted the number of endosialin-expressing cells in preclinical models of breast cancer, which resulted in slowed primary tumour growth and, in some cases, decreased metastasis to the lungs. As discussed in Chapter 1.2.3.3, conflicting reports have been published concerning the effect of pericyte ablation on tumour progression (Xian *et al.* 2006; Cooke *et al.* 2012), however it is likely that different tumour types respond in different ways to pericyte ablation depending on their vascular architecture. Ablation of endosialin expressing cells by Endo3 CAR T-cell therapy tended to result in a modest effect on primary tumour growth and significant limitation of metastasis in models with an aberrant vasculature, but significant effects on primary tumour growth and no effect on metastasis in tumours with a well organised and abundant vasculature. Therefore, in the clinical setting, examination of tumour architecture may play an important role in determining suitable patients for Endo3 CAR T-cell therapy.

8.3 Is Endo3 CAR T-cell associated toxicity relevant to humans?

In Chapters 4 and 5, Endo3 CAR T-cell therapy was associated with fatal toxicity when delivered to 4T1-tumour bearing mice. This toxicity was not alleviated by co-administering anti-IL-6R treatment and was only partially alleviated by giving multiple lower Endo3 CAR T-cell doses. In contrast, no toxicity was observed when C57BL/6 mice bearing either AT-3 or LLC tumours were given up to 3-fold higher doses of Endo3 CAR T-cells. The most notable difference *in vivo* between Endo3 CAR T-cells delivered to BALB/c mice and those delivered to C57BL/6 mice is the greater levels of expansion in the circulation of BALB/c mice. Onset of CAR T-cell related toxicities in patients treated with CD19 targeting CAR T-cells often correlates with peak expansion of CAR T-cells in the circulation and higher levels of CAR T-cell expansion are associated with more severe toxicity (Teachey *et al.* 2016; Mackall and Miklos 2017). Therefore, it is likely that

the greater Endo3 CAR T-cell expansion in tumour-bearing BALB/c mice is at least in part responsible for the toxicity observed in this model.

Data published by Chinnasamy and colleagues suggests that strain specific toxicity in BALB/c mice may be due to increased numbers of CD4⁺ CAR T-cells in the BALB/c CAR T-cell product. Interestingly, selection of only CD8⁺ CAR T-cells alleviated toxicity in BALB/c mice and selection of CD4⁺ CAR T-cells induced toxicity in C57BL/6 mice (Chinnasamy *et al.* 2010). This finding is further supported by Cheadle and colleagues who also see strain specific CAR T-cell toxicity in BALB/c mice and attribute this to increased CD4⁺ CAR T-cell numbers (Cheadle *et al.* 2014). Indeed, in this thesis, BALB/c derived Endo3 CAR T-cells were found to have higher numbers of CD4⁺ CAR T-cells than C57BL/6 derived Endo3 CAR T-cells. Therefore, it is likely that the BALB/c specific toxicity observed in this thesis is comparable to that observed in these two studies.

Key differences in the innate immune response exist between BALB/c and C57BL/6 mice. Both strains have polarised innate immune systems, however C57BL/6 mice are polarised towards Th1 response and BALB/c mice are polarised towards Th2 response. CD4⁺ CAR T-cells are more effective at stimulating the hosts immune response (Boulch *et al.* 2021), so this coupled with the polarisation towards a Th2 response may explain the systemic toxicities observed in the BALB/c model. In support of this, no toxicity was observed when the same dose of BALB/c CAR T-cells was delivered to NSG mice bearing 4T1 tumours.

As toxicity in tumour-bearing BALB/c mice treated with Endo3 CAR T-cells could not be alleviated in this thesis, it is important to consider whether this toxicity may be observed in human patients. A key difference between the cytotoxic response in mice and humans is that in humans both CD4⁺ and CD8⁺ cytotoxic T-cells utilise the perforin/granzyme system to kill antigen expressing cells (Yasukawa *et al.* 2000),

whereas in mice CD8⁺ and CD4⁺ cytotoxic T-cells rely on the perforin/granzyme and Fas/Fas Ligand pathways, respectively (Kägi *et al.* 1994; Stalder *et al.* 1994). Owing to this, the behaviour of mouse and human CD4⁺ CAR T-cells is not directly comparable.

Current FDA approved CAR T-cells are delivered to patients at various CD4⁺:CD8⁺ ratios. It has been reported that apheresis products with an initial CD4⁺:CD8⁺ ratio of <1 tend to expand with an increased ratio, whereas products with an initial CD4⁺:CD8⁺ ratio of >1 have a decreased ratio after expansion (Castella *et al.* 2020). Therefore, it is likely that patients are treated with both CD4⁺ and CD8⁺ heavy CAR T-cell populations. To date, no correlation between the number of CD4⁺ CAR T-cells present in the infused product and the severity of associated toxicity has been reported. On the contrary, a study by Hay and colleagues found a correlation between the number of CD8⁺ CAR T-cells and the severity of CRS in patients (Hay *et al.* 2017).

Considering the differences in cytotoxic T-cell killing between mouse and human systems and the fact that correlations have only been found between CD8⁺ CAR T-cell number and toxicity in humans, it is unlikely that the Endo3 CAR T-cell associated toxicity observed in tumour-bearing BALB/c mice would be relevant in the majority of human patients. The studies performed in this thesis utilise inbred mouse strains with polarised immune responses, which does not reflect the human patient population. However, it must be considered that some patients may have conditions that give them a Th2 bias in their innate immune response, similar to BALB/c mice. These conditions include patients with zinc deficiency, allergies and lymphoma (Mori *et al.* 2001; Kawamoto *et al.* 2006; Uciechowski *et al.* 2008). Therefore, caution should be taken in treating these subsets of patients.

8.4 Next steps for Endo3 CAR T-cell therapy

Endo3 CAR T-cell therapy has demonstrated promising activity against solid tumours in multiple preclinical models as reported in this thesis. However, Endo3 CAR T-cell efficacy was variable between these models, thus it will be important to gain understanding on what tumour characteristics, beyond the presence of endosialin-expressing cells, will determine a suitable candidate for Endo3 CAR T-cell therapy. It is likely that Endo3 CAR T-cell therapy is more efficacious against tumours with a more aberrant, disorganised vasculature, however the reason for this remains unclear and requires further investigation. It must also be considered that the efficacy of Endo3 CAR T-cells in this thesis may have been limited by the doses delivered, especially in the absence of associated toxicity. Future studies may explore increasing the delivered dose further, or alternatively delivering multiple doses at regular intervals. Studies utilising C57BL/6 mice may particularly benefit from multi-dosing, as Endo3 CAR T-cells do not expand in these models, which may limit the anti-tumour effects.

In this thesis, Endo3 CAR T-cell therapy was explored in the context of breast and lung cancer. However, as previously discussed, endosialin is upregulated in the stroma of other solid tumour types (Rouleau *et al.* 2008; Simonavicius *et al.* 2008). In addition, in some tumour types such as sarcoma, endosialin is also expressed by the tumour cells (Rouleau *et al.* 2008; Thway *et al.* 2016). Therefore, it would be interesting to explore the efficacy of Endo3 CAR T-cell therapy in the context of endosialin-positive sarcomas and other solid tumours with endosialin-positive stromal cells, such as glioblastomas.

As discussed in Section 8.3 the toxicity observed in Endo3 CAR T-cell treated BALB/c mice is likely a strain dependent effect and is unlikely to be relevant to human patients. However, approaches to improve the safety of Endo3 CAR T-cells may be taken. Endo3 CAR T-cell toxicity in BALB/c mice likely results from the rapid expansion

of Endo3 CAR T-cells observed between 6 and 8 days post-T-cell therapy, which in turn is likely to result in increased cytokine release and systemic inflammation. Engineering Endo3 CAR T-cells to include a suicide switch (Casucci *et al.* 2012; Minagawa *et al.* 2016) that can be triggered by the administration of a small molecule would allow control of the maximum levels of circulating Endo3 CAR T-cells, which can be monitored by regular blood sampling. Alternatively, to preserve Endo3 CAR T-cells whilst transiently inhibiting their function, Endo3 CAR T-cells could be engineered to have their CAR function disrupted by a small molecule. A recent example of such technology is the STOP CAR developed by Giordano-Attianese and colleagues. The STOP CAR separates the CAR into two chains, a recognition chain (containing scFv and CD28) and a signalling chain (containing CD3 ζ), that spontaneously dimerise to form a functional heterodimer. Administration of a small molecule can disrupt the dimer, resulting in loss of CAR function for as long as the molecule is present, with full CAR function returning after cessation of molecule delivery (Giordano-Attianese *et al.* 2020).

A question not answered by this thesis is how rapidly and in what quantity Endo3 CAR T-cells reach the tumour tissue and how are they changed in that environment, for example looking at markers of T-cell exhaustion. Investigating these characteristics will be important in determining whether Endo3 CAR T-cells are suitable as second generation CAR T-cells or whether they would benefit from next generation engineering to improve their tumour honing or survival in the circulation. An interesting consideration is the AngioSense reagent utilised in Chapter 5 of this thesis. AngioSense is a fluorescent macromolecule that pools specifically in the tumour vasculature to allow visualisation of vascular density in a solid tumour. Examination of the properties allowing AngioSense to pool specifically in the tumour vasculature may reveal interesting prospects for improving the honing of Endo3 CAR T-cells to the tumour tissue, thus improving the efficacy of this therapy.

As well as advances in next generation CAR T-cell engineering, progress is being made in understanding how to successfully engineer allogenic CAR T-cells (Cruz *et al.* 2013; Brudno *et al.* 2016). At present, all CAR T-cells delivered to patients are engineered from autologous lymphocytes. Although CAR T-cell production protocols have been optimised and generally result in successful generation of enough CAR T-cells to dose a patient, the process is both slow and costly. Allogenic CAR T-cells would allow advance manufacturing of CAR T-cell doses, thus reducing the time a patient must wait before receiving treatment. Additionally, allogenic CAR T-cells would also benefit patients that have impacted immune quality due to previous treatments. Multiple research groups are currently working to develop allogenic CAR T-cells, thus a final future consideration for Endo3 CAR T-cell therapy would be transduction into allogenic T-cells for a more accessible approach to treating patients.

8.5 Concluding remarks

In summary, the data obtained during this PhD suggest that Endo3 CAR T-cells are a novel CAR T-cell approach that successfully deplete tumour-associated endosialin expressing cells resulting in slowed tumour progression. Future studies should focus on establishing the best dosing strategy for Endo3 CAR T-cell therapy, improving the understanding of Endo3 CAR T-cell characteristics in the tumour tissue, evaluating Endo3 CAR T-cell therapy in the context of additional solid tumours and considering further engineering approaches to improve the safety and efficacy of Endo3 CAR T-cell therapy prior to clinical translation.

References

- Abramson, J.S., Palomba, M.L., Gordon, L.I., Lunning, M.A., Wang, M., Arnason, J., Mehta, A., Purev, E., Maloney, D.G., Andreadis, C., Sehgal, A., Solomon, S.R., Ghosh, N., Albertson, T.M., Garcia, J., Kostic, A., Mallaney, M., Ogasawara, K., Newhall, K., Kim, Y., Li, D. and Siddiqi, T. (2020) 'Lisocabtagene maraleucel for patients with relapsed or refractory large B-cell lymphomas (TRANSCEND NHL 001): a multicentre seamless design study', *The Lancet*, 396(10254), 839-852, available: [http://dx.doi.org/10.1016/S0140-6736\(20\)31366-0](http://dx.doi.org/10.1016/S0140-6736(20)31366-0).
- Adachi, K., Kano, Y., Nagai, T., Okuyama, N., Sakoda, Y. and Tamada, K. (2018) 'IL-7 and CCL19 expression in CAR-T cells improves immune cell infiltration and CAR-T cell survival in the tumor', *Nat Biotechnol*, 36(4), 346-351, available: <http://dx.doi.org/10.1038/nbt.4086>.
- Ahmed, N., Brawley, V.S., Hegde, M., Robertson, C., Ghazi, A., Gerken, C., Liu, E., Dakhova, O., Ashoori, A., Corder, A., Gray, T., Wu, M.-F., Liu, H., Hicks, J., Rainusso, N., Dotti, G., Mei, Z., Grilley, B., Gee, A., Rooney, C.M., Brenner, M.K., Heslop, H.E., Wels, W.S., Wang, L.L., Anderson, P. and Gottschalk, S. (2015) 'Human Epidermal Growth Factor Receptor 2 (HER2) –Specific Chimeric Antigen Receptor–Modified T Cells for the Immunotherapy of HER2-Positive Sarcoma', *Journal of Clinical Oncology*, 33(15), 1688-1696, available: <http://dx.doi.org/10.1200/JCO.2014.58.0225>.
- Ahmed, N., Brawley, V.S., Hegde, M., Robertson, C., Ghazi, A., Gerken, C., Liu, E., Dakhova, O., Ashoori, A., Corder, A., Gray, T., Wu, M.F., Liu, H., Hicks, J., Rainusso, N., Dotti, G., Mei, Z., Grilley, B., Gee, A., Rooney, C.M., Brenner, M.K., Heslop, H.E., Wels, W.S., Wang, L.L., Anderson, P. and Gottschalk, S. (2015) 'Human Epidermal Growth Factor Receptor 2 (HER2) -Specific Chimeric Antigen Receptor-Modified T Cells for the Immunotherapy of HER2-Positive Sarcoma', *J Clin Oncol*, 33(15), 1688-96, available: <http://dx.doi.org/10.1200/jco.2014.58.0225>.
- Albert, S., Arndt, C., Feldmann, A., Bergmann, R., Bachmann, D., Koristka, S., Ludwig, F., Ziller-Walter, P., Kegler, A., Gärtner, S., Schmitz, M., Ehninger, A., Cartellieri, M., Ehninger, G., Pietzsch, H.-J., Pietzsch, J., Steinbach, J. and Bachmann, M. (2017) 'A novel nanobody-based target module for retargeting of T lymphocytes to EGFR-expressing cancer cells via the modular UniCAR platform', *Onc Immunology*, 6(4), e1287246, available: <http://dx.doi.org/10.1080/2162402X.2017.1287246>.
- Albert, S., Arndt, C., Koristka, S., Berndt, N., Bergmann, R., Feldmann, A., Schmitz, M., Pietzsch, J., Steinbach, J. and Bachmann, M. (2018) 'From mono- to bivalent: improving theranostic properties of target modules for redirection of UniCAR T cells against EGFR-expressing tumor cells in vitro and in vivo', *Oncotarget*, 9(39), 25597-25616, available: <http://dx.doi.org/10.18632/oncotarget.25390>.
- Alessi, P., Leali, D., Camozzi, M., Cantelmo, A., Albini, A. and Presta, M. (2009) 'Anti-FGF2 approaches as a strategy to compensate resistance to anti-VEGF therapy: long-

References

- pentraxin 3 as a novel antiangiogenic FGF2-antagonist', *Eur Cytokine Netw*, 20(4), 225-34, available: <http://dx.doi.org/10.1684/ecn.2009.0175>.
- Amrolia, P.J., Wynn, R., Hough, R., Vora, A., Bonney, D., Veys, P., Rao, K., Chiesa, R., Al-Hajj, M., Cordoba, S.P., Onuoha, S., Kotsopoulou, E., Khokhar, N.Z., Pule, M. and Peddareddigari, V.G.R. (2018) 'Simultaneous Targeting of CD19 and CD22: Phase I Study of AUTO3, a Bicistronic Chimeric Antigen Receptor (CAR) T-Cell Therapy, in Pediatric Patients with Relapsed/Refractory B-Cell Acute Lymphoblastic Leukemia (r/r B-ALL): Amelia Study', *Blood*, 132(Supplement 1), 279-279, available: <http://dx.doi.org/10.1182/blood-2018-99-118616>.
- An, N., Hou, Y.N., Zhang, Q.X., Li, T., Zhang, Q.L., Fang, C., Chen, H., Lee, H.C., Zhao, Y.J. and Du, X. (2018) 'Anti-Multiple Myeloma Activity of Nanobody-Based Anti-CD38 Chimeric Antigen Receptor T Cells', *Mol Pharm*, 15(10), 4577-4588, available: <http://dx.doi.org/10.1021/acs.molpharmaceut.8b00584>.
- Andersen, M.H., Schrama, D., thor Straten, P. and Becker, J.C. (2006) 'Cytotoxic T Cells', *Journal of Investigative Dermatology*, 126(1), 32-41, available: <http://dx.doi.org/https://doi.org/10.1038/sj.jid.5700001>.
- Andonegui-Elguera, M.A., Alfaro-Mora, Y., Cáceres-Gutiérrez, R., Caro-Sánchez, C.H.S., Herrera, L.A. and Díaz-Chávez, J. (2020) 'An Overview of Vasculogenic Mimicry in Breast Cancer', *Frontiers in oncology*, 10, 220-220, available: <http://dx.doi.org/10.3389/fonc.2020.00220>.
- Antoniou, A.C., Casadei, S., Heikkinen, T., Barrowdale, D., Pylkäs, K., Roberts, J., Lee, A., Subramanian, D., De Leeneer, K., Fostira, F., Tomiak, E., Neuhausen, S.L., Teo, Z.L., Khan, S., Aittomäki, K., Moilanen, J.S., Turnbull, C., Seal, S., Mannermaa, A., Kallioniemi, A., Lindeman, G.J., Buys, S.S., Andrulis, I.L., Radice, P., Tondini, C., Manoukian, S., Toland, A.E., Miron, P., Weitzel, J.N., Domchek, S.M., Poppe, B., Claes, K.B.M., Yannoukacos, D., Concannon, P., Bernstein, J.L., James, P.A., Easton, D.F., Goldgar, D.E., Hopper, J.L., Rahman, N., Peterlongo, P., Nevanlinna, H., King, M.-C., Couch, F.J., Southey, M.C., Winqvist, R., Foulkes, W.D. and Tischkowitz, M. (2014) 'Breast-Cancer Risk in Families with Mutations in PALB2', *New England Journal of Medicine*, 371(6), 497-506, available: <http://dx.doi.org/10.1056/NEJMoa1400382>.
- Anurathapan, U., Chan, R.C., Hindi, H.F., Mucharla, R., Bajgain, P., Hayes, B.C., Fisher, W.E., Heslop, H.E., Rooney, C.M., Brenner, M.K., Leen, A.M. and Vera, J.F. (2014) 'Kinetics of tumor destruction by chimeric antigen receptor-modified T cells', *Mol Ther*, 22(3), 623-633, available: <http://dx.doi.org/10.1038/mt.2013.262>.
- Appleton, E., Hassan, J., Chan Wah Hak, C., Sivamanoharan, N., Wilkins, A., Samson, A., Ono, M., Harrington, K.J., Melcher, A. and Wennerberg, E. (2021) 'Kickstarting Immunity in Cold Tumours: Localised Tumour Therapy Combinations With Immune Checkpoint Blockade', *Frontiers in Immunology*, 12, available: <http://dx.doi.org/10.3389/fimmu.2021.754436>.

References

- Ariga, N., Sato, E., Ohuchi, N., Nagura, H. and Ohtani, H. (2001) 'Stromal expression of fibroblast activation protein/seprase, a cell membrane serine proteinase and gelatinase, is associated with longer survival in patients with invasive ductal carcinoma of breast', *International Journal of Cancer*, 95(1), 67-72, available: [http://dx.doi.org/https://doi.org/10.1002/1097-0215\(20010120\)95:1<67::AID-IJC1012>3.0.CO;2-U](http://dx.doi.org/https://doi.org/10.1002/1097-0215(20010120)95:1<67::AID-IJC1012>3.0.CO;2-U).
- Armulik, A., Abramsson, A. and Betsholtz, C. (2005) 'Endothelial/Pericyte Interactions', *Circulation Research*, 97(6), 512-523, available: <http://dx.doi.org/doi:10.1161/01.RES.0000182903.16652.d7>.
- Arndt, C., Loureiro, L.R., Feldmann, A., Jureczek, J., Bergmann, R., Máthé, D., Hegedüs, N., Berndt, N., Koristka, S., Mitwasi, N., Fasslrunner, F., Lamprecht, C., Kegler, A., Hoffmann, A., Bartsch, T., Köseer, A.S., Egan, G., Schmitz, M., Hořejší, V., Krause, M., Dubrovská, A. and Bachmann, M. (2020) 'UniCAR T cell immunotherapy enables efficient elimination of radioresistant cancer cells', *Oncotarget*, 9(1), 1743036, available: <http://dx.doi.org/10.1080/2162402X.2020.1743036>.
- Aslakson, C.J. and Miller, F.R. (1992) 'Selective Events in the Metastatic Process Defined by Analysis of the Sequential Dissemination of Subpopulations of a Mouse Mammary Tumor', *Cancer Res*, 52(6), 1399.
- Aston, W.J., Hope, D.E., Nowak, A.K., Robinson, B.W., Lake, R.A. and Lesterhuis, W.J. (2017) 'A systematic investigation of the maximum tolerated dose of cytotoxic chemotherapy with and without supportive care in mice', *BMC Cancer*, 17(1), 684-684, available: <http://dx.doi.org/10.1186/s12885-017-3677-7>.
- Bachmann, D., Aliperta, R., Bergmann, R., Feldmann, A., Koristka, S., Arndt, C., Loff, S., Welzel, P., Albert, S., Kegler, A., Ehninger, A., Cartellieri, M., Ehninger, G., Bornhäuser, M., von Bonin, M., Werner, C., Pietzsch, J., Steinbach, J. and Bachmann, M. (2017) 'Retargeting of UniCAR T cells with an in vivo synthesized target module directed against CD19 positive tumor cells', *Oncotarget*, 9(7), 7487-7500, available: <http://dx.doi.org/10.18632/oncotarget.23556>.
- Bachmann, M. (2019) 'The UniCAR system: A modular CAR T cell approach to improve the safety of CAR T cells', *Immunology Letters*, 211, 13-22, available: <http://dx.doi.org/https://doi.org/10.1016/j.imlet.2019.05.003>.
- Balkwill, F.R., Capasso, M. and Hagemann, T. (2012) 'The tumor microenvironment at a glance', *Journal of Cell Science*, 125(23), 5591, available: <http://dx.doi.org/10.1242/jcs.116392>.
- Bartis, D., Crowley, L.E., D'Souza, V.K., Borthwick, L., Fisher, A.J., Croft, A.P., Pongracz, J.E., Thompson, R., Langman, G., Buckley, C.D. and Thickett, D.R. (2016) 'Role of CD248 as a

References

- potential severity marker in idiopathic pulmonary fibrosis', *BMC Pulm Med*, 16(1), 51, available: <http://dx.doi.org/10.1186/s12890-016-0211-7>.
- Bartoschek, M., Oskolkov, N., Bocci, M., Lötvrot, J., Larsson, C., Sommarin, M., Madsen, C.D., Lindgren, D., Pekar, G., Karlsson, G., Ringnér, M., Bergh, J., Björklund, Å. and Pietras, K. (2018) 'Spatially and functionally distinct subclasses of breast cancer-associated fibroblasts revealed by single cell RNA sequencing', *Nature communications*, 9(1), 5150-5150, available: <http://dx.doi.org/10.1038/s41467-018-07582-3>.
- Baum, J. and Duffy, H.S. (2011) 'Fibroblasts and myofibroblasts: what are we talking about?', *Journal of cardiovascular pharmacology*, 57(4), 376-379, available: <http://dx.doi.org/10.1097/FJC.0b013e3182116e39>.
- Beatty, G.L., Haas, A.R., Maus, M.V., Torigian, D.A., Soulen, M.C., Plesa, G., Chew, A., Zhao, Y., Levine, B.L., Albelda, S.M., Kalos, M. and June, C.H. (2014) 'Mesothelin-specific chimeric antigen receptor mRNA-engineered T cells induce anti-tumor activity in solid malignancies', *Cancer Immunol Res*, 2(2), 112-20, available: <http://dx.doi.org/10.1158/2326-6066.Cir-13-0170>.
- Becker, R., Lenter, M.C., Vollkommer, T., Boos, A.M., Pfaff, D., Augustin, H.G. and Christian, S. (2008) 'Tumor stroma marker endosialin (Tem1) is a binding partner of metastasis-related protein Mac-2 BP/90K', *Faseb j*, 22(8), 3059-67, available: <http://dx.doi.org/10.1096/fj.07-101386>.
- Bentolila, L.A., Prakash, R., Mihic-Probst, D., Wadehra, M., Kleinman, H.K., Carmichael, T.S., Péault, B., Barnhill, R.L. and Lugassy, C. (2016) 'Imaging of Angiotropism/Vascular Co-Option in a Murine Model of Brain Melanoma: Implications for Melanoma Progression along Extravascular Pathways', *Sci Rep*, 6, 23834, available: <http://dx.doi.org/10.1038/srep23834>.
- Bernsen, H., Van der Laak, J., Küsters, B., Van der Ven, A. and Wesseling, P. (2005) 'Gliomatosis cerebri: quantitative proof of vessel recruitment by cooptation instead of angiogenesis', *J Neurosurg*, 103(4), 702-6, available: <http://dx.doi.org/10.3171/jns.2005.103.4.0702>.
- Betsholtz, C. (2004) 'Insight into the physiological functions of PDGF through genetic studies in mice', *Cytokine Growth Factor Rev*, 15(4), 215-28, available: <http://dx.doi.org/10.1016/j.cytogfr.2004.03.005>.
- Bielenberg, D.R. and Zetter, B.R. (2015) 'The Contribution of Angiogenesis to the Process of Metastasis', *Cancer journal (Sudbury, Mass.)*, 21(4), 267-273, available: <http://dx.doi.org/10.1097/PPO.000000000000138>.
- Bohlsón, S.S., Silva, R., Fonseca, M.I. and Tenner, A.J. (2005) 'CD93 Is Rapidly Shed from the Surface of Human Myeloid Cells and the Soluble Form Is Detected in Human Plasma',

References

- The Journal of Immunology*, 175(2), 1239, available: <http://dx.doi.org/10.4049/jimmunol.175.2.1239>.
- Bos, R., van der Groep, P., Greijer, A.E., Shvarts, A., Meijer, S., Pinedo, H.M., Semenza, G.L., van Diest, P.J. and van der Wall, E. (2003) 'Levels of hypoxia-inducible factor-1alpha independently predict prognosis in patients with lymph node negative breast carcinoma', *Cancer*, 97(6), 1573-81, available: <http://dx.doi.org/10.1002/cncr.11246>.
- Boulch, M., Cazaux, M., Loe-Mie, Y., Thibaut, R., Corre, B., Lemaître, F., Grandjean, C.L., Garcia, Z. and Bousso, P. (2021) 'A cross-talk between CAR T cell subsets and the tumor microenvironment is essential for sustained cytotoxic activity', *Sci Immunol*, 6(57), available: <http://dx.doi.org/10.1126/sciimmunol.abd4344>.
- Brady, J., Neal, J., Sadakar, N. and Gasque, P. (2004) 'Human endosialin (tumor endothelial marker 1) is abundantly expressed in highly malignant and invasive brain tumors', *J Neuropathol Exp Neurol*, 63(12), 1274-83, available: <http://dx.doi.org/10.1093/jnen/63.12.1274>.
- Brentjens, R.J., Davila, M.L., Riviere, I., Park, J., Wang, X., Cowell, L.G., Bartido, S., Stefanski, J., Taylor, C., Olszewska, M., Borquez-Ojeda, O., Qu, J., Wasielewska, T., He, Q., Bernal, Y., Rijo, I.V., Hedvat, C., Kobos, R., Curran, K., Steinherz, P., Jurcic, J., Rosenblatt, T., Maslak, P., Frattini, M. and Sadelain, M. (2013) 'CD19-targeted T cells rapidly induce molecular remissions in adults with chemotherapy-refractory acute lymphoblastic leukemia', *Science translational medicine*, 5(177), 177ra38, available: <http://dx.doi.org/10.1126/scitranslmed.3005930>.
- Brentjens, R.J., Riviere, I., Park, J., Davilla, M., Wang, X., Yeh, R., Lamanna, N., Frattini, M.G. and Sadelain, M. (2011a) 'Lymphodepletion and tumor burden govern clinical responses in patients with B-cell malignancies treated with autologous, CD19-targeted T cells', *Journal of Clinical Oncology*, 29(15_suppl), 2534-2534, available: http://dx.doi.org/10.1200/jco.2011.29.15_suppl.2534.
- Brentjens, R.J., Rivière, I., Park, J.H., Davila, M.L., Wang, X., Stefanski, J., Taylor, C., Yeh, R., Bartido, S., Borquez-Ojeda, O., Olszewska, M., Bernal, Y., Pegram, H., Przybylowski, M., Hollyman, D., Usachenko, Y., Pirraglia, D., Hosey, J., Santos, E., Halton, E., Maslak, P., Scheinberg, D., Jurcic, J., Heaney, M., Heller, G., Frattini, M. and Sadelain, M. (2011b) 'Safety and persistence of adoptively transferred autologous CD19-targeted T cells in patients with relapsed or chemotherapy refractory B-cell leukemias', *Blood*, 118(18), 4817-28, available: <http://dx.doi.org/10.1182/blood-2011-04-348540>.
- Brentjens, R.J., Santos, E., Nikhamin, Y., Yeh, R., Matsushita, M., La Perle, K., Quintás-Cardama, A., Larson, S.M. and Sadelain, M. (2007) 'Genetically Targeted T Cells Eradicate Systemic Acute Lymphoblastic Leukemia Xenografts', *Clinical Cancer Research*, 13(18), 5426, available: <http://dx.doi.org/10.1158/1078-0432.CCR-07-0674>.

References

- Broad, R.V., Jones, S.J., Teske, M.C., Wastall, L.M., Hanby, A.M., Thorne, J.L. and Hughes, T.A. (2021) 'Inhibition of interferon-signalling halts cancer-associated fibroblast-dependent protection of breast cancer cells from chemotherapy', *British journal of cancer*, available: <http://dx.doi.org/10.1038/s41416-020-01226-4>.
- Brocker, T. and Karjalainen, K. (1995) 'Signals through T cell receptor-zeta chain alone are insufficient to prime resting T lymphocytes', *J Exp Med*, 181(5), 1653-9, available: <http://dx.doi.org/10.1084/jem.181.5.1653>.
- Brudno, J.N., Somerville, R.P., Shi, V., Rose, J.J., Halverson, D.C., Fowler, D.H., Gea-Banacloche, J.C., Pavletic, S.Z., Hickstein, D.D., Lu, T.L., Feldman, S.A., Iwamoto, A.T., Kurlander, R., Maric, I., Goy, A., Hansen, B.G., Wilder, J.S., Blacklock-Schuver, B., Hakim, F.T., Rosenberg, S.A., Gress, R.E. and Kochenderfer, J.N. (2016) 'Allogeneic T Cells That Express an Anti-CD19 Chimeric Antigen Receptor Induce Remissions of B-Cell Malignancies That Progress After Allogeneic Hematopoietic Stem-Cell Transplantation Without Causing Graft-Versus-Host Disease', *Journal of clinical oncology : official journal of the American Society of Clinical Oncology*, 34(10), 1112-21, available: <http://dx.doi.org/10.1200/jco.2015.64.5929>.
- Brufsky, A.M., Hurvitz, S., Perez, E., Swamy, R., Valero, V., O'Neill, V. and Rugo, H.S. (2011) 'RIBBON-2: a randomized, double-blind, placebo-controlled, phase III trial evaluating the efficacy and safety of bevacizumab in combination with chemotherapy for second-line treatment of human epidermal growth factor receptor 2-negative metastatic breast cancer', *Journal of clinical oncology : official journal of the American Society of Clinical Oncology*, 29(32), 4286-93, available: <http://dx.doi.org/10.1200/jco.2010.34.1255>.
- Buckanovich, R.J., Facciabene, A., Kim, S., Benencia, F., Sasaroli, D., Balint, K., Katsaros, D., O'Brien-Jenkins, A., Gimotty, P.A. and Coukos, G. (2008) 'Endothelin B receptor mediates the endothelial barrier to T cell homing to tumors and disables immune therapy', *Nat Med*, 14(1), 28-36, available: <http://dx.doi.org/10.1038/nm1699>.
- Budde, L.E., Berger, C., Lin, Y., Wang, J., Lin, X., Frayo, S.E., Brouns, S.A., Spencer, D.M., Till, B.G., Jensen, M.C., Riddell, S.R. and Press, O.W. (2013) 'Combining a CD20 chimeric antigen receptor and an inducible caspase 9 suicide switch to improve the efficacy and safety of T cell adoptive immunotherapy for lymphoma', *PLOS ONE*, 8(12), e82742, available: <http://dx.doi.org/10.1371/journal.pone.0082742>.
- Byrd, T.T., Fousek, K., Pignata, A., Szot, C., Samaha, H., Seaman, S., Dobrolecki, L., Salsman, V.S., Oo, H.Z., Bielamowicz, K., Landi, D., Rainusso, N., Hicks, J., Powell, S., Baker, M.L., Wels, W.S., Koch, J., Sorensen, P.H., Deneen, B., Ellis, M.J., Lewis, M.T., Hegde, M., Fletcher, B.S., St Croix, B. and Ahmed, N. (2018) 'TEM8/ANTXR1-Specific CAR T Cells as a Targeted Therapy for Triple-Negative Breast Cancer', *Cancer Res*, 78(2), 489-500, available: <http://dx.doi.org/10.1158/0008-5472.CAN-16-1911>.

References

- Cairo, M.S., Coiffier, B., Reiter, A., Younes, A. and on behalf of the, T.L.S.E.P. (2010) 'Recommendations for the evaluation of risk and prophylaxis of tumour lysis syndrome (TLS) in adults and children with malignant diseases: an expert TLS panel consensus', *British Journal of Haematology*, 149(4), 578-586, available: <http://dx.doi.org/10.1111/j.1365-2141.2010.08143.x>.
- CancerResearchInstitute (2020) *What is Immunotherapy?*, available: <https://www.cancerresearch.org/immunotherapy/what-is-immunotherapy> [accessed 27/04/2020].
- Cao, X., Leonard, K., Collins, L.I., Cai, S.F., Mayer, J.C., Payton, J.E., Walter, M.J., Piwnica-Worms, D., Schreiber, R.D. and Ley, T.J. (2009) 'Interleukin 12 stimulates IFN-gamma-mediated inhibition of tumor-induced regulatory T-cell proliferation and enhances tumor clearance', *Cancer Res*, 69(22), 8700-9, available: <http://dx.doi.org/10.1158/0008-5472.Can-09-1145>.
- Cao, Y., Zhang, Z.-L., Zhou, M., Elson, P., Rini, B., Aydin, H., Feenstra, K., Tan, M.-H., Berghuis, B., Tabbey, R., Resau, J.H., Zhou, F.-J., Teh, B.T. and Qian, C.-N. (2013) 'Pericyte coverage of differentiated vessels inside tumor vasculature is an independent unfavorable prognostic factor for patients with clear cell renal cell carcinoma', *Cancer*, 119(2), 313-324, available: <http://dx.doi.org/https://doi.org/10.1002/cncr.27746>.
- Capone, E., Piccolo, E., Fichera, I., Ciufici, P., Barcaroli, D., Sala, A., De Laurenzi, V., Iacobelli, V., Iacobelli, S. and Sala, G. (2017) 'Generation of a novel Antibody-Drug Conjugate targeting endosialin: potent and durable antitumor response in sarcoma', *Oncotarget*, 8(36), 60368-60377, available: <http://dx.doi.org/10.18632/oncotarget.19499>.
- Caporarello, N., D'Angeli, F., Cambria, M.T., Candido, S., Giallongo, C., Salmeri, M., Lombardo, C., Longo, A., Giurdanella, G., Anfuso, C.D. and Lupo, G. (2019) 'Pericytes in Microvessels: From "Mural" Function to Brain and Retina Regeneration', *Int J Mol Sci*, 20(24), available: <http://dx.doi.org/10.3390/ijms20246351>.
- Cartellieri, M., Feldmann, A., Koristka, S., Arndt, C., Loff, S., Ehninger, A., von Bonin, M., Bejestani, E.P., Ehninger, G. and Bachmann, M.P. (2016) 'Switching CAR T cells on and off: a novel modular platform for retargeting of T cells to AML blasts', *Blood Cancer Journal*, 6(8), e458-e458, available: <http://dx.doi.org/10.1038/bcj.2016.61>.
- Cartellieri, M., Loff, S., von Bonin, M., Bejestani, E.P., Ehninger, A., Feldmann, A., Koristka, S., Arndt, C., Ehninger, G. and Bachmann, M.P. (2015) 'Unicar: A Novel Modular Retargeting Platform Technology for CAR T Cells', *Blood*, 126(23), 5549-5549, available: <http://dx.doi.org/10.1182/blood.V126.23.5549.5549>.
- Castella, M., Boronat, A., Martín-Ibáñez, R., Rodríguez, V., Suñé, G., Caballero, M., Marzal, B., Pérez-Amill, L., Martín-Antonio, B., Castaño, J., Bueno, C., Balagué, O., González-Navarro, E.A., Serra-Pages, C., Engel, P., Vilella, R., Benitez-Ribas, D., Ortiz-Maldonado,

References

- V., Cid, J., Tabera, J., Canals, J.M., Lozano, M., Baumann, T., Vilarrodona, A., Trias, E., Campo, E., Menendez, P., Urbano-Ispizua, Á., Yagüe, J., Pérez-Galán, P., Rives, S., Delgado, J. and Juan, M. (2019) 'Development of a Novel Anti-CD19 Chimeric Antigen Receptor: A Paradigm for an Affordable CAR T Cell Production at Academic Institutions', *Molecular Therapy - Methods & Clinical Development*, 12, 134-144, available: <http://dx.doi.org/10.1016/j.omtm.2018.11.010>.
- Castella, M., Caballero-Baños, M., Ortiz-Maldonado, V., González-Navarro, E.A., Suñé, G., Antoñana-Vidósola, A., Boronat, A., Marzal, B., Millán, L., Martín-Antonio, B., Cid, J., Lozano, M., García, E., Tabera, J., Trias, E., Perpiña, U., Canals, J.M., Baumann, T., Benítez-Ribas, D., Campo, E., Yagüe, J., Urbano-Ispizua, Á., Rives, S., Delgado, J. and Juan, M. (2020) 'Point-Of-Care CAR T-Cell Production (ARI-0001) Using a Closed Semi-automatic Bioreactor: Experience From an Academic Phase I Clinical Trial', *Frontiers in Immunology*, 11, available: <http://dx.doi.org/10.3389/fimmu.2020.00482>.
- Casucci, M., di Robilant, B.N., Falcone, L., Camisa, B., Genovese, P., Gentner, B., Naldini, L., Savoldo, B., Ciceri, F., Bordignon, C., Dotti, G., Bonini, C. and Bondanza, A. (2012) 'Co-Expression of a Suicide Gene in CAR-Redirected T Cells Enables the Safe Targeting of CD44v6 for Leukemia and Myeloma Eradication', *Blood*, 120(21), 949-949, available: <http://dx.doi.org/10.1182/blood.V120.21.949.949>.
- Cazaux, M., Grandjean, C.L., Lemaître, F., Garcia, Z., Beck, R.J., Milo, I., Postat, J., Beltman, J.B., Cheadle, E.J. and Bousso, P. (2019) 'Single-cell imaging of CAR T cell activity in vivo reveals extensive functional and anatomical heterogeneity', *Journal of Experimental Medicine*, 216(5), 1038-1049, available: <http://dx.doi.org/10.1084/jem.20182375>.
- Chacko, A.M., Li, C., Nayak, M., Mikitsh, J.L., Hu, J., Hou, C., Grasso, L., Nicolaides, N.C., Muzykantov, V.R., Divgi, C.R. and Coukos, G. (2014) 'Development of 124I immuno-PET targeting tumor vascular TEM1/endothelial', *J Nucl Med*, 55(3), 500-507, available: <http://dx.doi.org/10.2967/jnumed.113.121905>.
- Chang, C.-H., Qiu, J., O'Sullivan, D., Buck, Michael D., Noguchi, T., Curtis, Jonathan D., Chen, Q., Gindin, M., Gubin, Matthew M., van der Windt, Gerritje J.W., Tonc, E., Schreiber, Robert D., Pearce, Edward J. and Pearce, Erika L. (2015) 'Metabolic Competition in the Tumor Microenvironment Is a Driver of Cancer Progression', *Cell*, 162(6), 1229-1241, available: <http://dx.doi.org/https://doi.org/10.1016/j.cell.2015.08.016>.
- Chantrain, C.F., Shimada, H., Jodele, S., Groshen, S., Ye, W., Shalinsky, D.R., Werb, Z., Coussens, L.M. and DeClerck, Y.A. (2004) 'Stromal matrix metalloproteinase-9 regulates the vascular architecture in neuroblastoma by promoting pericyte recruitment', *Cancer Res*, 64(5), 1675-86, available: <http://dx.doi.org/10.1158/0008-5472.can-03-0160>.
- Chatenoud, L., Ferran, C., Reuter, A., Legendre, C., Gevaert, Y., Kreis, H., Franchimont, P. and Bach, J.F. (1989) 'Systemic reaction to the anti-T-cell monoclonal antibody OKT3 in relation to serum levels of tumor necrosis factor and interferon-gamma [corrected]', *N*

References

- Engl J Med*, 320(21), 1420-1, available:
<http://dx.doi.org/10.1056/nejm198905253202117>.
- Chaudhary, A., Hilton, M.B., Seaman, S., Haines, D.C., Stevenson, S., Lemotte, P.K., Tschantz, W.R., Zhang, X.M., Saha, S., Fleming, T. and St Croix, B. (2012) 'TEM8/ANTXR1 blockade inhibits pathological angiogenesis and potentiates tumoricidal responses against multiple cancer types', *Cancer Cell*, 21(2), 212-26, available:
<http://dx.doi.org/10.1016/j.ccr.2012.01.004>.
- Cheadle, E.J., Sheard, V., Rothwell, D.G., Bridgeman, J.S., Ashton, G., Hanson, V., Mansoor, A.W., Hawkins, R.E. and Gilham, D.E. (2014) 'Differential Role of Th1 and Th2 Cytokines in Autotoxicity Driven by CD19-Specific Second-Generation Chimeric Antigen Receptor T Cells in a Mouse Model', *The Journal of Immunology*, 192(8), 3654-3665, available:
<http://dx.doi.org/10.4049/jimmunol.1302148>.
- Chen, J., Flurkey, K. and Harrison, D.E. (2002) 'A reduced peripheral blood CD4+ lymphocyte proportion is a consistent ageing phenotype', *Mechanisms of Ageing and Development*, 123(2), 145-153, available:
[http://dx.doi.org/https://doi.org/10.1016/S0047-6374\(01\)00347-5](http://dx.doi.org/https://doi.org/10.1016/S0047-6374(01)00347-5).
- Chen, M., Sun, R., Shi, B., Wang, Y., Di, S., Luo, H., Sun, Y., Li, Z., Zhou, M. and Jiang, H. (2019) 'Antitumor efficacy of chimeric antigen receptor T cells against EGFRvIII-expressing glioblastoma in C57BL/6 mice', *Biomedicine & Pharmacotherapy*, 113, 108734, available: <http://dx.doi.org/https://doi.org/10.1016/j.biopha.2019.108734>.
- Chen, S., Giannakou, A., Wyman, S., Gruzdas, J., Golas, J., Zhong, W., Loreth, C., Sridharan, L., Yamin, T.T., Damelin, M. and Geles, K.G. (2018) 'Cancer-associated fibroblasts suppress SOX2-induced dysplasia in a lung squamous cancer coculture', *Proc Natl Acad Sci U S A*, 115(50), E11671-e11680, available: <http://dx.doi.org/10.1073/pnas.1803718115>.
- Cheung, Kevin J., Gabrielson, E., Werb, Z. and Ewald, Andrew J. (2013) 'Collective Invasion in Breast Cancer Requires a Conserved Basal Epithelial Program', *Cell*, 155(7), 1639-1651, available: <http://dx.doi.org/10.1016/j.cell.2013.11.029>.
- Chinnasamy, D., Yu, Z., Theoret, M.R., Zhao, Y., Shrimali, R.K., Morgan, R.A., Feldman, S.A., Restifo, N.P. and Rosenberg, S.A. (2010) 'Gene therapy using genetically modified lymphocytes targeting VEGFR-2 inhibits the growth of vascularized syngenic tumors in mice', *J Clin Invest*, 120(11), 3953-68, available: <http://dx.doi.org/10.1172/jci43490>.
- Chitturi, R.T., Balasubramaniam, A.M., Parameswar, R.A., Kesavan, G., Haris, K.T.M. and Mohideen, K. (2015) 'The role of myofibroblasts in wound healing, contraction and its clinical implications in cleft palate repair', *Journal of international oral health : JIOH*, 7(3), 75-80.

References

- Chlebowski, R.T., Chen, Z., Anderson, G.L., Rohan, T., Aragaki, A., Lane, D., Dolan, N.C., Paskett, E.D., McTiernan, A., Hubbell, F.A., Adams-Campbell, L.L. and Prentice, R. (2005) 'Ethnicity and Breast Cancer: Factors Influencing Differences in Incidence and Outcome', *JNCI: Journal of the National Cancer Institute*, 97(6), 439-448, available: <http://dx.doi.org/10.1093/jnci/dji064>.
- Chmielewski, M. and Abken, H. (2017) 'CAR T Cells Releasing IL-18 Convert to T-Bet(high) FoxO1(low) Effectors that Exhibit Augmented Activity against Advanced Solid Tumors', *Cell Rep*, 21(11), 3205-3219, available: <http://dx.doi.org/10.1016/j.celrep.2017.11.063>.
- Chow, M.T. and Luster, A.D. (2014) 'Chemokines in cancer', *Cancer Immunol Res*, 2(12), 1125-1131, available: <http://dx.doi.org/10.1158/2326-6066.CIR-14-0160>.
- Christian, S., Ahorn, H., Koehler, A., Eisenhaber, F., Rodi, H.P., Garin-Chesa, P., Park, J.E., Rettig, W.J. and Lenter, M.C. (2001) 'Molecular cloning and characterization of endosialin, a C-type lectin-like cell surface receptor of tumor endothelium', *J Biol Chem*, 276(10), 7408-14, available: <http://dx.doi.org/10.1074/jbc.M009604200>.
- Christian, S., Ahorn, H., Novatchkova, M., Garin-Chesa, P., Park, J.E., Weber, G., Eisenhaber, F., Rettig, W.J. and Lenter, M.C. (2001) 'Molecular Cloning and Characterization of EndoGlyx-1, an EMILIN-like Multisubunit Glycoprotein of Vascular Endothelium', *Journal of Biological Chemistry*, 276(51), 48588-48595.
- Cicone, F., Denoel, T., Gnesin, S., Riggi, N., Irving, M., Jakka, G., Schaefer, N., Viertl, D., Coukos, G. and Prior, J.O. (2020) 'Preclinical Evaluation and Dosimetry of [(111)In]CHX-DTPA-scFv78-Fc Targeting Endosialin/Tumor Endothelial Marker 1 (TEM1)', *Mol Imaging Biol*, 2020/01/30, available: <http://dx.doi.org/10.1007/s11307-020-01479-8>.
- ClinicalTrials.gov (2020), available: <https://clinicaltrials.gov/ct2/results?cond=&term=MORAb-004&cntry=&state=&city=&dist=> [accessed 24/04/2020].
- Colladel, R., Pellicani, R., Andreuzzi, E., Paulitti, A., Tarticchio, G., Todaro, F., Colombatti, A. and Mongiat, M. (2016) 'MULTIMERIN2 binds VEGF-A primarily via the carbohydrate chains exerting an angiostatic function and impairing tumor growth', *Oncotarget*, 7(2), 2022-37, available: <http://dx.doi.org/10.18632/oncotarget.6515>.
- Colpaert, C.G., Vermeulen, P.B., Van Beest, P., Soubry, A., Goovaerts, G., Dirix, L.Y., Harris, A.L. and Van Marck, E.A. (2003) 'Cutaneous breast cancer deposits show distinct growth patterns with different degrees of angiogenesis, hypoxia and fibrin deposition', *Histopathology*, 42(6), 530-40, available: <http://dx.doi.org/10.1046/j.1365-2559.2003.01629.x>.
- Cooke, Vesselina G., LeBleu, Valerie S., Keskin, D., Khan, Z., O'Connell, Joyce T., Teng, Y., Duncan, Michael B., Xie, L., Maeda, G., Vong, S., Sugimoto, H., Rocha, Rafael M., Damascena, A., Brentani, Ricardo R. and Kalluri, R. (2012) 'Pericyte Depletion Results in

References

Hypoxia-Associated Epithelial-to-Mesenchymal Transition and Metastasis Mediated by Met Signaling Pathway', *Cancer Cell*, 21(1), 66-81, available: <http://dx.doi.org/https://doi.org/10.1016/j.ccr.2011.11.024>.

Cortes, J., Cescon, D.W., Rugo, H.S., Nowecki, Z., Im, S.-A., Yusof, M.M., Gallardo, C., Lipatov, O., Barrios, C.H., Holgado, E., Iwata, H., Masuda, N., Otero, M.T., Gokmen, E., Loi, S., Guo, Z., Zhao, J., Aktan, G., Karantza, V., Schmid, P., Luis, F., Gonzalo, G.A., Diego, K., Ruben, K., Matias, M., Mirta, V., Sally, B.-H., Stephen, B., Philip, C., Sherene, L., Dhanusha, S., Andrea, G., Donatienne, T., Carlos, B., Leandro, B., Fabiano, C., Ruffo, d.F.J., Roberto, H., Domicio Carvalho, L., Fernando Cezar Toniazzi, L., Roberto Odebrecht, R., Antonio Orlando, S.N., Felipe, S., David, C., Danielle, C., Cristiano, F., Xinni, S., Joanne, Y., Alejandro, A., Carlos, G., Claudio, S., Cesar, S., Eduardo, Y., Alvaro, G.D., Jesus, S., Petra, H., Zdenek, K., Bohuslav, M., Katarina, P., Jana, P., Vesna, G., Erik, J., Jeanette, J., Soren, L., Tamas, L., Herve, B., Isabelle, D., Anthony, G., Anne-Claire, H.-B., Luis, T., Jens-Uwe, B., Peter, F., Dirk, F., Nadia, H., Jens, H., Anna, K.F.d.S., Christian, K., Sibylle, L., Diana, L., Tjoung-Won, P.-S., Raquel Von, S., Pauline, W., Louis, C., Ava, K., Kai Cheong Roger, N., Peter, A., Tibor, C., Zsuzsanna, K., Laszlo, L., Karoly, M., Gabor, R., John, C., Catherine, K., Seamus, O.R., Saverio, C., Antonietta, D., Enrico, R., Tomoyuki, A., Takaaki, F., Kenichi, I., *et al.* (2020) 'Pembrolizumab plus chemotherapy versus placebo plus chemotherapy for previously untreated locally recurrent inoperable or metastatic triple-negative breast cancer (KEYNOTE-355): a randomised, placebo-controlled, double-blind, phase 3 clinical trial', *The Lancet*, 396(10265), 1817-1828, available: [http://dx.doi.org/10.1016/S0140-6736\(20\)32531-9](http://dx.doi.org/10.1016/S0140-6736(20)32531-9).

Craddock, J.A., Lu, A., Bear, A., Pule, M., Brenner, M.K., Rooney, C.M. and Foster, A.E. (2010) 'Enhanced tumor trafficking of GD2 chimeric antigen receptor T cells by expression of the chemokine receptor CCR2b', *Journal of immunotherapy (Hagerstown, Md. : 1997)*, 33(8), 780-788, available: <http://dx.doi.org/10.1097/CJI.0b013e3181ee6675>.

Croix, B.S., Rago, C., Velculescu, V., Traverso, G., Romans, K.E., Montgomery, E., Lal, A., Riggins, G.J., Lengauer, C., Vogelstein, B. and Kinzler, K.W. (2000) 'Genes Expressed in Human Tumor Endothelium', *Science*, 289(5482), 1197, available: <http://dx.doi.org/10.1126/science.289.5482.1197>.

CRUK (2022) *Breast Cancer Statistics*, available: <https://www.cancerresearchuk.org/health-professional/cancer-statistics/statistics-by-cancer-type/breast-cancer#heading-Zero> [accessed 3rd March].

Cruz, C.R., Micklethwaite, K.P., Savoldo, B., Ramos, C.A., Lam, S., Ku, S., Diouf, O., Liu, E., Barrett, A.J., Ito, S., Shpall, E.J., Krance, R.A., Kamble, R.T., Carrum, G., Hosing, C.M., Gee, A.P., Mei, Z., Grilley, B.J., Heslop, H.E., Rooney, C.M., Brenner, M.K., Bollard, C.M. and Dotti, G. (2013) 'Infusion of donor-derived CD19-redirected virus-specific T cells for B-cell malignancies relapsed after allogeneic stem cell transplant: a phase 1 study', *Blood*, 122(17), 2965-73, available: <http://dx.doi.org/10.1182/blood-2013-06-506741>.

Cullen, M., Seaman, S., Chaudhary, A., Yang, M.Y., Hilton, M.B., Logsdon, D., Haines, D.C., Tessarollo, L. and St Croix, B. (2009) 'Host-derived tumor endothelial marker 8

References

- promotes the growth of melanoma', *Cancer Res*, 69(15), 6021-6026, available: <http://dx.doi.org/10.1158/0008-5472.CAN-09-1086>.
- D'Angelo, S.P., Hamid, O.A., Tarhini, A., Schadendorf, D., Chmielowski, B., Collichio, F.A., Pavlick, A.C., Lewis, K.D., Weil, S.C., Heyburn, J., Schweizer, C., O'Shannessy, D.J. and Carvajal, R.D. (2018) 'A phase 2 study of ontuxizumab, a monoclonal antibody targeting endosialin, in metastatic melanoma', *Invest New Drugs*, 36(1), 103-113, available: <http://dx.doi.org/10.1007/s10637-017-0530-4>.
- Davila, M.L., Riviere, I., Wang, X., Bartido, S., Park, J., Curran, K., Chung, S.S., Stefanski, J., Borquez-Ojeda, O., Olszewska, M., Qu, J., Wasielewska, T., He, Q., Fink, M., Shinglot, H., Youssif, M., Satter, M., Wang, Y., Hosey, J., Quintanilla, H., Halton, E., Bernal, Y., Bouhassira, D.C., Arcila, M.E., Gonen, M., Roboz, G.J., Maslak, P., Douer, D., Frattini, M.G., Giral, S., Sadelain, M. and Brentjens, R. (2014) 'Efficacy and toxicity management of 19-28z CAR T cell therapy in B cell acute lymphoblastic leukemia', *Science translational medicine*, 6(224), 224ra25, available: <http://dx.doi.org/10.1126/scitranslmed.3008226>.
- de Kruijf, E.M., van Nes, J.G.H., van de Velde, C.J.H., Putter, H., Smit, V.T.H.B.M., Liefers, G.J., Kuppen, P.J.K., Tollenaar, R.A.E.M. and Mesker, W.E. (2011) 'Tumor–stroma ratio in the primary tumor is a prognostic factor in early breast cancer patients, especially in triple-negative carcinoma patients', *Breast Cancer Research and Treatment*, 125(3), 687-696, available: <http://dx.doi.org/10.1007/s10549-010-0855-6>.
- De Munter, S., Van Parys, A., Bral, L., Ingels, J., Goetgeluk, G., Bonte, S., Pille, M., Billiet, L., Weening, K., Verhee, A., Van der Heyden, J., Taghon, T., Leclercq, G., Kerre, T., Tavernier, J. and Vandekerckhove, B. (2020) 'Rapid and Effective Generation of Nanobody Based CARs using PCR and Gibson Assembly', *Int J Mol Sci*, 21(3), available: <http://dx.doi.org/10.3390/ijms21030883>.
- Dekker, T.J.A., van de Velde, C.J.H., van Pelt, G.W., Kroep, J.R., Julien, J.P., Smit, V.T.H.B.M., Tollenaar, R.A.E.M. and Mesker, W.E. (2013) 'Prognostic significance of the tumor-stroma ratio: validation study in node-negative premenopausal breast cancer patients from the EORTC perioperative chemotherapy (POP) trial (10854)', *Breast Cancer Research and Treatment*, 139(2), 371-379, available: <http://dx.doi.org/10.1007/s10549-013-2571-5>.
- Di Matteo, A., Franceschini, M., Chiarella, S., Rocchio, S., Travaglini-Allocatelli, C. and Federici, L. (2016) 'Molecules that target nucleophosmin for cancer treatment: an update', *Oncotarget*, 7(28), 44821-44840, available: <http://dx.doi.org/10.18632/oncotarget.8599>.
- Di Stasi, A., De Angelis, B., Rooney, C.M., Zhang, L., Mahendravada, A., Foster, A.E., Heslop, H.E., Brenner, M.K., Dotti, G. and Savoldo, B. (2009) 'T lymphocytes coexpressing CCR4 and a chimeric antigen receptor targeting CD30 have improved homing and antitumor

References

- activity in a Hodgkin tumor model', *Blood*, 113(25), 6392-402, available: <http://dx.doi.org/10.1182/blood-2009-03-209650>.
- Di Stasi, A., Tey, S.K., Dotti, G., Fujita, Y., Kennedy-Nasser, A., Martinez, C., Straathof, K., Liu, E., Durett, A.G., Grilley, B., Liu, H., Cruz, C.R., Savoldo, B., Gee, A.P., Schindler, J., Krance, R.A., Heslop, H.E., Spencer, D.M., Rooney, C.M. and Brenner, M.K. (2011) 'Inducible apoptosis as a safety switch for adoptive cell therapy', *N Engl J Med*, 365(18), 1673-83, available: <http://dx.doi.org/10.1056/NEJMoa1106152>.
- Diaconu, I., Ballard, B., Zhang, M., Chen, Y., West, J., Dotti, G. and Savoldo, B. (2017) 'Inducible Caspase-9 Selectively Modulates the Toxicities of CD19-Specific Chimeric Antigen Receptor-Modified T Cells', *Mol Ther*, 25(3), 580-592, available: <http://dx.doi.org/10.1016/j.ymthe.2017.01.011>.
- Diaz, L.A., Jr., Coughlin, C.M., Weil, S.C., Fishel, J., Gounder, M.M., Lawrence, S., Azad, N., O'Shannessy, D.J., Grasso, L., Wustner, J., Ebel, W. and Carvajal, R.D. (2015) 'A first-in-human phase I study of MORAb-004, a monoclonal antibody to endosialin in patients with advanced solid tumors', *Clinical cancer research : an official journal of the American Association for Cancer Research*, 21(6), 1281-1288, available: <http://dx.doi.org/10.1158/1078-0432.CCR-14-1829>.
- Dimitriou, F., Matter, A.V., Mangana, J., Urosevic-Maiwald, M., Micaletto, S., Braun, R.P., French, L.E. and Dummer, R. (2019) 'Cytokine Release Syndrome During Sequential Treatment With Immune Checkpoint Inhibitors and Kinase Inhibitors for Metastatic Melanoma', *Journal of immunotherapy (Hagerstown, Md. : 1997)*, 42(1), 29-32, available: <http://dx.doi.org/10.1097/cji.000000000000236>.
- Dittmer, J. (2017) 'Mechanisms governing metastatic dormancy in breast cancer', *Semin Cancer Biol*, 44, 72-82, available: <http://dx.doi.org/10.1016/j.semcancer.2017.03.006>.
- Doi, T., Aramaki, T., Yasui, H., Muro, K., Ikeda, M., Okusaka, T., Inaba, Y., Nakai, K., Ikezawa, H. and Nakajima, R. (2019) 'A phase I study of ontuxizumab, a humanized monoclonal antibody targeting endosialin, in Japanese patients with solid tumors', *Invest New Drugs*, 37(5), 1061-1074, available: <http://dx.doi.org/10.1007/s10637-018-0713-7>.
- Dolznic, H., Schweifer, N., Puri, C., Kraut, N., Rettig, W.J., Kerjaschki, D. and Garin-Chesa, P. (2005) 'Characterization of cancer stroma markers: In silico&/em> analysis of an mRNA expression database for fibroblast activation protein and endosialin', *Cancer Immunity Archive*, 5(1), 10.
- Döme, B., Paku, S., Somlai, B. and Tímár, J. (2002) 'Vascularization of cutaneous melanoma involves vessel co-option and has clinical significance', *J Pathol*, 197(3), 355-62, available: <http://dx.doi.org/10.1002/path.1124>.

References

- Dotti, G., Gottschalk, S., Savoldo, B. and Brenner, M.K. (2014) 'Design and development of therapies using chimeric antigen receptor-expressing T cells', *Immunol Rev*, 257(1), 107-26, available: <http://dx.doi.org/10.1111/imr.12131>.
- Drent, E., Poels, R., Mulders, M.J., van de Donk, N., Themeli, M., Lokhorst, H.M. and Mutis, T. (2018) 'Feasibility of controlling CD38-CAR T cell activity with a Tet-on inducible CAR design', *PLOS ONE*, 13(5), e0197349, available: <http://dx.doi.org/10.1371/journal.pone.0197349>.
- Drummond, R., Cauvi, D.M., Hawisher, D., Song, D., Niño, D.F., Coimbra, R., Bickler, S. and De Maio, A. (2012a) 'Deletion of scavenger receptor A gene in mice resulted in protection from septic shock and modulation of TLR4 signaling in isolated peritoneal macrophages', *Innate Immunity*, 19(1), 30-41, available: <http://dx.doi.org/10.1177/1753425912449548>.
- Drummond, R., Song, D., Hawisher, D., Wolf, P.L., Vazquez, D.E., Nino, D., Coimbra, R., Cauvi, D.M. and De Maio, A. (2012b) 'Acute acalculous cholecystitis-like phenotype in scavenger receptor A knockout mice', *The Journal of Surgical Research*, 174(2), 344-351, available: <http://dx.doi.org/10.1016/j.jss.2010.12.033>.
- Dudley, M.E., Yang, J.C., Sherry, R., Hughes, M.S., Royal, R., Kammula, U., Robbins, P.F., Huang, J., Citrin, D.E., Leitman, S.F., Wunderlich, J., Restifo, N.P., Thomasian, A., Downey, S.G., Smith, F.O., Klapper, J., Morton, K., Laurencot, C., White, D.E. and Rosenberg, S.A. (2008) 'Adoptive Cell Therapy for Patients With Metastatic Melanoma: Evaluation of Intensive Myeloablative Chemoradiation Preparative Regimens', *Journal of Clinical Oncology*, 26(32), 5233-5239, available: <http://dx.doi.org/10.1200/JCO.2008.16.5449>.
- Duong, M.T., Collinson-Pautz, M.R., Morschl, E., Lu, A., Szymanski, S.P., Zhang, M., Brandt, M.E., Chang, W.C., Sharp, K.L., Toler, S.M., Slawin, K.M., Foster, A.E., Spencer, D.M. and Bayle, J.H. (2019) 'Two-Dimensional Regulation of CAR-T Cell Therapy with Orthogonal Switches', *Molecular therapy oncolytics*, 12, 124-137, available: <http://dx.doi.org/10.1016/j.omto.2018.12.009>.
- Easton, D.F., Pooley, K.A., Dunning, A.M., Pharoah, P.D.P., Thompson, D., Ballinger, D.G., Struewing, J.P., Morrison, J., Field, H., Luben, R., Wareham, N., Ahmed, S., Healey, C.S., Bowman, R., Luccarini, C., Conroy, D., Shah, M., Munday, H., Jordan, C., Perkins, B., West, J., Redman, K., Driver, K., Meyer, K.B., Haiman, C.A., Kolonel, L.K., Henderson, B.E., Le Marchand, L., Brennan, P., Sangrajrang, S., Gaborieau, V., Odefrey, F., Shen, C.-Y., Wu, P.-E., Wang, H.-C., Eccles, D., Evans, D.G., Peto, J., Fletcher, O., Johnson, N., Seal, S., Stratton, M.R., Rahman, N., Chenevix-Trench, G., Bojesen, S.E., Nordestgaard, B.G., Axelsson, C.K., Garcia-Closas, M., Brinton, L., Chanock, S., Lissowska, J., Peplonska, B., Nevanlinna, H., Fagerholm, R., Eerola, H., Kang, D., Yoo, K.-Y., Noh, D.-Y., Ahn, S.-H., Hunter, D.J., Hankinson, S.E., Cox, D.G., Hall, P., Wedren, S., Liu, J., Low, Y.-L., Bogdanova, N., Schürmann, P., Dörk, T., Tollenaar, R.A.E.M., Jacobi, C.E., Devilee, P., Klijn, J.G.M., Sigurdson, A.J., Doody, M.M., Alexander, B.H., Zhang, J., Cox, A., Brock, I.W., MacPherson, G., Reed, M.W.R., Couch, F.J., Goode, E.L., Olson, J.E., Meijers-Heijboer, H., van den Ouweland, A., Uitterlinden, A., Rivadeneira, F., Milne, R.L., Ribas,

References

- G., Gonzalez-Neira, A., Benitez, J., Hopper, J.L., McCredie, M., Southey, M., Giles, G.G., Schroen, C., Justenhoven, C., Brauch, H., Hamann, U., *et al.* (2007) 'Genome-wide association study identifies novel breast cancer susceptibility loci', *Nature*, 447(7148), 1087-1093, available: <http://dx.doi.org/10.1038/nature05887>.
- Ebright, R.Y., Zachariah, M.A., Micalizzi, D.S., Wittner, B.S., Niederhoffer, K.L., Nieman, L.T., Chirn, B., Wiley, D.F., Wesley, B., Shaw, B., Nieblas-Bedolla, E., Atlas, L., Szabolcs, A., lafrate, A.J., Toner, M., Ting, D.T., Brastianos, P.K., Haber, D.A. and Maheswaran, S. (2020) 'HIF1A signaling selectively supports proliferation of breast cancer in the brain', *Nature communications*, 11(1), 6311, available: <http://dx.doi.org/10.1038/s41467-020-20144-w>.
- Eckhardt, B.L., Parker, B.S., van Laar, R.K., Restall, C.M., Natoli, A.L., Tavaría, M.D., Stanley, K.L., Sloan, E.K., Moseley, J.M. and Anderson, R.L. (2005) 'Genomic analysis of a spontaneous model of breast cancer metastasis to bone reveals a role for the extracellular matrix', *Mol Cancer Res*, 3(1), 1-13.
- Enblad, G., Karlsson, H., Gammelgård, G., Wenthe, J., Lövgren, T., Amini, R.M., Wikstrom, K.I., Essand, M., Savoldo, B., Hallböök, H., Höglund, M., Dotti, G., Brenner, M.K., Hagberg, H. and Loskog, A. (2018) 'A Phase I/IIa Trial Using CD19-Targeted Third-Generation CAR T Cells for Lymphoma and Leukemia', *Clinical Cancer Research*, 24(24), 6185, available: <http://dx.doi.org/10.1158/1078-0432.CCR-18-0426>.
- Erdogan, B. and Webb, D.J. (2017) 'Cancer-associated fibroblasts modulate growth factor signaling and extracellular matrix remodeling to regulate tumor metastasis', *Biochem Soc Trans*, 45(1), 229-236, available: <http://dx.doi.org/10.1042/bst20160387>.
- Eyquem, J., Mansilla-Soto, J., Giavridis, T., van der Stegen, S.J., Hamieh, M., Cunanan, K.M., Odak, A., Gonen, M. and Sadelain, M. (2017) 'Targeting a CAR to the TRAC locus with CRISPR/Cas9 enhances tumour rejection', *Nature*, 543(7643), 113-117, available: <http://dx.doi.org/10.1038/nature21405>.
- Farrington-Rock, C., Crofts, N.J., Doherty, M.J., Ashton, B.A., Griffin-Jones, C. and Canfield, A.E. (2004) 'Chondrogenic and adipogenic potential of microvascular pericytes', *Circulation*, 110(15), 2226-32, available: <http://dx.doi.org/10.1161/01.Cir.0000144457.55518.E5>.
- Feldmann, A., Arndt, C., Bergmann, R., Loff, S., Cartellieri, M., Bachmann, D., Aliperta, R., Hetzenecker, M., Ludwig, F., Albert, S., Ziller-Walter, P., Kegler, A., Koristka, S., Gärtner, S., Schmitz, M., Ehninger, A., Ehninger, G., Pietzsch, J., Steinbach, J. and Bachmann, M. (2017) 'Retargeting of T lymphocytes to PSCA- or PSMA positive prostate cancer cells using the novel modular chimeric antigen receptor platform technology "UniCAR"', *Oncotarget*, 8(19), 31368-31385, available: <http://dx.doi.org/10.18632/oncotarget.15572>.

References

- Fernando, S. and Fletcher, B.S. (2009) 'Targeting tumor endothelial marker 8 in the tumor vasculature of colorectal carcinomas in mice', *Cancer Res*, 69(12), 5126-32, available: <http://dx.doi.org/10.1158/0008-5472.Can-09-0725>.
- Fierle, J.K., Brioschi, M., de Tiani, M., Wetterwald, L., Atsaves, V., Abram-Saliba, J., Petrova, T.V., Coukos, G. and Dunn, S.M. (2021) 'Soluble trivalent engagers redirect cytolytic T cell activity toward tumor endothelial marker 1', *Cell Reports Medicine*, 2(8), 100362, available: <http://dx.doi.org/https://doi.org/10.1016/j.xcrm.2021.100362>.
- Finak, G., Bertos, N., Pepin, F., Sadekova, S., Souleimanova, M., Zhao, H., Chen, H., Omeroglu, G., Meterissian, S., Omeroglu, A., Hallett, M. and Park, M. (2008) 'Stromal gene expression predicts clinical outcome in breast cancer', *Nat Med*, 14(5), 518-27, available: <http://dx.doi.org/10.1038/nm1764>.
- Finney, H.M., Akbar, A.N. and Lawson, A.D. (2004) 'Activation of resting human primary T cells with chimeric receptors: costimulation from CD28, inducible costimulator, CD134, and CD137 in series with signals from the TCR zeta chain', *J Immunol*, 172(1), 104-13, available: <http://dx.doi.org/10.4049/jimmunol.172.1.104>.
- Finney, H.M., Lawson, A.D., Bebbington, C.R. and Weir, A.N. (1998) 'Chimeric receptors providing both primary and costimulatory signaling in T cells from a single gene product', *J Immunol*, 161(6), 2791-7.
- Ford, K., Hanley, C.J., Mellone, M., Szyndralewicz, C., Heitz, F., Wiesel, P., Wood, O., Machado, M., Lopez, M.A., Ganesan, A.P., Wang, C., Chakravarthy, A., Fenton, T.R., King, E.V., Vijayanand, P., Ottensmeier, C.H., Al-Shamkhani, A., Savelyeva, N. and Thomas, G.J. (2020) 'NOX4 Inhibition Potentiates Immunotherapy by Overcoming Cancer-Associated Fibroblast-Mediated CD8 T-cell Exclusion from Tumors', *Cancer Res*, 80(9), 1846-1860, available: <http://dx.doi.org/10.1158/0008-5472.Can-19-3158>.
- Frantz, C., Stewart, K.M. and Weaver, V.M. (2010) 'The extracellular matrix at a glance', *Journal of Cell Science*, 123(24), 4195, available: <http://dx.doi.org/10.1242/jcs.023820>.
- Freeman, G.J., Long, A.J., Iwai, Y., Bourque, K., Chernova, T., Nishimura, H., Fitz, L.J., Malenkovich, N., Okazaki, T., Byrne, M.C., Horton, H.F., Fouser, L., Carter, L., Ling, V., Bowman, M.R., Carreno, B.M., Collins, M., Wood, C.R. and Honjo, T. (2000) 'Engagement of the PD-1 immunoinhibitory receptor by a novel B7 family member leads to negative regulation of lymphocyte activation', *J Exp Med*, 192(7), 1027-34, available: <http://dx.doi.org/10.1084/jem.192.7.1027>.
- Frey, N.V., Shaw, P.A., Hexner, E.O., Gill, S., Marcucci, K., Luger, S.M., Mangan, J.K., Grupp, S.A., Maude, S.L., Ericson, S., Levine, B., Lacey, S.F., Melenhorst, J.J., June, C.H. and Porter, D.L. (2016) 'Optimizing chimeric antigen receptor (CAR) T cell therapy for adult patients with relapsed or refractory (r/r) acute lymphoblastic leukemia (ALL)', *Journal*

References

- of Clinical Oncology*, 34(15_suppl), 7002-7002, available: http://dx.doi.org/10.1200/JCO.2016.34.15_suppl.7002.
- Friedman, K.M., Garrett, T.E., Evans, J.W., Horton, H.M., Latimer, H.J., Seidel, S.L., Horvath, C.J. and Morgan, R.A. (2018) 'Effective Targeting of Multiple B-Cell Maturation Antigen-Expressing Hematological Malignancies by Anti-B-Cell Maturation Antigen Chimeric Antigen Receptor T Cells', *Hum Gene Ther*, 29(5), 585-601, available: <http://dx.doi.org/10.1089/hum.2018.001>.
- Fu, W., Lei, C., Liu, S., Cui, Y., Wang, C., Qian, K., Li, T., Shen, Y., Fan, X., Lin, F., Ding, M., Pan, M., Ye, X., Yang, Y. and Hu, S. (2019) 'CAR exosomes derived from effector CAR-T cells have potent antitumour effects and low toxicity', *Nature communications*, 10(1), 4355, available: <http://dx.doi.org/10.1038/s41467-019-12321-3>.
- Fu, X., Rivera, A., Tao, L. and Zhang, X. (2013) 'Genetically modified T cells targeting neovasculature efficiently destroy tumor blood vessels, shrink established solid tumors and increase nanoparticle delivery', *Int J Cancer*, 133(10), 2483-92, available: <http://dx.doi.org/10.1002/ijc.28269>.
- Fujiwara, K., Masutani, M., Tachibana, M. and Okada, N. (2020) 'Impact of scFv structure in chimeric antigen receptor on receptor expression efficiency and antigen recognition properties', *Biochemical and Biophysical Research Communications*, 527(2), 350-357, available: <http://dx.doi.org/https://doi.org/10.1016/j.bbrc.2020.03.071>.
- Furuhashi, M., Sjöblom, T., Abramsson, A., Ellingsen, J., Micke, P., Li, H., Bergsten-Folestad, E., Eriksson, U., Heuchel, R., Betsholtz, C., Heldin, C.-H. and Östman, A. (2004) 'Platelet-Derived Growth Factor Production by B16 Melanoma Cells Leads to Increased Pericyte Abundance in Tumors and an Associated Increase in Tumor Growth Rate', *Cancer Res*, 64(8), 2725, available: <http://dx.doi.org/10.1158/0008-5472.CAN-03-1489>.
- Fuyuhiko, Y., Yashiro, M., Noda, S., Matsuoka, J., Hasegawa, T., Kato, Y., Sawada, T. and Hirakawa, K. (2012) 'Cancer-associated orthotopic myofibroblasts stimulates the motility of gastric carcinoma cells', *Cancer science*, 103(4), 797-805, available: <http://dx.doi.org/10.1111/j.1349-7006.2012.02209.x>.
- Gabbiani, G., Ryan, G.B. and Majne, G. (1971) 'Presence of modified fibroblasts in granulation tissue and their possible role in wound contraction', *Experientia*, 27(5), 549-50, available: <http://dx.doi.org/10.1007/bf02147594>.
- Gaengel, K., Genové, G., Armulik, A. and Betsholtz, C. (2009) 'Endothelial-Mural Cell Signaling in Vascular Development and Angiogenesis', *Arterioscler Thromb Vasc Biol*, 29(5), 630-638, available: <http://dx.doi.org/10.1161/ATVBAHA.107.161521>.

References

- Garin-Chesa, P., Old, L.J. and Rettig, W.J. (1990) 'Cell surface glycoprotein of reactive stromal fibroblasts as a potential antibody target in human epithelial cancers', *Proc Natl Acad Sci U S A*, 87(18), 7235-9, available: <http://dx.doi.org/10.1073/pnas.87.18.7235>.
- Generali, D., Berruti, A., Brizzi, M.P., Campo, L., Bonardi, S., Wigfield, S., Bersiga, A., Allevi, G., Milani, M., Aguggini, S., Gandolfi, V., Dogliotti, L., Bottini, A., Harris, A.L. and Fox, S.B. (2006) 'Hypoxia-inducible factor-1alpha expression predicts a poor response to primary chemoendocrine therapy and disease-free survival in primary human breast cancer', *Clinical cancer research : an official journal of the American Association for Cancer Research*, 12(15), 4562-8, available: <http://dx.doi.org/10.1158/1078-0432.Ccr-05-2690>.
- Ghorashian, S., Kramer, A.M., Onuoha, S., Wright, G., Bartram, J., Richardson, R., Albon, S.J., Casanovas-Company, J., Castro, F., Popova, B., Villanueva, K., Yeung, J., Vetharoy, W., Guvenel, A., Wawrzyniecka, P.A., Mekkaoui, L., Cheung, G.W., Pinner, D., Chu, J., Lucchini, G., Silva, J., Ciocarlie, O., Lazareva, A., Inglott, S., Gilmour, K.C., Ahsan, G., Ferrari, M., Manzoor, S., Champion, K., Brooks, T., Lopes, A., Hackshaw, A., Farzaneh, F., Chiesa, R., Rao, K., Bonney, D., Samarasinghe, S., Goulden, N., Vora, A., Veys, P., Hough, R., Wynn, R., Pule, M.A. and Amrolia, P.J. (2019) 'Enhanced CAR T cell expansion and prolonged persistence in pediatric patients with ALL treated with a low-affinity CD19 CAR', *Nat Med*, 25(9), 1408-1414, available: <http://dx.doi.org/10.1038/s41591-019-0549-5>.
- Gianni, L., Romieu, G.H., Lichinitser, M., Serrano, S.V., Mansutti, M., Pivot, X., Mariani, P., Andre, F., Chan, A., Lipatov, O., Chan, S., Wardley, A., Greil, R., Moore, N., Prot, S., Pallaud, C. and Semiglazov, V. (2013) 'AVEREL: a randomized phase III Trial evaluating bevacizumab in combination with docetaxel and trastuzumab as first-line therapy for HER2-positive locally recurrent/metastatic breast cancer', *Journal of clinical oncology : official journal of the American Society of Clinical Oncology*, 31(14), 1719-25, available: <http://dx.doi.org/10.1200/jco.2012.44.7912>.
- Giavridis, T., van der Stegen, S.J.C., Eyquem, J., Hamieh, M., Piersigilli, A. and Sadelain, M. (2018) 'CAR T cell-induced cytokine release syndrome is mediated by macrophages and abated by IL-1 blockade', *Nat Med*, 24(6), 731-738, available: <http://dx.doi.org/10.1038/s41591-018-0041-7>.
- Giordano-Attianese, G., Gainza, P., Gray-Gaillard, E., Cribioli, E., Shui, S., Kim, S., Kwak, M.-J., Vollers, S., Corria Osorio, A.D.J., Reichenbach, P., Bonet, J., Oh, B.-H., Irving, M., Coukos, G. and Correia, B.E. (2020) 'A computationally designed chimeric antigen receptor provides a small-molecule safety switch for T-cell therapy', *Nature Biotechnology*, 38(4), 426-432, available: <http://dx.doi.org/10.1038/s41587-019-0403-9>.
- Gomes da Silva, D., Mukherjee, M., Srinivasan, M., Dakhova, O., Liu, H., Grilley, B., Gee, A.P., Neelapu, S.S., Rooney, C.M., Heslop, H.E., Savoldo, B., Dotti, G., Brenner, M.K., Mamonkin, M. and Ramos, C.A. (2016) 'Direct Comparison of In Vivo Fate of Second and Third-Generation CD19-Specific Chimeric Antigen Receptor (CAR)-T Cells in

References

- Patients with B-Cell Lymphoma: Reversal of Toxicity from Tonic Signaling', *Blood*, 128(22), 1851-1851, available: <http://dx.doi.org/10.1182/blood.V128.22.1851.1851>.
- Grada, Z., Hegde, M., Byrd, T., Shaffer, D.R., Ghazi, A., Brawley, V.S., Corder, A., Schönfeld, K., Koch, J., Dotti, G., Heslop, H.E., Gottschalk, S., Wels, W.S., Baker, M.L. and Ahmed, N. (2013) 'TanCAR: A Novel Bispecific Chimeric Antigen Receptor for Cancer Immunotherapy', *Molecular therapy. Nucleic acids*, 2(7), e105-e105, available: <http://dx.doi.org/10.1038/mtna.2013.32>.
- Gregório, A.C., Fonseca, N.A., Moura, V., Lacerda, M., Figueiredo, P., Simões, S., Dias, S. and Moreira, J.N. (2016) 'Inoculated Cell Density as a Determinant Factor of the Growth Dynamics and Metastatic Efficiency of a Breast Cancer Murine Model', *PLOS ONE*, 11(11), e0165817, available: <http://dx.doi.org/10.1371/journal.pone.0165817>.
- Gross, G., Gorochov, G., Waks, T. and Eshhar, Z. (1989) 'Generation of effector T cells expressing chimeric T cell receptor with antibody type-specificity', *Transplant Proc*, 21(1 Pt 1), 127-30.
- Grothey, A., Strosberg, J.R., Renfro, L.A., Hurwitz, H.I., Marshall, J.L., Safran, H., Guarino, M.J., Kim, G.P., Hecht, J.R., Weil, S.C., Heyburn, J., Wang, W., Schweizer, C., O'Shannessy, D.J. and Diaz, L.A., Jr. (2018) 'A Randomized, Double-Blind, Placebo-Controlled Phase II Study of the Efficacy and Safety of Monotherapy Ontuxizumab (MORAb-004) Plus Best Supportive Care in Patients with Chemorefractory Metastatic Colorectal Cancer', *Clinical cancer research : an official journal of the American Association for Cancer Research*, 24(2), 316-325, available: <http://dx.doi.org/10.1158/1078-0432.Ccr-17-1558>.
- Gruber, G., Greiner, R.H., Hlushchuk, R., Aebersold, D.M., Altermatt, H.J., Berclaz, G. and Djonov, V. (2004) 'Hypoxia-inducible factor 1 alpha in high-risk breast cancer: an independent prognostic parameter?', *Breast Cancer Res*, 6(3), R191-8, available: <http://dx.doi.org/10.1186/bcr775>.
- Grupp, S.A., Kalos, M., Barrett, D., Aplenc, R., Porter, D.L., Rheingold, S.R., Teachey, D.T., Chew, A., Hauck, B., Wright, J.F., Milone, M.C., Levine, B.L. and June, C.H. (2013) 'Chimeric antigen receptor-modified T cells for acute lymphoid leukemia', *N Engl J Med*, 368(16), 1509-1518, available: <http://dx.doi.org/10.1056/NEJMoa1215134>.
- Gu, X., He, D., Li, C., Wang, H. and Yang, G. (2018) 'Development of Inducible CD19-CAR T Cells with a Tet-On System for Controlled Activity and Enhanced Clinical Safety', *Int J Mol Sci*, 19(11), available: <http://dx.doi.org/10.3390/ijms19113455>.
- Guo, P., Hu, B., Gu, W., Xu, L., Wang, D., Huang, H.-J.S., Cavenee, W.K. and Cheng, S.-Y. (2003) 'Platelet-Derived Growth Factor-B Enhances Glioma Angiogenesis by Stimulating Vascular Endothelial Growth Factor Expression in Tumor Endothelia and by Promoting

References

- Pericyte Recruitment', *Am J Pathol*, 162(4), 1083-1093, available: [http://dx.doi.org/https://doi.org/10.1016/S0002-9440\(10\)63905-3](http://dx.doi.org/https://doi.org/10.1016/S0002-9440(10)63905-3).
- Guo, Y., Hu, J., Wang, Y., Peng, X., Min, J., Wang, J., Matthaiou, E., Cheng, Y., Sun, K., Tong, X., Fan, Y., Zhang, P.J., Kandalaf, L.E., Irving, M., Coukos, G. and Li, C. (2018) 'Tumour endothelial marker 1/endosialin-mediated targeting of human sarcoma', *Eur J Cancer*, 90, 111-121, available: <http://dx.doi.org/10.1016/j.ejca.2017.10.035>.
- Gust, J., Hay, K.A., Hanafi, L.-A., Li, D., Myerson, D., Gonzalez-Cuyar, L.F., Yeung, C., Liles, W.C., Wurfel, M., Lopez, J.A., Chen, J., Chung, D., Harju-Baker, S., Özpolat, T., Fink, K.R., Riddell, S.R., Maloney, D.G. and Turtle, C.J. (2017) 'Endothelial Activation and Blood-Brain Barrier Disruption in Neurotoxicity after Adoptive Immunotherapy with CD19 CAR-T Cells', *Cancer discovery*, 7(12), 1404-1419, available: <http://dx.doi.org/10.1158/2159-8290.CD-17-0698>.
- Guyach, S.E., Bryan, M.A. and Norris, K.A. (2009) 'Differences in antibody and immune responses between Balb/c and C57Bl/6 mice infected with *Trypanosoma cruzi* (129.5)', *The Journal of Immunology*, 182(1 Supplement), 129.5-129.5.
- Hajari Taheri, F., Hassani, M., Sharifzadeh, Z., Behdani, M., Arashkia, A. and Abolhassani, M. (2019) 'T cell engineered with a novel nanobody-based chimeric antigen receptor against VEGFR2 as a candidate for tumor immunotherapy', *IUBMB Life*, 71(9), 1259-1267, available: <http://dx.doi.org/10.1002/iub.2019>.
- Hale, M., Lee, B., Honaker, Y., Leung, W.H., Grier, A.E., Jacobs, H.M., Sommer, K., Sahni, J., Jackson, S.W., Scharenberg, A.M., Astrakhan, A. and Rawlings, D.J. (2017) 'Homology-Directed Recombination for Enhanced Engineering of Chimeric Antigen Receptor T Cells', *Mol Ther Methods Clin Dev*, 4, 192-203, available: <http://dx.doi.org/10.1016/j.omtm.2016.12.008>.
- Hamieh, M., Dobrin, A., Cabriolu, A., van der Stegen, S.J.C., Giavridis, T., Mansilla-Soto, J., Eyquem, J., Zhao, Z., Whitlock, B.M., Miele, M.M., Li, Z., Cunanan, K.M., Huse, M., Hendrickson, R.C., Wang, X., Rivière, I. and Sadelain, M. (2019) 'CAR T cell trogocytosis and cooperative killing regulate tumour antigen escape', *Nature*, 568(7750), 112-116, available: <http://dx.doi.org/10.1038/s41586-019-1054-1>.
- Hanahan, D. (2022) 'Hallmarks of Cancer: New Dimensions', *Cancer discovery*, 12(1), 31-46, available: <http://dx.doi.org/10.1158/2159-8290.Cd-21-1059>.
- Hanahan, D. and Folkman, J. (1996) 'Patterns and Emerging Mechanisms of the Angiogenic Switch during Tumorigenesis', *Cell*, 86(3), 353-364, available: [http://dx.doi.org/https://doi.org/10.1016/S0092-8674\(00\)80108-7](http://dx.doi.org/https://doi.org/10.1016/S0092-8674(00)80108-7).
- Hanahan, D. and Weinberg, R.A. (2000) 'The hallmarks of cancer', *Cell*, 100(1), 57-70, available: [http://dx.doi.org/10.1016/s0092-8674\(00\)81683-9](http://dx.doi.org/10.1016/s0092-8674(00)81683-9).

References

- Hanahan, D. and Weinberg, Robert A. (2011) 'Hallmarks of Cancer: The Next Generation', *Cell*, 144(5), 646-674, available: <http://dx.doi.org/10.1016/j.cell.2011.02.013>.
- Hanly, A.M., Hayanga, A., Winter, D.C. and Bouchier-Hayes, D.J. (2005) 'Thrombomodulin: tumour biology and prognostic implications', *Eur J Surg Oncol*, 31(3), 217-20, available: <http://dx.doi.org/10.1016/j.ejso.2004.11.017>.
- Hara, T., Nakaoka, H.J., Hayashi, T., Mimura, K., Hoshino, D., Inoue, M., Nagamura, F., Murakami, Y., Seiki, M. and Sakamoto, T. (2017) 'Control of metastatic niche formation by targeting APBA3/Mint3 in inflammatory monocytes', *Proceedings of the National Academy of Sciences*, 114(22), E4416-E4424, available: <http://dx.doi.org/doi:10.1073/pnas.1703171114>.
- Harbeck, N., Penault-Llorca, F., Cortes, J., Gnant, M., Houssami, N., Poortmans, P., Ruddy, K., Tsang, J. and Cardoso, F. (2019) 'Breast cancer', *Nature Reviews Disease Primers*, 5(1), 66, available: <http://dx.doi.org/10.1038/s41572-019-0111-2>.
- Hardie, D.L., Baldwin, M.J., Naylor, A., Haworth, O.J., Hou, T.Z., Lax, S., Curnow, S.J., Willcox, N., MacFadyen, J., Isacke, C.M. and Buckley, C.D. (2011) 'The stromal cell antigen CD248 (endosialin) is expressed on naive CD8+ human T cells and regulates proliferation', *Immunology*, 133(3), 288-95, available: <http://dx.doi.org/10.1111/j.1365-2567.2011.03437.x>.
- Hartwich, J., Orr, W.S., Ng, C.Y., Spence, Y., Morton, C. and Davidoff, A.M. (2013) 'HIF-1 α activation mediates resistance to anti-angiogenic therapy in neuroblastoma xenografts', *J Pediatr Surg*, 48(1), 39-46, available: <http://dx.doi.org/10.1016/j.jpedsurg.2012.10.016>.
- Hasanov, Z., Ruckdeschel, T., Konig, C., Mogler, C., Kapel, S.S., Korn, C., Spegg, C., Eichwald, V., Wieland, M., Appak, S. and Augustin, H.G. (2017) 'Endosialin Promotes Atherosclerosis Through Phenotypic Remodeling of Vascular Smooth Muscle Cells', *Arterioscler Thromb Vasc Biol*, 37(3), 495-505, available: <http://dx.doi.org/10.1161/atvbaha.116.308455>.
- Hashizume, H., Baluk, P., Morikawa, S., McLean, J.W., Thurston, G., Roberge, S., Jain, R.K. and McDonald, D.M. (2000) 'Openings between defective endothelial cells explain tumor vessel leakiness', *Am J Pathol*, 156(4), 1363-1380, available: [http://dx.doi.org/10.1016/S0002-9440\(10\)65006-7](http://dx.doi.org/10.1016/S0002-9440(10)65006-7).
- Hassani, M., Hajari Taheri, F., Sharifzadeh, Z., Arashkia, A., Hadjati, J., van Weerden, W.M., Abdoli, S., Modarressi, M.H. and Abolhassani, M. (2020) 'Engineered Jurkat Cells for Targeting Prostate-Specific Membrane Antigen on Prostate Cancer Cells by Nanobody-Based Chimeric Antigen Receptor', *Iran Biomed J*, 24(2), 81-8.

References

- Hassani, M., Hajari Taheri, F., Sharifzadeh, Z., Arashkia, A., Hadjati, J., van Weerden, W.M., Modarressi, M.H. and Abolhassani, M. (2019) 'Construction of a chimeric antigen receptor bearing a nanobody against prostate a specific membrane antigen in prostate cancer', *J Cell Biochem*, 120(6), 10787-10795, available: <http://dx.doi.org/10.1002/jcb.28370>.
- Hay, K.A., Hanafi, L.-A., Li, D., Gust, J., Liles, W.C., Wurfel, M.M., López, J.A., Chen, J., Chung, D., Harju-Baker, S., Cherian, S., Chen, X., Riddell, S.R., Maloney, D.G. and Turtle, C.J. (2017) 'Kinetics and biomarkers of severe cytokine release syndrome after CD19 chimeric antigen receptor-modified T-cell therapy', *Blood*, 130(21), 2295-2306, available: <http://dx.doi.org/10.1182/blood-2017-06-793141>.
- Hayward, C.P.M., Hassell, J.A., Denomme, G.A., Rachubinski, R.A., Brown, C. and Kelton, J.G. (1995) 'The cDNA Sequence of Human Endothelial Cell Multimerin: A UNIQUE PROTEIN WITH RGDS, COILED-COIL, AND EPIDERMAL GROWTH FACTOR-LIKE DOMAINS AND A CARBOXYL TERMINUS SIMILAR TO THE GLOBULAR DOMAIN OF COMPLEMENT C1q AND COLLAGENS TYPE VIII AND X', *Journal of Biological Chemistry*, 270(31), 18246-18251.
- Heczey, A., Louis, C.U., Savoldo, B., Dakhova, O., Durett, A., Grilley, B., Liu, H., Wu, M.F., Mei, Z., Gee, A., Mehta, B., Zhang, H., Mahmood, N., Tashiro, H., Heslop, H.E., Dotti, G., Rooney, C.M. and Brenner, M.K. (2017) 'CAR T Cells Administered in Combination with Lymphodepletion and PD-1 Inhibition to Patients with Neuroblastoma', *Mol Ther*, 25(9), 2214-2224, available: <http://dx.doi.org/10.1016/j.ymthe.2017.05.012>.
- Hellstrom, M., Kalen, M., Lindahl, P., Abramsson, A. and Betsholtz, C. (1999) 'Role of PDGF-B and PDGFR-beta in recruitment of vascular smooth muscle cells and pericytes during embryonic blood vessel formation in the mouse', *Development*, 126(14), 3047-55.
- Hildemann, S.K., Eberlein, J., Davenport, B., Nguyen, T.T., Victorino, F. and Homann, D. (2013) 'High Efficiency of Antiviral CD4+ Killer T Cells', *PLOS ONE*, 8(4), e60420, available: <http://dx.doi.org/10.1371/journal.pone.0060420>.
- Hillyer, P., Mordelet, E., Flynn, G. and Male, D. (2003) 'Chemokines, chemokine receptors and adhesion molecules on different human endothelia: discriminating the tissue-specific functions that affect leucocyte migration', *Clin Exp Immunol*, 134(3), 431-41, available: <http://dx.doi.org/10.1111/j.1365-2249.2003.02323.x>.
- Hirata, E., Girotti, M.R., Viros, A., Hooper, S., Spencer-Dene, B., Matsuda, M., Larkin, J., Marais, R. and Sahai, E. (2015) 'Intravital imaging reveals how BRAF inhibition generates drug-tolerant microenvironments with high integrin β 1/FAK signaling', *Cancer Cell*, 27(4), 574-88, available: <http://dx.doi.org/10.1016/j.ccell.2015.03.008>.
- Hofheinz, R.D., al-Batran, S.E., Hartmann, F., Hartung, G., Jager, D., Renner, C., Tanswell, P., Kunz, U., Amelsberg, A., Kuthan, H. and Stehle, G. (2003) 'Stromal antigen targeting by

References

- a humanised monoclonal antibody: an early phase II trial of sibrotuzumab in patients with metastatic colorectal cancer', *Onkologie*, 26(1), 44-8, available: <http://dx.doi.org/10.1159/000069863>.
- Hong, Y.K., Lee, Y.C., Cheng, T.L., Lai, C.H., Hsu, C.K., Kuo, C.H., Hsu, Y.Y., Li, J.T., Chang, B.I., Ma, C.Y., Lin, S.W., Wang, K.C., Shi, G.Y. and Wu, H.L. (2019) 'Tumor Endothelial Marker 1 (TEM1/Endosialin/CD248) Enhances Wound Healing by Interacting with Platelet-Derived Growth Factor Receptors', *J Invest Dermatol*, 139(10), 2204-2214.e7, available: <http://dx.doi.org/10.1016/j.jid.2019.03.1149>.
- Honjo, O., Kubo, T., Sugaya, F., Nishizaka, T., Kato, K., Hirohashi, Y., Takahashi, H. and Torigoe, T. (2019) 'Severe cytokine release syndrome resulting in purpura fulminans despite successful response to nivolumab therapy in a patient with pleomorphic carcinoma of the lung: a case report', *Journal for ImmunoTherapy of Cancer*, 7(1), 97, available: <http://dx.doi.org/10.1186/s40425-019-0582-4>.
- Hosaka, K., Yang, Y., Seki, T., Fischer, C., Dubey, O., Fredlund, E., Hartman, J., Religa, P., Morikawa, H., Ishii, Y., Sasahara, M., Larsson, O., Cossu, G., Cao, R., Lim, S. and Cao, Y. (2016) 'Pericyte-fibroblast transition promotes tumor growth and metastasis', *Proc Natl Acad Sci U S A*, 113(38), E5618-27, available: <http://dx.doi.org/10.1073/pnas.1608384113>.
- Hossain, N., Sahaf, B., Abramian, M., Spiegel, J.Y., Kong, K., Kim, S., Mavroukakis, S., Oak, J., Natkunam, Y., Meyer, E.H., Frank, M.J., Feldman, S.A., Long, S.R., Qin, H., Fry, T.J., Muffly, L.S., Mackall, C.L. and Miklos, D.B. (2018) 'Phase I Experience with a Bi-Specific CAR Targeting CD19 and CD22 in Adults with B-Cell Malignancies', *Blood*, 132(Supplement 1), 490-490, available: <http://dx.doi.org/10.1182/blood-2018-99-110142>.
- Howard, S.C., Pui, C.-H. and Ribeiro, R.C. (2014) 'Chapter 4 - Tumor Lysis Syndrome' in Finkel, K. W. and Howard, S. C., eds., *Renal Disease in Cancer Patients* Academic Press, 39-64.
- Hoyos, V., Savoldo, B., Quintarelli, C., Mahendravada, A., Zhang, M., Vera, J., Heslop, H.E., Rooney, C.M., Brenner, M.K. and Dotti, G. (2010) 'Engineering CD19-specific T lymphocytes with interleukin-15 and a suicide gene to enhance their anti-lymphoma/leukemia effects and safety', *Leukemia*, 24(6), 1160-70, available: <http://dx.doi.org/10.1038/leu.2010.75>.
- Hu, B., Ren, J., Luo, Y., Keith, B., Young, R.M., Scholler, J., Zhao, Y. and June, C.H. (2017) 'Augmentation of Antitumor Immunity by Human and Mouse CAR T Cells Secreting IL-18', *Cell Rep*, 20(13), 3025-3033, available: <http://dx.doi.org/10.1016/j.celrep.2017.09.002>.
- Hurwitz, H., Fehrenbacher, L., Novotny, W., Cartwright, T., Hainsworth, J., Heim, W., Berlin, J., Baron, A., Griffing, S., Holmgren, E., Ferrara, N., Fyfe, G., Rogers, B., Ross, R. and

References

- Kabbinavar, F. (2004) 'Bevacizumab plus irinotecan, fluorouracil, and leucovorin for metastatic colorectal cancer', *N Engl J Med*, 350(23), 2335-42, available: <http://dx.doi.org/10.1056/NEJMoa032691>.
- Huyan, X.-H., Lin, Y.-P., Gao, T., Chen, R.-Y. and Fan, Y.-M. (2011) 'Immunosuppressive effect of cyclophosphamide on white blood cells and lymphocyte subpopulations from peripheral blood of Balb/c mice', *International Immunopharmacology*, 11(9), 1293-1297, available: <http://dx.doi.org/https://doi.org/10.1016/j.intimp.2011.04.011>.
- Jiang, H., Hegde, S. and DeNardo, D.G. (2017) 'Tumor-associated fibrosis as a regulator of tumor immunity and response to immunotherapy', *Cancer immunology, immunotherapy : CII*, 66(8), 1037-1048, available: <http://dx.doi.org/10.1007/s00262-017-2003-1>.
- Jin, L., Tao, H., Karachi, A., Long, Y., Hou, A.Y., Na, M., Dyson, K.A., Grippin, A.J., Deleyrolle, L.P., Zhang, W., Rajon, D.A., Wang, Q.J., Yang, J.C., Kresak, J.L., Saylor, E.J., Rahman, M., Bova, F.J., Lin, Z., Mitchell, D.A. and Huang, J. (2019) 'CXCR1- or CXCR2-modified CAR T cells co-opt IL-8 for maximal antitumor efficacy in solid tumors', *Nature communications*, 10(1), 4016, available: <http://dx.doi.org/10.1038/s41467-019-11869-4>.
- Jing, S.W., Wang, Y.D., Kuroda, M., Su, J.W., Sun, G.G., Liu, Q., Cheng, Y.J. and Yang, C.R. (2012) 'HIF-1 α contributes to hypoxia-induced invasion and metastasis of esophageal carcinoma via inhibiting E-cadherin and promoting MMP-2 expression', *Acta Med Okayama*, 66(5), 399-407, available: <http://dx.doi.org/10.18926/amo/48964>.
- John, L.B., Devaud, C., Duong, C.P., Yong, C.S., Beavis, P.A., Haynes, N.M., Chow, M.T., Smyth, M.J., Kershaw, M.H. and Darcy, P.K. (2013) 'Anti-PD-1 antibody therapy potently enhances the eradication of established tumors by gene-modified T cells', *Clinical cancer research : an official journal of the American Association for Cancer Research*, 19(20), 5636-46, available: <http://dx.doi.org/10.1158/1078-0432.Ccr-13-0458>.
- Jones, G.L., Will, A., Jackson, G.H., Webb, N.J.A., Rule, S. and the British Committee for Standards in, H. (2015) 'Guidelines for the management of tumour lysis syndrome in adults and children with haematological malignancies on behalf of the British Committee for Standards in Haematology', *British Journal of Haematology*, 169(5), 661-671, available: <http://dx.doi.org/10.1111/bjh.13403>.
- Jones, R.L., Chawla, S.P., Attia, S., Schoffski, P., Gelderblom, H., Chmielowski, B., Le Cesne, A., Van Tine, B.A., Trent, J.C., Patel, S., Wagner, A.J., Chugh, R., Heyburn, J.W., Weil, S.C., Wang, W., Viele, K. and Maki, R.G. (2019) 'A phase 1 and randomized controlled phase 2 trial of the safety and efficacy of the combination of gemcitabine and docetaxel with ontuxizumab (MORAb-004) in metastatic soft-tissue sarcomas', *Cancer*, 125(14), 2445-2454, available: <http://dx.doi.org/10.1002/cncr.32084>.

References

- Juillerat, A., Tkach, D., Busser, B.W., Temburni, S., Valton, J., Duclert, A., Poirot, L., Depil, S. and Duchateau, P. (2019) 'Modulation of chimeric antigen receptor surface expression by a small molecule switch', *BMC Biotechnol*, 19(1), 44, available: <http://dx.doi.org/10.1186/s12896-019-0537-3>.
- Junghans, R.P., Ma, Q., Rathore, R., Gomes, E.M., Bais, A.J., Lo, A.S., Abedi, M., Davies, R.A., Cabral, H.J., Al-Homsi, A.S. and Cohen, S.I. (2016) 'Phase I Trial of Anti-PSMA Designer CAR-T Cells in Prostate Cancer: Possible Role for Interacting Interleukin 2-T Cell Pharmacodynamics as a Determinant of Clinical Response', *Prostate*, 76(14), 1257-70, available: <http://dx.doi.org/10.1002/pros.23214>.
- Junttila, M.R. and de Sauvage, F.J. (2013) 'Influence of tumour micro-environment heterogeneity on therapeutic response', *Nature*, 501(7467), 346-354, available: <http://dx.doi.org/10.1038/nature12626>.
- Kaech, S.M., Wherry, E.J. and Ahmed, R. (2002) 'Effector and memory T-cell differentiation: implications for vaccine development', *Nature Reviews Immunology*, 2(4), 251-262, available: <http://dx.doi.org/10.1038/nri778>.
- Kägi, D., Ledermann, B., Bürki, K., Seiler, P., Odermatt, B., Olsen, K.J., Podack, E.R., Zinkernagel, R.M. and Hengartner, H. (1994) 'Cytotoxicity mediated by T cells and natural killer cells is greatly impaired in perforin-deficient mice', *Nature*, 369(6475), 31-7, available: <http://dx.doi.org/10.1038/369031a0>.
- Kakarla, S., Chow, K.K., Mata, M., Shaffer, D.R., Song, X.T., Wu, M.F., Liu, H., Wang, L.L., Rowley, D.R., Pfizenmaier, K. and Gottschalk, S. (2013) 'Antitumor effects of chimeric receptor engineered human T cells directed to tumor stroma', *Mol Ther*, 21(8), 1611-20, available: <http://dx.doi.org/10.1038/mt.2013.110>.
- Kalos, M., Levine, B.L., Porter, D.L., Katz, S., Grupp, S.A., Bagg, A. and June, C.H. (2011) 'T cells with chimeric antigen receptors have potent antitumor effects and can establish memory in patients with advanced leukemia', *Science translational medicine*, 3(95), 95ra73-95ra73, available: <http://dx.doi.org/10.1126/scitranslmed.3002842>.
- Karagiannis, G.S., Pastoriza, J.M., Wang, Y., Harney, A.S., Entenberg, D., Pignatelli, J., Sharma, V.P., Xue, E.A., Cheng, E., D'Alfonso, T.M., Jones, J.G., Anampa, J., Rohan, T.E., Sparano, J.A., Condeelis, J.S. and Oktay, M.H. (2017) 'Neoadjuvant chemotherapy induces breast cancer metastasis through a TMEM-mediated mechanism', *Science translational medicine*, 9(397), eaan0026, available: <http://dx.doi.org/doi:10.1126/scitranslmed.aan0026>.
- Karlsson, M., Zhang, C., Méar, L., Zhong, W., Digre, A., Katona, B., Sjöstedt, E., Butler, L., Odeberg, J., Dusart, P., Edfors, F., Oksvold, P., Feilitzten, K.v., Zwahlen, M., Arif, M., Altay, O., Li, X., Ozcan, M., Mardinoglu, A., Fagerberg, L., Mulder, J., Luo, Y., Ponten, F., Uhlén, M. and Lindskog, C. (2021) 'A single-cell type transcriptomics map of

References

- human tissues', *Science Advances*, 7(31), eabh2169, available: <http://dx.doi.org/doi:10.1126/sciadv.abh2169>.
- Karp, N.A., Wilson, Z., Stalker, E., Mooney, L., Lazic, S.E., Zhang, B. and Hardaker, E. (2020) 'A multi-batch design to deliver robust estimates of efficacy and reduce animal use – a syngeneic tumour case study', *Sci Rep*, 10(1), 6178, available: <http://dx.doi.org/10.1038/s41598-020-62509-7>.
- Kassam, F., Enright, K., Dent, R., Dranitsaris, G., Myers, J., Flynn, C., Fralick, M., Kumar, R. and Clemons, M. (2009) 'Survival outcomes for patients with metastatic triple-negative breast cancer: implications for clinical practice and trial design', *Clin Breast Cancer*, 9(1), 29-33, available: <http://dx.doi.org/10.3816/CBC.2009.n.005>.
- Katz, S.C., Burga, R.A., McCormack, E., Wang, L.J., Mooring, W., Point, G.R., Khare, P.D., Thorn, M., Ma, Q., Stainken, B.F., Assanah, E.O., Davies, R., Espat, N.J. and Junghans, R.P. (2015) 'Phase I Hepatic Immunotherapy for Metastases Study of Intra-Arterial Chimeric Antigen Receptor-Modified T-cell Therapy for CEA+ Liver Metastases', *Clinical cancer research : an official journal of the American Association for Cancer Research*, 21(14), 3149-59, available: <http://dx.doi.org/10.1158/1078-0432.Ccr-14-1421>.
- Kawamoto, N., Kaneko, H., Takemura, M., Seishima, M., Sakurai, S., Fukao, T., Kasahara, K., Iwasa, S. and Kondo, N. (2006) 'Age-related changes in intracellular cytokine profiles and Th2 dominance in allergic children', *Pediatr Allergy Immunol*, 17(2), 125-33, available: <http://dx.doi.org/10.1111/j.1399-3038.2005.00363.x>.
- Kennecke, H., Yerushalmi, R., Woods, R., Cheang, M.C.U., Voduc, D., Speers, C.H., Nielsen, T.O. and Gelmon, K. (2010) 'Metastatic Behavior of Breast Cancer Subtypes', *Journal of Clinical Oncology*, 28(20), 3271-3277, available: <http://dx.doi.org/10.1200/jco.2009.25.9820>.
- Kershaw, M.H., Westwood, J.A., Parker, L.L., Wang, G., Eshhar, Z., Mavroukakis, S.A., White, D.E., Wunderlich, J.R., Canevari, S., Rogers-Freezer, L., Chen, C.C., Yang, J.C., Rosenberg, S.A. and Hwu, P. (2006) 'A phase I study on adoptive immunotherapy using gene-modified T cells for ovarian cancer', *Clinical cancer research : an official journal of the American Association for Cancer Research*, 12(20 Pt 1), 6106-15, available: <http://dx.doi.org/10.1158/1078-0432.Ccr-06-1183>.
- Khan, K.A., McMurray, J.L., Mohammed, F. and Bicknell, R. (2019) 'C-type lectin domain group 14 proteins in vascular biology, cancer and inflammation', *The FEBS Journal*, 286(17), 3299-3332, available: <http://dx.doi.org/10.1111/febs.14985>.
- Khan, K.A., Naylor, A.J., Khan, A., Noy, P.J., Mambretti, M., Lodhia, P., Athwal, J., Korzystka, A., Buckley, C.D., Willcox, B.E., Mohammed, F. and Bicknell, R. (2017) 'Multimerin-2 is a ligand for group 14 family C-type lectins CLEC14A, CD93 and CD248 spanning the

References

- endothelial pericyte interface', *Oncogene*, 36(44), 6097-6108, available: <http://dx.doi.org/10.1038/onc.2017.214>.
- Kieffer, Y., Hocine, H.R., Gentric, G., Pelon, F., Bernard, C., Bourachot, B., Lameiras, S., Albergante, L., Bonneau, C., Guyard, A., Tarte, K., Zinovyev, A., Baulande, S., Zalcman, G., Vincent-Salomon, A. and Mechta-Grigoriou, F. (2020) 'Single-Cell Analysis Reveals Fibroblast Clusters Linked to Immunotherapy Resistance in Cancer', *Cancer discovery*, 10(9), 1330-1351, available: <http://dx.doi.org/10.1158/2159-8290.Cd-19-1384>.
- Kim, K.J., Kwon, S.H., Yun, J.H., Jeong, H.S., Kim, H.R., Lee, E.H., Ye, S.K. and Cho, C.H. (2017) 'STAT3 activation in endothelial cells is important for tumor metastasis via increased cell adhesion molecule expression', *Oncogene*, 36(39), 5445-5459, available: <http://dx.doi.org/10.1038/onc.2017.148>.
- Kinoshita, T., Ishii, G., Hiraoka, N., Hirayama, S., Yamauchi, C., Aokage, K., Hishida, T., Yoshida, J., Nagai, K. and Ochiai, A. (2013) 'Forkhead box P3 regulatory T cells coexisting with cancer associated fibroblasts are correlated with a poor outcome in lung adenocarcinoma', *Cancer science*, 104(4), 409-415, available: <http://dx.doi.org/10.1111/cas.12099>.
- Kloss, C.C., Condomines, M., Cartellieri, M., Bachmann, M. and Sadelain, M. (2013) 'Combinatorial antigen recognition with balanced signaling promotes selective tumor eradication by engineered T cells', *Nat Biotechnol*, 31(1), 71-5, available: <http://dx.doi.org/10.1038/nbt.2459>.
- Kochenderfer, J.N., Dudley, M.E., Carpenter, R.O., Kassim, S.H., Rose, J.J., Telford, W.G., Hakim, F.T., Halverson, D.C., Fowler, D.H., Hardy, N.M., Mato, A.R., Hickstein, D.D., Gea-Banacloche, J.C., Pavletic, S.Z., Sportes, C., Maric, I., Feldman, S.A., Hansen, B.G., Wilder, J.S., Blacklock-Schuber, B., Jena, B., Bishop, M.R., Gress, R.E. and Rosenberg, S.A. (2013) 'Donor-derived CD19-targeted T cells cause regression of malignancy persisting after allogeneic hematopoietic stem cell transplantation', *Blood*, 122(25), 4129-4139, available: <http://dx.doi.org/10.1182/blood-2013-08-519413>.
- Kochenderfer, J.N., Dudley, M.E., Feldman, S.A., Wilson, W.H., Spaner, D.E., Maric, I., Stetler-Stevenson, M., Phan, G.Q., Hughes, M.S., Sherry, R.M., Yang, J.C., Kammula, U.S., Devillier, L., Carpenter, R., Nathan, D.-A.N., Morgan, R.A., Laurencot, C. and Rosenberg, S.A. (2012) 'B-cell depletion and remissions of malignancy along with cytokine-associated toxicity in a clinical trial of anti-CD19 chimeric-antigen-receptor-transduced T cells', *Blood*, 119(12), 2709-2720, available: <http://dx.doi.org/10.1182/blood-2011-10-384388>.
- Kochenderfer, J.N., Dudley, M.E., Kassim, S.H., Somerville, R.P.T., Carpenter, R.O., Stetler-Stevenson, M., Yang, J.C., Phan, G.Q., Hughes, M.S., Sherry, R.M., Raffeld, M., Feldman, S., Lu, L., Li, Y.F., Ngo, L.T., Goy, A., Feldman, T., Spaner, D.E., Wang, M.L., Chen, C.C., Kranick, S.M., Nath, A., Nathan, D.-A.N., Morton, K.E., Toomey, M.A. and Rosenberg, S.A. (2015) 'Chemotherapy-refractory diffuse large B-cell lymphoma and indolent B-cell

References

- malignancies can be effectively treated with autologous T cells expressing an anti-CD19 chimeric antigen receptor', *Journal of clinical oncology : official journal of the American Society of Clinical Oncology*, 33(6), 540-549, available: <http://dx.doi.org/10.1200/JCO.2014.56.2025>.
- Kochenderfer, J.N., Feldman, S.A., Zhao, Y., Xu, H., Black, M.A., Morgan, R.A., Wilson, W.H. and Rosenberg, S.A. (2009) 'Construction and preclinical evaluation of an anti-CD19 chimeric antigen receptor', *Journal of immunotherapy (Hagerstown, Md. : 1997)*, 32(7), 689-702, available: <http://dx.doi.org/10.1097/CJI.0b013e3181ac6138>.
- Kochenderfer, J.N., Somerville, R.P.T., Lu, T., Shi, V., Bot, A., Rossi, J., Xue, A., Goff, S.L., Yang, J.C., Sherry, R.M., Klebanoff, C.A., Kammula, U.S., Sherman, M., Perez, A., Yuan, C.M., Feldman, T., Friedberg, J.W., Roschewski, M.J., Feldman, S.A., McIntyre, L., Toomey, M.A. and Rosenberg, S.A. (2017) 'Lymphoma Remissions Caused by Anti-CD19 Chimeric Antigen Receptor T Cells Are Associated With High Serum Interleukin-15 Levels', *Journal of clinical oncology : official journal of the American Society of Clinical Oncology*, 35(16), 1803-1813, available: <http://dx.doi.org/10.1200/JCO.2016.71.3024>.
- Kochenderfer, J.N., Somerville, R.P.T., Lu, T., Yang, J.C., Sherry, R.M., Feldman, S.A., McIntyre, L., Bot, A., Rossi, J., Lam, N. and Rosenberg, S.A. (2017) 'Long-Duration Complete Remissions of Diffuse Large B Cell Lymphoma after Anti-CD19 Chimeric Antigen Receptor T Cell Therapy', *Mol Ther*, 25(10), 2245-2253, available: <http://dx.doi.org/10.1016/j.ymthe.2017.07.004>.
- Kochenderfer, J.N., Wilson, W.H., Janik, J.E., Dudley, M.E., Stetler-Stevenson, M., Feldman, S.A., Maric, I., Raffeld, M., Nathan, D.A., Lanier, B.J., Morgan, R.A. and Rosenberg, S.A. (2010) 'Eradication of B-lineage cells and regression of lymphoma in a patient treated with autologous T cells genetically engineered to recognize CD19', *Blood*, 116(20), 4099-102, available: <http://dx.doi.org/10.1182/blood-2010-04-281931>.
- Kochenderfer, J.N., Yu, Z., Frasheri, D., Restifo, N.P. and Rosenberg, S.A. (2010) 'Adoptive transfer of syngeneic T cells transduced with a chimeric antigen receptor that recognizes murine CD19 can eradicate lymphoma and normal B cells', *Blood*, 116(19), 3875-3886, available: <http://dx.doi.org/10.1182/blood-2010-01-265041>.
- Koneru, M., Purdon, T.J., Spriggs, D., Koneru, S. and Brentjens, R.J. (2015) 'IL-12 secreting tumor-targeted chimeric antigen receptor T cells eradicate ovarian tumors in vivo', *Onc Immunology*, 4(3), e994446, available: <http://dx.doi.org/10.4161/2162402x.2014.994446>.
- Koristka, S., Cartellieri, M., Feldmann, A., Arndt, C., Loff, S., Michalk, I., Aliperta, R., von Bonin, M., Bornhäuser, M., Ehninger, A., Ehninger, G. and Bachmann, M.P. (2014) 'Flexible Antigen-Specific Redirection of Human Regulatory T Cells Via a Novel Universal Chimeric Antigen Receptor System', *Blood*, 124(21), 3494-3494, available: <http://dx.doi.org/10.1182/blood.V124.21.3494.3494>.

References

- Kraman, M., Bambrough, P.J., Arnold, J.N., Roberts, E.W., Magiera, L., Jones, J.O., Gopinathan, A., Tuveson, D.A. and Fearon, D.T. (2010) 'Suppression of antitumor immunity by stromal cells expressing fibroblast activation protein-alpha', *Science*, 330(6005), 827-30, available: <http://dx.doi.org/10.1126/science.1195300>.
- Krause, A., Guo, H.-F., Latouche, J.-B., Tan, C., Cheung, N.-K.V. and Sadelain, M. (1998) 'Antigen-dependent CD28 Signaling Selectively Enhances Survival and Proliferation in Genetically Modified Activated Human Primary T Lymphocytes', *Journal of Experimental Medicine*, 188(4), 619-626, available: <http://dx.doi.org/10.1084/jem.188.4.619>.
- Kuchenbaecker, K.B., Hopper, J.L., Barnes, D.R., Phillips, K.-A., Mooij, T.M., Roos-Blom, M.-J., Jervis, S., van Leeuwen, F.E., Milne, R.L., Andrieu, N., Goldgar, D.E., Terry, M.B., Rookus, M.A., Easton, D.F., Antoniou, A.C., BRCA1, a.t. and Consortium, B.C. (2017) 'Risks of Breast, Ovarian, and Contralateral Breast Cancer for BRCA1 and BRCA2 Mutation Carriers', *JAMA*, 317(23), 2402-2416, available: <http://dx.doi.org/10.1001/jama.2017.7112>.
- Kuczynski, E.A., Vermeulen, P.B., Pezzella, F., Kerbel, R.S. and Reynolds, A.R. (2019) 'Vessel co-option in cancer', *Nature Reviews Clinical Oncology*, 16(8), 469-493, available: <http://dx.doi.org/10.1038/s41571-019-0181-9>.
- Kueberuwa, G., Kalaitidou, M., Cheadle, E., Hawkins, R.E. and Gilham, D.E. (2018a) 'CD19 CAR T Cells Expressing IL-12 Eradicate Lymphoma in Fully Lymphoreplete Mice through Induction of Host Immunity', *Molecular Therapy - Oncolytics*, 8, 41-51, available: <http://dx.doi.org/10.1016/j.omto.2017.12.003>.
- Kueberuwa, G., Zheng, W., Kalaitidou, M., Gilham, D.E. and Hawkins, R.E. (2018b) 'A Syngeneic Mouse B-Cell Lymphoma Model for Pre-Clinical Evaluation of CD19 CAR T Cells', *Journal of visualized experiments : JoVE*, (140), 58492, available: <http://dx.doi.org/10.3791/58492>.
- Lakins, M.A., Ghorani, E., Munir, H., Martins, C.P. and Shields, J.D. (2018) 'Cancer-associated fibroblasts induce antigen-specific deletion of CD8 (+) T Cells to protect tumour cells', *Nature communications*, 9(1), 948-948, available: <http://dx.doi.org/10.1038/s41467-018-03347-0>.
- Lamers, C.H., Sleijfer, S., van Steenberghe, S., van Elzakker, P., van Krimpen, B., Groot, C., Vulto, A., den Bakker, M., Oosterwijk, E., Debets, R. and Gratama, J.W. (2013) 'Treatment of metastatic renal cell carcinoma with CAIX CAR-engineered T cells: clinical evaluation and management of on-target toxicity', *Molecular therapy : the journal of the American Society of Gene Therapy*, 21(4), 904-912, available: <http://dx.doi.org/10.1038/mt.2013.17>.

References

- Lamers, C.H., Sleijfer, S., Vulto, A.G., Kruit, W.H., Kliffen, M., Debets, R., Gratama, J.W., Stoter, G. and Oosterwijk, E. (2006) 'Treatment of metastatic renal cell carcinoma with autologous T-lymphocytes genetically retargeted against carbonic anhydrase IX: first clinical experience', *Journal of clinical oncology : official journal of the American Society of Clinical Oncology*, 24(13), e20-2, available: <http://dx.doi.org/10.1200/jco.2006.05.9964>.
- Lange, S.E., Zheleznyak, A., Studer, M., O'Shannessy, D.J., Lapi, S.E. and Van Tine, B.A. (2016) 'Development of 89Zr-Ontuxizumab for in vivo TEM-1/Endosialin PET applications', *Oncotarget*, 7(11), 13082-92, available: <http://dx.doi.org/10.18632/oncotarget.7552>.
- Langenkamp, E., Zhang, L., Lugano, R., Huang, H., Elhassan, T.E., Georganaki, M., Bazzar, W., Loof, J., Trendelenburg, G., Essand, M., Ponten, F., Smits, A. and Dimberg, A. (2015) 'Elevated expression of the C-type lectin CD93 in the glioblastoma vasculature regulates cytoskeletal rearrangements that enhance vessel function and reduce host survival', *Cancer Res*, 75(21), 4504-16, available: <http://dx.doi.org/10.1158/0008-5472.Can-14-3636>.
- Lanitis, E., Kosti, P., Ronet, C., Cribioli, E., Rota, G., Spill, A., Reichenbach, P., Zoete, V., Dangaj Laniti, D., Coukos, G. and Irving, M. (2021) 'VEGFR-2 redirected CAR-T cells are functionally impaired by soluble VEGF-A competition for receptor binding', *J Immunother Cancer*, 9(8), available: <http://dx.doi.org/10.1136/jitc-2020-002151>.
- Lanitis, E., Poussin, M., Hagemann, I.S., Coukos, G., Sandaltzopoulos, R., Scholler, N. and Powell, D.J., Jr. (2012) 'Redirected antitumor activity of primary human lymphocytes transduced with a fully human anti-mesothelin chimeric receptor', *Mol Ther*, 20(3), 633-43, available: <http://dx.doi.org/10.1038/mt.2011.256>.
- Lanitis, E., Poussin, M., Klattenhoff, A.W., Song, D., Sandaltzopoulos, R., June, C.H. and Powell, D.J., Jr. (2013) 'Chimeric antigen receptor T Cells with dissociated signaling domains exhibit focused antitumor activity with reduced potential for toxicity in vivo', *Cancer Immunol Res*, 1(1), 43-53, available: <http://dx.doi.org/10.1158/2326-6066.Cir-13-0008>.
- Lanitis, E., Rota, G., Kosti, P., Ronet, C., Spill, A., Seijo, B., Romero, P., Dangaj, D., Coukos, G. and Irving, M. (2020) 'Optimized gene engineering of murine CAR-T cells reveals the beneficial effects of IL-15 coexpression', *Journal of Experimental Medicine*, 218(2), available: <http://dx.doi.org/10.1084/jem.20192203>.
- Lax, S., Hou, T.Z., Jenkinson, E., Salmon, M., MacFadyen, J.R., Isacke, C.M., Anderson, G., Cunningham, A.F. and Buckley, C.D. (2007) 'CD248/Endosialin is dynamically expressed on a subset of stromal cells during lymphoid tissue development, splenic remodeling and repair', *FEBS Lett*, 581(18), 3550-6, available: <http://dx.doi.org/10.1016/j.febslet.2007.06.063>.

References

- Le, R.Q., Li, L., Yuan, W., Shord, S.S., Nie, L., Habtemariam, B.A., Przepiorka, D., Farrell, A.T. and Pazdur, R. (2018) 'FDA Approval Summary: Tocilizumab for Treatment of Chimeric Antigen Receptor T Cell-Induced Severe or Life-Threatening Cytokine Release Syndrome', *Oncologist*, 23(8), 943-947, available: <http://dx.doi.org/10.1634/theoncologist.2018-0028>.
- Leach, D.R., Krummel, M.F. and Allison, J.P. (1996) 'Enhancement of antitumor immunity by CTLA-4 blockade', *Science*, 271(5256), 1734-6, available: <http://dx.doi.org/10.1126/science.271.5256.1734>.
- Lee, D.W., Gardner, R., Porter, D.L., Louis, C.U., Ahmed, N., Jensen, M., Grupp, S.A. and Mackall, C.L. (2014) 'Current concepts in the diagnosis and management of cytokine release syndrome', *Blood*, 124(2), 188-195, available: <http://dx.doi.org/10.1182/blood-2014-05-552729>.
- Lee, D.W., Kochenderfer, J.N., Stetler-Stevenson, M., Cui, Y.K., Delbrook, C., Feldman, S.A., Fry, T.J., Orentas, R., Sabatino, M., Shah, N.N., Steinberg, S.M., Stroncek, D., Tschernia, N., Yuan, C., Zhang, H., Zhang, L., Rosenberg, S.A., Wayne, A.S. and Mackall, C.L. (2015) 'T cells expressing CD19 chimeric antigen receptors for acute lymphoblastic leukaemia in children and young adults: a phase 1 dose-escalation trial', *Lancet*, 385(9967), 517-528, available: [http://dx.doi.org/10.1016/s0140-6736\(14\)61403-3](http://dx.doi.org/10.1016/s0140-6736(14)61403-3).
- Lee, D.W., Santomasso, B.D., Locke, F.L., Ghobadi, A., Turtle, C.J., Brudno, J.N., Maus, M.V., Park, J.H., Mead, E., Pavletic, S., Go, W.Y., Eldjerou, L., Gardner, R.A., Frey, N., Curran, K.J., Peggs, K., Pasquini, M., DiPersio, J.F., van den Brink, M.R.M., Komanduri, K.V., Grupp, S.A. and Neelapu, S.S. (2019) 'ASTCT Consensus Grading for Cytokine Release Syndrome and Neurologic Toxicity Associated with Immune Effector Cells', *Biol Blood Marrow Transplant*, 25(4), 625-638, available: <http://dx.doi.org/10.1016/j.bbmt.2018.12.758>.
- Lee, H.-J. and Zheng, J.J. (2010) 'PDZ domains and their binding partners: structure, specificity, and modification', *Cell Communication and Signaling*, 8(1), 8, available: <http://dx.doi.org/10.1186/1478-811X-8-8>.
- Lee, S., Rho, S.S., Park, H., Park, J.A., Kim, J., Lee, I.K., Koh, G.Y., Mochizuki, N., Kim, Y.M. and Kwon, Y.G. (2017) 'Carbohydrate-binding protein CLEC14A regulates VEGFR-2- and VEGFR-3-dependent signals during angiogenesis and lymphangiogenesis', *J Clin Invest*, 127(2), 457-471, available: <http://dx.doi.org/10.1172/jci85145>.
- Lee, Y.G., Chu, H., Lu, Y., Leamon, C.P., Srinivasarao, M., Putt, K.S. and Low, P.S. (2019) 'Regulation of CAR T cell-mediated cytokine release syndrome-like toxicity using low molecular weight adapters', *Nature communications*, 10(1), 2681, available: <http://dx.doi.org/10.1038/s41467-019-10565-7>.

References

- Levéen, P., Pekny, M., Gebre-Medhin, S., Swolin, B., Larsson, E. and Betsholtz, C. (1994) 'Mice deficient for PDGF B show renal, cardiovascular, and hematological abnormalities', *Genes Dev*, 8(16), 1875-87, available: <http://dx.doi.org/10.1101/gad.8.16.1875>.
- Li, G., Boucher, J.C., Kotani, H., Park, K., Zhang, Y., Shrestha, B., Wang, X., Guan, L., Beatty, N., Abate-Daga, D. and Davila, M.L. (2018) '4-1BB enhancement of CAR T function requires NF- κ B and TRAFs', *JCI insight*, 3(18), e121322, available: <http://dx.doi.org/10.1172/jci.insight.121322>.
- Li, M., Cheng, X., Rong, R., Gao, Y., Tang, X. and Chen, Y. (2020) 'High expression of fibroblast activation protein (FAP) predicts poor outcome in high-grade serous ovarian cancer', *BMC Cancer*, 20(1), 1032, available: <http://dx.doi.org/10.1186/s12885-020-07541-6>.
- Liao, Q., Mao, Y., He, H., Ding, X., Zhang, X. and Xu, J. (2020) 'PD-L1 chimeric costimulatory receptor improves the efficacy of CAR-T cells for PD-L1-positive solid tumors and reduces toxicity in vivo', *Biomarker Research*, 8(1), 57, available: <http://dx.doi.org/10.1186/s40364-020-00237-w>.
- Lindahl, P., Johansson, B.R., Levéen, P. and Betsholtz, C. (1997) 'Pericyte loss and microaneurysm formation in PDGF-B-deficient mice', *Science*, 277(5323), 242-5, available: <http://dx.doi.org/10.1126/science.277.5323.242>.
- Liu, C., Pham, K., Luo, D., Reynolds, B.A., Hothi, P., Foltz, G. and Harrison, J.K. (2013) 'Expression and Functional Heterogeneity of Chemokine Receptors CXCR4 and CXCR7 in Primary Patient-Derived Glioblastoma Cells', *PLOS ONE*, 8(3), e59750, available: <http://dx.doi.org/10.1371/journal.pone.0059750>.
- Liu, L., Bi, E., Ma, X., Xiong, W., Qian, J., Ye, L., Su, P., Wang, Q., Xiao, L., Yang, M., Lu, Y. and Yi, Q. (2020) 'Enhanced CAR-T activity against established tumors by polarizing human T cells to secrete interleukin-9', *Nature communications*, 11(1), 5902, available: <http://dx.doi.org/10.1038/s41467-020-19672-2>.
- Liu, X., Jiang, S., Fang, C., Yang, S., Olalere, D., Pequignot, E.C., Cogdill, A.P., Li, N., Ramones, M., Granda, B., Zhou, L., Loew, A., Young, R.M., June, C.H. and Zhao, Y. (2015) 'Affinity-Tuned ErbB2 or EGFR Chimeric Antigen Receptor T Cells Exhibit an Increased Therapeutic Index against Tumors in Mice', *Cancer Res*, 75(17), 3596-607, available: <http://dx.doi.org/10.1158/0008-5472.Can-15-0159>.
- Locke, F.L., Ghobadi, A., Jacobson, C.A., Miklos, D.B., Lekakis, L.J., Oluwole, O.O., Lin, Y., Braunschweig, I., Hill, B.T., Timmerman, J.M., Deol, A., Reagan, P.M., Stiff, P., Flinn, I.W., Farooq, U., Goy, A., McSweeney, P.A., Munoz, J., Siddiqi, T., Chavez, J.C., Herrera, A.F., Bartlett, N.L., Wieszorek, J.S., Navale, L., Xue, A., Jiang, Y., Bot, A., Rossi, J.M., Kim, J.J., Go, W.Y. and Neelapu, S.S. (2019) 'Long-term safety and activity of axicabtagene ciloleucel in refractory large B-cell lymphoma (ZUMA-1): a single-arm, multicentre,

References

- phase 1-2 trial', *Lancet Oncol*, 20(1), 31-42, available: [http://dx.doi.org/10.1016/s1470-2045\(18\)30864-7](http://dx.doi.org/10.1016/s1470-2045(18)30864-7).
- Locke, F.L., Neelapu, S.S., Bartlett, N.L., Siddiqi, T., Chavez, J.C., Hosing, C.M., Ghobadi, A., Budde, L.E., Bot, A., Rossi, J.M., Jiang, Y., Xue, A.X., Elias, M., Aycok, J., Wiezorek, J. and Go, W.Y. (2017) 'Phase 1 Results of ZUMA-1: A Multicenter Study of KTE-C19 Anti-CD19 CAR T Cell Therapy in Refractory Aggressive Lymphoma', *Mol Ther*, 25(1), 285-295, available: <http://dx.doi.org/10.1016/j.ymthe.2016.10.020>.
- Loghmani, H. and Conway, E.M. (2018) 'Exploring traditional and nontraditional roles for thrombomodulin', *Blood*, 132(2), 148-158, available: <http://dx.doi.org/10.1182/blood-2017-12-768994>.
- Lohi, O., Urban, S. and Freeman, M. (2004) 'Diverse Substrate Recognition Mechanisms for Rhomboids: Thrombomodulin Is Cleaved by Mammalian Rhomboids', *Current Biology*, 14(3), 236-241, available: <http://dx.doi.org/https://doi.org/10.1016/j.cub.2004.01.025>.
- Long, A.H., Haso, W.M., Shern, J.F., Wanhainen, K.M., Murgai, M., Ingaramo, M., Smith, J.P., Walker, A.J., Kohler, M.E., Venkateshwara, V.R., Kaplan, R.N., Patterson, G.H., Fry, T.J., Orentas, R.J. and Mackall, C.L. (2015) '4-1BB costimulation ameliorates T cell exhaustion induced by tonic signaling of chimeric antigen receptors', *Nat Med*, 21(6), 581-590, available: <http://dx.doi.org/10.1038/nm.3838>.
- Long, A.H., Highfill, S.L., Cui, Y., Smith, J.P., Walker, A.J., Ramakrishna, S., El-Etriby, R., Galli, S., Tsokos, M.G., Orentas, R.J. and Mackall, C.L. (2016) 'Reduction of MDSCs with All-trans Retinoic Acid Improves CAR Therapy Efficacy for Sarcomas', *Cancer Immunol Res*, 4(10), 869-880, available: <http://dx.doi.org/10.1158/2326-6066.Cir-15-0230>.
- Long, X., Xiong, W., Zeng, X., Qi, L., Cai, Y., Mo, M., Jiang, H., Zhu, B., Chen, Z. and Li, Y. (2019) 'Cancer-associated fibroblasts promote cisplatin resistance in bladder cancer cells by increasing IGF-1/ER β /Bcl-2 signalling', *Cell death & disease*, 10(5), 375, available: <http://dx.doi.org/10.1038/s41419-019-1581-6>.
- Lorenzon, E., Colladel, R., Andreuzzi, E., Marastoni, S., Todaro, F., Schiappacassi, M., Ligresti, G., Colombatti, A. and Mongiat, M. (2012) 'MULTIMERIN2 impairs tumor angiogenesis and growth by interfering with VEGF-A/VEGFR2 pathway', *Oncogene*, 31(26), 3136-47, available: <http://dx.doi.org/10.1038/onc.2011.487>.
- Loureiro, L.R., Feldmann, A., Bergmann, R., Koristka, S., Berndt, N., Arndt, C., Pietzsch, J., Novo, C., Videira, P. and Bachmann, M. (2018) 'Development of a novel target module redirecting UniCAR T cells to Sialyl Tn-expressing tumor cells', *Blood Cancer Journal*, 8(9), 81, available: <http://dx.doi.org/10.1038/s41408-018-0113-4>.

References

- Lu, Y.J., Chu, H., Wheeler, L.W., Nelson, M., Westrick, E., Matthaei, J.F., Cardle, I., Johnson, A., Gustafson, J., Parker, N., Vetzal, M., Xu, L.C., Wang, E.Z., Jensen, M.C., Klein, P.J., Low, P.S. and Leamon, C.P. (2019) 'Preclinical Evaluation of Bispecific Adaptor Molecule Controlled Folate Receptor CAR-T Cell Therapy With Special Focus on Pediatric Malignancies', *Frontiers in oncology*, 9, 151, available: <http://dx.doi.org/10.3389/fonc.2019.00151>.
- Lugano, R., Ramachandran, M. and Dimberg, A. (2020) 'Tumor angiogenesis: causes, consequences, challenges and opportunities', *Cellular and Molecular Life Sciences*, 77(9), 1745-1770, available: <http://dx.doi.org/10.1007/s00018-019-03351-7>.
- MacFadyen, J., Savage, K., Wienke, D. and Isacke, C.M. (2007) 'Endosialin is expressed on stromal fibroblasts and CNS pericytes in mouse embryos and is downregulated during development', *Gene Expression Patterns*, 7(3), 363-369, available: <http://dx.doi.org/https://doi.org/10.1016/j.modgep.2006.07.006>.
- MacFadyen, J.R., Haworth, O., Roberston, D., Hardie, D., Webster, M.-T., Morris, H.R., Panico, M., Sutton-Smith, M., Dell, A., van der Geer, P., Wienke, D., Buckley, C.D. and Isacke, C.M. (2005) 'Endosialin (TEM1, CD248) is a marker of stromal fibroblasts and is not selectively expressed on tumour endothelium', *FEBS Letters*, 579(12), 2569-2575, available: <http://dx.doi.org/10.1016/j.febslet.2005.03.071>.
- MacIver, N.J., Michalek, R.D. and Rathmell, J.C. (2013) 'Metabolic Regulation of T Lymphocytes', *Annual Review of Immunology*, 31(1), 259-283, available: <http://dx.doi.org/10.1146/annurev-immunol-032712-095956>.
- Mackall, C.L. and Miklos, D.B. (2017) 'CNS Endothelial Cell Activation Emerges as a Driver of CAR T Cell-Associated Neurotoxicity', *Cancer discovery*, 7(12), 1371-1373, available: <http://dx.doi.org/10.1158/2159-8290.Cd-17-1084>.
- MacLeod, D.T., Antony, J., Martin, A.J., Moser, R.J., Hekele, A., Wetzal, K.J., Brown, A.E., Triggiano, M.A., Hux, J.A., Pham, C.D., Bartsevich, V.V., Turner, C.A., Lape, J., Kirkland, S., Beard, C.W., Smith, J., Hirsch, M.L., Nicholson, M.G., Jantz, D. and McCreedy, B. (2017) 'Integration of a CD19 CAR into the TCR Alpha Chain Locus Streamlines Production of Allogeneic Gene-Edited CAR T Cells', *Mol Ther*, 25(4), 949-961, available: <http://dx.doi.org/10.1016/j.ymthe.2017.02.005>.
- Maher, J., Brentjens, R.J., Gunset, G., Rivière, I. and Sadelain, M. (2002) 'Human T-lymphocyte cytotoxicity and proliferation directed by a single chimeric TCR ζ /CD28 receptor', *Nature Biotechnology*, 20(1), 70-75, available: <http://dx.doi.org/10.1038/nbt0102-70>.
- Maia, M., de Vriese, A., Janssens, T., Moons, M., van Landuyt, K., Tavernier, J., Lories, R.J. and Conway, E.M. (2010) 'CD248 and its cytoplasmic domain: a therapeutic target for arthritis', *Arthritis Rheum*, 62(12), 3595-606, available: <http://dx.doi.org/10.1002/art.27701>.

References

- Maia, M., DeVriese, A., Janssens, T., Moons, M., Lories, R.J., Tavernier, J. and Conway, E.M. (2011) 'CD248 facilitates tumor growth via its cytoplasmic domain', *BMC Cancer*, 11, 162, available: <http://dx.doi.org/10.1186/1471-2407-11-162>.
- Majzner, R.G., Weber, E.W., Lynn, R.C., Xu, P. and Mackall, C.L. (2018) 'Neurotoxicity Associated with a High-Affinity GD2 CAR—Letter', *Cancer Immunol Res*, 6(4), 494-495, available: <http://dx.doi.org/10.1158/2326-6066.Cir-18-0089>.
- Mall, C., Sckisel, G.D., Proia, D.A., Mirsoian, A., Grossenbacher, S.K., Pai, C.-C.S., Chen, M., Monjazeb, A.M., Kelly, K., Blazar, B.R. and Murphy, W.J. (2015) 'Repeated PD-1/PD-L1 monoclonal antibody administration induces fatal xenogeneic hypersensitivity reactions in a murine model of breast cancer', *Oncotmunology*, 5(2), e1075114-e1075114, available: <http://dx.doi.org/10.1080/2162402X.2015.1075114>.
- Mammadova-Bach, E., Zigrino, P., Brucker, C., Bourdon, C., Freund, M., De Arcangelis, A., Abrams, S.I., Orend, G., Gachet, C. and Mangin, P.H. (2016) 'Platelet integrin $\alpha\beta 1$ controls lung metastasis through direct binding to cancer cell-derived ADAM9', *JCI insight*, 1(14), e88245-e88245, available: <http://dx.doi.org/10.1172/jci.insight.88245>.
- Maniotis, A.J., Folberg, R., Hess, A., Seftor, E.A., Gardner, L.M., Pe'er, J., Trent, J.M., Meltzer, P.S. and Hendrix, M.J. (1999) 'Vascular channel formation by human melanoma cells in vivo and in vitro: vasculogenic mimicry', *Am J Pathol*, 155(3), 739-52, available: [http://dx.doi.org/10.1016/s0002-9440\(10\)65173-5](http://dx.doi.org/10.1016/s0002-9440(10)65173-5).
- Mapelli, L., Gagliano, G., Soda, T., Laforenza, U., Moccia, F. and Angelo, E.U. (2017) 'Granular Layer Neurons Control Cerebellar Neurovascular Coupling Through an NMDA Receptor/NO-Dependent System', *The Journal of Neuroscience*, 37(5), 1340, available: <http://dx.doi.org/10.1523/JNEUROSCI.2025-16.2016>.
- Mata, M., Gerken, C., Nguyen, P., Krenciute, G., Spencer, D.M. and Gottschalk, S. (2017) 'Inducible Activation of MyD88 and CD40 in CAR T Cells Results in Controllable and Potent Antitumor Activity in Preclinical Solid Tumor Models', *Cancer discovery*, 7(11), 1306-1319, available: <http://dx.doi.org/10.1158/2159-8290.Cd-17-0263>.
- Matsugi, T., Chen, Q. and Anderson, D.R. (1997) 'Suppression of CO₂-induced relaxation of bovine retinal pericytes by angiotensin II', *Invest Ophthalmol Vis Sci*, 38(3), 652-7.
- Matthaiou, E.I., Barar, J., Sandaltzopoulos, R., Li, C., Coukos, G. and Omid, Y. (2014) 'Shikonin-loaded antibody-armed nanoparticles for targeted therapy of ovarian cancer', *Int J Nanomedicine*, 9, 1855-70, available: <http://dx.doi.org/10.2147/ijn.S51880>.
- Maude, S.L., Frey, N., Shaw, P.A., Aplenc, R., Barrett, D.M., Bunin, N.J., Chew, A., Gonzalez, V.E., Zheng, Z., Lacey, S.F., Mahnke, Y.D., Melenhorst, J.J., Rheingold, S.R., Shen, A., Teachey, D.T., Levine, B.L., June, C.H., Porter, D.L. and Grupp, S.A. (2014) 'Chimeric

References

- antigen receptor T cells for sustained remissions in leukemia', *N Engl J Med*, 371(16), 1507-1517, available: <http://dx.doi.org/10.1056/NEJMoa1407222>.
- Maude, S.L., Laetsch, T.W., Buechner, J., Rives, S., Boyer, M., Bittencourt, H., Bader, P., Verneris, M.R., Stefanski, H.E., Myers, G.D., Qayed, M., De Moerloose, B., Hiramatsu, H., Schlis, K., Davis, K.L., Martin, P.L., Nemecek, E.R., Yanik, G.A., Peters, C., Baruchel, A., Boissel, N., Mechinaud, F., Balduzzi, A., Krueger, J., June, C.H., Levine, B.L., Wood, P., Taran, T., Leung, M., Mueller, K.T., Zhang, Y., Sen, K., Lebwohl, D., Pulsipher, M.A. and Grupp, S.A. (2018) 'Tisagenlecleucel in Children and Young Adults with B-Cell Lymphoblastic Leukemia', *N Engl J Med*, 378(5), 439-448, available: <http://dx.doi.org/10.1056/NEJMoa1709866>.
- McCarthy, E.F. (2006) 'The toxins of William B. Coley and the treatment of bone and soft-tissue sarcomas', *The Iowa orthopaedic journal*, 26, 154-158.
- Mills, C.D., Kincaid, K., Alt, J.M., Heilman, M.J. and Hill, A.M. (2000) 'M-1/M-2 Macrophages and the Th1/Th2 Paradigm', *The Journal of Immunology*, 164(12), 6166-6173, available: <http://dx.doi.org/10.4049/jimmunol.164.12.6166>.
- Milone, M.C., Fish, J.D., Carpenito, C., Carroll, R.G., Binder, G.K., Teachey, D., Samanta, M., Lakhali, M., Gloss, B., Danet-Desnoyers, G., Campana, D., Riley, J.L., Grupp, S.A. and June, C.H. (2009) 'Chimeric receptors containing CD137 signal transduction domains mediate enhanced survival of T cells and increased antileukemic efficacy in vivo', *Mol Ther*, 17(8), 1453-1464, available: <http://dx.doi.org/10.1038/mt.2009.83>.
- Minagawa, K., Jamil, M.O., Al-Obaidi, M., Pereboeva, L., Salzman, D., Erba, H.P., Lamb, L.S., Bhatia, R., Mineishi, S. and Di Stasi, A. (2016) 'In Vitro Pre-Clinical Validation of Suicide Gene Modified Anti-CD33 Redirected Chimeric Antigen Receptor T-Cells for Acute Myeloid Leukemia', *PLOS ONE*, 11(12), e0166891, available: <http://dx.doi.org/10.1371/journal.pone.0166891>.
- Minn, A.J., Kang, Y., Serganova, I., Gupta, G.P., Giri, D.D., Doubrovin, M., Ponomarev, V., Gerald, W.L., Blasberg, R. and Massagué, J. (2005) 'Distinct organ-specific metastatic potential of individual breast cancer cells and primary tumors', *J Clin Invest*, 115(1), 44-55, available: <http://dx.doi.org/10.1172/jci22320>.
- Minn, I., Huss, D.J., Ahn, H.-H., Chinn, T.M., Park, A., Jones, J., Brummet, M., Rowe, S.P., Sosa-Shah, P., Du, Y., Levitsky, H.I. and Pomper, M.G. (2019) 'Imaging CAR T cell therapy with PSMA-targeted positron emission tomography', *Science Advances*, 5(7), eaaw5096, available: <http://dx.doi.org/10.1126/sciadv.aaw5096>.
- Mitwasi, N., Feldmann, A., Bergmann, R., Berndt, N., Arndt, C., Koristka, S., Kegler, A., Jureczek, J., Hoffmann, A., Ehninger, A., Cartellieri, M., Albert, S., Rossig, C., Ehninger, G., Pietzsch, J., Steinbach, J. and Bachmann, M. (2017) 'Development of novel target

References

- modules for retargeting of UniCAR T cells to GD2 positive tumor cells', *Oncotarget*, 8(65), 108584-108603, available: <http://dx.doi.org/10.18632/oncotarget.21017>.
- Moccia, K.D., Olsen, C.H., Mitchell, J.M. and Landauer, M.R. (2010) 'Evaluation of hydration and nutritional gels as supportive care after total-body irradiation in mice (*Mus musculus*)', *Journal of the American Association for Laboratory Animal Science : JAALAS*, 49(3), 323-328.
- Mogler, C., Wieland, M., Konig, C., Hu, J., Runge, A., Korn, C., Besemfelder, E., Breitkopf-Heinlein, K., Komljenovic, D., Dooley, S., Schirmacher, P., Longerich, T. and Augustin, H.G. (2015) 'Hepatic stellate cell-expressed endosialin balances fibrogenesis and hepatocyte proliferation during liver damage', *EMBO Mol Med*, 7(3), 332-8, available: <http://dx.doi.org/10.15252/emmm.201404246>.
- Moon, E.K., Wang, L.C., Dolfi, D.V., Wilson, C.B., Ranganathan, R., Sun, J., Kapoor, V., Scholler, J., Pure, E., Milone, M.C., June, C.H., Riley, J.L., Wherry, E.J. and Albelda, S.M. (2014) 'Multifactorial T-cell hypofunction that is reversible can limit the efficacy of chimeric antigen receptor-transduced human T cells in solid tumors', *Clinical cancer research : an official journal of the American Association for Cancer Research*, 20(16), 4262-73, available: <http://dx.doi.org/10.1158/1078-0432.Ccr-13-2627>.
- Moorman, A.M., Vink, R., Heijmans, H.J., van der Palen, J. and Kouwenhoven, E.A. (2012) 'The prognostic value of tumour-stroma ratio in triple-negative breast cancer', *European Journal of Surgical Oncology (EJSO)*, 38(4), 307-313, available: <http://dx.doi.org/https://doi.org/10.1016/j.ejso.2012.01.002>.
- Morgan, R.A., Yang, J.C., Kitano, M., Dudley, M.E., Laurencot, C.M. and Rosenberg, S.A. (2010) 'Case Report of a Serious Adverse Event Following the Administration of T Cells Transduced With a Chimeric Antigen Receptor Recognizing ERBB2', *Molecular Therapy*, 18(4), 843-851, available: <http://dx.doi.org/https://doi.org/10.1038/mt.2010.24>.
- Mori, T., Takada, R., Watanabe, R., Okamoto, S. and Ikeda, Y. (2001) 'T-helper (Th)1/Th2 imbalance in patients with previously untreated B-cell diffuse large cell lymphoma', *Cancer immunology, immunotherapy : CII*, 50(10), 566-8, available: <http://dx.doi.org/10.1007/s00262-001-0232-8>.
- Morikawa, S., Baluk, P., Kaidoh, T., Haskell, A., Jain, R.K. and McDonald, D.M. (2002) 'Abnormalities in pericytes on blood vessels and endothelial sprouts in tumors', *Am J Pathol*, 160(3), 985-1000, available: [http://dx.doi.org/10.1016/s0002-9440\(10\)64920-6](http://dx.doi.org/10.1016/s0002-9440(10)64920-6).
- Mosely, S.I., Prime, J.E., Sainson, R.C., Koopmann, J.O., Wang, D.Y., Greenawalt, D.M., Ahdesmaki, M.J., Leyland, R., Mullins, S., Pacelli, L., Marcus, D., Anderton, J., Watkins, A., Coates Ulrichsen, J., Brohawn, P., Higgs, B.W., McCourt, M., Jones, H., Harper, J.A., Morrow, M., Valge-Archer, V., Stewart, R., Dovedi, S.J. and Wilkinson, R.W. (2017)

References

- 'Rational Selection of Syngeneic Preclinical Tumor Models for Immunotherapeutic Drug Discovery', *Cancer Immunol Res*, 5(1), 29-41, available: <http://dx.doi.org/10.1158/2326-6066.Cir-16-0114>.
- Mount, C., Majzner, R., Sundaresh, S., Arnold, E., Kadapakkam, M., Monje-Deisseroth, M. and Mackall, C. (2017) 'PDTM-39. GD2-DIRECTED CHIMERIC ANTIGEN RECEPTOR T CELLS AS A POTENT IMMUNOTHERAPY REGIMEN IN XENOGRAFT MODELS OF DIFFUSE INTRINSIC PONTINE GLIOMA', *Neuro-Oncology*, 19(suppl_6), vi198-vi198, available: <http://dx.doi.org/10.1093/neuonc/nox168.802>.
- Munshi, N.C., Anderson, L.D., Jr., Shah, N., Madduri, D., Berdeja, J., Lonial, S., Raje, N., Lin, Y., Siegel, D., Oriol, A., Moreau, P., Yakoub-Agha, I., Delforge, M., Cavo, M., Einsele, H., Goldschmidt, H., Weisel, K., Rambaldi, A., Reece, D., Petrocca, F., Massaro, M., Connarn, J.N., Kaiser, S., Patel, P., Huang, L., Campbell, T.B., Hege, K. and San-Miguel, J. (2021) 'Idecabtagene Vicleucel in Relapsed and Refractory Multiple Myeloma', *N Engl J Med*, 384(8), 705-716, available: <http://dx.doi.org/10.1056/NEJMoa2024850>.
- Mura, M., Swain, R.K., Zhuang, X., Vorschmitt, H., Reynolds, G., Durant, S., Beesley, J.F., Herbert, J.M., Sheldon, H., Andre, M., Sanderson, S., Glen, K., Luu, N.T., McGettrick, H.M., Antczak, P., Falciani, F., Nash, G.B., Nagy, Z.S. and Bicknell, R. (2012) 'Identification and angiogenic role of the novel tumor endothelial marker CLEC14A', *Oncogene*, 31(3), 293-305, available: <http://dx.doi.org/10.1038/onc.2011.233>.
- Muranski, P., Boni, A., Wrzesinski, C., Citrin, D.E., Rosenberg, S.A., Childs, R. and Restifo, N.P. (2006) 'Increased intensity lymphodepletion and adoptive immunotherapy--how far can we go?', *Nature clinical practice. Oncology*, 3(12), 668-681, available: <http://dx.doi.org/10.1038/ncponc0666>.
- Murray, P.J. (2007) 'The JAK-STAT signaling pathway: input and output integration', *J Immunol*, 178(5), 2623-9, available: <http://dx.doi.org/10.4049/jimmunol.178.5.2623>.
- Nagarsheth, N., Wicha, M.S. and Zou, W. (2017) 'Chemokines in the cancer microenvironment and their relevance in cancer immunotherapy', *Nature Reviews Immunology*, 17(9), 559-572, available: <http://dx.doi.org/10.1038/nri.2017.49>.
- Nakashima, O., Sugihara, S., Kage, M. and Kojiro, M. (1995) 'Pathomorphologic characteristics of small hepatocellular carcinoma: a special reference to small hepatocellular carcinoma with indistinct margins', *Hepatology*, 22(1), 101-5.
- Nanda, A., Carson-Walter, E.B., Seaman, S., Barber, T.D., Stampfl, J., Singh, S., Vogelstein, B., Kinzler, K.W. and St Croix, B. (2004) 'TEM8 interacts with the cleaved C5 domain of collagen alpha 3(VI)', *Cancer Res*, 64(3), 817-20, available: <http://dx.doi.org/10.1158/0008-5472.can-03-2408>.

References

- Nanda, A., Karim, B., Peng, Z., Liu, G., Qiu, W., Gan, C., Vogelstein, B., St Croix, B., Kinzler, K.W. and Huso, D.L. (2006) 'Tumor endothelial marker 1 (Tem1) functions in the growth and progression of abdominal tumors', *Proc Natl Acad Sci U S A*, 103(9), 3351-6, available: <http://dx.doi.org/10.1073/pnas.0511306103>.
- Naylor, A.J., Azzam, E., Smith, S., Croft, A., Poyser, C., Duffield, J.S., Huso, D.L., Gay, S., Ospelt, C., Cooper, M.S., Isacke, C., Goodyear, S.R., Rogers, M.J. and Buckley, C.D. (2012) 'The mesenchymal stem cell marker CD248 (endosialin) is a negative regulator of bone formation in mice', *Arthritis Rheum*, 64(10), 3334-3343, available: <http://dx.doi.org/10.1002/art.34556>.
- NCI (2022) *Cancer Stat Facts: Female Breast Cancer Subtypes*, available: <https://seer.cancer.gov/statfacts/html/breast-subtypes.html> [accessed 3rd March].
- Neelapu, S.S., Locke, F.L., Bartlett, N.L., Lekakis, L.J., Miklos, D.B., Jacobson, C.A., Braunschweig, I., Oluwole, O.O., Siddiqi, T., Lin, Y., Timmerman, J.M., Stiff, P.J., Friedberg, J.W., Flinn, I.W., Goy, A., Hill, B.T., Smith, M.R., Deol, A., Farooq, U., McSweeney, P., Munoz, J., Avivi, I., Castro, J.E., Westin, J.R., Chavez, J.C., Ghobadi, A., Komanduri, K.V., Levy, R., Jacobsen, E.D., Witzig, T.E., Reagan, P., Bot, A., Rossi, J., Navale, L., Jiang, Y., Aycock, J., Elias, M., Chang, D., Wieszorek, J. and Go, W.Y. (2017) 'Axicabtagene Ciloleucel CAR T-Cell Therapy in Refractory Large B-Cell Lymphoma', *N Engl J Med*, 377(26), 2531-2544, available: <http://dx.doi.org/10.1056/NEJMoa1707447>.
- Neelapu, S.S., Tummala, S., Kebriaei, P., Wierda, W., Gutierrez, C., Locke, F.L., Komanduri, K.V., Lin, Y., Jain, N., Daver, N., Westin, J., Gulbis, A.M., Lohin, M.E., de Groot, J.F., Adkins, S., Davis, S.E., Rezvani, K., Hwu, P. and Shpall, E.J. (2018) 'Chimeric antigen receptor T-cell therapy - assessment and management of toxicities', *Nature reviews. Clinical oncology*, 15(1), 47-62, available: <http://dx.doi.org/10.1038/nrclinonc.2017.148>.
- Nelson, R.A., Guye, M.L., Luu, T. and Lai, L.L. (2015) 'Survival Outcomes of Metaplastic Breast Cancer Patients: Results from a US Population-based Analysis', *Annals of Surgical Oncology*, 22(1), 24-31, available: <http://dx.doi.org/10.1245/s10434-014-3890-4>.
- Nishimoto, N., Terao, K., Mima, T., Nakahara, H., Takagi, N. and Kakehi, T. (2008) 'Mechanisms and pathologic significances in increase in serum interleukin-6 (IL-6) and soluble IL-6 receptor after administration of an anti-IL-6 receptor antibody, tocilizumab, in patients with rheumatoid arthritis and Castleman disease', *Blood*, 112(10), 3959-3964, available: <http://dx.doi.org/10.1182/blood-2008-05-155846>.
- Nordby, Y., Richardsen, E., Rakae, M., Ness, N., Donnem, T., Patel, H.R.H., Busund, L.-T., Bremnes, R.M. and Andersen, S. (2017) 'High expression of PDGFR- β in prostate cancer stroma is independently associated with clinical and biochemical prostate cancer recurrence', *Sci Rep*, 7(1), 43378, available: <http://dx.doi.org/10.1038/srep43378>.

References

- Norelli, M., Camisa, B., Barbiera, G., Falcone, L., Purevdorj, A., Genua, M., Sanvito, F., Ponzoni, M., Doglioni, C., Cristofori, P., Traversari, C., Bordignon, C., Ciceri, F., Ostuni, R., Bonini, C., Casucci, M. and Bondanza, A. (2018) 'Monocyte-derived IL-1 and IL-6 are differentially required for cytokine-release syndrome and neurotoxicity due to CAR T cells', *Nat Med*, 24(6), 739-748, available: <http://dx.doi.org/10.1038/s41591-018-0036-4>.
- Norris, R.E., Fox, E., Reid, J.M., Ralya, A., Liu, X.W., Minard, C. and Weigel, B.J. (2018) 'Phase 1 trial of ontuxizumab (MORAb-004) in children with relapsed or refractory solid tumors: A report from the Children's Oncology Group Phase 1 Pilot Consortium (ADV1213)', *Pediatr Blood Cancer*, 65(5), e26944, available: <http://dx.doi.org/10.1002/pbc.26944>.
- Norton, K.A., Popel, A.S. and Pandey, N.B. (2015) 'Heterogeneity of chemokine cell-surface receptor expression in triple-negative breast cancer', *Am J Cancer Res*, 5(4), 1295-307.
- Noy, P.J., Lodhia, P., Khan, K., Zhuang, X., Ward, D.G., Verissimo, A.R., Bacon, A. and Bicknell, R. (2015) 'Blocking CLEC14A-MMRN2 binding inhibits sprouting angiogenesis and tumour growth', *Oncogene*, 34(47), 5821-5831, available: <http://dx.doi.org/10.1038/onc.2015.34>.
- Noy, P.J., Swain, R.K., Khan, K., Lodhia, P. and Bicknell, R. (2016) 'Sprouting angiogenesis is regulated by shedding of the C-type lectin family 14, member A (CLEC14A) ectodomain, catalyzed by rhomboid-like 2 protein (RHBDL2)', *Faseb j*, 30(6), 2311-23, available: <http://dx.doi.org/10.1096/fj.201500122R>.
- O'Keefe, M.B., Devlin, A.H., Burns, A.J., Gardiner, T.A., Logan, I.D., Hirst, D.G. and McKeown, S.R. (2008) 'Investigation of pericytes, hypoxia, and vascularity in bladder tumors: association with clinical outcomes', *Oncol Res*, 17(3), 93-101, available: <http://dx.doi.org/10.3727/096504008785055530>.
- O'Shannessy, D.J., Smith, M.F., Somers, E.B., Jackson, S.M., Albone, E., Tomkowicz, B., Cheng, X., Park, Y., Fernando, D., Milinichik, A., Kline, B., Fulton, R., Oberoi, P. and Nicolaidis, N.C. (2016) 'Novel antibody probes for the characterization of endosialin/TEM-1', *Oncotarget*, 7(43), 69420-69435, available: <http://dx.doi.org/10.18632/oncotarget.11018>.
- O'Rourke, D.M., Nasrallah, M.P., Morrisette, J., Melenhorst, J.J., Lacey, S.F., Mansfield, K., Martinez-Lage, M., Desai, A., Brem, S., Maloney, E., Mohan, S., Wang, S., Verma, G., Navenot, J.-M., Shen, A., Zheng, Z., Levine, B.L., Okada, H., June, C.H. and Maus, M.V. (2016) 'Abstract LB-083: Phase I study of T cells redirected to EGFRvIII with a chimeric antigen receptor in patients with EGFRvIII+ glioblastoma', *Cancer Res*, 76(14 Supplement), LB-083, available: <http://dx.doi.org/10.1158/1538-7445.AM2016-LB-083>.

References

- Ochs, K., Sahm, F., Opitz, C.A., Lanz, T.V., Oezen, I., Couraud, P.-O., von Deimling, A., Wick, W. and Platten, M. (2013) 'Immature mesenchymal stem cell-like pericytes as mediators of immunosuppression in human malignant glioma', *Journal of Neuroimmunology*, 265(1), 106-116, available: <http://dx.doi.org/https://doi.org/10.1016/j.jneuroim.2013.09.011>.
- Ohradanova, A., Gradin, K., Barathova, M., Zatovicova, M., Holotnakova, T., Kopacek, J., Parkkila, S., Poellinger, L., Pastorekova, S. and Pastorek, J. (2008) 'Hypoxia upregulates expression of human endosialin gene via hypoxia-inducible factor 2', *British journal of cancer*, 99(8), 1348-1356, available: <http://dx.doi.org/10.1038/sj.bjc.6604685>.
- Opavsky, R., Haviernik, P., Jurkovicova, D., Garin, M.T., Copeland, N.G., Gilbert, D.J., Jenkins, N.A., Bies, J., Garfield, S., Pastorekova, S., Oue, A. and Wolff, L. (2001) 'Molecular Characterization of the MouseTem1/endosialin Gene Regulated by Cell Density in Vitro and Expressed in Normal Tissues in Vivo', *Journal of Biological Chemistry*, 276(42), 38795-38807.
- Osborn, M.J., Webber, B.R., Knipping, F., Lonetree, C.L., Tennis, N., DeFeo, A.P., McElroy, A.N., Starker, C.G., Lee, C., Merkel, S., Lund, T.C., Kelly-Spratt, K.S., Jensen, M.C., Voytas, D.F., von Kalle, C., Schmidt, M., Gabriel, R., Hippen, K.L., Miller, J.S., Scharenberg, A.M., Tolar, J. and Blazar, B.R. (2016) 'Evaluation of TCR Gene Editing Achieved by TALENs, CRISPR/Cas9, and megaTAL Nucleases', *Mol Ther*, 24(3), 570-81, available: <http://dx.doi.org/10.1038/mt.2015.197>.
- Ozawa, C.R., Banfi, A., Glazer, N.L., Thurston, G., Springer, M.L., Kraft, P.E., McDonald, D.M. and Blau, H.M. (2004) 'Microenvironmental VEGF concentration, not total dose, determines a threshold between normal and aberrant angiogenesis', *J Clin Invest*, 113(4), 516-527, available: <http://dx.doi.org/10.1172/JCI18420>.
- Özdemir, B.C., Pentcheva-Hoang, T., Carstens, J.L., Zheng, X., Wu, C.C., Simpson, T.R., Laklai, H., Sugimoto, H., Kahlert, C., Novitskiy, S.V., De Jesus-Acosta, A., Sharma, P., Heidari, P., Mahmood, U., Chin, L., Moses, H.L., Weaver, V.M., Maitra, A., Allison, J.P., LeBleu, V.S. and Kalluri, R. (2014) 'Depletion of carcinoma-associated fibroblasts and fibrosis induces immunosuppression and accelerates pancreas cancer with reduced survival', *Cancer Cell*, 25(6), 719-34, available: <http://dx.doi.org/10.1016/j.ccr.2014.04.005>.
- Pabst, T., Joncourt, R., Shumilov, E., Heini, A., Wiedemann, G., Legros, M., Seipel, K., Schild, C., Jalowiec, K., Mansouri Taleghani, B., Fux, M., Novak, U., Porret, N., Zeerleder, S. and Bacher, U. (2020) 'Analysis of IL-6 serum levels and CAR T cell-specific digital PCR in the context of cytokine release syndrome', *Experimental hematology*, 88, 7-14.e3, available: <http://dx.doi.org/https://doi.org/10.1016/j.exphem.2020.07.003>.
- Pan, J., Yang, J.F., Deng, B.P., Zhao, X.J., Zhang, X., Lin, Y.H., Wu, Y.N., Deng, Z.L., Zhang, Y.L., Liu, S.H., Wu, T., Lu, P.H., Lu, D.P., Chang, A.H. and Tong, C.R. (2017) 'High efficacy and safety of low-dose CD19-directed CAR-T cell therapy in 51 refractory or relapsed B

References

- acute lymphoblastic leukemia patients', *Leukemia*, 31(12), 2587-2593, available: <http://dx.doi.org/10.1038/leu.2017.145>.
- Parikh, J.G., Kulkarni, A. and Johns, C. (2014) ' α -smooth muscle actin-positive fibroblasts correlate with poor survival in hepatocellular carcinoma', *Oncology letters*, 7(2), 573-575, available: <http://dx.doi.org/10.3892/ol.2013.1720>.
- Park, A.K., Fong, Y., Kim, S.-I., Yang, J., Murad, J.P., Lu, J., Jeang, B., Chang, W.-C., Chen, N.G., Thomas, S.H., Forman, S.J. and Priceman, S.J. (2020) 'Effective combination immunotherapy using oncolytic viruses to deliver CAR targets to solid tumors', *Science translational medicine*, 12(559), eaaz1863, available: <http://dx.doi.org/10.1126/scitranslmed.aaz1863>.
- Patin, E.C., Soulard, D., Fleury, S., Hassane, M., Dombrowicz, D., Faveeuw, C., Trottein, F. and Paget, C. (2018) 'Type I IFN Receptor Signaling Controls IL7-Dependent Accumulation and Activity of Protumoral IL17A-Producing $\gamma\delta$ T Cells in Breast Cancer', *Cancer Res*, 78(1), 195, available: <http://dx.doi.org/10.1158/0008-5472.CAN-17-1416>.
- Paulsson, J., Sjöblom, T., Micke, P., Pontén, F., Landberg, G., Heldin, C.-H., Bergh, J., Brennan, D.J., Jirstrom, K. and Östman, A. (2009) 'Prognostic Significance of Stromal Platelet-Derived Growth Factor β -Receptor Expression in Human Breast Cancer', *Am J Pathol*, 175(1), 334-341, available: <http://dx.doi.org/https://doi.org/10.2353/ajpath.2009.081030>.
- Pellicani, R., Poletto, E., Andreuzzi, E., Paulitti, A., Doliana, R., Bizzotto, D., Braghetta, P., Colladel, R., Tarticchio, G., Sabatelli, P., Bucciotti, F., Bressan, G., Iozzo, R.V., Colombatti, A., Bonaldo, P. and Mongiat, M. (2020) 'Multimerin-2 maintains vascular stability and permeability', *Matrix Biology*, 87, 11-25, available: <http://dx.doi.org/https://doi.org/10.1016/j.matbio.2019.08.002>.
- Perou, C.M., Sørli, T., Eisen, M.B., van de Rijn, M., Jeffrey, S.S., Rees, C.A., Pollack, J.R., Ross, D.T., Johnsen, H., Akslen, L.A., Fluge, Ø., Pergamenschikov, A., Williams, C., Zhu, S.X., Lønning, P.E., Børresen-Dale, A.-L., Brown, P.O. and Botstein, D. (2000) 'Molecular portraits of human breast tumours', *Nature*, 406(6797), 747-752, available: <http://dx.doi.org/10.1038/35021093>.
- Pezzella, F., Pastorino, U., Tagliabue, E., Andreola, S., Sozzi, G., Gasparini, G., Menard, S., Gatter, K.C., Harris, A.L., Fox, S., Buyse, M., Pilotti, S., Pierotti, M. and Rilke, F. (1997) 'Non-small-cell lung carcinoma tumor growth without morphological evidence of neoangiogenesis', *Am J Pathol*, 151(5), 1417-23.
- Pietrzyk, L. and Wdowiak, P. (2020) 'Endosialin (TEM1) as a Diagnostic, Progression, and Prognostic Serum Marker for Patients With Colorectal Cancer-A Preliminary Study', *Cancer Control*, 27(1), 1073274820903351, available: <http://dx.doi.org/10.1177/1073274820903351>.

References

- Pinchuk, L.M. and Filipov, N.M. (2008) 'Differential effects of age on circulating and splenic leukocyte populations in C57BL/6 and BALB/c male mice', *Immunity & ageing : I & A*, 5, 1-1, available: <http://dx.doi.org/10.1186/1742-4933-5-1>.
- Pircher, M., Schuberth, P., Gulati, P., Sulser, S., Weder, W., Curioni, A., Renner, C. and Petrusch, U. (2015) 'FAP-specific re-directed T cells first in-man study in malignant pleural mesothelioma: experience of the first patient treated', *Journal for ImmunoTherapy of Cancer*, 3(Suppl 2), P120-P120, available: <http://dx.doi.org/10.1186/2051-1426-3-S2-P120>.
- Poirot, L., Philip, B., Schiffer-Mannioui, C., Le Clerre, D., Chion-Sotinel, I., Derniame, S., Potrel, P., Bas, C., Lemaire, L., Galetto, R., Lebuhotel, C., Eyquem, J., Cheung, G.W., Duclert, A., Gouble, A., Arnould, S., Peggs, K., Pule, M., Scharenberg, A.M. and Smith, J. (2015) 'Multiplex Genome-Edited T-cell Manufacturing Platform for "Off-the-Shelf" Adoptive T-cell Immunotherapies', *Cancer Res*, 75(18), 3853-64, available: <http://dx.doi.org/10.1158/0008-5472.Can-14-3321>.
- Ponnaiya, B., Cornforth, M.N. and Ullrich, R.L. (1997) 'Radiation-induced chromosomal instability in BALB/c and C57BL/6 mice: the difference is as clear as black and white', *Radiat Res*, 147(2), 121-5.
- Porter, D.L., Levine, B.L., Kalos, M., Bagg, A. and June, C.H. (2011) 'Chimeric antigen receptor-modified T cells in chronic lymphoid leukemia', *N Engl J Med*, 365(8), 725-33, available: <http://dx.doi.org/10.1056/NEJMoa1103849>.
- Potente, M., Gerhardt, H. and Carmeliet, P. (2011) 'Basic and Therapeutic Aspects of Angiogenesis', *Cell*, 146(6), 873-887, available: <http://dx.doi.org/https://doi.org/10.1016/j.cell.2011.08.039>.
- Powell, D.W., Mifflin, R.C., Valentich, J.D., Crowe, S.E., Saada, J.I. and West, A.B. (1999) 'Myofibroblasts. I. Paracrine cells important in health and disease', *Am J Physiol*, 277(1), C1-9, available: <http://dx.doi.org/10.1152/ajpcell.1999.277.1.C1>.
- proteinatlas.org (2020), available: [accessed 14/05/2020].
- Pulaski, B.A. and Ostrand-Rosenberg, S. (1998) 'Reduction of established spontaneous mammary carcinoma metastases following immunotherapy with major histocompatibility complex class II and B7.1 cell-based tumor vaccines', *Cancer Res*, 58(7), 1486-93.
- Qin, H., Ramakrishna, S., Nguyen, S., Fountaine, T.J., Ponduri, A., Stetler-Stevenson, M., Yuan, C.M., Haso, W., Shern, J.F., Shah, N.N. and Fry, T.J. (2018) 'Preclinical Development of Bivalent Chimeric Antigen Receptors Targeting Both CD19 and CD22', *Molecular*

References

- therapy oncolytics*, 11, 127-137, available: <http://dx.doi.org/10.1016/j.omto.2018.10.006>.
- Quintarelli, C., Vera, J.F., Savoldo, B., Giordano Attianese, G.M., Pule, M., Foster, A.E., Heslop, H.E., Rooney, C.M., Brenner, M.K. and Dotti, G. (2007) 'Co-expression of cytokine and suicide genes to enhance the activity and safety of tumor-specific cytotoxic T lymphocytes', *Blood*, 110(8), 2793-802, available: <http://dx.doi.org/10.1182/blood-2007-02-072843>.
- Rafiq, S., Yeku, O.O., Jackson, H.J., Purdon, T.J., van Leeuwen, D.G., Drakes, D.J., Song, M., Miele, M.M., Li, Z., Wang, P., Yan, S., Xiang, J., Ma, X., Seshan, V.E., Hendrickson, R.C., Liu, C. and Brentjens, R.J. (2018) 'Targeted delivery of a PD-1-blocking scFv by CAR-T cells enhances anti-tumor efficacy in vivo', *Nature Biotechnology*, 36(9), 847-856, available: <http://dx.doi.org/10.1038/nbt.4195>.
- Raj, D., Yang, M.-H., Rodgers, D., Hampton, E.N., Begum, J., Mustafa, A., Lorizio, D., Garces, I., Propper, D., Kench, J.G., Kocher, H.M., Young, T.S., Aicher, A. and Heeschen, C. (2019) 'Switchable CAR-T cells mediate remission in metastatic pancreatic ductal adenocarcinoma', *Gut*, 68(6), 1052, available: <http://dx.doi.org/10.1136/gutjnl-2018-316595>.
- Raje, N., Berdeja, J., Lin, Y., Siegel, D., Jagannath, S., Madduri, D., Liedtke, M., Rosenblatt, J., Maus, M.V., Turka, A., Lam, L.-P., Morgan, R.A., Friedman, K., Massaro, M., Wang, J., Russotti, G., Yang, Z., Campbell, T., Hege, K., Petrocca, F., Quigley, M.T., Munshi, N. and Kochenderfer, J.N. (2019) 'Anti-BCMA CAR T-Cell Therapy bb2121 in Relapsed or Refractory Multiple Myeloma', *New England Journal of Medicine*, 380(18), 1726-1737, available: <http://dx.doi.org/10.1056/NEJMoa1817226>.
- Ramani, V.C., Lemaire, C.A., Triboulet, M., Casey, K.M., Heirich, K., Renier, C., Vilches-Moure, J.G., Gupta, R., Razmara, A.M., Zhang, H., Sledge, G.W., Sollier, E. and Jeffrey, S.S. (2019) 'Investigating circulating tumor cells and distant metastases in patient-derived orthotopic xenograft models of triple-negative breast cancer', *Breast Cancer Research*, 21(1), 98, available: <http://dx.doi.org/10.1186/s13058-019-1182-4>.
- Ren, J., Zhang, X., Liu, X., Fang, C., Jiang, S., June, C.H. and Zhao, Y. (2017) 'A versatile system for rapid multiplex genome-edited CAR T cell generation', *Oncotarget*, 8(10), 17002-17011, available: <http://dx.doi.org/10.18632/oncotarget.15218>.
- Rettig, W.J., Garin-Chesa, P., Beresford, H.R., Oettgen, H.F., Melamed, M.R. and Old, L.J. (1988) 'Cell-surface glycoproteins of human sarcomas: differential expression in normal and malignant tissues and cultured cells', *Proc Natl Acad Sci U S A*, 85(9), 3110-4, available: <http://dx.doi.org/10.1073/pnas.85.9.3110>.
- Rettig, W.J., Garin-Chesa, P., Healey, J.H., Su, S.L., Jaffe, E.A. and Old, L.J. (1992) 'Identification of endosialin, a cell surface glycoprotein of vascular endothelial cells in human cancer',

References

Proceedings of the National Academy of Sciences of the United States of America, 89(22), 10832-10836, available: <http://dx.doi.org/10.1073/pnas.89.22.10832>.

- Rhim, A.D., Oberstein, P.E., Thomas, D.H., Mirek, E.T., Palermo, C.F., Sastra, S.A., Dekleva, E.N., Saunders, T., Becerra, C.P., Tattersall, I.W., Westphalen, C.B., Kitajewski, J., Fernandez-Barrena, M.G., Fernandez-Zapico, M.E., Iacobuzio-Donahue, C., Olive, K.P. and Stanger, B.Z. (2014) 'Stromal elements act to restrain, rather than support, pancreatic ductal adenocarcinoma', *Cancer Cell*, 25(6), 735-47, available: <http://dx.doi.org/10.1016/j.ccr.2014.04.021>.
- Ribeiro, A.L. and Okamoto, O.K. (2015) 'Combined Effects of Pericytes in the Tumor Microenvironment', *Stem Cells International*, 2015, 868475, available: <http://dx.doi.org/10.1155/2015/868475>.
- Richman, S.A., Nunez-Cruz, S., Moghimi, B., Li, L.Z., Gershenson, Z.T., Mourelatos, Z., Barrett, D.M., Grupp, S.A. and Milone, M.C. (2018) 'High-Affinity GD2-Specific CAR T Cells Induce Fatal Encephalitis in a Preclinical Neuroblastoma Model', *Cancer Immunol Res*, 6(1), 36-46, available: <http://dx.doi.org/10.1158/2326-6066.Cir-17-0211>.
- Robertson, M.J., Kirkwood, J.M., Logan, T.F., Koch, K.M., Kathman, S., Kirby, L.C., Bell, W.N., Thurmond, L.M., Weisenbach, J. and Dar, M.M. (2008) 'A dose-escalation study of recombinant human interleukin-18 using two different schedules of administration in patients with cancer', *Clinical cancer research : an official journal of the American Association for Cancer Research*, 14(11), 3462-9, available: <http://dx.doi.org/10.1158/1078-0432.Ccr-07-4740>.
- Rodriguez-Garcia, A., Lynn, R.C., Poussin, M., Eiva, M.A., Shaw, L.C., O'Connor, R.S., Minutolo, N.G., Casado-Medrano, V., Lopez, G., Matsuyama, T. and Powell, D.J. (2021) 'CAR-T cell-mediated depletion of immunosuppressive tumor-associated macrophages promotes endogenous antitumor immunity and augments adoptive immunotherapy', *Nature communications*, 12(1), 877, available: <http://dx.doi.org/10.1038/s41467-021-20893-2>.
- Rotz, S.J., Leino, D., Szabo, S., Mangino, J.L., Turpin, B.K. and Pressey, J.G. (2017) 'Severe cytokine release syndrome in a patient receiving PD-1-directed therapy', *Pediatr Blood Cancer*, 64(12), available: <http://dx.doi.org/10.1002/pbc.26642>.
- Rouleau, C., Curiel, M., Weber, W., Smale, R., Kurtzberg, L., Mascarello, J., Berger, C., Wallar, G., Bagley, R., Honma, N., Hasegawa, K., Ishida, I., Kataoka, S., Thurberg, B.L., Mehraein, K., Horten, B., Miller, G. and Teicher, B.A. (2008) 'Endosialin Protein Expression and Therapeutic Target Potential in Human Solid Tumors: Sarcoma versus Carcinoma', *Clinical Cancer Research*, 14(22), 7223, available: <http://dx.doi.org/10.1158/1078-0432.CCR-08-0499>.

References

- Rouleau, C., Gianolio, D.A., Smale, R., Roth, S.D., Krumbholz, R., Harper, J., Munroe, K.J., Green, T.L., Horten, B.C., Schmid, S.M. and Teicher, B.A. (2015) 'Anti-Endosialin Antibody-Drug Conjugate: Potential in Sarcoma and Other Malignancies', *Mol Cancer Ther*, 14(9), 2081-9, available: <http://dx.doi.org/10.1158/1535-7163.Mct-15-0312>.
- Rouleau, C., Smale, R., Fu, Y.S., Hui, G., Wang, F., Hutto, E., Fogle, R., Jones, C.M., Krumbholz, R., Roth, S., Curiel, M., Ren, Y., Bagley, R.G., Wallar, G., Miller, G., Schmid, S., Horten, B. and Teicher, B.A. (2011) 'Endosialin is expressed in high grade and advanced sarcomas: evidence from clinical specimens and preclinical modeling', *Int J Oncol*, 39(1), 73-89, available: <http://dx.doi.org/10.3892/ijo.2011.1020>.
- Rouso-Noori, L., Mastandrea, I., Talmor, S., Waks, T., Globerson Levin, A., Haugas, M., Teesalu, T., Alvarez-Vallina, L., Eshhar, Z. and Friedmann-Morvinski, D. (2021) 'P32-specific CAR T cells with dual antitumor and antiangiogenic therapeutic potential in gliomas', *Nature communications*, 12(1), 3615, available: <http://dx.doi.org/10.1038/s41467-021-23817-2>.
- Rucker, H.K., Wynder, H.J. and Thomas, W.E. (2000) 'Cellular mechanisms of CNS pericytes', *Brain Research Bulletin*, 51(5), 363-369, available: [http://dx.doi.org/https://doi.org/10.1016/S0361-9230\(99\)00260-9](http://dx.doi.org/https://doi.org/10.1016/S0361-9230(99)00260-9).
- Ruella, M., Barrett, D.M., Kenderian, S.S., Shestova, O., Hofmann, T.J., Perazzelli, J., Klichinsky, M., Aikawa, V., Nazimuddin, F., Kozlowski, M., Scholler, J., Lacey, S.F., Melenhorst, J.J., Morrisette, J.J.D., Christian, D.A., Hunter, C.A., Kalos, M., Porter, D.L., June, C.H., Grupp, S.A. and Gill, S. (2016) 'Dual CD19 and CD123 targeting prevents antigen-loss relapses after CD19-directed immunotherapies', *J Clin Invest*, 126(10), 3814-3826, available: <http://dx.doi.org/10.1172/JCI87366>.
- Rupp, C., Dolznig, H., Puri, C., Sommergruber, W., Kerjaschki, D., Rettig, W.J. and Garin-Chesa, P. (2006) 'Mouse endosialin, a C-type lectin-like cell surface receptor: Expression during embryonic development and induction in experimental cancer neoangiogenesis', *Cancer Immunity Archive*, 6(1), 10.
- Russell, J.H. and Ley, T.J. (2002) 'Lymphocyte-Mediated Cytotoxicity', *Annual Review of Immunology*, 20(1), 323-370, available: <http://dx.doi.org/10.1146/annurev.immunol.20.100201.131730>.
- Rybinski, K., Imtiyaz, H.Z., Mittica, B., Drozdowski, B., Fulmer, J., Furuuchi, K., Fernando, S., Henry, M., Chao, Q., Kline, B., Albone, E., Wustner, J., Lin, J., Nicolaidis, N.C., Grasso, L. and Zhou, Y. (2015) 'Targeting endosialin/CD248 through antibody-mediated internalization results in impaired pericyte maturation and dysfunctional tumor microvasculature', *Oncotarget*, 6(28), 25429-25440, available: <http://dx.doi.org/10.18632/oncotarget.4559>.

References

- Saadi, A., Shannon, N.B., Lao-Sirieix, P., O'Donovan, M., Walker, E., Clemons, N.J., Hardwick, J.S., Zhang, C., Das, M., Save, V., Novelli, M., Balkwill, F. and Fitzgerald, R.C. (2010) 'Stromal genes discriminate preinvasive from invasive disease, predict outcome, and highlight inflammatory pathways in digestive cancers', *Proc Natl Acad Sci U S A*, 107(5), 2177-82, available: <http://dx.doi.org/10.1073/pnas.0909797107>.
- Sahai, E., Astsaturon, I., Cukierman, E., DeNardo, D.G., Egeblad, M., Evans, R.M., Fearon, D., Greten, F.R., Hingorani, S.R., Hunter, T., Hynes, R.O., Jain, R.K., Janowitz, T., Jorgensen, C., Kimmelman, A.C., Kolonin, M.G., Maki, R.G., Powers, R.S., Puré, E., Ramirez, D.C., Scherz-Shouval, R., Sherman, M.H., Stewart, S., Tlsty, T.D., Tuveson, D.A., Watt, F.M., Weaver, V., Weeraratna, A.T. and Werb, Z. (2020) 'A framework for advancing our understanding of cancer-associated fibroblasts', *Nature Reviews Cancer*, 20(3), 174-186, available: <http://dx.doi.org/10.1038/s41568-019-0238-1>.
- Sakemura, R., Terakura, S., Watanabe, K., Julamanee, J., Takagi, E., Miyao, K., Koyama, D., Goto, T., Hanajiri, R., Nishida, T., Murata, M. and Kiyoi, H. (2016) 'A Tet-On Inducible System for Controlling CD19-Chimeric Antigen Receptor Expression upon Drug Administration', *Cancer Immunol Res*, 4(8), 658-68, available: <http://dx.doi.org/10.1158/2326-6066.Cir-16-0043>.
- Sanderson, R., Romero-Toledo, A. and Gribben, J.G. (2019) 'CAR T Cells Derived from Healthy Mice Lead to Cytokine Release Syndrome (CRS) in the TCL1 Chronic Lymphocytic Leukemia Model; Mice with CLL Treated with Acalabrutinib or Ibrutinib Have Improved CAR T Cell Function without Increasing the Cytokines of CRS', *Blood*, 134(Supplement_1), 249-249, available: <http://dx.doi.org/10.1182/blood-2019-125647>.
- Santomasso, B.D., Park, J.H., Salloum, D., Riviere, I., Flynn, J., Mead, E., Halton, E., Wang, X., Senechal, B., Purdon, T., Cross, J.R., Liu, H., Vachha, B., Chen, X., DeAngelis, L.M., Li, D., Bernal, Y., Gonen, M., Wendel, H.-G., Sadelain, M. and Brentjens, R.J. (2018) 'Clinical and Biological Correlates of Neurotoxicity Associated with CAR T-cell Therapy in Patients with B-cell Acute Lymphoblastic Leukemia', *Cancer discovery*, 8(8), 958-971, available: <http://dx.doi.org/10.1158/2159-8290.CD-17-1319>.
- Schaaf, M.B., Garg, A.D. and Agostinis, P. (2018) 'Defining the role of the tumor vasculature in antitumor immunity and immunotherapy', *Cell death & disease*, 9(2), 115-115, available: <http://dx.doi.org/10.1038/s41419-017-0061-0>.
- Scheuermann, R.H. and Racila, E. (1995) 'CD19 Antigen in Leukemia and Lymphoma Diagnosis and Immunotherapy', *Leukemia & Lymphoma*, 18(5-6), 385-397, available: <http://dx.doi.org/10.3109/10428199509059636>.
- Schmid, P., Cortes, J., Dent, R., Puzstai, L., McArthur, H., Kümmel, S., Bergh, J., Denkert, C., Park, Y.H., Hui, R., Harbeck, N., Takahashi, M., Untch, M., Fasching, P.A., Cardoso, F., Andersen, J., Patt, D., Danso, M., Ferreira, M., Mouret-Reynier, M.-A., Im, S.-A., Ahn, J.-H., Gion, M., Baron-Hay, S., Boileau, J.-F., Ding, Y., Tryfonidis, K., Aktan, G., Karantza, V.

References

- and O'Shaughnessy, J. (2022) 'Event-free Survival with Pembrolizumab in Early Triple-Negative Breast Cancer', *New England Journal of Medicine*, 386(6), 556-567, available: <http://dx.doi.org/10.1056/NEJMoa2112651>.
- Schneider, D., Xiong, Y., Wu, D., Nille, V., Schmitz, S., Haso, W., Kaiser, A., Dropulic, B. and Orentas, R.J. (2017) 'A tandem CD19/CD20 CAR lentiviral vector drives on-target and off-target antigen modulation in leukemia cell lines', *J Immunother Cancer*, 5, 42, available: <http://dx.doi.org/10.1186/s40425-017-0246-1>.
- Schuberth, P.C., Hagedorn, C., Jensen, S.M., Gulati, P., van den Broek, M., Mischo, A., Soltermann, A., Jüngel, A., Marroquin Belaunzaran, O., Stahel, R., Renner, C. and Petrusch, U. (2013) 'Treatment of malignant pleural mesothelioma by fibroblast activation protein-specific re-directed T cells', *Journal of translational medicine*, 11, 187-187, available: <http://dx.doi.org/10.1186/1479-5876-11-187>.
- Schultz, L.M., Muffly, L.S., Spiegel, J.Y., Ramakrishna, S., Hossain, N., Baggott, C., Sahaf, B., Patel, S., Craig, J., Yoon, J., Kadapakkam, M., Majzner, R.G., Frank, M.J., Erickson, C., Marcy, A.C., Fujimoto, M., Bhatia, N., Meyer, E.H., Kong, K.A., Egeler, E., Mavroukakis, S., Qin, H., Fry, T.J., Feldman, S.A., Miklos, D.B., Mackall, C.L. and Davis, K.L. (2019) 'Phase I Trial Using CD19/CD22 Bispecific CAR T Cells in Pediatric and Adult Acute Lymphoblastic Leukemia (ALL)', *Blood*, 134(Supplement_1), 744-744, available: <http://dx.doi.org/10.1182/blood-2019-129411>.
- Schuster, S.J., Bishop, M.R., Tam, C.S., Waller, E.K., Borchmann, P., McGuirk, J.P., Jäger, U., Jaglowski, S., Andreadis, C., Westin, J.R., Fleury, I., Bachanova, V., Foley, S.R., Ho, P.J., Mielke, S., Magenau, J.M., Holte, H., Pantano, S., Pacaud, L.B., Awasthi, R., Chu, J., Anak, Ö., Salles, G. and Maziarz, R.T. (2018) 'Tisagenlecleucel in Adult Relapsed or Refractory Diffuse Large B-Cell Lymphoma', *New England Journal of Medicine*, 380(1), 45-56, available: <http://dx.doi.org/10.1056/NEJMoa1804980>.
- Schuster, S.J., Svoboda, J., Chong, E.A., Nasta, S.D., Mato, A.R., Anak, Ö., Brogdon, J.L., Pruteanu-Malinici, I., Bhoj, V., Landsburg, D., Wasik, M., Levine, B.L., Lacey, S.F., Melenhorst, J.J., Porter, D.L. and June, C.H. (2017) 'Chimeric Antigen Receptor T Cells in Refractory B-Cell Lymphomas', *New England Journal of Medicine*, 377(26), 2545-2554, available: <http://dx.doi.org/10.1056/NEJMoa1708566>.
- Scott, A.M., Wiseman, G., Welt, S., Adjei, A., Lee, F.T., Hopkins, W., Divgi, C.R., Hanson, L.H., Mitchell, P., Gansen, D.N., Larson, S.M., Ingle, J.N., Hoffman, E.W., Tanswell, P., Ritter, G., Cohen, L.S., Bette, P., Arvay, L., Amelsberg, A., Vlock, D., Rettig, W.J. and Old, L.J. (2003) 'A Phase I dose-escalation study of sibrotuzumab in patients with advanced or metastatic fibroblast activation protein-positive cancer', *Clinical cancer research : an official journal of the American Association for Cancer Research*, 9(5), 1639-47.
- Seidel, J.A., Otsuka, A. and Kabashima, K. (2018) 'Anti-PD-1 and Anti-CTLA-4 Therapies in Cancer: Mechanisms of Action, Efficacy, and Limitations', *Frontiers in oncology*, 8, 86-86, available: <http://dx.doi.org/10.3389/fonc.2018.00086>.

References

- Seimetz, D., Heller, K. and Richter, J. (2019) 'Approval of First CAR-Ts: Have we Solved all Hurdles for ATMPs?', *Cell Medicine*, 11, 2155179018822781, available: <http://dx.doi.org/10.1177/2155179018822781>.
- Selli, C. and Sims, A.H. (2019) 'Neoadjuvant Therapy for Breast Cancer as a Model for Translational Research', *Breast cancer : basic and clinical research*, 13, 1178223419829072-1178223419829072, available: <http://dx.doi.org/10.1177/1178223419829072>.
- Shah, B.D., Ghobadi, A., Oluwole, O.O., Logan, A., Boissel, N., Cassaday, R.D., Forcade, E., Bishop, M.R., Topp, M.S., Tzachanis, D., O'Dwyer, K.M., Arellano, M.L., Lin, Y., Baer, M.R., Schiller, G.J., Dong, J., Shen, T., Milletti, F., Masouleh, B.K. and Houot, R. (2021) 'Phase 2 results of the ZUMA-3 study evaluating KTE-X19, an anti-CD19 chimeric antigen receptor (CAR) T-cell therapy, in adult patients (pts) with relapsed/refractory B-cell acute lymphoblastic leukemia (R/R B-ALL)', *Journal of Clinical Oncology*, 39(15_suppl), 7002-7002, available: http://dx.doi.org/10.1200/JCO.2021.39.15_suppl.7002.
- Sherman, M.H., Yu, R.T., Engle, D.D., Ding, N., Atkins, A.R., Tiriach, H., Collisson, E.A., Connor, F., Van Dyke, T., Kozlov, S., Martin, P., Tseng, T.W., Dawson, D.W., Donahue, T.R., Masamune, A., Shimosegawa, T., Apte, M.V., Wilson, J.S., Ng, B., Lau, S.L., Gunton, J.E., Wahl, G.M., Hunter, T., Drebin, J.A., O'Dwyer, P.J., Liddle, C., Tuveson, D.A., Downes, M. and Evans, R.M. (2014) 'Vitamin D receptor-mediated stromal reprogramming suppresses pancreatitis and enhances pancreatic cancer therapy', *Cell*, 159(1), 80-93, available: <http://dx.doi.org/10.1016/j.cell.2014.08.007>.
- Shimabukuro-Vornhagen, A., Gödel, P., Subklewe, M., Stemmler, H.J., SchlöBer, H.A., Schlaak, M., Kochanek, M., Böll, B. and von Bergwelt-Baildon, M.S. (2018) 'Cytokine release syndrome', *Journal for ImmunoTherapy of Cancer*, 6(1), 56-56, available: <http://dx.doi.org/10.1186/s40425-018-0343-9>.
- Shimao, Y., Nabeshima, K., Inoue, T. and Koono, M. (1999) 'Role of fibroblasts in HGF/SF-induced cohort migration of human colorectal carcinoma cells: fibroblasts stimulate migration associated with increased fibronectin production via upregulated TGF-beta1', *Int J Cancer*, 82(3), 449-58, available: [http://dx.doi.org/10.1002/\(sici\)1097-0215\(19990730\)82:3<449::aid-ijc20>3.0.co;2-h](http://dx.doi.org/10.1002/(sici)1097-0215(19990730)82:3<449::aid-ijc20>3.0.co;2-h).
- Shirakawa, K., Tsuda, H., Heike, Y., Kato, K., Asada, R., Inomata, M., Sasaki, H., Kasumi, F., Yoshimoto, M., Iwanaga, T., Konishi, F., Terada, M. and Wakasugi, H. (2001) 'Absence of endothelial cells, central necrosis, and fibrosis are associated with aggressive inflammatory breast cancer', *Cancer Res*, 61(2), 445-51.
- Simonavicius, N., Ashenden, M., van Weverwijk, A., Lax, S., Huso, D.L., Buckley, C.D., Huijbers, I.J., Yarwood, H. and Isacke, C.M. (2012) 'Pericytes promote selective vessel regression

References

- to regulate vascular patterning', *Blood*, 120(7), 1516-27, available: <http://dx.doi.org/10.1182/blood-2011-01-332338>.
- Simonavicius, N., Robertson, D., Bax, D.A., Jones, C., Huijbers, I.J. and Isacke, C.M. (2008) 'Endosialin (CD248) is a marker of tumor-associated pericytes in high-grade glioma', *Mod Pathol*, 21(3), 308-15, available: <http://dx.doi.org/10.1038/modpathol.3801006>.
- Sims, D.E. (1986) 'The pericyte--a review', *Tissue Cell*, 18(2), 153-74, available: [http://dx.doi.org/10.1016/0040-8166\(86\)90026-1](http://dx.doi.org/10.1016/0040-8166(86)90026-1).
- Sinha, D., Chong, L., George, J., Schlüter, H., Mönchgesang, S., Mills, S., Li, J., Parish, C., Bowtell, D. and Kaur, P. (2016) 'Pericytes Promote Malignant Ovarian Cancer Progression in Mice and Predict Poor Prognosis in Serous Ovarian Cancer Patients', *Clinical Cancer Research*, 22(7), 1813, available: <http://dx.doi.org/10.1158/1078-0432.CCR-15-1931>.
- Sinn, M., Denkert, C., Striefler, J.K., Pelzer, U., Stieler, J.M., Bahra, M., Lohneis, P., Dörken, B., Oettle, H., Riess, H. and Sinn, B.V. (2014) 'α-Smooth muscle actin expression and desmoplastic stromal reaction in pancreatic cancer: results from the CONKO-001 study', *British journal of cancer*, 111(10), 1917-1923, available: <http://dx.doi.org/10.1038/bjc.2014.495>.
- Slovin, S.F., Wang, X., Hullings, M., Arauz, G., Bartido, S., Lewis, J.S., Schöder, H., Zanzonico, P., Scher, H.I. and Riviere, I. (2013) 'Chimeric antigen receptor (CAR+) modified T cells targeting prostate specific membrane antigen (PSMA) in patients (pts) with castrate metastatic prostate cancer (CMPC)', *Journal of Clinical Oncology*, 31(15_suppl), TPS3115-TPS3115, available: http://dx.doi.org/10.1200/jco.2013.31.15_suppl.tps3115.
- Smith-Garvin, J.E., Koretzky, G.A. and Jordan, M.S. (2009) 'T cell activation', *Annu Rev Immunol*, 27, 591-619, available: <http://dx.doi.org/10.1146/annurev.immunol.021908.132706>.
- Smith, S.W., Croft, A.P., Morris, H.L., Naylor, A.J., Huso, D.L., Isacke, C.M., Savage, C.O.S. and Buckley, C.D. (2015) 'Genetic Deletion of the Stromal Cell Marker CD248 (Endosialin) Protects against the Development of Renal Fibrosis', *Nephron*, 131(4), 265-277, available: <http://dx.doi.org/10.1159/000438754>.
- Sommermeier, D., Hudecek, M., Kosasih, P.L., Gogishvili, T., Maloney, D.G., Turtle, C.J. and Riddell, S.R. (2016) 'Chimeric antigen receptor-modified T cells derived from defined CD8+ and CD4+ subsets confer superior antitumor reactivity in vivo', *Leukemia*, 30(2), 492-500, available: <http://dx.doi.org/10.1038/leu.2015.247>.
- Soriano, P. (1994) 'Abnormal kidney development and hematological disorders in PDGF beta-receptor mutant mice', *Genes Dev*, 8(16), 1888-96, available: <http://dx.doi.org/10.1101/gad.8.16.1888>.

References

- Stalder, T., Hahn, S. and Erb, P. (1994) 'Fas antigen is the major target molecule for CD4+ T cell-mediated cytotoxicity', *J Immunol*, 152(3), 1127-33.
- Stavrou, M., Philip, B., Traynor-White, C., Davis, C.G., Onuoha, S., Cordoba, S., Thomas, S. and Pule, M. (2018) 'A Rapamycin-Activated Caspase 9-Based Suicide Gene', *Mol Ther*, 26(5), 1266-1276, available: <http://dx.doi.org/10.1016/j.ymthe.2018.03.001>.
- Stessels, F., Van den Eynden, G., Van der Auwera, I., Salgado, R., Van den Heuvel, E., Harris, A.L., Jackson, D.G., Colpaert, C.G., van Marck, E.A., Dirix, L.Y. and Vermeulen, P.B. (2004) 'Breast adenocarcinoma liver metastases, in contrast to colorectal cancer liver metastases, display a non-angiogenic growth pattern that preserves the stroma and lacks hypoxia', *British journal of cancer*, 90(7), 1429-36, available: <http://dx.doi.org/10.1038/sj.bjc.6601727>.
- Stewart, T.J. and Abrams, S.I. (2007) 'Altered Immune Function during Long-Term Host-Tumor Interactions Can Be Modulated to Retard Autochthonous Neoplastic Growth', *The Journal of Immunology*, 179(5), 2851-2859, available: <http://dx.doi.org/10.4049/jimmunol.179.5.2851>.
- Straathof, K., Flutter, B., Wallace, R., Jain, N., Loka, T., Depani, S., Wright, G., Thomas, S., Cheung, G.W.-K., Gileadi, T., Stafford, S., Kokalaki, E., Barton, J., Marriott, C., Rampling, D., Ogunbiyi, O., Akarca, A.U., Marafioti, T., Inglott, S., Gilmour, K., Al-Hajj, M., Day, W., McHugh, K., Biassoni, L., Sizer, N., Barton, C., Edwards, D., Dragoni, I., Silvester, J., Dyer, K., Traub, S., Elson, L., Brook, S., Westwood, N., Robson, L., Bedi, A., Howe, K., Barry, A., Duncan, C., Barone, G., Pule, M. and Anderson, J. (2020) 'Antitumor activity without on-target off-tumor toxicity of GD2–chimeric antigen receptor T cells in patients with neuroblastoma', *Science translational medicine*, 12(571), eabd6169, available: <http://dx.doi.org/doi:10.1126/scitranslmed.abd6169>.
- Straathof, K.C., Pule, M.A., Yotnda, P., Dotti, G., Vanin, E.F., Brenner, M.K., Heslop, H.E., Spencer, D.M. and Rooney, C.M. (2005) 'An inducible caspase 9 safety switch for T-cell therapy', *Blood*, 105(11), 4247-54, available: <http://dx.doi.org/10.1182/blood-2004-11-4564>.
- Straussman, R., Morikawa, T., Shee, K., Barzily-Rokni, M., Qian, Z.R., Du, J., Davis, A., Mongare, M.M., Gould, J., Frederick, D.T., Cooper, Z.A., Chapman, P.B., Solit, D.B., Ribas, A., Lo, R.S., Flaherty, K.T., Ogino, S., Wargo, J.A. and Golub, T.R. (2012) 'Tumour micro-environment elicits innate resistance to RAF inhibitors through HGF secretion', *Nature*, 487(7408), 500-4, available: <http://dx.doi.org/10.1038/nature11183>.
- Sun, S., Hao, H., Yang, G., Zhang, Y. and Fu, Y. (2018) 'Immunotherapy with CAR-Modified T Cells: Toxicities and Overcoming Strategies', *Journal of immunology research*, 2018, 2386187-2386187, available: <http://dx.doi.org/10.1155/2018/2386187>.

References

- Sun, Y.-S., Zhao, Z., Yang, Z.-N., Xu, F., Lu, H.-J., Zhu, Z.-Y., Shi, W., Jiang, J., Yao, P.-P. and Zhu, H.-P. (2017) 'Risk Factors and Preventions of Breast Cancer', *International journal of biological sciences*, 13(11), 1387-1397, available: <http://dx.doi.org/10.7150/ijbs.21635>.
- Sung, H., Ferlay, J., Siegel, R.L., Laversanne, M., Soerjomataram, I., Jemal, A. and Bray, F. (2021) 'Global Cancer Statistics 2020: GLOBOCAN Estimates of Incidence and Mortality Worldwide for 36 Cancers in 185 Countries', *CA: A Cancer Journal for Clinicians*, 71(3), 209-249, available: <http://dx.doi.org/https://doi.org/10.3322/caac.21660>.
- Suresh Babu, S., Valdez, Y., Xu, A., O'Byrne, A.M., Calvo, F., Lei, V. and Conway, E.M. (2014) 'TGF β -mediated suppression of CD248 in non-cancer cells via canonical Smad-dependent signaling pathways is uncoupled in cancer cells', *BMC Cancer*, 14, 113-113, available: <http://dx.doi.org/10.1186/1471-2407-14-113>.
- Surowiak, P., Murawa, D., Materna, V., Maciejczyk, A., Pudelko, M., Ciesla, S., Breborowicz, J.A.N., Murawa, P., Zabel, M., Dietel, M. and Lage, H. (2007) 'Occurrence of Stromal Myofibroblasts in the Invasive Ductal Breast Cancer Tissue is an Unfavourable Prognostic Factor', *Anticancer Research*, 27(4C), 2917.
- Taberero, J., Yoshino, T., Cohn, A.L., Obermannova, R., Bodoky, G., Garcia-Carbonero, R., Ciuleanu, T.-E., Portnoy, D.C., Van Cutsem, E., Grothey, A., Prausová, J., Garcia-Alfonso, P., Yamazaki, K., Clingan, P.R., Lonardi, S., Kim, T.W., Simms, L., Chang, S.-C. and Nasroulah, F. (2015) 'Ramucirumab versus placebo in combination with second-line FOLFIRI in patients with metastatic colorectal carcinoma that progressed during or after first-line therapy with bevacizumab, oxaliplatin, and a fluoropyrimidine (RAISE): a randomised, double-blind, multicentre, phase 3 study', *The Lancet Oncology*, 16(5), 499-508, available: [http://dx.doi.org/https://doi.org/10.1016/S1470-2045\(15\)70127-0](http://dx.doi.org/https://doi.org/10.1016/S1470-2045(15)70127-0).
- Tadros, A.B., Sevilimedu, V., Giri, D.D., Zabor, E.C., Morrow, M. and Plitas, G. (2021) 'Survival Outcomes for Metaplastic Breast Cancer Differ by Histologic Subtype', *Annals of Surgical Oncology*, 28(8), 4245-4253, available: <http://dx.doi.org/10.1245/s10434-020-09430-5>.
- Tai, Y.-T., Acharya, C., Zhong, M.Y., Cea, M., Cagnetta, A., Richardson, P.G., Munshi, N.C. and Anderson, K.C. (2013) 'Constitutive B-Cell Maturation Antigen (BCMA) Activation In Human Multiple Myeloma Cells Promotes Myeloma Cell Growth and Survival In The Bone Marrow Microenvironment Via Upregulated MCL-1 and NF κ B Signaling', *Blood*, 122(21), 681-681, available: <http://dx.doi.org/10.1182/blood.V122.21.681.681>.
- Teachey, D.T., Lacey, S.F., Shaw, P.A., Melenhorst, J.J., Maude, S.L., Frey, N., Pequignot, E., Gonzalez, V.E., Chen, F., Finklestein, J., Barrett, D.M., Weiss, S.L., Fitzgerald, J.C., Berg, R.A., Aplenc, R., Callahan, C., Rheingold, S.R., Zheng, Z., Rose-John, S., White, J.C., Nazimuddin, F., Wertheim, G., Levine, B.L., June, C.H., Porter, D.L. and Grupp, S.A. (2016) 'Identification of Predictive Biomarkers for Cytokine Release Syndrome after Chimeric Antigen Receptor T-cell Therapy for Acute Lymphoblastic Leukemia', *Cancer discovery*, 6(6), 664-679, available: <http://dx.doi.org/10.1158/2159-8290.CD-16-0040>.

References

- Teachey, D.T., Rheingold, S.R., Maude, S.L., Zugmaier, G., Barrett, D.M., Seif, A.E., Nichols, K.E., Suppa, E.K., Kalos, M., Berg, R.A., Fitzgerald, J.C., Aplenc, R., Gore, L. and Grupp, S.A. (2013) 'Cytokine release syndrome after blinatumomab treatment related to abnormal macrophage activation and ameliorated with cytokine-directed therapy', *Blood*, 121(26), 5154-7, available: <http://dx.doi.org/10.1182/blood-2013-02-485623>.
- Thiery, J.P., Acloque, H., Huang, R.Y. and Nieto, M.A. (2009) 'Epithelial-mesenchymal transitions in development and disease', *Cell*, 139(5), 871-90, available: <http://dx.doi.org/10.1016/j.cell.2009.11.007>.
- Thway, K., Robertson, D., Jones, R.L., Selfe, J., Shipley, J., Fisher, C. and Isacke, C.M. (2016) 'Endosialin expression in soft tissue sarcoma as a potential marker of undifferentiated mesenchymal cells', *British journal of cancer*, 115(4), 473-479, available: <http://dx.doi.org/10.1038/bjc.2016.214>.
- Till, B.G., Jensen, M.C., Wang, J., Qian, X., Gopal, A.K., Maloney, D.G., Lindgren, C.G., Lin, Y., Pagel, J.M., Budde, L.E., Raubitschek, A., Forman, S.J., Greenberg, P.D., Riddell, S.R. and Press, O.W. (2012) 'CD20-specific adoptive immunotherapy for lymphoma using a chimeric antigen receptor with both CD28 and 4-1BB domains: pilot clinical trial results', *Blood*, 119(17), 3940-3950, available: <http://dx.doi.org/10.1182/blood-2011-10-387969>.
- Tokarew, N., Ogonek, J., Endres, S., von Bergwelt-Baildon, M. and Kobold, S. (2019) 'Teaching an old dog new tricks: next-generation CAR T cells', *British journal of cancer*, 120(1), 26-37, available: <http://dx.doi.org/10.1038/s41416-018-0325-1>.
- Tomkowicz, B., Rybinski, K., Sebeck, D., Sass, P., Nicolaidis, N.C., Grasso, L. and Zhou, Y. (2010) 'Endosialin/TEM-1/CD248 regulates pericyte proliferation through PDGF receptor signaling', *Cancer Biology & Therapy*, 9(11), 908-915, available: <http://dx.doi.org/10.4161/cbt.9.11.11731>.
- Torikai, H., Reik, A., Liu, P.Q., Zhou, Y., Zhang, L., Maiti, S., Huls, H., Miller, J.C., Kebriaei, P., Rabinovich, B., Lee, D.A., Champlin, R.E., Bonini, C., Naldini, L., Rebar, E.J., Gregory, P.D., Holmes, M.C. and Cooper, L.J. (2012) 'A foundation for universal T-cell based immunotherapy: T cells engineered to express a CD19-specific chimeric-antigen-receptor and eliminate expression of endogenous TCR', *Blood*, 119(24), 5697-705, available: <http://dx.doi.org/10.1182/blood-2012-01-405365>.
- Tran, E., Chinnasamy, D., Yu, Z., Morgan, R.A., Lee, C.C., Restifo, N.P. and Rosenberg, S.A. (2013) 'Immune targeting of fibroblast activation protein triggers recognition of multipotent bone marrow stromal cells and cachexia', *J Exp Med*, 210(6), 1125-35, available: <http://dx.doi.org/10.1084/jem.20130110>.

References

- Trayes, K.P. and Cokenakes, S.E.H. (2021) 'Breast Cancer Treatment', *Am Fam Physician*, 104(2), 171-178.
- Uciechowski, P., Kahmann, L., Plümäkers, B., Malavolta, M., Mocchegiani, E., Dedoussis, G., Herbein, G., Jajte, J., Fulop, T. and Rink, L. (2008) 'TH1 and TH2 cell polarization increases with aging and is modulated by zinc supplementation', *Experimental Gerontology*, 43(5), 493-498, available: <http://dx.doi.org/https://doi.org/10.1016/j.exger.2007.11.006>.
- van der Stegen, S.J.C., Davies, D.M., Wilkie, S., Foster, J., Sosabowski, J.K., Burnet, J., Whilding, L.M., Petrovic, R.M., Ghaem-Maghami, S., Mather, S., Jeannon, J.-P., Parente-Pereira, A.C. and Maher, J. (2013) 'Preclinical In Vivo Modeling of Cytokine Release Syndrome Induced by ErbB-Retargeted Human T Cells: Identifying a Window of Therapeutic Opportunity?', *The Journal of Immunology*, 191(9), 4589, available: <http://dx.doi.org/10.4049/jimmunol.1301523>.
- Vaupel, P., Fortmeyer, H.P., Runkel, S. and Kallinowski, F. (1987) 'Blood Flow, Oxygen Consumption, and Tissue Oxygenation of Human Breast Cancer Xenografts in Nude Rats', *Cancer Res*, 47(13), 3496.
- Virgintino, D., Girolamo, F., Errede, M., Capobianco, C., Robertson, D., Stallcup, W.B., Perris, R. and Roncali, L. (2007) 'An intimate interplay between precocious, migrating pericytes and endothelial cells governs human fetal brain angiogenesis', *Angiogenesis*, 10(1), 35-45, available: <http://dx.doi.org/10.1007/s10456-006-9061-x>.
- Viski, C., Konig, C., Kijewska, M., Mogler, C., Isacke, C.M. and Augustin, H.G. (2016) 'Endosialin-Expressing Pericytes Promote Metastatic Dissemination', *Cancer Res*, 76(18), 5313-25, available: <http://dx.doi.org/10.1158/0008-5472.Can-16-0932>.
- Vogel, P., Pletcher, J.M. and Liang, Y. (2010) 'Spontaneous Acute Tumor Lysis Syndrome as a Cause of Early Deaths in Short-Term Carcinogenicity Studies Using p53+/- Mice', *Veterinary Pathology*, 47(4), 719-724, available: <http://dx.doi.org/10.1177/0300985810363484>.
- Vrdoljak, E., Marschner, N., Zielinski, C., Gligorov, J., Cortes, J., Puglisi, F., Apro, M., Fallowfield, L., Fontana, A., Inbar, M., Kahan, Z., Welt, A., Lévy, C., Brain, E., Pivot, X., Putzu, C., González Martín, A., de Ducla, S., Easton, V. and von Minckwitz, G. (2016) 'Final results of the TANIA randomised phase III trial of bevacizumab after progression on first-line bevacizumab therapy for HER2-negative locally recurrent/metastatic breast cancer', *Ann Oncol*, 27(11), 2046-2052, available: <http://dx.doi.org/10.1093/annonc/mdw316>.
- Wang, L.-C.S., Lo, A., Scholler, J., Sun, J., Majumdar, R.S., Kapoor, V., Antzis, M., Cotner, C.E., Johnson, L.A., Durham, A.C., Solomides, C.C., June, C.H., Puré, E. and Albelda, S.M. (2014) 'Targeting fibroblast activation protein in tumor stroma with chimeric antigen

References

- receptor T cells can inhibit tumor growth and augment host immunity without severe toxicity', *Cancer Immunol Res*, 2(2), 154-166, available: <http://dx.doi.org/10.1158/2326-6066.CIR-13-0027>.
- Wang, X. and Rivière, I. (2016) 'Clinical manufacturing of CAR T cells: foundation of a promising therapy', *Molecular Therapy - Oncolytics*, 3, 16015, available: <http://dx.doi.org/https://doi.org/10.1038/mt.2016.15>.
- Wang, Y., Qi, K., Cheng, H., Cao, J., Shi, M., Qiao, J., Yan, Z., Jing, G., Pan, B., Sang, W., Li, D., Wang, X., Fu, C., Zhu, F., Zheng, J., Li, Z. and Xu, K. (2019) 'Coagulation Disorders after Chimeric Antigen Receptor T Cell Therapy: Analysis of 100 Patients with Relapsed and Refractory Hematologic Malignancies', *Biology of Blood and Marrow Transplantation*, available: <http://dx.doi.org/https://doi.org/10.1016/j.bbmt.2019.11.027>.
- Warburg, O., Karlfried, G. and August-Wilhelm, G. (1958) 'Stoffwechsel der weißen Blutzellen', *Zeitschrift für Naturforschung B*, 13(8), 515-516, available: <http://dx.doi.org/https://doi.org/10.1515/znb-1958-0806>.
- Watanabe, H., Numata, K., Ito, T., Takagi, K. and Matsukawa, A. (2004) 'INNATE IMMUNE RESPONSE IN TH1- AND TH2-DOMINANT MOUSE STRAINS', *Shock*, 22(5), 460-466, available: <http://dx.doi.org/10.1097/01.shk.0000142249.08135.e9>.
- Welt, S., Divgi, C.R., Scott, A.M., Garin-Chesa, P., Finn, R.D., Graham, M., Carswell, E.A., Cohen, A., Larson, S.M., Old, L.J. and et al. (1994) 'Antibody targeting in metastatic colon cancer: a phase I study of monoclonal antibody F19 against a cell-surface protein of reactive tumor stromal fibroblasts', *Journal of clinical oncology : official journal of the American Society of Clinical Oncology*, 12(6), 1193-203, available: <http://dx.doi.org/10.1200/jco.1994.12.6.1193>.
- Whilding, L.M., Halim, L., Draper, B., Parente-Pereira, A.C., Zabinski, T., Davies, D.M. and Maher, J. (2019) 'CAR T-Cells Targeting the Integrin $\alpha\beta6$ and Co-Expressing the Chemokine Receptor CXCR2 Demonstrate Enhanced Homing and Efficacy against Several Solid Malignancies', *Cancers*, 11(5), 674, available: <http://dx.doi.org/10.3390/cancers11050674>.
- WHO (2022) *Breast Cancer*, available: <https://www.who.int/news-room/fact-sheets/detail/breast-cancer> [accessed 3rd March].
- Wilhelm, A., Aldridge, V., Haldar, D., Naylor, A.J., Weston, C.J., Hedegaard, D., Garg, A., Fear, J., Reynolds, G.M., Croft, A.P., Henderson, N.C., Buckley, C.D. and Newsome, P.N. (2016) 'CD248/endothelial critically regulates hepatic stellate cell proliferation during chronic liver injury via a PDGF-regulated mechanism', *Gut*, 65(7), 1175-85, available: <http://dx.doi.org/10.1136/gutjnl-2014-308325>.

References

- Wilkie, S., van Schalkwyk, M.C., Hobbs, S., Davies, D.M., van der Stegen, S.J., Pereira, A.C., Burbridge, S.E., Box, C., Eccles, S.A. and Maher, J. (2012) 'Dual targeting of ErbB2 and MUC1 in breast cancer using chimeric antigen receptors engineered to provide complementary signaling', *J Clin Immunol*, 32(5), 1059-70, available: <http://dx.doi.org/10.1007/s10875-012-9689-9>.
- Williams, K.M., Hakim, F.T. and Gress, R.E. (2007) 'T cell immune reconstitution following lymphodepletion', *Seminars in immunology*, 19(5), 318-330, available: <http://dx.doi.org/10.1016/j.smim.2007.10.004>.
- Wong, P.-P., Muñoz-Félix, J.M., Hijazi, M., Kim, H., Robinson, S.D., De Luxán-Delgado, B., Rodríguez-Hernández, I., Maiques, O., Meng, Y.-M., Meng, Q., Bodrug, N., Dukinfield, M.S., Reynolds, L.E., Elia, G., Clear, A., Harwood, C., Wang, Y., Campbell, J.J., Singh, R., Zhang, P., Schall, T.J., Matchett, K.P., Henderson, N.C., Szlosarek, P.W., Dreger, S.A., Smith, S., Jones, J.L., Gribben, J.G., Cutillas, P.R., Meier, P., Sanz-Moreno, V. and Hovalda-Dilke, K.M. (2020) 'Cancer Burden Is Controlled by Mural Cell- α 3 β 3-Integrin Regulated Crosstalk with Tumor Cells', *Cell*, 181(6), 1346-1363.e21, available: <http://dx.doi.org/10.1016/j.cell.2020.02.003>.
- Wu, C.Y., Roybal, K.T., Puchner, E.M., Onuffer, J. and Lim, W.A. (2015) 'Remote control of therapeutic T cells through a small molecule-gated chimeric receptor', *Science*, 350(6258), aab4077, available: <http://dx.doi.org/10.1126/science.aab4077>.
- Wu, S.Z., Roden, D.L., Al-Eryani, G., Bartonicek, N., Harvey, K., Cazet, A.S., Chan, C.-L., Junankar, S., Hui, M.N., Millar, E.A., Beretov, J., Horvath, L., Joshua, A.M., Stricker, P., Wilmott, J.S., Quek, C., Long, G.V., Scolyer, R.A., Yeung, B.Z., Segara, D., Mak, C., Warriar, S., Powell, J.E., O'Toole, S., Lim, E. and Swarbrick, A. (2021) 'Cryopreservation of human cancers conserves tumour heterogeneity for single-cell multi-omics analysis', *Genome Medicine*, 13(1), 81, available: <http://dx.doi.org/10.1186/s13073-021-00885-z>.
- Xian, X., Håkansson, J., Ståhlberg, A., Lindblom, P., Betsholtz, C., Gerhardt, H. and Semb, H. (2006) 'Pericytes limit tumor cell metastasis', *J Clin Invest*, 116(3), 642-651, available: <http://dx.doi.org/10.1172/JCI25705>.
- Xie, Y.J., Dougan, M., Jalkhani, N., Ingram, J., Fang, T., Kummer, L., Momin, N., Pishesha, N., Rickelt, S., Hynes, R.O. and Ploegh, H. (2019) 'Nanobody-based CAR T cells that target the tumor microenvironment inhibit the growth of solid tumors in immunocompetent mice', *Proceedings of the National Academy of Sciences*, 116(16), 7624, available: <http://dx.doi.org/10.1073/pnas.1817147116>.
- Yamazaki, T. and Mukoyama, Y.-s. (2018) 'Tissue Specific Origin, Development, and Pathological Perspectives of Pericytes', *Frontiers in Cardiovascular Medicine*, 5(78), available: <http://dx.doi.org/10.3389/fcvm.2018.00078>.

References

- Yáñez, L., Sánchez-Escamilla, M. and Perales, M.-A. (2019) 'CAR T Cell Toxicity: Current Management and Future Directions', *HemaSphere*, 3(2), e186, available: <http://dx.doi.org/10.1097/hs9.000000000000186>.
- Yang, Y., Andersson, P., Hosaka, K., Zhang, Y., Cao, R., Iwamoto, H., Yang, X., Nakamura, M., Wang, J., Zhuang, R., Morikawa, H., Xue, Y., Braun, H., Beyaert, R., Samani, N., Nakae, S., Hams, E., Dissing, S., Fallon, P.G., Langer, R. and Cao, Y. (2016) 'The PDGF-BB-SOX7 axis-modulated IL-33 in pericytes and stromal cells promotes metastasis through tumour-associated macrophages', *Nature communications*, 7, 11385, available: <http://dx.doi.org/10.1038/ncomms11385>.
- Yasukawa, M., Ohminami, H., Arai, J., Kasahara, Y., Ishida, Y. and Fujita, S. (2000) 'Granule exocytosis, and not the fas/fas ligand system, is the main pathway of cytotoxicity mediated by alloantigen-specific CD4(+) as well as CD8(+) cytotoxic T lymphocytes in humans', *Blood*, 95(7), 2352-5.
- Yeku, O.O., Purdon, T.J., Koneru, M., Spriggs, D. and Brentjens, R.J. (2017) 'Armored CAR T cells enhance antitumor efficacy and overcome the tumor microenvironment', *Sci Rep*, 7(1), 10541, available: <http://dx.doi.org/10.1038/s41598-017-10940-8>.
- Yixuan, Z., Jiwei, B., Shuai, W., Hua, G., Mingxuan, L., Chuzhong, L., Songbai, G. and Yazhuo, Z. (2018) 'Analysis of clinical factors and PDGFR- β in predicting prognosis of patients with clival chordoma', *Journal of Neurosurgery JNS*, 129(6), 1429-1437, available: <http://dx.doi.org/10.3171/2017.6.JNS17562>.
- Yonenaga, Y., Mori, A., Onodera, H., Yasuda, S., Oe, H., Fujimoto, A., Tachibana, T. and Imamura, M. (2005) 'Absence of Smooth Muscle Actin-Positive Pericyte Coverage of Tumor Vessels Correlates with Hematogenous Metastasis and Prognosis of Colorectal Cancer Patients', *Oncology*, 69(2), 159-166, available: <http://dx.doi.org/10.1159/000087840>.
- Yu, L.X., Yan, L., Yang, W., Wu, F.Q., Ling, Y., Chen, S.Z., Tang, L., Tan, Y.X., Cao, D., Wu, M.C., Yan, H.X. and Wang, H.Y. (2014) 'Platelets promote tumour metastasis via interaction between TLR4 and tumour cell-released high-mobility group box1 protein', *Nature communications*, 5, 5256, available: <http://dx.doi.org/10.1038/ncomms6256>.
- Zah, E., Lin, M.-Y., Silva-Benedict, A., Jensen, M.C. and Chen, Y.Y. (2016) 'T Cells Expressing CD19/CD20 Bispecific Chimeric Antigen Receptors Prevent Antigen Escape by Malignant B Cells', *Cancer Immunol Res*, 4(6), 498-508, available: <http://dx.doi.org/10.1158/2326-6066.CIR-15-0231>.
- Zanivan, S., Maione, F., Hein, M.Y., Hernandez-Fernaund, J.R., Ostasiewicz, P., Giraud, E. and Mann, M. (2013) 'SILAC-based proteomics of human primary endothelial cell morphogenesis unveils tumor angiogenic markers', *Mol Cell Proteomics*, 12(12), 3599-611, available: <http://dx.doi.org/10.1074/mcp.M113.031344>.

References

- Zelensky, A.N. and Gready, J.E. (2005) 'The C-type lectin-like domain superfamily', *The FEBS Journal*, 272(24), 6179-6217, available: <http://dx.doi.org/10.1111/j.1742-4658.2005.05031.x>.
- Zhang, L., Steele, M.B., Jenks, N., Grell, J., Behrens, M., Nace, R., Naik, S., Federspiel, M.J., Russell, S.J. and Peng, K.-W. (2016) 'Robust Oncolytic Virotherapy Induces Tumor Lysis Syndrome and Associated Toxicities in the MPC-11 Plasmacytoma Model', *Molecular Therapy*, 24(12), 2109-2117, available: <http://dx.doi.org/10.1038/mt.2016.167>.
- Zhang, Y., Guo, J., Zhang, X.L., Li, D.P., Zhang, T.T., Gao, F.F., Liu, N.F. and Sheng, X.G. (2015) 'Antibody fragment-armed mesoporous silica nanoparticles for the targeted delivery of bevacizumab in ovarian cancer cells', *Int J Pharm*, 496(2), 1026-33, available: <http://dx.doi.org/10.1016/j.ijpharm.2015.10.080>.
- Zimmermann, K.W. (1923) 'Der feinere Bau der Blutcapillaren', *Zeitschrift für Anatomie und Entwicklungsgeschichte*, 68(1), 29-109, available: <http://dx.doi.org/10.1007/BF02593544>.